

NIST NCSTAR 1-5

**Federal Building and Fire Safety Investigation of the
World Trade Center Disaster**

Reconstruction of the Fires in the World Trade Center Towers

Richard G. Gann
Anthony Hamins
Kevin B. McGrattan
George W. Mulholland
Harold E. Nelson
Thomas J. Ohlemiller
William M. Pitts
Kuldeep R. Prasad

NIST NCSTAR 1-5

**Federal Building and Fire Safety Investigation of the
World Trade Center Disaster**

**Reconstruction of the Fires in the
World Trade Center Towers**

Richard G. Gann
Anthony Hamins
Kevin B. McGrattan
George W. Mulholland
*Building and Fire Research Laboratory
National Institute of Standards and Technology*

Harold E. Nelson
Contractor

Thomas J. Ohlemiller
William M. Pitts
Kuldeep R. Prasad
*Building and Fire Research Laboratory
National Institute of Standards and Technology*

September 2005



U.S. Department of Commerce
Carlos M. Gutierrez, Secretary

Technology Administration
Michelle O'Neill, Acting Under Secretary for Technology

National Institute of Standards and Technology
William Jeffrey, Director

Disclaimer No. 1

Certain commercial entities, equipment, products, or materials are identified in this document in order to describe a procedure or concept adequately or to trace the history of the procedures and practices used. Such identification is not intended to imply recommendation, endorsement, or implication that the entities, products, materials, or equipment are necessarily the best available for the purpose. Nor does such identification imply a finding of fault or negligence by the National Institute of Standards and Technology.

Disclaimer No. 2

The policy of NIST is to use the International System of Units (metric units) in all publications. In this document, however, units are presented in metric units or the inch-pound system, whichever is prevalent in the discipline.

Disclaimer No. 3

Pursuant to section 7 of the National Construction Safety Team Act, the NIST Director has determined that certain evidence received by NIST in the course of this Investigation is "voluntarily provided safety-related information" that is "not directly related to the building failure being investigated" and that "disclosure of that information would inhibit the voluntary provision of that type of information" (15 USC 7306c).

In addition, a substantial portion of the evidence collected by NIST in the course of the Investigation has been provided to NIST under nondisclosure agreements.

Disclaimer No. 4

NIST takes no position as to whether the design or construction of a WTC building was compliant with any code since, due to the destruction of the WTC buildings, NIST could not verify the actual (or as-built) construction, the properties and condition of the materials used, or changes to the original construction made over the life of the buildings. In addition, NIST could not verify the interpretations of codes used by applicable authorities in determining compliance when implementing building codes. Where an Investigation report states whether a system was designed or installed as required by a code *provision*, NIST has documentary or anecdotal evidence indicating whether the requirement was met, or NIST has independently conducted tests or analyses indicating whether the requirement was met.

Use in Legal Proceedings

No part of any report resulting from a NIST investigation into a structural failure or from an investigation under the National Construction Safety Team Act may be used in any suit or action for damages arising out of any matter mentioned in such report (15 USC 281a; as amended by P.L. 107-231).

**National Institute of Standards and Technology National Construction Safety Team Act Report 1-5
Natl. Inst. Stand. Technol. Natl. Constr. Sfty. Tm. Act Rpt. 1-5, 240 pages (September 2005)
CODEN: NSPUE2**

U.S. GOVERNMENT PRINTING OFFICE
WASHINGTON: 2005

For sale by the Superintendent of Documents, U.S. Government Printing Office
Internet: bookstore.gpo.gov — Phone: (202) 512-1800 — Fax: (202) 512-2250
Mail: Stop SSOP, Washington, DC 20402-0001

ABSTRACT

The collapses of the World Trade Center towers on September 11, 2001, resulted from a combination of aircraft impact damage and the ensuing fires. This report documents:

- The information obtained on the factors that affected the nature, duration, and location of the fires and how this was obtained;
- The development and validation of the fire model used to simulate the fires;
- Descriptions of the most likely fires, as they were reconstructed; and
- The modeling and validation of the heat transfer from the fires to the buildings' structural members.

Keywords: Fire, fire model validation, fire modeling, fire tests, World Trade Center.

This page intentionally left blank.

TABLE OF CONTENTS

Abstract	iii
List of Figures	xi
List of Tables	xvii
List of Acronyms and Abbreviations	xix
Metric Conversion Table	xxi
Preface	xxv
Acknowledgments.....	xxxv
Executive Summary	xxxvii
Chapter 1	
Introduction	1
1.1 Objective and Approach	1
1.2 Document Content	3
Chapter 2	
Visual Evidence.....	5
2.1 Introduction.....	5
2.1.1 Magnitude.....	5
2.1.2 Sources	6
2.2 Evidence Regarding WTC 1	6
2.2.1 Time Line for the First 30 Seconds	6
2.2.2 Estimated Aircraft Speed.....	9
2.2.3 Observed Impact Damage	9
2.2.4 Observed Fire Behavior in WTC 1 Following the Aircraft Strike	10
2.3 Evidence Regarding WTC 2	21
2.3.1 Time Line for the First 10 Seconds	21
2.3.2 Estimated Aircraft Speed.....	24
2.3.3 Determination of Primary Oscillation Period.....	24
2.3.4 Observed Impact Damage	27
2.3.5 Debris Expelled by the Aircraft Impact.....	28
2.3.6 Fire Behavior Following the Aircraft Strike.....	29
2.3.7 Observed Fire Behavior in WTC 2.....	29
2.3.8 Other Structural Changes	39

2.4	References.....	40
Chapter 3		
Building Interiors and Combustibles		41
3.1	Data on the Building Interiors.....	41
3.1.1	Focus	41
3.1.2	Floor Plans.....	41
3.1.3	Ceilings.....	45
3.1.4	Ventilation Paths	49
3.2	Building Combustibles.....	50
3.2.1	Nature of Combustibles.....	50
3.2.2	Flammability of Workstations.....	52
3.3	Aircraft Combustibles.....	58
3.3.1	Liquid Fuels.....	58
3.3.2	Other Combustibles	58
3.4	Insulation	60
3.4.1	Identification	60
3.4.2	Thermal and Mechanical Properties.....	60
3.4.3	Thermal Behavior in Fires.....	61
3.5	Other Considerations for the Fire Reconstruction	66
3.6	References.....	66
Chapter 4		
Fire Modeling.....		69
4.1	Introduction.....	69
4.2	Description of the Fire Dynamics Simulator	69
4.3	FDS Accuracy for Fires of Known Heat Release Rate	71
4.4	Modeling of the Building Combustibles.....	73
4.5	Compartment Fire Experiments Involving Workstations	75
4.6	Summary	80
4.7	References.....	81
Chapter 5		
Heat Transfer Modeling		83
5.1	Introduction.....	83
5.2	Description of the Fire Structure Interface	83
5.3	Sensitivity of the Heat Transfer Process	84

5.4 Accuracy Assessment of FSI	86
5.4.1 Rendition of Structural Elements	86
5.4.2 Test 1	90
5.4.3 Test 5	94
5.5 Summary	102
5.6 References.....	102
Chapter 6	
Simulation of the WTC Fires and Thermal Environments.....	103
6.1 General.....	103
6.2 Fire Dynamics Simulator Simulation Assumptions and Variables.....	103
6.2.1 Assumptions and Fixed Parameters.....	104
6.2.2 Variables.....	105
6.2.3 Presentation of Results	105
6.3 Simulation Results for WTC 1, Case A	106
6.3.1 Floor 92	106
6.3.2 Floor 93	106
6.3.3 Floor 94	107
6.3.4 Floor 95	107
6.3.5 Floor 96	107
6.3.6 Floor 97	108
6.3.7 Floor 98	108
6.3.8 Floor 99	108
6.3.9 Observations.....	108
6.4 Simulation of Fires in WTC 1, Case B	108
6.5 Simulation of Fires in WTC 2, Case C	109
6.5.1 Floor 78	109
6.5.2 Floor 79	109
6.5.3 Floor 80	110
6.5.4 Floor 81	110
6.5.5 Floor 82	110
6.5.6 Floor 83	110
6.6 Simulation of Fires in WTC 2, Case D	111
6.7 Discussion of FDS Results.....	140
6.7.1 Fire Spread Patterns.....	140

6.7.2	Fire Temperatures.....	141
6.7.3	Global Heat Release Rates	141
6.8	Data Transfer	142
6.9	Thermal Response Simulations.....	142
6.10	Global Thermal Response of WTC 1, Case A	143
6.10.1	Floor 93	158
6.10.2	Floor 94	158
6.10.3	Floor 95	159
6.10.4	Floor 96	160
6.10.5	Floor 97	160
6.10.6	Floor 98	161
6.10.7	Floor 99	162
6.11	Global Thermal Response of WTC 1, Case B	162
6.11.1	Floor 93	162
6.11.2	Floor 94	162
6.11.3	Floor 95	163
6.11.4	Floor 96	163
6.11.5	Floor 97, 98, and 99.....	163
6.12	Global Thermal Response of WTC 2, Case C	163
6.12.1	Floor 79	174
6.12.2	Floor 80	174
6.12.3	Floor 81	175
6.12.4	Floor 82	176
6.12.5	Floor 83	177
6.13	Global Thermal Response of WTC 2, Case D	178
6.13.1	Floor 79	178
6.13.2	Floor 80	178
6.13.3	Floor 81	178
6.13.4	Floor 82	179
6.13.5	Floor 83	179
6.14	Summary of Thermal Response of Structural Components.....	179
6.15	Fire in an Undamaged Tower	180
6.16	References.....	181

Chapter 7
Findings 183

- 7.1 Characteristics of the Buildings 183
- 7.2 Characteristics of the Fires..... 183
- 7.3 Capability for Large Fire Reconstruction 184
- 7.4 Simulations of the WTC Fires 184

This page intentionally left blank.

LIST OF FIGURES

Figure P–1.	The eight projects in the federal building and fire safety investigation of the WTC disaster.	xxvii
Figure 2–1.	Series of frames from videos that show the aircraft striking WTC 1 and the immediate aftermath. The times relative to the plane strike are shown in the upper right-hand corner.	7
Figure 2–2.	Photograph of the north face of WTC 1 around 9:30 a.m. showing the area damaged by the aircraft strike.	10
Figure 2–3.	View of the south face of WTC 1, cropped from a photograph shot from a helicopter at 10:22:59 a.m. It has been enhanced by adjusting the intensity levels, and column and floor numbers have been added.	18
Figure 2–4.	Maps of integrated fire observations between 8:47 a.m. and 10:28 a.m. for the four faces of WTC 1.	19
Figure 2–5.	The nascent fireballs and dust clouds formed on WTC 2 1.2 s after the aircraft struck WTC 2.	23
Figure 2–6.	Photograph of the towers recorded from the north-northeast 4.3 s after the aircraft struck WTC 2.	23
Figure 2–7.	Sequential cropped frames taken from a video showing the aircraft approaching WTC 2. The frames are separated by 33.3 ms.	25
Figure 2–8.	Plots of pixel locations for the nose and tail of the aircraft that struck WTC 2 as a function of time taken from the images shown in Figure 2–7.	26
Figure 2–9.	Displacement of the left-most window line on the 70 th floor of WTC 2 as a function of time, determined using Moiré analysis.	26
Figure 2–10.	Photograph was shot from the northeast, showing east face of WTC 2 at 9:44:50 a.m. The original intensity levels have been adjusted, and column and floor numbers have been added.	33
Figure 2–11.	Cropped photograph of the east face of WTC 2 at 9:58:02 a.m. The intensity levels have been adjusted, and column and floor numbers have been added.	35
Figure 2–12.	Maps of observed fire distributions on the four faces of WTC 2 shortly after the aircraft impact (near 9:04 a.m.) and corresponding integrated fire observations for the entire period between 9:03 a.m. and 9:59 a.m.	37
Figure 3–1.	Top and bottom views of a ceiling system similar to that originally installed in the tenant spaces.	46
Figure 3–2.	Bottom and top views of a ceiling system similar to that originally installed in the core areas.	47
Figure 3–3.	Test frame mounted on the shaking table at the University at Buffalo.	48

Figure 3–4. Furnishings and partitions layout of the 97th floor of WTC 1..... 52

Figure 3–5. Photographs of the generic workstation..... 53

Figure 3–6. Photographs of the WTC workstation..... 53

Figure 3–7. Annotated partial HRR curve from Test 2. 55

Figure 3–8. Photographs of a burning workstation at beginning of test, 165 s into test, near the peak heat release rate at 533 s, and at 965 s..... 56

Figure 3–9. Steel components in test compartment for Tests 1, 2, and 3..... 62

Figure 3–10. SFRM-coated steel components prior to a test. 63

Figure 3–11. Temperature-time history for truss A in Test 5..... 65

Figure 3–12. Temperature-time history for truss A in Test 3..... 65

Figure 4–1. Simulated centerline gas temperatures in a spray burner test. 72

Figure 4–2. Comparison of predicted and measured gas temperatures at various heights above the floor, Test 5..... 72

Figure 4–3. Heat Release Rates for the single workstation fire experiments. Clockwise from upper left: a single, undamaged workstation; a workstation with ceiling tiles added; a workstation with tiles and jet fuel applied; and a workstation with just jet fuel applied..... 74

Figure 4–4. View of the fire compartment before the start of Test 6. 76

Figure 4–5. Disassembled workstation burned in Test 5..... 76

Figure 4–6. Multiple workstation fire experiment. 77

Figure 4–7. Coarse grid simulation of a multiple workstation experiment. 77

Figure 4–8. Upper layer temperatures at 4 locations, Test 1. 78

Figure 4–9. Heat Release Rates for multiple workstation experiments. 79

Figure 5–1. Finite element model of light box shape core column and temperature contours (Kelvin) at one instant in time..... 84

Figure 5–2. Temperature rise (K) in a plate with a 12 in. gap in the thermal insulation..... 85

Figure 5–3. Rates of temperature rise in a 1 in. steel plate as a function of the length of a gap and the variability in the applied insulation for several insulation thicknesses. 86

Figure 5–4. FSI grid structure of insulated steel rod (with dimensions in meters) showing the elements used to model the steel (in blue) and the SFRM (in violet), and the temperature contours after 2,000 s in Test 5. 87

Figure 5–5. Perspective and top view of the finite element model of the steel column with SFRM. 87

Figure 5–6. Temperature (in K) contours on the outer surface of the SFRM and the ceiling after 2,000 s in Test 5. 88

Figure 5–7. Finite element model of the insulated steel truss, the ceiling and the floor used in the thermal analysis of Test 5. 88

Figure 5–8.	Finite element representation of the insulated steel truss (blue), the SFRM (violet), and the ceiling (red) used in the thermal analysis of Test 5.	89
Figure 5–9.	Temperature contours (in K) on the ceiling, floor and the surface of the SFRM on Truss A after 1,000 s in Test 5.	89
Figure 5–10.	Comparison of numerical simulations with measurements for the steel surface temperature at four locations on the west bar in Test 1.	91
Figure 5–11.	Comparison of numerical simulations with measurements for the steel surface temperature at four locations 3.69 m above the floor on the column in Test 1.	92
Figure 5–12.	Comparison of numerical simulations with measurements for the steel surface temperature at four locations 2.89 m above the floor on the north truss in Test 1.	93
Figure 5–13.	Comparison of numerical simulations with measurements for the steel surface temperature at four locations 3.70 m above the floor on the north truss in Test 1.	94
Figure 5–14.	Comparison of numerical simulations with measurements for the temperature of the SFRM surface at four locations on the insulated bar in Test 5.	95
Figure 5–15.	Comparison of numerical simulations with measurements for the temperature of the steel surface at four locations on the insulated bar in Test 5.	96
Figure 5–16.	Comparison of numerical simulations with measurements for the temperature of the SFRM surface at four locations 3.69 m above the floor on the insulated steel column in Test 5.	97
Figure 5–17.	Comparison of numerical simulations with measurements for the temperature of the steel surface at four locations 3.69 m above the floor on the insulated steel column in Test 5.	98
Figure 5–18.	Comparison of numerical simulations with measurements for the temperature of the SFRM surface at four locations 3.70 m above the floor on the north truss in Test 5.	99
Figure 5–19.	Comparison of numerical simulations with measurements for the temperature of the steel surface at four locations 3.70 m above the floor on the north truss in Test 5.	100
Figure 6–1.	Simulated upper layer temperatures on floor 92 of WTC 1, Case A.	112
Figure 6–2.	Simulated upper layer temperatures on floor 92 of WTC 1, Case B.	113
Figure 6–3.	Simulated upper layer temperatures on floor 93 of WTC 1, Case A.	114
Figure 6–4.	Simulated upper layer temperatures on floor 93 of WTC 1, Case B.	115
Figure 6–5.	Simulated upper layer temperatures on floor 94 of WTC 1, Case A.	116
Figure 6–6.	Simulated upper layer temperatures on floor 94 of WTC 1, Case B.	117
Figure 6–7.	Simulated upper layer temperatures on floor 95 of WTC 1, Case A.	118
Figure 6–8.	Simulated upper layer temperatures on floor 95 of WTC 1, Case B.	119
Figure 6–9.	Simulated upper layer temperatures on floor 96 of WTC 1, Case A.	120
Figure 6–10.	Simulated upper layer temperatures on floor 96 of WTC 1, Case B.	121
Figure 6–11.	Simulated upper layer temperatures on floor 97 of WTC 1, Case A.	122
Figure 6–12.	Simulated upper layer temperatures on floor 97 of WTC 1, Case B.	123

Figure 6–13. Simulated upper layer temperatures on floor 98 of WTC 1, Case A. 124

Figure 6–14. Simulated upper layer temperatures on floor 98 of WTC 1, Case B. 125

Figure 6–15. Simulated upper layer temperatures on floor 99 of WTC 1, Case A. 126

Figure 6–16. Simulated upper layer temperatures on floor 99 of WTC 1, Case B. 127

Figure 6–17. Simulated upper layer temperatures on floor 78 of WTC 2, Case C. 128

Figure 6–18. Simulated upper layer temperatures on floor 78 of WTC 2, Case D. 129

Figure 6–19. Simulated upper layer temperatures on floor 79 of WTC 2, Case C. 130

Figure 6–20. Simulated upper layer temperatures on floor 79 of WTC 2, Case D. 131

Figure 6–21. Simulated upper layer temperatures on floor 80 of WTC 2, Case C. 132

Figure 6–22. Simulated upper layer temperatures on floor 80 of WTC 2, Case D. 133

Figure 6–23. Simulated upper layer temperatures on floor 81 of WTC 2, Case C. 134

Figure 6–24. Simulated upper layer temperatures on floor 81 of WTC 2, Case D. 135

Figure 6–25. Simulated upper layer temperatures on floor 82 of WTC 2, Case C. 136

Figure 6–26. Simulated upper layer temperatures on floor 82 of WTC 2, Case D. 137

Figure 6–27. Simulated upper layer temperatures on floor 83 of WTC 2, Case C. 138

Figure 6–28. Simulated upper layer temperatures on floor 83 of WTC 2, Case D. 139

Figure 6–29. Direction of simulated fire movement on floors 94 and 97 of WTC 1. 140

Figure 6–30. Predicted heat release rates for fires in WTC 1 and WTC 2. 142

Figure 6–31. Thermal response of floor 93 of WTC 1, Case A. 144

Figure 6–32. Thermal response of floor 93 of WTC 1, Case B. 145

Figure 6–33. Thermal response of floor 94 of WTC 1, Case A. 146

Figure 6–34. Thermal response of floor 94 of WTC 1, Case B. 147

Figure 6–35. Thermal response of floor 95 of WTC 1, Case A. 148

Figure 6–36. Thermal response of floor 95 of WTC 1, Case B. 149

Figure 6–37. Thermal response of floor 96 of WTC 1, Case A. 150

Figure 6–38. Thermal response of floor 96 of WTC 1, Case B. 151

Figure 6–39. Thermal response of floor 97 of WTC 1, Case A. 152

Figure 6–40. Thermal response of floor 97 of WTC 1, Case B. 153

Figure 6–41. Thermal response of floor 98 of WTC 1, Case A. 154

Figure 6–42. Thermal response of floor 98 of WTC 1, Case B. 155

Figure 6–43. Thermal response of floor 99 of WTC 1, Case A. 156

Figure 6–44. Thermal response of floor 99 of WTC 1, Case B. 157

Figure 6–45. Structural and insulation damage to floor 94 of WTC 1, Case A. 158

Figure 6–46. Structural and insulation damage to floor 95 of WTC 1, Case A. 159

Figure 6–47. Structural and insulation damage to floor 96 of WTC 1, Case A. 160

Figure 6–48. Structural and insulation damage to floor 97 of WTC 1, Case A.	161
Figure 6–49. Structural and insulation damage to floor 98 of WTC 1, Case A.	162
Figure 6–50. Thermal response of floor 79 of WTC 2, Case C.	164
Figure 6–51. Thermal response of floor 79 of WTC 2, Case D.	165
Figure 6–52. Thermal response of floor 80 of WTC 2, Case C.	166
Figure 6–53. Thermal response of floor 80 of WTC 2, Case D.	167
Figure 6–54. Thermal response of floor 81 of WTC 2, Case C.	168
Figure 6–55. Thermal response of floor 81 of WTC 2, Case D.	169
Figure 6–56. Thermal response of floor 82 of WTC 2, Case C.	170
Figure 6–57. Thermal response of floor 82 of WTC 2, Case D.	171
Figure 6–58. Thermal response of floor 83 of WTC 2, Case C.	172
Figure 6–59. Thermal response of floor 83 of WTC 2, Case D.	173
Figure 6–60. Structural and insulation damage on floor 79 of WTC 2, Case C.....	174
Figure 6–61. Structural and insulation damage on floor 80 of WTC 2, Case C.....	175
Figure 6–62. Structural and insulation damage on floor 81 of WTC 2, Case C.....	176
Figure 6–63. Structural and insulation damage on floor 82 of WTC 2, Case C.....	177
Figure 6–64. Structural and insulation damage on floor 83 of WTC 2, Case C.....	178

This page intentionally left blank.

LIST OF TABLES

Table P-1.	Federal building and fire safety investigation of the WTC disaster.....	xxvi
Table P-2.	Public meetings and briefings of the WTC Investigation.	xxix
Table 2-1.	Time line for events immediately following the aircraft strike on WTC 1.....	9
Table 2-2.	Time line for events immediately following the plane strike on WTC 2.....	22
Table 2-3.	Summary of open windows observed on faces (78 th through 84 th floors) of WTC 2 at 9:03 a.m. and 9:58 a.m.....	29
Table 3-1.	Floor layout information obtained.	43
Table 3-2.	Use of space on focus floors in WTC 1.	51
Table 3-3.	Contents of workstations.....	54
Table 3-4.	Experimental test plan for single workstation fire tests.	55
Table 3-5.	Key results from the workstation fire test burns.	57
Table 3-6.	Combustible contents of aircraft.	59
Table 3-7.	Importance of combustible contents of aircraft.....	60
Table 3-8.	Types and locations of sprayed insulation on focus floors.	61
Table 3-9.	Test matrix for steel exposure fire tests.	63
Table 3-10.	Summary of insulation on steel components.....	64
Table 4-1.	Test matrix.	75
Table 5-1.	Times (h) at which modeled columns reached target temperatures.	85
Table 6-1.	Values of WTC fire simulation variables.....	104
Table 6-2.	Sources of WTC thermal response inputs.	143
Table 6-3.	Regions in WTC 1 in which temperatures of structural steel exceeded 600 °C.	179
Table 6-4.	Regions in WTC 2 in which temperatures of structural steel exceeded 600 °C.	179

This page intentionally left blank.

LIST OF ACRONYMS AND ABBREVIATIONS

Acronyms

ASTM	ASTM International
BFRL	NIST Building Fire and Research Laboratory
CFD	computational fluid dynamics
CPU	central processing unit
FDNY	New York City Fire Department
FDS	Fire Dynamics Simulator
FEMA	Federal Emergency Management Agency
FSI	Fire Structure Interface
HRR	Heat Release Rate
HVAC	heating, ventilating, and air conditioning
LES	large eddy simulation
MLR	mass loss rate
NIST	National Institute of Standards and Technology
NYPD	New York Police Department
PANYNJ	The Port Authority of New York and New Jersey
SFRM	sprayed fire-resistive material
USC	United States Code
WTC	World Trade Center
WTC 1	World Trade Center 1 (North Tower)
WTC 2	World Trade Center 2 (South Tower)
WTC 7	World Trade Center 7

Abbreviations

°C	degrees Celsius
°F	degrees Fahrenheit
cm	centimeter
ft	foot
gal	gallon

GJ	gigajoule
GW	gigawatt
in.	inch
K	kelvin
kg	kilogram
L	liter
lb	pound
m	meter
min	minute
MJ	megajoule
mm	millimeter
ms	millisecond
s	second
W	watt

METRIC CONVERSION TABLE

To convert from	to	Multiply by
-----------------	----	-------------

AREA AND SECOND MOMENT OF AREA

square foot (ft ²)	square meter (m ²)	9.290 304 E-02
square inch (in. ²)	square meter (m ²)	6.4516 E-04
square inch (in. ²)	square centimeter (cm ²)	6.4516 E+00
square yard (yd ²)	square meter (m ²)	8.361 274 E-01

ENERGY (includes WORK)

kilowatt hour (kW · h)	joule (J)	3.6 E+06
quad (1015 BtuIT)	joule (J)	1.055 056 E+18
therm (U.S.)	joule (J)	1.054 804 E+08
ton of TNT (energy equivalent)	joule (J)	4.184 E+09
watt hour (W · h)	joule (J)	3.6 E+03
watt second (W · s)	joule (J)	1.0 E+00

FORCE

dyne (dyn)	newton (N)	1.0 E-05
kilogram-force (kgf)	newton (N)	9.806 65 E+00
kilopond (kilogram-force) (kp)	newton (N)	9.806 65 E+00
kip (1 kip=1,000 lbf)	newton (N)	4.448 222 E+03
kip (1 kip=1,000 lbf)	kilonewton (kN)	4.448 222 E+00
pound-force (lbf)	newton (N)	4.448 222 E+00

FORCE DIVIDED BY LENGTH

pound-force per foot (lbf/ft)	newton per meter (N/m)	1.459 390 E+01
pound-force per inch (lbf/in.)	newton per meter (N/m)	1.751 268 E+02

HEAT FLOW RATE

calorieth per minute (calth/min)	watt (W)	6.973 333 E-02
calorieth per second (calth/s)	watt (W)	4.184 E+00
kilocalorieth per minute (kcalth/min)	watt (W)	6.973 333 E+01
kilocalorieth per second (kcalth/s)	watt (W)	4.184 E+03

To convert from	to	Multiply by
TEMPERATURE		
degree Celsius (°C)	kelvin (K)	$T/K = t/^{\circ}C + 273.15$
degree centigrade	degree Celsius (°C)	$t/^{\circ}C \approx t / \text{deg. cent.}$
degree Fahrenheit (°F)	degree Celsius (°C)	$t/^{\circ}C = (t/^{\circ}F - 32)/1.8$
degree Fahrenheit (°F)	kelvin (K)	$T/K = (t/^{\circ}F + 459.67)/1.8$
kelvin (K)	degree Celsius (°C)	$t/^{\circ}C = T/K - 273.15$
TEMPERATURE INTERVAL		
degree Celsius (°C)	kelvin (K)	1.0 E+00
degree centigrade	degree Celsius (°C)	1.0 E+00
degree Fahrenheit (°F)	degree Celsius (°C)	5.555 556 E-01
degree Fahrenheit (°F)	kelvin (K)	5.555 556 E-01
degree Rankine (°R)	kelvin (K)	5.555 556 E-01
VELOCITY (includes SPEED)		
foot per second (ft/s)	meter per second (m/s)	3.048 E-01
inch per second (in./s)	meter per second (m/s)	2.54 E-02
kilometer per hour (km/h)	meter per second (m/s)	2.777 778 E-01
mile per hour (mi/h)	kilometer per hour (km/h)	1.609 344 E+00
mile per minute (mi/min)	meter per second (m/s)	2.682 24 E+01
VOLUME (includes CAPACITY)		
cubic foot (ft ³)	cubic meter (m ³)	2.831 685 E-02
cubic inch (in. ³)	cubic meter (m ³)	1.638 706 E-05
cubic yard (yd ³)	cubic meter (m ³)	7.645 549 E-01
gallon (U.S.) (gal)	cubic meter (m ³)	3.785 412 E-03
gallon (U.S.) (gal)	liter (L)	3.785 412 E+00
liter (L)	cubic meter (m ³)	1.0 E-03
ounce (U.S. fluid) (fl oz)	cubic meter (m ³)	2.957 353 E-05
ounce (U.S. fluid) (fl oz)	milliliter (mL)	2.957 353 E+01

This page intentionally left blank.

PREFACE

Genesis of This Investigation

Immediately following the terrorist attack on the World Trade Center (WTC) on September 11, 2001, the Federal Emergency Management Agency (FEMA) and the American Society of Civil Engineers began planning a building performance study of the disaster. The week of October 7, as soon as the rescue and search efforts ceased, the Building Performance Study Team went to the site and began its assessment. This was to be a brief effort, as the study team consisted of experts who largely volunteered their time away from their other professional commitments. The Building Performance Study Team issued its report in May 2002, fulfilling its goal “to determine probable failure mechanisms and to identify areas of future investigation that could lead to practical measures for improving the damage resistance of buildings against such unforeseen events.”

On August 21, 2002, with funding from the U.S. Congress through FEMA, the National Institute of Standards and Technology (NIST) announced its building and fire safety investigation of the WTC disaster. On October 1, 2002, the National Construction Safety Team Act (Public Law 107-231), was signed into law. The NIST WTC Investigation was conducted under the authority of the National Construction Safety Team Act.

The goals of the investigation of the WTC disaster were:

- To investigate the building construction, the materials used, and the technical conditions that contributed to the outcome of the WTC disaster.
- To serve as the basis for:
 - Improvements in the way buildings are designed, constructed, maintained, and used;
 - Improved tools and guidance for industry and safety officials;
 - Recommended revisions to current codes, standards, and practices; and
 - Improved public safety.

The specific objectives were:

1. Determine why and how WTC 1 and WTC 2 collapsed following the initial impacts of the aircraft and why and how WTC 7 collapsed;
2. Determine why the injuries and fatalities were so high or low depending on location, including all technical aspects of fire protection, occupant behavior, evacuation, and emergency response;
3. Determine what procedures and practices were used in the design, construction, operation, and maintenance of WTC 1, 2, and 7; and
4. Identify, as specifically as possible, areas in current building and fire codes, standards, and practices that warrant revision.

NIST is a nonregulatory agency of the U.S. Department of Commerce’s Technology Administration. The purpose of NIST investigations is to improve the safety and structural integrity of buildings in the United States, and the focus is on fact finding. NIST investigative teams are authorized to assess building performance and emergency response and evacuation procedures in the wake of any building failure that has resulted in substantial loss of life or that posed significant potential of substantial loss of life. NIST does not have the statutory authority to make findings of fault nor negligence by individuals or organizations. Further, no part of any report resulting from a NIST investigation into a building failure or from an investigation under the National Construction Safety Team Act may be used in any suit or action for damages arising out of any matter mentioned in such report (15 USC 281a, as amended by Public Law 107-231).

Organization of the Investigation

The National Construction Safety Team for this Investigation, appointed by the then NIST Director, Dr. Arden L. Bement, Jr., was led by Dr. S. Shyam Sunder. Dr. William L. Grosshandler served as Associate Lead Investigator, Mr. Stephen A. Cauffman served as Program Manager for Administration, and Mr. Harold E. Nelson served on the team as a private sector expert. The Investigation included eight interdependent projects whose leaders comprised the remainder of the team. A detailed description of each of these eight projects is available at <http://wtc.nist.gov>. The purpose of each project is summarized in Table P–1, and the key interdependencies among the projects are illustrated in Fig. P–1.

Table P–1. Federal building and fire safety investigation of the WTC disaster.

Technical Area and Project Leader	Project Purpose
Analysis of Building and Fire Codes and Practices; Project Leaders: Dr. H. S. Lew and Mr. Richard W. Bukowski	Document and analyze the code provisions, procedures, and practices used in the design, construction, operation, and maintenance of the structural, passive fire protection, and emergency access and evacuation systems of WTC 1, 2, and 7.
Baseline Structural Performance and Aircraft Impact Damage Analysis; Project Leader: Dr. Fahim H. Sadek	Analyze the baseline performance of WTC 1 and WTC 2 under design, service, and abnormal loads, and aircraft impact damage on the structural, fire protection, and egress systems.
Mechanical and Metallurgical Analysis of Structural Steel; Project Leader: Dr. Frank W. Gayle	Determine and analyze the mechanical and metallurgical properties and quality of steel, weldments, and connections from steel recovered from WTC 1, 2, and 7.
Investigation of Active Fire Protection Systems; Project Leader: Dr. David D. Evans; Dr. William Grosshandler	Investigate the performance of the active fire protection systems in WTC 1, 2, and 7 and their role in fire control, emergency response, and fate of occupants and responders.
Reconstruction of Thermal and Tenability Environment; Project Leader: Dr. Richard G. Gann	Reconstruct the time-evolving temperature, thermal environment, and smoke movement in WTC 1, 2, and 7 for use in evaluating the structural performance of the buildings and behavior and fate of occupants and responders.
Structural Fire Response and Collapse Analysis; Project Leaders: Dr. John L. Gross and Dr. Therese P. McAllister	Analyze the response of the WTC towers to fires with and without aircraft damage, the response of WTC 7 in fires, the performance of composite steel-trussed floor systems, and determine the most probable structural collapse sequence for WTC 1, 2, and 7.
Occupant Behavior, Egress, and Emergency Communications; Project Leader: Mr. Jason D. Averill	Analyze the behavior and fate of occupants and responders, both those who survived and those who did not, and the performance of the evacuation system.
Emergency Response Technologies and Guidelines; Project Leader: Mr. J. Randall Lawson	Document the activities of the emergency responders from the time of the terrorist attacks on WTC 1 and WTC 2 until the collapse of WTC 7, including practices followed and technologies used.

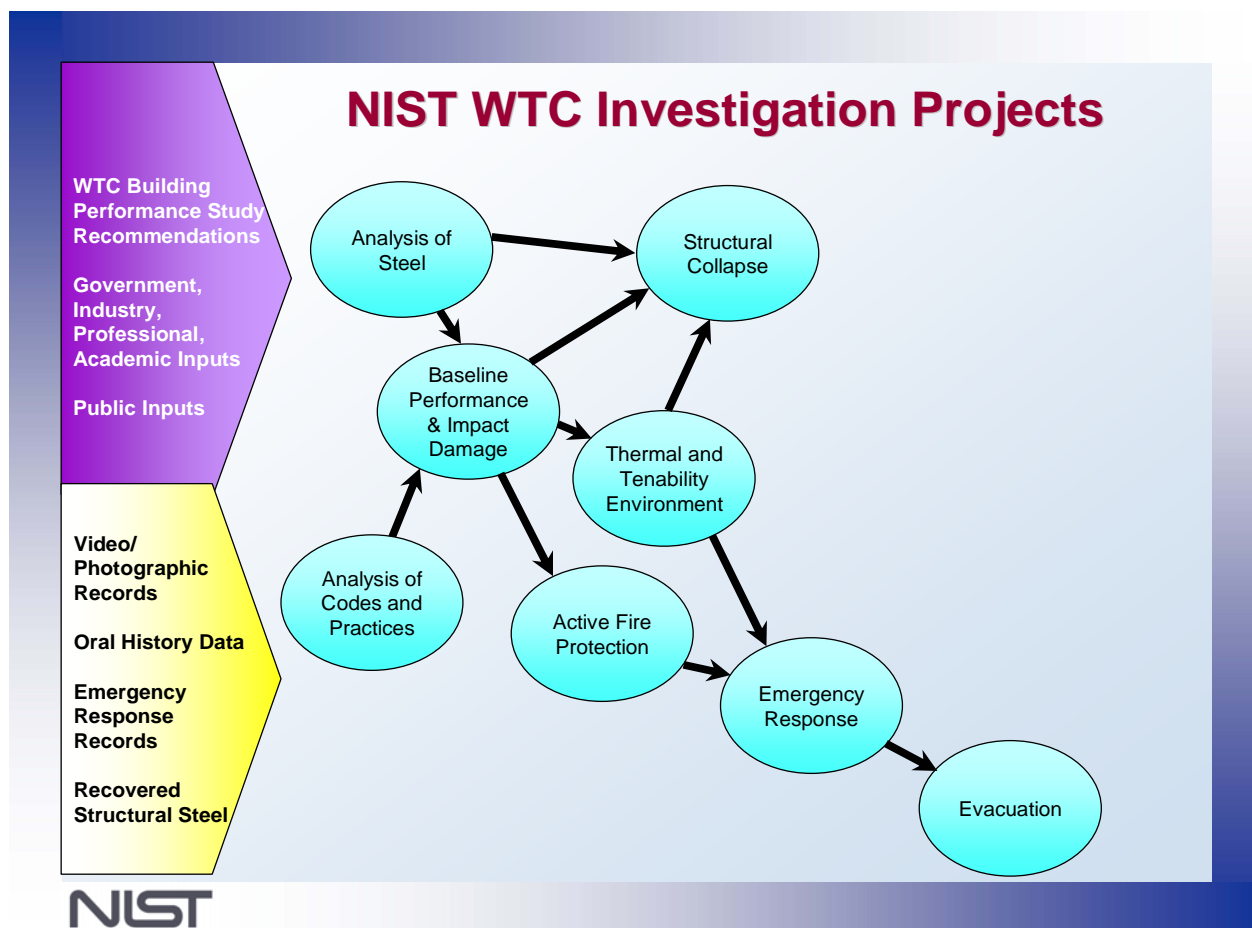


Figure P-1. The eight projects in the federal building and fire safety investigation of the WTC disaster.

National Construction Safety Team Advisory Committee

The NIST Director also established an advisory committee as mandated under the National Construction Safety Team Act. The initial members of the committee were appointed following a public solicitation. These were:

- Paul Fitzgerald, Executive Vice President (retired) FM Global, National Construction Safety Team Advisory Committee Chair
- John Barsom, President, Barsom Consulting, Ltd.
- John Bryan, Professor Emeritus, University of Maryland
- David Collins, President, The Preview Group, Inc.
- Glenn Corbett, Professor, John Jay College of Criminal Justice
- Philip DiNunno, President, Hughes Associates, Inc.

- Robert Hanson, Professor Emeritus, University of Michigan
- Charles Thornton, Co-Chairman and Managing Principal, The Thornton-Tomasetti Group, Inc.
- Kathleen Tierney, Director, Natural Hazards Research and Applications Information Center, University of Colorado at Boulder
- Forman Williams, Director, Center for Energy Research, University of California at San Diego

This National Construction Safety Team Advisory Committee provided technical advice during the Investigation and commentary on drafts of the Investigation reports prior to their public release. NIST has benefited from the work of many people in the preparation of these reports, including the National Construction Safety Team Advisory Committee. The content of the reports and recommendations, however, are solely the responsibility of NIST.

Public Outreach

During the course of this Investigation, NIST held public briefings and meetings (listed in Table P-2) to solicit input from the public, present preliminary findings, and obtain comments on the direction and progress of the Investigation from the public and the Advisory Committee.

NIST maintained a publicly accessible Web site during this Investigation at <http://wtc.nist.gov>. The site contained extensive information on the background and progress of the Investigation.

NIST's WTC Public-Private Response Plan

The collapse of the WTC buildings has led to broad reexamination of how tall buildings are designed, constructed, maintained, and used, especially with regard to major events such as fires, natural disasters, and terrorist attacks. Reflecting the enhanced interest in effecting necessary change, NIST, with support from Congress and the Administration, has put in place a program, the goal of which is to develop and implement the standards, technology, and practices needed for cost-effective improvements to the safety and security of buildings and building occupants, including evacuation, emergency response procedures, and threat mitigation.

The strategy to meet this goal is a three-part NIST-led public-private response program that includes:

- A federal building and fire safety investigation to study the most probable factors that contributed to post-aircraft impact collapse of the WTC towers and the 47-story WTC 7 building, and the associated evacuation and emergency response experience.
- A research and development (R&D) program to (a) facilitate the implementation of recommendations resulting from the WTC Investigation, and (b) provide the technical basis for cost-effective improvements to national building and fire codes, standards, and practices that enhance the safety of buildings, their occupants, and emergency responders.

Table P–2. Public meetings and briefings of the WTC Investigation.

Date	Location	Principal Agenda
June 24, 2002	New York City, NY	Public meeting: Public comments on the <i>Draft Plan</i> for the pending WTC Investigation.
August 21, 2002	Gaithersburg, MD	Media briefing announcing the formal start of the Investigation.
December 9, 2002	Washington, DC	Media briefing on release of the <i>Public Update</i> and NIST request for photographs and videos.
April 8, 2003	New York City, NY	Joint public forum with Columbia University on first-person interviews.
April 29–30, 2003	Gaithersburg, MD	NCST Advisory Committee meeting on plan for and progress on WTC Investigation with a public comment session.
May 7, 2003	New York City, NY	Media briefing on release of <i>May 2003 Progress Report</i> .
August 26–27, 2003	Gaithersburg, MD	NCST Advisory Committee meeting on status of the WTC investigation with a public comment session.
September 17, 2003	New York City, NY	Media and public briefing on initiation of first-person data collection projects.
December 2–3, 2003	Gaithersburg, MD	NCST Advisory Committee meeting on status and initial results and release of the <i>Public Update</i> with a public comment session.
February 12, 2004	New York City, NY	Public meeting on progress and preliminary findings with public comments on issues to be considered in formulating final recommendations.
June 18, 2004	New York City, NY	Media/public briefing on release of <i>June 2004 Progress Report</i> .
June 22–23, 2004	Gaithersburg, MD	NCST Advisory Committee meeting on the status of and preliminary findings from the WTC Investigation with a public comment session.
August 24, 2004	Northbrook, IL	Public viewing of standard fire resistance test of WTC floor system at Underwriters Laboratories, Inc.
October 19–20, 2004	Gaithersburg, MD	NCST Advisory Committee meeting on status and near complete set of preliminary findings with a public comment session.
November 22, 2004	Gaithersburg, MD	NCST Advisory Committee discussion on draft annual report to Congress, a public comment session, and a closed session to discuss pre-draft recommendations for WTC Investigation.
April 5, 2005	New York City, NY	Media and public briefing on release of the probable collapse sequence for the WTC towers and draft reports for the projects on codes and practices, evacuation, and emergency response.
June 23, 2005	New York City, NY	Media and public briefing on release of all draft reports for the WTC towers and draft recommendations for public comment.
September 12–13, 2005	Gaithersburg, MD	NCST Advisory Committee meeting on disposition of public comments and update to draft reports for the WTC towers.
September 13–15, 2005	Gaithersburg, MD	WTC Technical Conference for stakeholders and technical community for dissemination of findings and recommendations and opportunity for public to make technical comments.

- A dissemination and technical assistance program (DTAP) to (a) engage leaders of the construction and building community in ensuring timely adoption and widespread use of proposed changes to practices, standards, and codes resulting from the WTC Investigation and the R&D program, and (b) provide practical guidance and tools to better prepare facility owners, contractors, architects, engineers, emergency responders, and regulatory authorities to respond to future disasters.

The desired outcomes are to make buildings, occupants, and first responders safer in future disaster events.

National Construction Safety Team Reports on the WTC Investigation

A final report on the collapse of the WTC towers is being issued as NIST NCSTAR 1. A companion report on the collapse of WTC 7 is being issued as NIST NCSTAR 1A. The present report is one of a set that provides more detailed documentation of the Investigation findings and the means by which these technical results were achieved. As such, it is part of the archival record of this Investigation. The titles of the full set of Investigation publications are:

NIST (National Institute of Standards and Technology). 2005. *Federal Building and Fire Safety Investigation of the World Trade Center Disaster: Final Report on the Collapse of the World Trade Center Towers*. NIST NCSTAR 1. Gaithersburg, MD, September.

NIST (National Institute of Standards and Technology). 2006. *Federal Building and Fire Safety Investigation of the World Trade Center Disaster: Final Report on the Collapse of World Trade Center 7*. NIST NCSTAR 1A. Gaithersburg, MD.

Lew, H. S., R. W. Bukowski, and N. J. Carino. 2005. *Federal Building and Fire Safety Investigation of the World Trade Center Disaster: Design, Construction, and Maintenance of Structural and Life Safety Systems*. NIST NCSTAR 1-1. National Institute of Standards and Technology. Gaithersburg, MD, September.

Fanella, D. A., A. T. Derecho, and S. K. Ghosh. 2005. *Federal Building and Fire Safety Investigation of the World Trade Center Disaster: Design and Construction of Structural Systems*. NIST NCSTAR 1-1A. National Institute of Standards and Technology. Gaithersburg, MD, September.

Ghosh, S. K., and X. Liang. 2005. *Federal Building and Fire Safety Investigation of the World Trade Center Disaster: Comparison of Building Code Structural Requirements*. NIST NCSTAR 1-1B. National Institute of Standards and Technology. Gaithersburg, MD, September.

Fanella, D. A., A. T. Derecho, and S. K. Ghosh. 2005. *Federal Building and Fire Safety Investigation of the World Trade Center Disaster: Maintenance and Modifications to Structural Systems*. NIST NCSTAR 1-1C. National Institute of Standards and Technology. Gaithersburg, MD, September.

Grill, R. A., and D. A. Johnson. 2005. *Federal Building and Fire Safety Investigation of the World Trade Center Disaster: Fire Protection and Life Safety Provisions Applied to the Design and Construction of World Trade Center 1, 2, and 7 and Post-Construction Provisions Applied after Occupancy*. NIST NCSTAR 1-1D. National Institute of Standards and Technology. Gaithersburg, MD, September.

Razza, J. C., and R. A. Grill. 2005. *Federal Building and Fire Safety Investigation of the World Trade Center Disaster: Comparison of Codes, Standards, and Practices in Use at the Time of the Design and Construction of World Trade Center 1, 2, and 7*. NIST NCSTAR 1-1E. National Institute of Standards and Technology. Gaithersburg, MD, September.

Grill, R. A., D. A. Johnson, and D. A. Fanella. 2005. *Federal Building and Fire Safety Investigation of the World Trade Center Disaster: Comparison of the 1968 and Current (2003) New*

- York City Building Code Provisions*. NIST NCSTAR 1-1F. National Institute of Standards and Technology. Gaithersburg, MD, September.
- Grill, R. A., and D. A. Johnson. 2005. *Federal Building and Fire Safety Investigation of the World Trade Center Disaster: Amendments to the Fire Protection and Life Safety Provisions of the New York City Building Code by Local Laws Adopted While World Trade Center 1, 2, and 7 Were in Use*. NIST NCSTAR 1-1G. National Institute of Standards and Technology. Gaithersburg, MD, September.
- Grill, R. A., and D. A. Johnson. 2005. *Federal Building and Fire Safety Investigation of the World Trade Center Disaster: Post-Construction Modifications to Fire Protection and Life Safety Systems of World Trade Center 1 and 2*. NIST NCSTAR 1-1H. National Institute of Standards and Technology. Gaithersburg, MD, September.
- Grill, R. A., D. A. Johnson, and D. A. Fanella. 2005. *Federal Building and Fire Safety Investigation of the World Trade Center Disaster: Post-Construction Modifications to Fire Protection, Life Safety, and Structural Systems of World Trade Center 7*. NIST NCSTAR 1-1I. National Institute of Standards and Technology. Gaithersburg, MD, September.
- Grill, R. A., and D. A. Johnson. 2005. *Federal Building and Fire Safety Investigation of the World Trade Center Disaster: Design, Installation, and Operation of Fuel System for Emergency Power in World Trade Center 7*. NIST NCSTAR 1-1J. National Institute of Standards and Technology. Gaithersburg, MD, September.
- Sadek, F. 2005. *Federal Building and Fire Safety Investigation of the World Trade Center Disaster: Baseline Structural Performance and Aircraft Impact Damage Analysis of the World Trade Center Towers*. NIST NCSTAR 1-2. National Institute of Standards and Technology. Gaithersburg, MD, September.
- Faschan, W. J., and R. B. Garlock. 2005. *Federal Building and Fire Safety Investigation of the World Trade Center Disaster: Reference Structural Models and Baseline Performance Analysis of the World Trade Center Towers*. NIST NCSTAR 1-2A. National Institute of Standards and Technology. Gaithersburg, MD, September.
- Kirkpatrick, S. W., R. T. Bocchieri, F. Sadek, R. A. MacNeill, S. Holmes, B. D. Peterson, R. W. Cilke, C. Navarro. 2005. *Federal Building and Fire Safety Investigation of the World Trade Center Disaster: Analysis of Aircraft Impacts into the World Trade Center Towers*, NIST NCSTAR 1-2B. National Institute of Standards and Technology. Gaithersburg, MD, September.
- Gayle, F. W., R. J. Fields, W. E. Luecke, S. W. Banovic, T. Foecke, C. N. McCowan, T. A. Siewert, and J. D. McColskey. 2005. *Federal Building and Fire Safety Investigation of the World Trade Center Disaster: Mechanical and Metallurgical Analysis of Structural Steel*. NIST NCSTAR 1-3. National Institute of Standards and Technology. Gaithersburg, MD, September.
- Luecke, W. E., T. A. Siewert, and F. W. Gayle. 2005. *Federal Building and Fire Safety Investigation of the World Trade Center Disaster: Contemporaneous Structural Steel Specifications*. NIST Special Publication 1-3A. National Institute of Standards and Technology. Gaithersburg, MD, September.

Banovic, S. W. 2005. *Federal Building and Fire Safety Investigation of the World Trade Center Disaster: Steel Inventory and Identification*. NIST NCSTAR 1-3B. National Institute of Standards and Technology. Gaithersburg, MD, September.

Banovic, S. W., and T. Foecke. 2005. *Federal Building and Fire Safety Investigation of the World Trade Center Disaster: Damage and Failure Modes of Structural Steel Components*. NIST NCSTAR 1-3C. National Institute of Standards and Technology. Gaithersburg, MD, September.

Luecke, W. E., J. D. McColskey, C. N. McCowan, S. W. Banovic, R. J. Fields, T. Foecke, T. A. Siewert, and F. W. Gayle. 2005. *Federal Building and Fire Safety Investigation of the World Trade Center Disaster: Mechanical Properties of Structural Steels*. NIST NCSTAR 1-3D. National Institute of Standards and Technology. Gaithersburg, MD, September.

Banovic, S. W., C. N. McCowan, and W. E. Luecke. 2005. *Federal Building and Fire Safety Investigation of the World Trade Center Disaster: Physical Properties of Structural Steels*. NIST NCSTAR 1-3E. National Institute of Standards and Technology. Gaithersburg, MD, September.

Evans, D. D., R. D. Peacock, E. D. Kuligowski, W. S. Dols, and W. L. Grosshandler. 2005. *Federal Building and Fire Safety Investigation of the World Trade Center Disaster: Active Fire Protection Systems*. NIST NCSTAR 1-4. National Institute of Standards and Technology. Gaithersburg, MD, September.

Kuligowski, E. D., D. D. Evans, and R. D. Peacock. 2005. *Federal Building and Fire Safety Investigation of the World Trade Center Disaster: Post-Construction Fires Prior to September 11, 2001*. NIST NCSTAR 1-4A. National Institute of Standards and Technology. Gaithersburg, MD, September.

Hopkins, M., J. Schoenrock, and E. Budnick. 2005. *Federal Building and Fire Safety Investigation of the World Trade Center Disaster: Fire Suppression Systems*. NIST NCSTAR 1-4B. National Institute of Standards and Technology. Gaithersburg, MD, September.

Keough, R. J., and R. A. Grill. 2005. *Federal Building and Fire Safety Investigation of the World Trade Center Disaster: Fire Alarm Systems*. NIST NCSTAR 1-4C. National Institute of Standards and Technology. Gaithersburg, MD, September.

Ferreira, M. J., and S. M. Strege. 2005. *Federal Building and Fire Safety Investigation of the World Trade Center Disaster: Smoke Management Systems*. NIST NCSTAR 1-4D. National Institute of Standards and Technology. Gaithersburg, MD, September.

Gann, R. G., A. Hamins, K. B. McGrattan, G. W. Mulholland, H. E. Nelson, T. J. Ohlemiller, W. M. Pitts, and K. R. Prasad. 2005. *Federal Building and Fire Safety Investigation of the World Trade Center Disaster: Reconstruction of the Fires in the World Trade Center Towers*. NIST NCSTAR 1-5. National Institute of Standards and Technology. Gaithersburg, MD, September.

Pitts, W. M., K. M. Butler, and V. Junker. 2005. *Federal Building and Fire Safety Investigation of the World Trade Center Disaster: Visual Evidence, Damage Estimates, and Timeline Analysis*. NIST NCSTAR 1-5A. National Institute of Standards and Technology. Gaithersburg, MD, September.

- Hamins, A., A. Maranghides, K. B. McGrattan, E. Johnsson, T. J. Ohlemiller, M. Donnelly, J. Yang, G. Mulholland, K. R. Prasad, S. Kukuck, R. Anleitner and T. McAllister. 2005. *Federal Building and Fire Safety Investigation of the World Trade Center Disaster: Experiments and Modeling of Structural Steel Elements Exposed to Fire*. NIST NCSTAR 1-5B. National Institute of Standards and Technology. Gaithersburg, MD, September.
- Ohlemiller, T. J., G. W. Mulholland, A. Maranghides, J. J. Filliben, and R. G. Gann. 2005. *Federal Building and Fire Safety Investigation of the World Trade Center Disaster: Fire Tests of Single Office Workstations*. NIST NCSTAR 1-5C. National Institute of Standards and Technology. Gaithersburg, MD, September.
- Gann, R. G., M. A. Riley, J. M. Repp, A. S. Whittaker, A. M. Reinhorn, and P. A. Hough. 2005. *Federal Building and Fire Safety Investigation of the World Trade Center Disaster: Reaction of Ceiling Tile Systems to Shocks*. NIST NCSTAR 1-5D. National Institute of Standards and Technology. Gaithersburg, MD, September.
- Hamins, A., A. Maranghides, K. B. McGrattan, T. J. Ohlemiller, and R. Anleitner. 2005. *Federal Building and Fire Safety Investigation of the World Trade Center Disaster: Experiments and Modeling of Multiple Workstations Burning in a Compartment*. NIST NCSTAR 1-5E. National Institute of Standards and Technology. Gaithersburg, MD, September.
- McGrattan, K. B., C. Bouldin, and G. Forney. 2005. *Federal Building and Fire Safety Investigation of the World Trade Center Disaster: Computer Simulation of the Fires in the World Trade Center Towers*. NIST NCSTAR 1-5F. National Institute of Standards and Technology. Gaithersburg, MD, September.
- Prasad, K. R., and H. R. Baum. 2005. *Federal Building and Fire Safety Investigation of the World Trade Center Disaster: Fire Structure Interface and Thermal Response of the World Trade Center Towers*. NIST NCSTAR 1-5G. National Institute of Standards and Technology. Gaithersburg, MD, September.
- Gross, J. L., and T. McAllister. 2005. *Federal Building and Fire Safety Investigation of the World Trade Center Disaster: Structural Fire Response and Probable Collapse Sequence of the World Trade Center Towers*. NIST NCSTAR 1-6. National Institute of Standards and Technology. Gaithersburg, MD, September.
- Carino, N. J., M. A. Starnes, J. L. Gross, J. C. Yang, S. Kukuck, K. R. Prasad, and R. W. Bukowski. 2005. *Federal Building and Fire Safety Investigation of the World Trade Center Disaster: Passive Fire Protection*. NIST NCSTAR 1-6A. National Institute of Standards and Technology. Gaithersburg, MD, September.
- Gross, J., F. Hervey, M. Izydorek, J. Mammoser, and J. Treadway. 2005. *Federal Building and Fire Safety Investigation of the World Trade Center Disaster: Fire Resistance Tests of Floor Truss Systems*. NIST NCSTAR 1-6B. National Institute of Standards and Technology. Gaithersburg, MD, September.
- Zarghamee, M. S., S. Bolourchi, D. W. Eggers, Ö. O. Erbay, F. W. Kan, Y. Kitane, A. A. Liepins, M. Mudlock, W. I. Naguib, R. P. Ojdrovic, A. T. Sarawit, P. R. Barrett, J. L. Gross, and

T. P. McAllister. 2005. *Federal Building and Fire Safety Investigation of the World Trade Center Disaster: Component, Connection, and Subsystem Structural Analysis*. NIST NCSTAR 1-6C. National Institute of Standards and Technology. Gaithersburg, MD, September.

Zarghamee, M. S., Y. Kitane, Ö. O. Erbay, T. P. McAllister, and J. L. Gross. 2005. *Federal Building and Fire Safety Investigation of the World Trade Center Disaster: Global Structural Analysis of the Response of the World Trade Center Towers to Impact Damage and Fire*. NIST NCSTAR 1-6D. National Institute of Standards and Technology. Gaithersburg, MD, September.

McAllister, T., R. W. Bukowski, R. G. Gann, J. L. Gross, K. B. McGrattan, H. E. Nelson, L. Phan, W. M. Pitts, K. R. Prasad, F. Sadek. 2006. *Federal Building and Fire Safety Investigation of the World Trade Center Disaster: Structural Fire Response and Probable Collapse Sequence of World Trade Center 7*. (Provisional). NIST NCSTAR 1-6E. National Institute of Standards and Technology. Gaithersburg, MD.

Gilsanz, R., V. Arbitrio, C. Anders, D. Chlebus, K. Ezzeldin, W. Guo, P. Moloney, A. Montalva, J. Oh, K. Rubenacker. 2006. *Federal Building and Fire Safety Investigation of the World Trade Center Disaster: Structural Analysis of the Response of World Trade Center 7 to Debris Damage and Fire*. (Provisional). NIST NCSTAR 1-6F. National Institute of Standards and Technology. Gaithersburg, MD.

Kim, W. 2006. *Federal Building and Fire Safety Investigation of the World Trade Center Disaster: Analysis of September 11, 2001, Seismogram Data*. (Provisional). NIST NCSTAR 1-6G. National Institute of Standards and Technology. Gaithersburg, MD.

Nelson, K. 2006. *Federal Building and Fire Safety Investigation of the World Trade Center Disaster: The Con Ed Substation in World Trade Center 7*. (Provisional). NIST NCSTAR 1-6H. National Institute of Standards and Technology. Gaithersburg, MD.

Averill, J. D., D. S. Mileti, R. D. Peacock, E. D. Kuligowski, N. Groner, G. Proulx, P. A. Reneke, and H. E. Nelson. 2005. *Federal Building and Fire Safety Investigation of the World Trade Center Disaster: Occupant Behavior, Egress, and Emergency Communication*. NIST NCSTAR 1-7. National Institute of Standards and Technology. Gaithersburg, MD, September.

Fahy, R., and G. Proulx. 2005. *Federal Building and Fire Safety Investigation of the World Trade Center Disaster: Analysis of Published Accounts of the World Trade Center Evacuation*. NIST NCSTAR 1-7A. National Institute of Standards and Technology. Gaithersburg, MD, September.

Zmud, J. 2005. *Federal Building and Fire Safety Investigation of the World Trade Center Disaster: Technical Documentation for Survey Administration*. NIST NCSTAR 1-7B. National Institute of Standards and Technology. Gaithersburg, MD, September.

Lawson, J. R., and R. L. Vettori. 2005. *Federal Building and Fire Safety Investigation of the World Trade Center Disaster: The Emergency Response Operations*. NIST NCSTAR 1-8. National Institute of Standards and Technology. Gaithersburg, MD, September.

ACKNOWLEDGMENTS

A large number of the National Institute Standards and Technology (NIST) staff performed tests and analyses that were at the heart of this report: Howard Baum, Lori Brassell, Kathy Butler, Dale Bentz, Charles Bouldin, Nick Carino, Laurean DeLauter, Michelle Donnelly, Glenn Forney, Erik Johnsson, Jack Lee, Alexander Maranghides, Therese McAllister, Jay McElroy, Roy McLane, Ronald Rehm, Michael Riley, Michael Selepak, David Stroup, Jiann Yang, Robert Zarr.

They were supported by a set of students: Mohsen Altafi, Jonathan Demarest, Joshua Novosel, Victor Ontiveros, Lisa Petersen, Rochelle Plummer, Schuyler Ruitberg, Jose Sanchez, Steven Sekellick, Laura Sugden, Brendan Williams.

James Filliben of the NIST Information Technology Laboratory guided and interpreted the results of the designed experiments and computations.

The efforts of Valentine Junker, a NIST Visual Media Consultant, were particularly valuable in obtaining photographic and videographic evidence.

Nancy Seliga, Gerry Gaeta, and Jeffrey Gertier, Building Managers from the Port Authority of New York and New Jersey, provided valuable information about the interiors of the World Trade Center (WTC) towers.

The staff of Marsh & McLennan provided detailed floor plans of their space in WTC 1, along with detailed descriptions of the office furnishings.

Representatives of Boeing, United Airlines, and American Airlines provided information on the combustible contents of the aircraft.

Paul Hough, Stephen Newcomer, Barry Buhay, and Tom Fritz, all of Armstrong World Industries, provided information regarding the ceiling system materials and construction and assisted with the test program.

Andrew Whitaker, Andrei Reinhorn, and Joshua Repp, all of the State University of New York at Buffalo, conducted the shake tests of the ceiling tile systems.

This page intentionally left blank.

EXECUTIVE SUMMARY

E.1 INTRODUCTION

The collapses of the World Trade Center (WTC) towers on September 11, 2001, resulted from a combination of aircraft impact damage and the ensuing fires. A prime focus of the National Institute of Standards and Technology (NIST) Investigation was to learn the relative importance of these two factors and their interaction leading to the collapses of the buildings. This entailed such facets as:

- What were the location, magnitude, and duration of the fires that brought about the collapses of the WTC towers?
- Were the natures of these fires typical of what might be expected in common occupancies, or were there special features that made these fires especially dangerous?
- Could an extreme but conventional fire, occurring without the aircraft impact, have led to the collapse of a WTC tower?

This effort began with the objective to reconstruct, with assessed uncertainty limits, the time-evolving temperature, thermal radiation, and smoke fields in WTC 1, 2, and 7 for use in understanding the behavior and fate of occupants and responders and the structural performance of the buildings. Operationally, this was divided into eight technical tasks:

- Acquisition and application of photographs, videos, and other relevant information to develop detailed time lines for the spread and growth of fires at the peripheries of the WTC buildings.
- Characterization of the types, mass, and distribution of combustibles in the pertinent floors of the WTC buildings at the time of the disaster.
- Location and characterization of the fire endurance properties of the internal partitions (floors, walls, and ceilings) in the pertinent floors of the WTC buildings.
- Determination of the effective thermal properties of the structural insulation systems, the effect of vibration, impact, and shock on their thermal insulation performance, and whether chemical interaction between the insulation materials and the steel at elevated temperatures could degrade the steel and insulation performance during thermal insult.
- Upgrade of the NIST Fire Dynamics Simulator (FDS) for its application to the reconstruction of the fires in the WTC buildings. Development of a computational methodology for mapping the FDS-generated thermal environment onto and through the buildings' structural elements.
- Conduct of experiments to provide input to and guidance for the FDS combustion sub-model.

- Reconstruction of the gaseous thermal environment surrounding the buildings' structural elements and the resulting temperature rise within them.
- Generation and use of experimental data for assessing the accuracy of the prediction of thermal insult on structural members such as columns, trusses, beams, and other support structures like those in WTC 1, 2, and 7.

This document reports the likely nature of the fires in WTC 1 and WTC 2 and how NIST was able to reconstruct them. The outcome of the fire reconstructions became a principal input to the assessment of the collapse of the buildings. A reconstruction of the fires in WTC 7 is presented in a separate report.

E.2 PHOTOGRAPHIC EVIDENCE

The destruction of the WTC towers on September 11, 2001, may have been the most heavily photographed disaster in history. This was valuable to this Investigation, since neither of the buildings remained, eliminating access to the telltale signs that fire investigators typically use to assess the path and intensity of a fire. There was a good amount of photographic material shot during the early stage, when only WTC 1 was damaged. By the time WTC 2 was struck, the number of cameras and the diversity of locations had increased. Following the collapse of WTC 2, the amount of visual material decreased markedly as people rushed to escape the area and the huge dust clouds generated by the collapse obscured the site.

NIST assembled a collection of nearly 150 segments of video footage (totaling in excess of 300 hours) and over 7,000 photographs. The sources included television networks and stations, the New York City Police Department (NYPD), the Fire Department (FDNY) of the City of New York, and assorted World Wide Web sites. The collection included the work of over 200 photographers and 40 videographers. The material was organized into a database in which the searchable properties included the name and location of the photographer, time of shot/video, copyright status, content, whether it included the key events, whether it included FDNY or NYPD people or apparatus, and other details (falling debris, people, building damage).

To construct a time line for fire growth and structural changes in the WTC buildings, times of known accuracy were assigned to the photographic assets. The touchstone was the moment the second plane struck WTC 2, which NIST established from the clocks in the September 11 telecasts as 9:02:59 a.m. Absolute times were then assigned to all frames of videos that showed the second plane strike. By matching photographs and other videos to specific events in these initially assigned videos, NIST staff created a time line extending over the entire day with assigned relative accuracies of ± 3 s or better. The resulting timing of the five major events of September 11 is shown in Table E-1 below.

In each photograph and each video frame, each window was coded by whether fire and/or smoke were present and whether the window was still in place or not. Graphical rendering of these results, combined with timed sequencing of the actual photographic frames, led to the construction of highly detailed time lines for the spread of the fires and changes in visible damage to the buildings.

Table E–1. Times for major September 11, 2001, events.

Event	Time
First aircraft strike	8:46:30 a.m.
Second aircraft strike	9:02:59 a.m.
Collapse of WTC 2	9:58:59 a.m.
Collapse of WTC 1	10:28:22 a.m.
Collapse of WTC 7	5:20:52 p.m.

E.3 BUILDING INTERIORS AND COMBUSTIBLES

NIST obtained architectural plans for most of the floors in the impact and fire zones of WTC 1 and WTC 2. These included the locations of interior walls, descriptions of the floor and ceiling construction, and additional features such as the locations of staircases within the tenant spaces.

Since the ceiling system could have served as a temporary protective barrier to heating of the floor structure above, shaking table experiments were conducted to determine the magnitude of building impact that could have led to significant dislodging of ceiling tiles. Forces of the order of 5g caused significant damage to the framing. Since the aircraft impact forces were estimated to have been about 100g, NIST assumed there was not enough of the ceiling system in place to provide significant thermal protection.

The most common floor plan was a continuous open space populated by a large array of workstations or cubicles. Although there were a variety of styles of such units, the cubicles were fundamentally similar. Each cubicle typically was bounded by privacy panels, with a single entrance opening. Within the area defined by the panels was a desktop, file storage, bookshelves, carpeting, chair, etc. In addition, there were a variety of amounts and locations of paper, both on the work surfaces and within the file cabinets and bookshelves. These cubicles were grouped in clusters or rows, with up to 215 units on a given floor.

NIST conducted fire tests of single representative workstations, both to obtain flammability data and to provide input for a combustion algorithm for FDS. The tests included the effects of the presence of jet fuel and of fallen inert material representative of ceiling tiles or wall fragments. The results were:

- A workstation generated a total heat release of approximately 3.9 GJ from a mass loss of approximately 200 kg. These values were insensitive to the addition of jet fuel or inert material. Approximately 75 percent of the heat release and mass loss occurred over a period of approximately 20 min. The peak heat release rate (HRR) was approximately 7 MW.
- The inert material reduced the peak HRR approximately in proportion to its coverage of the burning surfaces.
- The jet fuel sharply shortened the time to involvement of all accessible combustible surfaces and, thus, the time to the peak HRR.

From the floor plans and the combustibility data, it was estimated that the combustible fuel load in the WTC tenant spaces was approximately 20 kg/m² (4 lb/ft²). The two aircraft introduced significant increments to this fuel loading along the paths of their entry into the buildings. United Airlines,

American Airlines, and Boeing (the manufacturer of the two hijacked aircraft) provided information on the combustibles that the aircraft brought into the respective buildings.

Insulation against damaging temperature rise in the structural elements was accomplished using a combination of sprayed fire-resistive materials (SFRMs) and gypsum wallboard. NIST measured the cohesive strength of the dominant SFRM and its adhesive strength to steel substrates with and without primer. NIST also obtained samples of the two types of sprayed insulation and four types of gypsum wallboard and sent them to testing laboratories for determination of their thermal conductivity, density, and heat capacity, all as a function of temperature from ambient. The sprayed material data were for 25 °C to 1,200 °C; the wallboard data were from 25 °C to 600 °C.

The thermal protection afforded by SFRMs is typically obtained under steady and uniform heating conditions in a test furnace such as that prescribed in the ASTM E 119 standard for fire resistance ratings. Actual fires can reach high irradiances faster, are generally not isotropic, and may wane and re-grow before running out of fuel or being extinguished. NIST conducted a series of experiments in the NIST Large-scale Fire Laboratory to obtain data on SFRM performance under realistic fire conditions. Within a large test compartment, an assortment of representative steel members was exposed to controlled fires from steady-state gas burner fires of different heat release rate and radiative intensity. The steel members were bare or coated with SFRM in two thicknesses. The thermal profile of the fire was measured at multiple locations within the compartment. Temperatures were also recorded at multiple locations on the surfaces of the steel, the insulation, and the compartment. The results were then used to guide the fire modeling effort.

E.4 FIRE MODELING

The required output of the simulations of the fires in the WTC towers was a set of three-dimensional, time varying renditions of the thermal and radiative environment to which the structural members in the tower were subjected from the time of aircraft impact until their collapses. These profiles were generated using the NIST FDS, a computational fluid dynamics model of fire-driven fluid flow with which NIST had extensive experience. FDS represents the space(s) in which the fire and its effluent are to be modeled as a grid of rectangular cells. The fire generates hot gas, which radiatively and convectively heats the surfaces of walls and combustibles. The rate at which each combustible generates combustible vapor depends on this heat flux to the surface and the fuel's effective heat of gasification. To create burning, FDS assumes that combustion occurs at the interface of two (adjacent) grid cells, when the first cell contains more air than is needed to combust the vaporized fuel within that cell and the second cell contains less air than is needed to combust the fuel within (the second) cell.

FDS predictions of the thermal environment in the steel exposure tests were generally within experimental uncertainty:

- The predicted upper layer gas temperatures were within 4 percent of the measurements.
- There was good agreement with measured gas velocities at the compartment inlets.
- Because of limited spatial resolution at the outlet window, the steep gradient in velocity was not captured by the model, but the integrated mass flux was.

- FDS predicted the leaning of the fire plume caused by asymmetric obstructions in the compartment, but underestimated the extent of the leaning. This adversely impacted predictions of the thermal behavior of structural components at some locations near the fire.
- The predictions of radiative heat fluxes in the upper layer were within 10 percent of the measurements.
- FDS predictions of the heat flux to the floor and column surfaces facing the fire were good; but were less so for the surfaces facing away due to the underprediction of the flame leaning.

In these experiments, the “fire” was a steady heat source whose combustion properties were steady and well known. The comparison between experiment and calculation was thus a test of the fluid mechanics and heat transfer capability in FDS. The good agreement indicated that no changes were needed in these aspects of FDS.

Capturing the behavior of the single workstation fires involved the additional features of a complex burning object. Data on the combustion of the combustible components of the workstation were obtained using a Cone Calorimeter (ASTM E 1354), with the test specimens exposed to varying incident heat fluxes and piloted ignition of the vapors. Predictions of the workstation combustion using these data were not satisfactory because (a) there were some features of the combustion that would be difficult for a simulation of current capability to capture (e.g., complex burning of the chair, ash formation from stacks of exposed paper, falling items that led to changes in the geometry of combustibles) and (b) some of the workstation components ignited from irradiance alone.

Thus, a modified combustion approach was implemented. The carpet, desk, and privacy panel data from the Cone Calorimeter were used as originally planned. The remaining components were represented as homogeneous “boxes,” which were assigned a burning rate. The prediction quality was much improved:

- The magnitudes of the peak HRR values were within 10 percent of the experimental values.
- The shape and magnitude of the subsequent, near-steady burning behavior were quite similar.
- The overall burning times were similar for the experiments and the simulations.
- The effects of the tiles in decreasing the peak HRR and the jet fuel in increasing the peak HRR and on the subsequent burning behavior were captured correctly.

However, the peak HRR in the simulations without jet fuel occurred sooner than in the experiments, a result of lumping the chair together with various other combustible items. In addition, the simulations underpredicted the large reduction in the time to the peak HRR for the addition of jet fuel.

Nonetheless, the chosen set of parameters and approximated component burning descriptions gave a reasonable description of the actual workstation HRR behavior and its dependence on the inert material coverage and presence of jet fuel. The localized differences between the simulations and experiments would become less important when several (or more) workstations were burning concurrently, as was the case in the large fires on September 11.

A third set of fire tests was then conducted to assess the accuracy with which FDS predicted the fire spread, heat release rate, and thermal environment in a large compartment in which three workstations were burning in a compartment configuration characteristic of that found in the WTC buildings. Again the effects of the presence of inert material and jet fuel were included, as was the effect of different degrees of “rubbleizing” the furniture. In these tests:

- The total mass loss was triple the mass loss from the single workstation tests.
- The peak HRR values were only about 50 percent higher than the single workstation burns, reflecting the ventilation-limited nature of the three-workstation tests. This is consistent with the HRR peaks being independent of the location of the fire in the compartment.

FDS simulation of each test was carried out before the test was conducted. The quality of the simulations was deemed satisfactory:

- The shapes and magnitudes of the predicted and measured HRR curves were close.
- The predicted times to the peak HRR region were within about a minute of the measured rise times. FDS captured the significant decrease in time to the peak HRR region due to the jet fuel.
- The predicted peak HRR values were within experimental uncertainty of the measured values.
- FDS consistently overpredicted the HRR in the region following the HRR peak. Repeating the simulations with an increased heat of gasification of the “box” combustibles greatly improved the fit, but at the expense of underpredicting the peak intensity. As a result, the decision was made to use the higher heat of gasification value in further simulations.
- The prediction of the HRR of the rubbleized furniture required only one adjusted parameter: since the mass loss was half that of the assembled workstations, the burning rate for the simulation was reduced by the same factor. Thus, this factor was used in the reconstruction of the WTC fires in the regions where highly damaged furnishings were expected.

In an assessment of the model, it is important to maintain perspective on the accuracy required to reconstruct the actual WTC fires. For fires that were sufficiently severe that they threatened the structural integrity of the building, many workstations burned concurrently. These workstations were at various stages of their combustion, and the aggregate burning of a large group of workstations would average out features that are not precisely modeled, which should improve model accuracy.

E.5 HEAT TRANSFER MODELING

Simulating the effect of a fire on structural integrity requires a means for transferring the heat generated by the FDS-simulated fire to the surface of the structural members and then conducting the heat through the (insulated) columns, trusses, and other elements that made up the tower structure. This process was made difficult for these large, geometrically complex buildings by the wide disparity in length and time scales that had to be taken into account in the simulations.

To overcome these difficulties, NIST developed the Fire Structure Interface (FSI). To use the FSI with a set of FDS-calculated gas phase temperatures:

- The compartment was divided into a hot, soot-laden upper layer and a cool, clear lower layer.
- Explicit formulae for the radiative heat flux were obtained as a function of temperature, hot layer depth, soot concentration, and orientation of each structural element.
- Structural components in the hot layer were also subject to convective fluxes based on the difference between their surface temperature and the local hot layer temperature.
- The thermophysical properties of the steel in the structural elements and of the SFRM were obtained from published data and new data developed under the Investigation.
- The resulting data set was subsequently read into the ANSYS 8.0 finite element program, which generated the thermal distribution within the structural elements.

The “transparency” of FSI was estimated by comparison of FDS-FSI predictions of steel and SFRM surface temperatures with those obtained in the steel element exposure tests. The FSI appeared to add little to the overall uncertainty in the simulation of the temperatures at the outer surfaces of bare steel elements and the surfaces of SFRM and, more importantly, at the SFRM-steel interface. On the average, the numerical predictions of the steel surface temperature were within 7 percent of the experimental measurements for bare steel elements and within 17 percent for the insulated steel elements. The former was determined to result from uncertainty in the heat release rate in the fire model. The increase in the latter was attributed to model sensitivity to the SFRM coating thickness and thermal conductivity.

E.6 RECONSTRUCTED FIRES

The simulations of the fires and of their heating of the building structure were the second and third computational steps, respectively, in the identification of the probable sequences leading to the collapses of the towers. They followed the simulation of the aircraft impacts and preceded the analysis of the behavior of the damaged and heated building structures.

After a number of simulations to gain insight into the factors having the most influence on the nature of the fires, for each tower, two fire scenarios (Case A and Case B for WTC 1 and Case C and Case D for WTC 2) were superimposed on two aircraft-driven damage patterns. For each of the four scenarios, FDS was used to generate a time-dependent gas temperature and radiation environment on each of the floors. The following apply to all the Cases:

- Eight floors were modeled in WTC 1 (92 through 99) and six floors were modeled in WTC 2 (78 through 83). Each floor was modeled separately, since examination of the photographic collection indicated little evidence for floor-to-floor fire spread in the times that the towers survived. Heat conduction through the floors was included.

- Detailed floor plans were available for the eight modeled floors in WTC 1 and the 80th floor of WTC 2. For the remaining floors in WTC 2, the layouts were estimated from the architectural drawings of the core space and from recollections by The Port Authority of New York and New Jersey (The Port Authority) staff and workers from the tenant spaces.
- The condition of the interior walls, whether intact or damaged by the aircraft debris, did not change during a fire simulation.
- The furnishings not in the debris path were assumed to be undamaged and were modeled as developed from the experiments mentioned above. Those furnishings deemed to be rubblized were assigned two-thirds the burning rate of the undamaged furnishings.
- During a simulation, windows were removed at the time indicated in the photographs.
- Vertical shafts in the core area were incorporated as shown in the architectural drawings. For undamaged floors, all the openings to the core area were assumed to total 5 m² in area.
- It was assumed that 40 percent of the jet fuel was available for combustion on the impact floors. The distribution was derived from the aircraft impact modeling.
- The mass of combustibles in each aircraft was obtained from the airlines and the aircraft manufacturer.
- In the FDS computational grid, each floor comprised 128 by 128 by 9 cells. Each cell was 0.5 m in width and depth and 0.4 m in height.
- Prior to aircraft impact, the SFRM was assumed to be consistent with the as-built condition and characterized by a uniform equivalent thickness. If a structural element was found to be in the path of a debris field of sufficient intensity, all the insulation (SFRM and gypsum board) was deemed to have been removed.
- Core walls impacted by sufficiently energetic debris were fully removed. This enabled rapid venting of combustion gases into the core shafts and reduced the burning rate of combustibles in the tenant spaces. In Cases B and D, a more severe representation of the damage was to leave a 1.2 m soffit that would maintain a hot upper layer on each fire floor. This produced a fire of longer duration near the core columns and the attached floor membranes.

Sensitivity tests identified those factors that were the most influential on the outcome of single floor FDS simulations. Table E-2 summarizes how those factors were incorporated into the four cases.

Table E–2. Values of WTC fire simulation variables.

Variable	WTC 1		WTC 2	
	Case A	Case B	Case C	Case D
Fuel load	20 kg/m ² (4 lb/ft ²)	25 kg/m ² (5 lb/ft ²)	20 kg/m ² (4 lb/ft ²)	25 kg/m ² (5 lb/ft ²)
Distribution of disturbed combustibles	Even	Weighted toward the core	Heavily concentrated in the northeast corner	Moderately concentrated in the northeast corner
Condition of combustibles	Undamaged except in impact zone	Displaced furniture rumbled	All rumbled	Undamaged except in impact zone
Representation of impacted core walls	Fully removed	Soffit remained	Fully removed	Soffit remained
Structural damage, NIST NCSTAR 1-2 ¹ Case	Base	More severe	Base	More severe
Insulation damage, NIST NCSTAR 1-2 ¹ Case	Base	More severe	Base	More severe

The results of the FDS simulations of the perimeter fires were compared with the fire duration and spread rate as seen in the photographs and videos. A sample of the basis for such a comparison is shown in Figure E–1. This depicts the room gas temperature 0.4 m below the ceiling slab (in the “upper layer” of the compartment). Surrounding this are “stripes,” each representing a window on that floor. Black stripes denote broken windows, orange stripes denote windows where flames have extended outward from the building, and yellow stripes denote fires that were seen inside the building. Fires deeper than a few meters inside the building could not be seen because of the smoke obscuration and the steep viewing angle of nearly all the photographs.

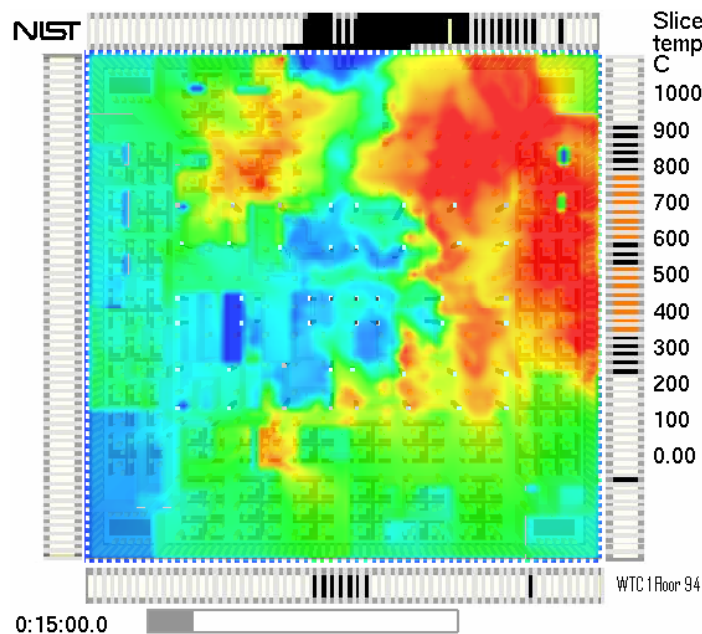


Figure E–1. Upper layer temperature of WTC 1, floor 94, 15 min after impact.

¹ This reference is to one of the companion documents from this Investigation. A list of these documents appears in the Preface to this report.

In WTC 1, much of the fire activity was initially in the vicinity of the impact area in the north part of the building, then it spread around the east and west faces, and was last observed to be concentrated in the south part of the building at the time of collapse. The fact that the simulated fires encircled the building in roughly the same amount of time as the actual fires supported the estimate of the overall combustible load of 20 kg/m² (4 lb/ft²). Simulations performed with higher loads required a proportionately longer amount of time to bring the fires around to the southeast because of the fact that the burn time was roughly proportional to the fuel mass in the oxygen-limited interior of the fire floors.

For WTC 2, relying mainly on Case D, there was less movement of the fires. The major burning occurred along the east side, with some spread to the north.

Much of the information needed to simulate the fires as described above came from laboratory-scale tests. While some of these involved enclosures several meters in dimension and fires that reached heat release rates of 10 MW and 12 GJ in total heat output, they were still far smaller than the fires that burned on September 11, 2001, in the WTC towers. Figure E-2 shows the heat release rates from the FDS simulations of the WTC fires. The peak plateau heat release rates were about 2 GW for WTC 1 and 1 GW for WTC 2. Integrating the area under these curves produced total heat outputs from the simulated fires of about 8,000 GJ from WTC 1 and 3,000 GJ from WTC 2. That adequate representations of disasters can be generated using data from experiments two orders of magnitude smaller is an indication of the capability within the fire research community.

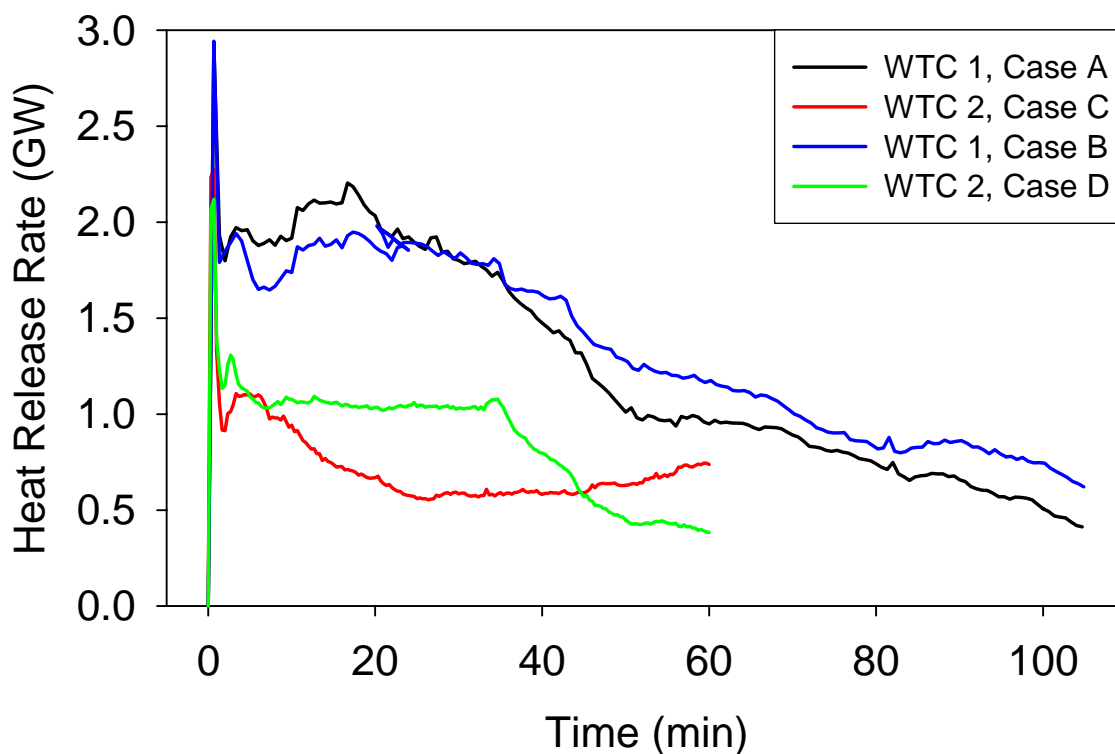


Figure E-2. Predicted heat release rates for fires in WTC 1 and WTC 2.

The results of the fire simulations were used in detailed calculations of the temperature histories of the structural components. The data from FDS were processed and used as boundary conditions for the finite-element calculation of the structural temperatures. Four quantities were transferred from FDS:

- The upper and lower layer gas temperatures, time-averaged over 100 s and spatially-averaged over 1 m. The upper layer gas temperatures were taken 0.4 m (one grid cell) below the ceiling. The lower layer temperatures were taken 0.4 m above the floor.
- The depth of the smoke layer, estimated from the vertical temperature profile.
- The absorption coefficient of the smoke layer 0.4 m below the ceiling.

The FSI was then used to “map” these onto and within the structural elements. Critical to the accuracy of this step was the status of the structural insulation following the aircraft impact. Figure E–3 shows a typical damage diagram generated from the Investigation's aircraft impact modeling and confirmed, where possible, using photographs and videos. Structural changes that occurred later, due to the fires, were not included. In the FSI computations, the concrete slab, trusses, or core beams in the areas marked by the red rectangles were removed. Figure E–4 depicts the structural steel thermal data generated by FSI. Similar data were generated for the concrete floor slab.

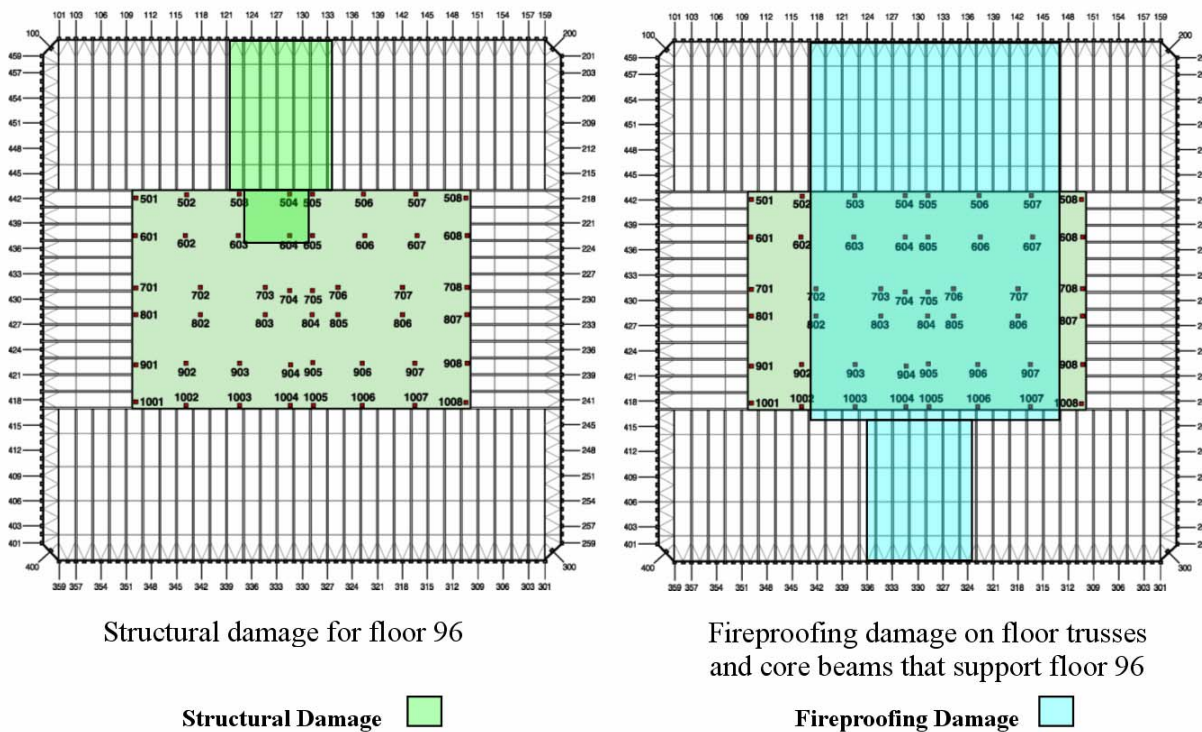


Figure E–3. Structural and insulation damage to floor 96 of WTC 1, Case B.

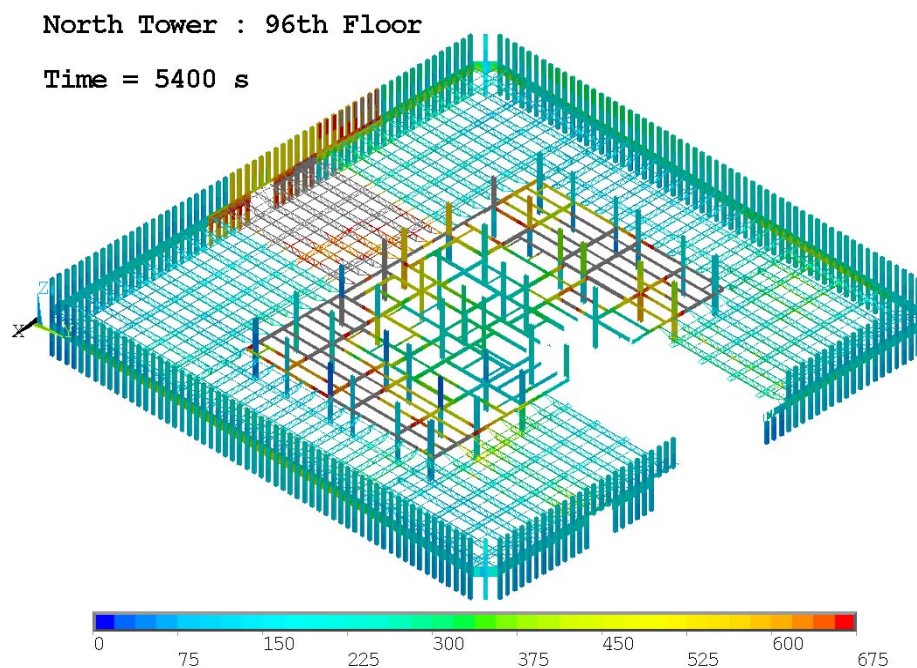


Figure E-4. Thermal response of floor 96 of WTC 1 at 5,400 s after impact, Case B.

The thermal data files then became input for the analysis of the changes in structural performance that resulted from exposure to the fire environments. The FSI calculations were performed at time steps ranging from 1 ms to 50 ms. Use of the resulting data set for structural analysis would have required a prohibitive amount of computation time. Thus, for each case, the instantaneous temperature and temperature gradient for each grid volume was provided at 10 min intervals after aircraft impact. For WTC 1, there were 10 such intervals, ending at 6,000 s; for WTC 2 there were six intervals, ending at 3,600 s. The data files were in a format consistent with ANSYS 8.0.

E.7 FIRE IN AN UNDAMAGED BUILDING

After incurring the direct damage from two different aircraft strike conditions, WTC 1 and WTC 2 stood for 102 min and 56 min, respectively. Structural models of the two aircraft-damaged buildings indicated that, in the absence of weakening by fires or other substantial insult, the buildings would have continued to stand indefinitely. The application of the fire scenarios in Cases B and D to the aircraft-damaged towers led to collapse.

To complete the assessment of the relative roles of aircraft impact and ensuing fires, NIST examined whether an extreme but conventional fire, occurring without the aircraft impact, could have led to the collapse of a WTC tower, were it in the same condition as it was prior to the aircraft impact on September 11, 2001.

The characteristics of such a maximum credible fire could have been:

- Ignition on a single floor by a small bomb or other explosion. If arson were involved, there might have been multiple small fires ignited on a few floors.

- Air supply determined by the building ventilation system.
- Moderate fire growth rate. In the case of arson, several gallons of an accelerant might have been applied to the building combustibles, igniting the equivalent of several workstations.
- Water supply to the sprinklers and standpipes maliciously compromised.
- Intact structural insulation and interior walls.

The four cases described in this report represented fires that were far more severe than this:

- The incident jet fuel created large and widespread early fires on several floors.
- The aircraft and subsequent fireballs created large open areas in the building exterior, through which air could flow to support the fires. In Case A, the fire was still limited by the total vent area (broken windows plus aircraft gash). In Case C, the fire had sufficient air. The fires in both cases were immense.
- About 10,000 gal of jet fuel were sprayed into multiple stories, simultaneously igniting hundreds of workstations.
- The impact and debris removed the insulation from a large number of structural elements that were then subjected to the heat from the fires.

In the four cases reported earlier in this chapter, none of the columns with intact insulation reached temperatures over 300 °C. Only a few isolated truss members with intact insulation were heated to temperatures over 400 °C in the WTC 1 simulations and to temperatures over 500 °C in the WTC 2 simulations.

In WTC 1, if the fires had been allowed to continue past the time of building collapse, complete burnout would likely have occurred within a short time since the fires had already traversed around the entire floor and most of the combustibles would already have been consumed.

In a simulation of WTC 2 that allowed the fires to continue to burn for 3 hours, the temperatures in the truss steel on the west side of the building (where the insulation was undamaged) did continue to increase. In WTC 2, if the fire simulation was extended for 2 hours past the time of building collapse with all windows broken, the temperatures in the truss steel on the west side of the building (where the insulation was undamaged) would likely have increased for about 40 min before falling off rapidly as the combustibles were consumed. Temperatures of 700 °C to 760 °C were reached over approximately 15 percent of the west floor area for less than 10 min. Approximately 60 percent of the floor steel had temperatures between 600 °C and 700 °C for about 15 min. Approximately 70 percent of the floor steel had temperatures that exceeded 500 °C for about 45 min. Based on Cases C and D, the temperatures of the insulated exterior and core columns would not have increased to the point where they would have experienced significant loss of strength or stiffness.

E.8 FINDINGS

E.8.1 Characteristics of the Buildings

- The floors which the aircraft impacted, and on which the major fires occurred, were mostly occupied by a single tenant. The floor plans were generally open, with few interior walls.
- The principal combustibles on the fire floors were workstations, each capable of generating a peak heat release rate 7 MW and a total (integrated) heat release of 4 GJ. The total combustible fuel load on the WTC floors was about 4 psf, 20 kg/m².
- The aircraft added significant combustible material to their paths (and the paths of their breakup fragments) through the buildings.
- The ceiling tile systems in the fire zones were heavily damaged by the shocks from the aircraft impacts and would have provided little, if any, barrier to fire exposure of the ceiling structure. This was consistent with multiple observations during the evacuation.

E.8.2 Characteristics of the Fires

- Upon aircraft impact, a significant fraction of 10,000 gal of jet fuel ignited within the building. The expansion of the hot combustion gases broke windows and blew some of the remaining fuel through them in large fireballs.
- The jet fuel fires consumed most of the oxygen within the fire floors, and the fires quickly died down. The fires grew as fresh air became available and the primed solid combustibles reached their full burning rates.
- The jet fuel was the primer for near-simultaneous ignition of large fires on multiple floors.
- The dominant fuel for the fires in the towers was the office combustibles. On the floors where the aircraft fuselage impacted, there was a significant, but secondary contribution from the combustibles in the aircraft. Most of the jet fuel in the fire zones was consumed in the first few minutes after impact, although there may have been unburned pockets of jet fuel that led to flare-ups late in the morning.
- The major fires in WTC 1 were on the 93rd through 99th floors. The fires generally moved both clockwise and counterclockwise from the north to the south of the tenant spaces. The fires were generally ventilation limited, i.e., they burned and spread only as fast as fresh air became available, generally from additional window breakage.
- The major fires in WTC 2 were on the 79th through 83rd floors, with the most significant fires being in the northeast corner of the 81st and 82nd floors. The fires moved far less than those in WTC 1, remaining in the east half of the floors. The fires had sufficient air to burn at a rate determined by the properties of the combustibles. This was in large part due to the extensive breakage of windows in the fire zone by the aircraft impact.

- At the time of the building collapses, there were still vigorous fires, indicating the unchecked fires could have burned for well over an hour.

E.8.3 Capability for Large Fire Reconstruction

- It was possible to reconstruct a complex fire in a large building, even if the building is no longer standing. However, this required extraordinary information to replace what might have been gleaned from an inspection of the post-fire premises. In the case of the WTC tower, this information included floor plans of the fire zones, burning behavior of the combustibles, simulations of damage to the building interior, and frequent photographic observations of the fire progress from the building exterior.
- Proper design and interpretation of laboratory fires over two orders of magnitude smaller (heat release rates of 10 MW and 12 GJ in total heat output) than the WTC fires provided valid information for simulating the WTC fires.
- Conventional office workstations reached a peak burning rate in about 10 min and continued burning for a total of about a half hour. Partial covering of surfaces with inert material reduced the peak burning rate proportional to the fraction covered, but did not affect the total amount of heat release during the entire burning.
- Jet fuel sprayed onto the surfaces of typical office workstations burned away within a few minutes. The jet fuel accelerated the burning of the workstation, but did not affect the overall heat released.
- The FDS was capable of prediction of the room temperatures and heat release rate values for complex fires to within 20 percent, when the building geometry, fire ventilation, and combustibles were properly described. Parallel processing was essential to keep computation times tractable.
- The Fire Structure Interface, developed for this Investigation, was able to map the fire-generated temperature and radiation fields onto and through layered structural materials to within the accuracy of the fire-generated fields and the thermophysical data for the structural components.

E.8.4 Simulations of the WTC Fires

- Insulation damage due to the aircraft impact was the single most important parameter affecting whether a structural member reached a temperature range likely to cause loss of structural strength.
- The fire spread rates in WTC 1 were consistent with a combusted fuel load of 4 psf (20 kg/m²). Higher combusted fuel loadings resulted in slower fire spread rates that did not match the patterns observed in the photographic evidence. Since these fires were ventilation-limited, the flame temperatures would not have varied significantly within a range of reasonable combusted fuel loadings.

- The plateau heat release rates from the fires were about 2 GW for WTC 1 and 1 GW for WTC 2. The total heat outputs were about 8,000 GJ from WTC 1 and 3,000 GJ from WTC 2.
- For fires of this magnitude, the important factors in determining burning rates were the ventilation area and location, the mass loading of the combustibles, their spatial distribution, and their heats of gasification. The presence of high volatility materials, such as jet fuel, were instrumental during the initiation phase, but mostly burned away rapidly and (except for a few flare-ups observed in WTC 2) played little or no role later.
- In the simulations, none of the columns with intact insulation reached temperatures over 300 °C. Only a few isolated truss members with intact insulation were heated to temperatures over 400 °C in the WTC 1 simulations and to temperatures over 500 °C in the WTC 2 simulations. In WTC 1, if the fires had been allowed to continue past the time of building collapse, complete burnout would likely have occurred within a short time since the fires had already traversed around the entire floor, and most of the combustibles would already have been consumed. In WTC 2, the temperatures in the truss steel on the west side of the building (where the insulation was undamaged) would likely have continued to increase. These temperatures could have exceeded 600 °C for about 15 min for large sections of the floor steel. The temperatures of the insulated exterior and core columns would not have increased to the point where they would have experienced significant loss of strength or stiffness.

Chapter 1

INTRODUCTION

1.1 OBJECTIVE AND APPROACH

The collapse of the towers in the World Trade Center (WTC) on September 11, 2001, resulted from a combination of aircraft impact damage and the ensuing fires. A prime focus of the Investigation of the WTC disaster was to learn the relative importance of these two factors and their interaction leading to the collapses of the buildings. This entailed developing answers to such questions as:

- What were the location, magnitude, and duration of the fires that brought about the collapses of the WTC towers?
- Were the natures of these fires typical of what might be expected in common occupancies, or were there special features that made these fires especially dangerous?
- Could an extreme but conventional fire, occurring without the aircraft impact, have led to the collapse of a WTC tower?

This effort began with the objective to reconstruct, with assessed uncertainty limits, the time-evolving temperature, thermal radiation, and smoke fields in WTC 1, 2, and 7 for use in understanding the behavior and fate of occupants and emergency responders and the structural performance of the buildings.

Addressing this objective required essential input from other efforts in the Investigation, for example:

- Degree and nature of aircraft impact damage,
- Extent and location of structural weakening needed for collapse to be initiated, and
- Eyewitness accounts of building damage and fire locations.

The output of this effort was, in turn, used elsewhere in the Investigation, for example:

- Description of fire and damage information to be requested of survivors, and
- Descriptions of the fire-induced temperatures throughout the exposed structural components for use in constructing the sequence of structural changes leading to collapse initiation.

Operationally, this effort was divided into eight technical tasks as follows:

Visual Collection and Time Line Development. To acquire and utilize photographs, videos, and other relevant information to develop detailed time lines for the spread and growth of fires at the peripheries of WTC 1, 2, and 7 and to organize the information such that it can be utilized by other Investigation Team members. The cataloging and analysis was to provide guidance on the initial conditions for modeling the

fires, the rates of spread of the fires, the floors on which the structural collapses appeared to have begun, etc. (NIST NCSTAR 1-5A).¹

Characterization of Combustibles. To gather data on and characterize the types, mass and distribution of combustibles in the pertinent floors of WTC 1, 2, and 7 at the time of the September 11, 2001, disaster and combustibles introduced by the incident aircraft. The results were to serve as input to the overall effort to reconstruct the thermal and tenability environment within the three buildings (NIST NCSTAR 1-5C).

Characterization of Partitions. To identify the location of and characterize the fire endurance properties of the internal partitions (floors, walls, and ceilings) on the pertinent floors of WTC 1, 2, and 7 at the time of the September 11, 2001, disaster. This entailed obtaining existing data on the fire performance of floor, wall, ceiling systems, and complementing this with additional measurements as needed. The results were to help in determining the potential rates of intercompartment fire spread and also the degree to which the interior of a building was visible in the photographs and videos.

Characterization of Structural Insulation. To determine the effective thermal properties of the structural insulation systems, the effect of vibration, impact, and shock on their thermal insulation performance, and whether chemical interaction between the insulation materials and the steel at elevated temperatures could degrade the steel and insulation performance during thermal insult. This was to enable simulation of the temperature rise within the structural elements as a result of the changing thermal environment (NIST NCSTAR 1-6A).

Model Development. To upgrade the NIST computational fluid dynamics (CFD) Fire Dynamics Simulator (FDS) for its application to the reconstruction of the fires in WTC 1, 2, and 7. This was to effect a pragmatic fire growth routine and also improve the efficiency of the model, enabling more extensive simulations during the time frame of the Investigation. In addition, this task was to develop a fire structure interface (FSI), a computational method for relating the turbulent fire environment to the transport of heat to and through an insulating layer to the underlying structural steel. This was to enable simulation of the temperature rise and resulting loss of structural capability of the steel (NIST NCSTAR 1-5F and NIST NCSTAR 1-5G).

Experiments for Model Development. To provide input parameters and guidance for the FDS combustion sub-model (NIST NCSTAR 1-5B and NIST NCSTAR 1-5C).

Fire Reconstruction: To reconstruct the gaseous thermal environment (radiation and temperature fields) surrounding the structural elements and in the inhabitable spaces within WTC 1, 2, and 7. Using such input information as the estimated aircraft damage and the contents and layout of the building from the above tasks, NIST would use FDS to simulate fully involved fires in the three buildings, with and without the initial damage from the aircraft or incident debris, enabling addressing the extent to which that damage affected the thermal environment felt by the structure. Parameters in the re-creation of the fires were to enable estimating the roles of jet fuel and building contents, ventilation system, compartment damage, pressurized core, and fire protection system on the growth and spread of fire. The use of statistical design for the sets of simulations were to lead to identification of those input conditions to

¹ This reference is to one of the companion documents from this Investigation. A list of these documents appears in the Preface to this report.

which the results were the most sensitive and those combinations of input conditions that led to the best agreement with the photographic evidence. The thermal environment was then to be transposed onto the structures of the two towers (NIST NCSTAR 1-5F and NIST NCSTAR 1-5G).

Reconstruction Validation. To generate and use experimental data for assessing the accuracy of the FDS predictions of complex fire growth and of the FSI predictions of thermal insult to structural members such as columns, trusses, beams, and other support structures like those in WTC 1, 2, and 7. Comparison of the data from these large-compartment tests were to establish the utility of FDS and FSI for simulating heat transfer and complex burning at a realistic scale (NIST NCSTAR 1-5B and NIST NCSTAR 1-5E).

As the Investigation progressed, it became clear that the simulation of tenability on the impact floors and above would be subject to gross uncertainty. The aircraft impacted the two buildings at different heights. In WTC 1, the stories above the aircraft impact floors were serviced by a ventilation system connected to the mechanical equipment located on the 108th and 109th floors. As a result, there were pre-impact ventilation pathways that could transport smoke and noxious gases directly from the fire floors. In WTC 2, the aircraft-impacted floors were serviced by the mechanical equipment on the 75th and 76th floors. The floors above the 93rd floor were connected to a separate system, and (in the absence of impact damage) there were no direct ventilation pathways to transport heat and smoke from the floors with active fires. However, smoke did reach the upper levels of WTC 2, perhaps transported through compromised elevator shafts. Unfortunately, there was no verifiable information available regarding damage between floors and damage to existing floor-to-floor air passages (vents). Furthermore, there was no quantitative information regarding the temperature and smoke conditions in the interior of the towers. These voids substantially increased the uncertainty in modeling the spread of heat and smoke from the fire floors to other parts of the building. Thus, with due consideration, it was decided not to attempt to model the smoke movement and, thus, the tenability conditions throughout the occupied portions of the buildings and to focus resources on modeling the fires that eventually led to the towers' collapses.

1.2 DOCUMENT CONTENT

This document reports the probable nature of the fires in WTC 1 and WTC 2 and how NIST was able to reconstruct them. The outcome of the reconstructions became a principal input to the assessment of the collapse of the buildings. Reconstruction of the fires in WTC 7 is presented in a separate report.

The widespread fires in the towers occurred as a result of the dispersion and ignition of jet fuel. The fires in the towers were characterized by their locations and their movement between the time of incidence and the collapses of the buildings, the length of time that they remained in these locations, and their thermal output and the transfer of that output to the buildings' structural components. The fires were controlled by the supply of combustibles (both those resident within the buildings and those introduced by the aircraft, and their distribution within the floors of the towers), the air supply through windows, interior shafts, and leakage through the floors, and barriers such as walls, floors, and ceilings.

The approach to reconstruction of these fires was unprecedented. Neither of the buildings remained, eliminating access to the telltale signs that fire investigators typically use to assess the path and intensity of a fire. However, this was perhaps the most photographed disaster in history, providing unparalleled information from the exterior of the buildings. In addition, there was some less quantitative information

garnered from examination of the interviews with survivors and the phone calls from people in and above the impact zones.

This unusual composition of available information led NIST to a high reliance on computational tools in recreating the fires. There had been extensive development of such software over the past decade. Nonetheless, for this Investigation, the state-of-the-art needed to be advanced to handle the wide ranges of times and length scales, the complex combustibles, etc. These improvements resulted from series of laboratory tests to clarify the phenomenology and provide magnitudes of fire properties, analysis of the photographic evidence from September 11, and algorithm development to capture the essence of these observations. The sensitivity of the outcome of the computer simulations to the various (unknown) aspects of the buildings and their contents was determined. The accuracy of the predictions was appraised by their consistency with the photographic evidence.

This report summarizes the results of the various experiments and simulations. Persons interested in the detailed development of these results are directed to the separately published companion reports.

Chapter 2

VISUAL EVIDENCE¹

2.1 INTRODUCTION

The destruction of the World Trade Center (WTC) on September 11, 2001, may have been the most heavily photographed and video recorded disaster in history. This evidence was extremely valuable, given the near total destruction of the buildings and the limited information available from inside the buildings during the unfolding tragedy. The photographic and video images constitute the largest body of evidence from which to extract knowledge of the structural damage from the aircraft, the progress of the ensuing fires, and the eventual collapse of the towers. However, as important as the visual evidence is, it must be recognized that the views were from the exterior, usually at a sharp angle looking up at the fires, and often obscured by smoke. There are few, if any, views of the situation from inside the buildings.

This chapter summarizes the building of the collection of visual material, its organization into a coherent body, the construction of a time line for the events of that day, and the extraction of specific information regarding the fires in the WTC towers.

2.1.1 Magnitude

The amount of visual material recorded on September 11 was extraordinary. The terrorist attacks occurred in an area that was the national home base of several news organizations, had several major newspapers, and was the center of the fashion industry. New York City is also a major tourist destination, and visitors often carried cameras to record their visits. Further, the very height that made the WTC towers accessible to the approaching aircraft also made them accessible to photographers. As a result there were hundreds of both professional and amateur photographers and videographers present, many equipped with excellent equipment and the knowledge to use it. These people were in the immediate area, as well as at other locations in Manhattan, Brooklyn, Queens, and New Jersey.

There was a good amount of photographic material shot during the early stage when only WTC 1 was damaged. By the time WTC 2 was struck, the number of cameras and the diversity of locations had increased. Following its collapse, the amount of visual material decreased markedly as people rushed to escape the area, and the huge dust clouds generated by the collapse obscured the site. There is a substantial, but less complete, amount of material covering the period from the WTC tower collapses to the collapse of WTC 7 at around 5:21 p.m.

In all, National Institute of Standards and Technology (NIST) assembled a collection of nearly 150 segments of video footage (totaling in excess of 300 hours) and over 7,000 photographs. The collection included the work of over 200 photographers and 40 videographers. The material was digitized

¹ Extensive detail of the material in this chapter is provided in NIST NCSTAR 1-5A. Further references to this report are not inserted in order to preserve continuity of this text. The reader should assume that unreferenced statements are supported by text in NIST NCSTAR 1-5A. This reference is to one of the companion documents from this Investigation. A list of these documents appears in the Preface to this report.

and stored on a local network that was isolated from external access due to the sensitive nature of some of the material and copyright issues. It was organized into a searchable database in which the searchable properties included the name and location of the photographer, time of shot/video, copyright status, content, whether it included the key events, whether it included Fire Department of the City of New York (FDNY) or New York Police Department (NYPD) people or apparatus, and other details (falling debris, people, building damage).

2.1.2 Sources

There were a variety of sources of visual material:

- Recordings of newscasts from September 11 and afterwards, documentaries, and other remembrances provided information directly and also pointed toward other potential sources of material. Sources included NBC, CBS, ABC, CNN, and local New York stations WABC, WCBS, WNBC, WPIX, WNYW and New York One.
- The major photo clearing houses such as AP, Reuters, and Corbis had web sites that were reviewed for material related to September 11. Several members of the media suggested additional sources. Direct contact was also made with local professional news organizations, including the New York Times, the Daily News, and the Star Ledger.
- Significant material was obtained from the NYPD and FDNY.
- Several collections of visual material were assembled for charitable or historical purposes. Collections from the Here is New York exhibition and the September 11 Digital Archive were reviewed.
- Many photos and videos began appearing on the World Wide Web as early as September 11, 2001. These could often be identified by Web searches, and in many cases contact information was provided.
- Public appeals for visual material were made during Investigation news conferences and updates. News accounts of these events led many to contact NIST using the toll free number or the Investigation web site. Frequently, a new source would provide information about other potential sources.

2.2 EVIDENCE REGARDING WTC 1

2.2.1 Time Line for the First 30 Seconds

The data regarding the events immediately following the impact of American Airlines Flight 11 on the north face of WTC 1 at 8:46:30 a.m. came exclusively from two videos and one set of a few still photographs. The two videos were shot from the north and the northwest of WTC 1, respectively. The photographs were shot from the southeast of the tower. These formed the basis for the following time line, estimation of the speed of the approaching aircraft, description of the immediate damage to the tower (strictly as seen from the outside), and characterization of the fire behavior in the immediate aftermath.

Figure 2–1 shows selected frames from the videos.



Figure 2-1. Series of frames from videos that show the aircraft striking WTC 1 and the immediate aftermath. The times relative to the plane strike are shown in the upper right-hand corner.



Figure 2-1. Series of frames from videos that show the aircraft striking WTC 1 and the immediate aftermath (cont.).

Table 2–1 captures the time line for the impact and the events that followed immediately.

Table 2–1. Time line for events immediately following the aircraft strike on WTC 1.

Time(s)	Observation
0:00	Plane struck tower.
0.03	Bright flash at front of plane.
0.20	Tail disappeared into building.
0.43	Dust cloud began to form on north face, appeared to be ignited.
0.67	Dust cloud apparent near the center of the east face.
1.43	Dust cloud appeared in vicinity of mechanical floors (108 and 109) near the center of the north face.
1.77	Dust clouds appeared at mechanical floors (108 and 109) at two locations on either side of center of the east face.
3.43	Fire appeared from behind southeast corner.
4.40	Area of fire evident on the east face.
9.43	Fireballs appeared to extinguish.
18.56	Substantial but diminishing fires on north and east faces.

The timing and appearance of the fireballs indicated that they were ignited inside the building. A calculation based on the oxygen contained within the building on the floors into which the fuel tanks entered indicated that up to 15 percent of the available jet fuel could have burned inside the building in this immediate event. These fires quickly depleted the available oxygen. The resulting pressure wave forced large amounts of unburned fuel through openings either created by direct impact of the aircraft and/or debris or windows blown out as a result of the overpressure generated inside the building by the fire itself. The presumably atomized fuel burned when it mixed with air outside of the building. The largest fireball formed on the north face, suggesting that the largest amount of jet fuel was blown backwards through the opening created by the aircraft entry. If roughly another 15 percent to 20 percent of the jet fuel burned outside the building as in WTC 2 (Section 2.4.1), then about two thirds of the jet fuel remained inside the building to burn later or just flow away from the fire zones.

Measurements and calculations estimated that the thermal expansion from a fire in a partially enclosed space could generate overpressures between about 1 lb/in² and 5 lb/in². For a window and frame area of over 10 ft², this amounts to thousands of pounds of pressure, more than enough to cause displacement.

2.2.2 Estimated Aircraft Speed

The speed of American Airlines Flight 11 as it entered the tower was estimated as 683 ft/s \pm 50 ft/s, or 466 mph \pm 34 mph (NIST NCSTAR 1-2B).

2.2.3 Observed Impact Damage

The aircraft struck near the center of the north face of WTC 1, centered on the 96th floor with wings impacting from the 93rd to the 99th floors (Figure 2–2). The impact created a hole about 15 ft wide by 4 stories high at its widest points. The aircraft fragments continued into the building to destroy portions of the concrete floor systems on the 94th through 97th floors. In addition to numerous windows broken out by the impact on the north face, there were about 15 windows blown out on the east side of the 94th floor

and about 10 on the south side of the 96th floor. The 94th and 96th floors were the areas struck by the wing fuel tanks. It is reasonable to surmise that these two floors were the source of the fireballs.

Immediately after the fireballs formed, large fires were evident from the north, east, and south faces during the period from 10 s to 30 s following the plane strike. Between 40 s and 45 s after the plane strike, there was an abrupt decrease in the size of the flames in the hole on the north face and the amount of smoke exiting the west face, likely a result of the aforementioned oxygen depletion. (During this period, unburned jet fuel did flow to other parts of the building. For instance, there were a number of accounts of fires in the lobby and of fires flashing from the elevators.)



Figure 2–2. Photograph of the north face of WTC 1 around 9:30 a.m. showing the area damaged by the aircraft strike.

2.2.4 Observed Fire Behavior in WTC 1 Following the Aircraft Strike

The following discussion of fire behavior in WTC 1 is broken into six time periods of roughly 15 min each. This summary focuses on fire observations. Details of the fire behavior as a function of time are documented in façade maps describing fire, smoke, and window condition observations included in 8:47 a.m. to 9:03 a.m.

WTC 1 from 8:47 a.m. to 9:03 a.m.

This period spanned the time between the first aircraft impact on WTC 1 and the second on WTC 2. As noted earlier, by 40 s after the aircraft impact on WTC 1, only relatively small fires were visible burning

on the north, east, and south faces. During the following few minutes, only minor changes in these initial fire distributions were observed. After this lull, fires began to appear, grow, and spread on all four faces of the tower.

Within a few minutes of the aircraft impact a substantial fire grew on the north face of the 97th floor to the immediate west of the aircraft impact cavity. Starting around 8:51 a.m. external flames also appeared on this floor from windows located a short distance to the east of the cavity and rapidly grew to fill several nearby windows. Around 8:57 a.m. smoke and flames suddenly came from windows on the east side of the 96th floor below the burning area on the 97th floor. The three fires on the 96th and 97th floors began spreading toward the edges of the face, with the fire on the west side of the 97th floor reaching the western edge of the tower by 9:03 a.m. and the two fires on the east side of the impact cavity spreading to the east before pausing outside of the walls of rooms located in the northeast corners of these floors. During the period, several small isolated fires were visible on other floors impacted by the aircraft.

On the east face of the tower the fire that was originally visible toward the center of the 94th floor spread and grew substantially. By 9:03 a.m. an intense fire was visible burning over a length of open windows that covered roughly a quarter of the face from a position on the north side to near the center of the face. Just before 8:57 a.m. flames appeared from windows on the 97th floor located just to the south of the internal wall of the room in the northeast corner of this floor. This fire appeared to spread and grow rapidly, covering more than a quarter of the length of the floor by 9:03 a.m. By this time several small fires were also visible on the northern sides of the 92nd, 93rd, and 95th floors and had just appeared on the 96th floor. Near the end of the period numerous people were observed falling from the 92nd and 93rd floors over short periods of time, which may be an indication that conditions at these locations on the east side were becoming untenable at this time.

The primary fire activity on the south face during the period was on the 96th floor. The fire on the western side of the face had grown and spread to cover nearly the entire western half of the floor. Flames were visible in the southwest corner of the floor where an aluminum panel covering the area had been removed during the aircraft impact. Near the end of the period relatively small fires began to appear on the western sides of the 95th and 97th floors.

No fires were visible on the west face until just after 8:55 a.m., when external flames and heavy smoke first appeared from a window on the 97th floor near the center of the face and then seemed to spread very rapidly in both directions. Within a minute, external flames were visible over a length of windows covering nearly a quarter of the face near the center. A second period of apparent rapid fire spread just after 9:01 a.m. increased this length to the south by roughly 50 percent in 8 s. Shortly after 9:02:15 a.m. another period of rapid fire spread appeared to fill in the remaining length between the existing fire and the north edge of the face. No fires were observed on other floors of this face during the period.

The most extensive fire growth took place on the 97th floor. The apparent rapid development of these fires, particularly on the west face, may be an indication that the fire growth and spread was accelerated by the presence of initially unburned aviation fuel that may have been dispersed over this floor during the aircraft impact.

Observations suggest that smoke from the developing fires was rapidly transported to the upper regions of the tower. Smoke was observed almost immediately coming from vents near the center of the north side of the mechanical equipment room on the 108th and 109th floors. Starting around 8:52 a.m., it appeared

that people began to break open windows on floors on each of the faces near the top of the tower, particularly on the 104th and 105th floors. Smoke began to flow immediately from many of these open windows.

Other observations summarized in the report are consistent with the observed fire behaviors during the period. A number of streamers were observed falling from façade areas where fires had recently appeared. The aluminum cladding next to windows where fires were present was marked by smoke in a manner which reflected the local fire intensity. In particular, distinct carets were present on the columns next to windows where flames extended from the openings.

Response of WTC 1 to the Impact of United Airlines Flight 175 on WTC 2

United Airlines Flight 175 struck WTC 2 at 9:02:59 a.m. The impact and subsequent fireballs briefly affected the fire behavior in WTC 1. The first effect was the sudden appearance of smoke and in a few cases fire from a number of open windows, indicating a weak pressure pulse had passed through the tower. A portion of the fireballs that formed on WTC 2 was adjacent to the east face of WTC 1. As the fireballs initially expanded they pushed smoke away from the east face of WTC 1 and revealed areas that had been hidden by smoke. As the fireballs grew larger, they entrained sufficient air that large amounts of smoke and air were drawn from open windows on the east face of WTC 1, while smoke flow was markedly decreased on the other faces. The disrupted smoke flow lasted for just over 10 s.

WTC 1 from 9:03 a.m. to 9:18 a.m.

Compared to the rapid fire spread observed on the north face periphery during the first time period, little additional fire spread occurred on this face during the following fifteen minutes. The intense fires that had grown on the 96th and 97th floors earlier retreated into the building and began to die down. Around 9:15 a.m. a fire appeared in windows on the west side of the aircraft impact cavity on the 94th floor. This was the first evidence of a fire in this area of the floor.

In contrast to the north face, the fires burning on the periphery of the east side of the tower continued to develop and spread during this time, initiating new areas of intense burning at the same time that areas ignited somewhat earlier were dying down. By 9:07 a.m. an extensive length of flame had appeared on the 92nd floor extending over roughly 20 percent of the width of the face to the north of the face center. Moderate fire growth had also occurred near the center of the 93rd floor, while an isolated fire was visible at the center of the 95th floor. An intense fire (with flames extended from windows) developed over a length running from just outside the wall of the room in the northeast corner to well past the center of the face on the 96th floor. On the 94th and 97th floors, the fires at windows that had been burning intensely during the earlier period were dying down, while new areas of fire had spread to the south.

During the initial part of this time period, the fires on the western half of the 96th floor on the south face continued to burn intensely. At this time, flames were not visible on other floors. By the end of the period the appearance of the south face had changed dramatically. While the fires on the 96th floor had begun to die down and recede back into the tower, extensive areas of flame became apparent on both the 95th and 97th floors. The fire on the 95th floor was visible over roughly 10 percent of the width of the face at a location on the east side of the western half of the floor. On the 97th floor a fire developed that covered most of the western half of the floor.

The fires on the west face during this time period continued to undergo unusual and dramatic changes in behavior. During the early part of the period, heavy flames and smoke were observed coming from roughly the same locations on the 97th floor as just prior to 9:03 a.m. At 9:06:27 a.m., a short-lived, but intense, burst of flame appeared near the top of a window near the southern edge of the floor. Very shortly afterward the amount of smoke and flames coming from open windows along the length of the 97th floor decreased dramatically, and it was possible to see parts of the west façade that had been hidden just before. At this time flames were visible near the southern edge of the face. Later images of the west face during the period show an extensive fire along the entire length of the floor, but with flames that have receded well into the windows and little smoke flow from the open windows. Around 9:08 a.m. a small fire became visible on the 96th floor near the southern edge. By the end of the period a relatively low-intensity fire was visible in several windows in this area. No other fires were observed on the face during the period.

WTC 1 from 9:18 a.m. to 9:35 a.m.

Very shortly after 9:18 a.m. intense fires with external flames appeared within the rooms on the northeast corners of the 96th and 97th floors. A similar fire was observed in the northeast corner room on the 94th floor around 9:25 a.m. Very shortly after these fires appeared, streamers began falling from the area. The intense flames in these windows only lasted a few minutes, having died down by 9:35 a.m. The fire observed on the west side of the 94th floor at the end of the previous period spread significantly and filled the length between the aircraft impact cavity and eastern wall of a room on the northwest corner of the floor. Even though these flames were extensive, there was no external flaming and very little smoke was coming from nearby windows. By 9:35 a.m. this fire was also dying down. Around 9:28 a.m. a small fire became visible on the 98th floor. Over the next few minutes this fire spread and by 9:35 a.m. covered roughly one-fourth of the floor width near the center of the face.

By 9:18 a.m., most of the fires observed earlier near the center of the face on multiple floors on the east face were dying down. As on the north face, fires were observed moving into rooms located on the northeast corners of the 96th and 97th floors around 9:19 a.m. and on the 94th floor around 9:23 a.m. A similar fire growth was observed in the room on the northeast corner of the 93rd floor starting at the end of the period. Fires which had recently spread west from the initial burning areas on the 92nd, 95th, 96th, and 97th floors continued to burn, but there was little additional fire spread during the period.

By the start of this period, extremely intense fires were present on the west side of the south face on the 95th, 96th, and 97th floors. On the two higher floors these flames extended from near the center of the face to the western edge, while on the 95th floor there appeared to be a barrier that prevented flame spread to the western edge. Over the course of the period, the fires on the 96th and 97th floors began to die down while those on the 95th floor remained intense. There was no indication of additional fire spread during the period on this face.

The fires on the west face were relatively quiet during this time. The extensive fire present earlier on the 97th floor continued to die down, becoming very spotty by the end of the period. Meanwhile, the low intensity fire that had earlier begun to spread north on the 96th floor from the south edge continued moving methodically across the floor, reaching near the center of the face by 9:33 a.m. Unlike the earlier fires on the 97th floor, these flames appeared to be burning near the floor at separated locations. Their appearance was very similar to the dying flames seen on the 97th floor.

In general, fire spread during this period was reduced compared to the first two periods. While intensely burning fires with extended flames developed in northeast corner rooms on several floors, most of the new fire growth involved less intense flames that did not extend from windows. Such fires included those on the west side of the 94th floor and the central part of the 98th floor on the north face and the south side of the 96th floor on the west face.

Most of the streamers during the period were observed at early times when fires were spreading into the northeast corner rooms and on the west side of the 94th floor. Relatively few people were observed falling from the upper floors of WTC 1 during this time. These observations are consistent with the observations indicating that the fires present during this period were less vigorous and extensive than during the two earlier periods.

WTC 1 from 9:35 a.m. to 9:59 a.m.

This period takes the time line for WTC 1 fire behavior up to the time that WTC 2 collapsed.

The fires that appeared on the north face at the 98th floor near the end of the previous period continued to spread and by the end of this period extended over two-thirds of the face starting at the east edge. Even though the flames were extensive, very little smoke and flame were evident coming from the 98th floor windows, and the fires were dying down by the end of the period. Around 9:40 a.m. smoke and flames appeared in windows at the western edge of the 94th floor, indicating that a nearby fire had entered a room located in this corner. This fire would spread slowly to west during the remainder of the period. At roughly the same time a similar fire grew in windows at the east edge of the 92nd floor, apparently having migrated from the east face. Another fire developed rapidly in a room on the northwest corner of the 96th floor around 9:53 a.m., apparently moving from the west face.

The most dramatic change in the fire distributions on the east face during this time was the appearance and spread of an intense fire on the 98th floor. At around 9:38 a.m. a jet of flame appeared from a window midway between the north edge and the center of the face. By the end of the period intense flames were coming from 98th floor windows over much of the northern half of the face. Meanwhile, fires on the 92nd, 94th, 95th, 96th, and 97th floors continued to spread from the center of the face toward the south. Due to growth and decay cycles of the spreading fires, the flames on these floors developed the appearance of waves moving slowly southward across the face. On the 93rd floor flames were evident on the north side of the face, including in windows inside a room on the northeast corner.

The distribution of fires on the south face also changed substantially during this period. The intense fires burning earlier on the west sides of the 95th, 96th, and 97th floors continued to die down throughout this time. Around 9:40 a.m. a flame jet suddenly erupted from the south side of the 98th floor. This new area of fire then spread and grew rapidly, covering most of the west side of the floor within a few minutes. This fire continued to burn until the end of the period. The first indications of a fire burning on the east side of the south face became apparent around 9:43 a.m. It was just possible to identify an area of small flames at a position roughly one-third of the way between the east edge of the face and center on the 94th floor. This fire did not grow substantially during the remainder of the period.

The most dramatic changes in fire distributions on the west face took place on the 94th and 98th floors. Earlier there were no visible signs of fire on these two floors. Sometime around 9:38 a.m. flames appeared on the 98th floor and, within a few minutes, relatively low intensity flames were visible over

more than half of the length of that floor starting at the south edge. By 9:59 a.m. the flames could be seen over more than three-fourths of the floor width. Even though extensive, these flames were not intense since there was no flame extension and very little smoke was flowing from nearby windows. At around 9:39 a.m. small fires appeared to develop rapidly near the center and northern edges of the 94th floor. Almost simultaneously eight people were seen falling or climbing down from 94th floor windows near the center of the face. By the end of the period relatively low intensity flames were visible in most windows on the floor from the north face to well beyond the center of the face. The northward movement of the low-intensity fire on the 96th floor continued during the period, finally reaching the edge of the face around 9:53 a.m.

The large number of people who fell from the west side of the 94th floor around 9:40 a.m. was mentioned above. During the period, additional people were observed falling from higher floors on the north, east, and west sides of the tower.

Response of WTC 1 to the Collapse of WTC 2

At 9:58:59 a.m., WTC 2 began to collapse, and roughly 10 s later debris reached the ground. Very shortly after the collapse began, fire and smoke were pushed out of the south face of WTC 1, probably due to a pressure pulse transmitted to WTC 1 from the collapsing tower. The most prominent effect was on the 98th floor where flames were pushed out of windows along the west side of the face. There was also a distinct increase in the flame intensity on the west side of the 96th floor. It is likely significant that flames did not appear elsewhere on the face, perhaps indicating that large flames were only present near the periphery of the face at these locations.

Videos showed that no flames were pushed from open windows on the north face of WTC 1, but that fires burning on the 92nd, 94th, and 96th floors brightened noticeably. On the east face, flames near the south edge on both the 92nd and 96th floors flared out at roughly the same time the changes were observed on the north and south faces. Shortly after the collapse of WTC 2, the flow of smoke from the north face of WTC 1 stopped momentarily. The period of decreased smoke flow lasted for approximately 40 s.

Videos shot from the east showed that debris from WTC 2 passed in an arc across the east face of WTC 1, creating damage on the façade of WTC 1 that is visible in images taken shortly after the collapse. The highest marks on the building were just below the mechanical equipment room on the 75th and 76th floors. The damage appeared relatively superficial, and it is considered unlikely that it affected the subsequent fire behavior in the tower. Videos and eyewitness accounts indicate that large amounts of dust and some debris entered the lower floors of WTC 1 during the collapse of WTC 2. It is not known if damage at these lower locations could influence the fires near the top of the tower.

WTC 1 from 9:59 a.m. to 10:18 a.m.

The collapse of WTC 2 resulted in changes in the quantity and quality of visual material showing the faces of WTC 1. People near the site were forced to flee or seek shelter. Many photographers and videographers located further away changed their focus to the large dust clouds that covered much of lower Manhattan. The dust reached levels near the top of WTC 1 and obscured the faces. This was particularly true on the downwind east and south sides. As a result, the visual information following the collapse of WTC 2 was considerably less detailed than prior to this time. However, other evidence

indicated that significant changes in fire behavior and distribution were taking place prior to the collapse of WTC 1 at 10:28:22 a.m.

The most complete information for the current period was available for the north face. Images recorded shortly after 10:00 a.m. showed that remarkably little fire was visible on the face and that the flames that were visible had low intensities. During the period, the fire burning on the east side of the 92nd floor continued spreading slowly to the west, apparently moving from room to room along the façade. By the end of the period it had reached roughly two-thirds of the way across the face. Only remnants of the earlier fires on the 94th and 96th floors were visible on the west side of the face. Starting around 10:10 a.m., an intense fire grew on the 98th floor near the west edge of the face.

Compared to the north face, it proved more difficult to characterize the fire behavior on the east face of WTC 1. Shortly after the collapse of WTC 2 a dust cloud rose from below and totally obscured the floors where fires were present. Just prior to the arrival of the dust from below, intense fires were visible coming from windows on the 94th, 96th, 97th, and 98th floors with similar distributions to those seen just prior to the collapse. As the dust began to clear around 10:07 a.m., the only fire visible was the intense band of flames on the north side of the 98th floor. Over the next several minutes the limited imagery available suggests that the fire distributions on the east face remained similar to those present prior to the collapse. There is some indication that the fires burning on the 96th and 97th floors may have spread further south, perhaps reaching as far as the southwest-corner room on the 96th floor and three-fourths of the way across the face on the 97th floor.

The quality of the imagery available for the south face of WTC 1 following the collapse of WTC 2 was similar to that for the east face. Shortly after 10:00 a.m. a long distance video showed an intense line of fire present on the western side of the 98th floor and a vigorous fire burning on the 97th floor near the center of the face. Shortly afterward, dust rose from below and totally obscured the floors with fire. When the dust began to clear around 10:06 a.m. the flame distribution did not appear to have changed markedly. At around 10:11 a.m. the dust cleared sufficiently to detect the presence of fires on the east side of the 96th floor, extending from near the eastern edge to at least half way to the center of the face, and on the 97th floor, concentrated toward the center of the face. Shortly afterward, flames were observed coming from the 99th floor on the west side of the face.

One of the more interesting fire spread behaviors in WTC 1 was observed on the west face shortly after the collapse of WTC 2, when a large fire developed rapidly on the south side of the 104th floor, well above floors where fire had been observed previously. A deep red glow along the 98th floor remained visible on the face, indicating that the interior fire on this floor continued to burn. The fire became extended across the entire width of the floor when it spread to the north edge during the period. Isolated flames were still visible on the north side of the 96th floor, while the low-intensity fire burning on the 94th floor spread south to cover three-fourths of the face width. Around 10:07 a.m. 13 people were observed falling from windows near the center of the 95th floor. Shortly afterwards, fire first became visible on this side of the floor nearly simultaneously at a number of windows. By 9:18 a.m. flames were visible over a three-fourths length of the 95th floor, extending from near the north edge. Though extensive, these flames appeared to have relatively low intensities, similar to the fires below on the 94th floor.

The large number of people observed falling from the 95th floor around 10:07 a.m. has already been discussed. Other people were observed falling from locations well above the fire floors on the north and

west faces. Most of these were seen near the end of the period, perhaps indicating that conditions on the upper floors had begun to rapidly deteriorate.

10:18 a.m. to Collapse of WTC 1 at 10:28:22 a.m.

By shortly after 10:18 a.m., the fire spreading toward the west on the north side of the 92nd floor was approaching the edge of the face. Despite the presence of flames over a significant length of the floor, the fire appeared to be burning with a low intensity at separated locations, with essentially no smoke coming from nearby open windows. An event took place within the tower at 10:18:48 a.m. that generated a pressure pulse with sufficient magnitude to force a large amount of smoke from the open windows on the 92nd floor, along with smaller amounts from open windows on other floors on the north face and on the other faces of the tower. While it seemed likely that the pressure pulse was generated by some sort of collapse within the tower, e.g., a portion of the core settling or a partial floor collapse, it has not been possible to determine the nature of the event or even its general location based on the visual record. Shortly after the pressure pulse, an intense fire appeared at the western edge of the 95th floor. Over the next several minutes, the fire on west side of the 92nd floor grew dramatically, with heavy internal flames visible over most of the western half of the floor. Fires present elsewhere on the north face were dying down during this period. When the tower began to collapse, it acted as a piston, forcing air downward onto other floors and out through openings. As a result, large volumes of fire and smoke were pushed from windows on the 92nd floor at several locations across the face, confirming the presence of an extensive area of fire. Flames were also pushed from windows in the northwest-corner room on the 95th floor, indicating that a significant fire was still present nearby. Flames were not expelled from elsewhere on the north face, providing additional evidence that intense fires observed earlier at other locations on the face had either died down or gone out.

Views of the east face during the final ten minutes were limited and partially obscured. A small fire was clearly burning near the center of the 101st floor. Several long-distance videos show that around 10:21:15 a.m. there was an intense burst of flame from the 98th floor at a location roughly half way between the center of the east face and the south end. This new region of intense fire rapidly expanded in both directions to cover about one-fourth of the width of the face. The new area of fire on the south side of the 98th floor remained the dominant feature on the east face until the collapse. Roughly 3 s prior to collapse initiation, this line of fire brightened noticeably. During the collapse, bright flames were expelled from the southern side of the 98th floor, confirming the presence of an intense fire in the area. Expelled fire was not visible coming from the other fire floors on the face, suggesting that the fires present elsewhere were much smaller than that on the south side of the 98th floor.

Views of the south face of WTC 1 were also limited for this time period, but several photographs taken from a helicopter flying relatively close to the tower provide a good indication of conditions on this face roughly half way through the period. Figure 2–3 shows a cropped view of one of these photographs shot from the southwest at 10:22:59 a.m. Fires are visible on the east side of the face on the 92nd through 98th floors. A long-distance video showed that the particularly intense fire on the 98th floor moved into the area around 10:19 a.m. Close inspection of the photograph reveals that many of the columns on the south face in the vicinity of 95th floor to the 98th floors were bowed inward at this time. Somewhat smaller flames are visible on the west side of the face on the 92nd, 96th, 98th, 99th, and 100th floors. Around 10:25 a.m. heavy smoke and fire appeared from windows in a room located on the southwest corner of the 94th floor. Long-distance videos show that during the period leading up to the tower

collapse, the line of fire on the 98th floor continued to burn vigorously. The fire on the 99th floor appeared to intensify and move towards the east, eventually reaching a location more than half way between the center of the face and the east edge. When WTC 1 began to collapse, a large amount of flame was pushed from openings on the south face with flames appearing to come from three separate locations. The first was from the vicinity of the intense fire burning on the east sides of the 98th and 99th floors, the second was from the fire burning on the western edge of the 94th floor, and the third came from around the center of the face near the 94th floor.



Figure 2–3. View of the south face of WTC 1, cropped from a photograph shot from a helicopter at 10:22:59 a.m. It has been enhanced by adjusting the intensity levels, and column and floor numbers have been added.

Minimal fire spread took place on the west face during the period. Fire moved into two adjacent rooms located in the northeast corner of the 92nd floor and into a southwest corner room on the 94th floor. Fires observed earlier on the 94th, 95th, and 98th floors were generally dying down. The fires on the 96th and 97th floors appeared to have died out since no flames were visible on these floors. The fire on the south side of the 104th floor continued to burn intensely. A video shot showed that smoke was forced out of

multiple west-face windows approximately 2 s before the collapse of WTC 1 began. As the tower collapsed, the resulting pressure increase pushed intense flames out of windows at the northern edge of the 92nd floor, at the northern edge of the 95th floor, at the southern edge of the 94th floor, and from the intensely burning region on the 104th floor, indicating the areas on the face where the most intense burning was taking place.

During this final period, people were observed falling from the upper floors of the north and west faces. It is likely that additional people fell on the other faces and were not identified due to the quality of the imagery. The fact that people continued to fall from upper floors suggests that conditions on these floors continued to deteriorate until the tower collapsed.

Summary and Additional Discussion of Observations for WTC 1 Fires

Fire growth and spread in WTC 1 was extensive during the 102 min between the aircraft impact and collapse of the tower. Figure 2–4 shows the results for the four faces of integrating the fire observations over the entire event. Extensive fires were observed from the 92nd to 99th floors. (Note that fires were also present on higher floors, including the intense fire on the south side of the west face of the 104th floor.) Fire seems to have spread over almost all of the 96th to 98th floors, while unburned areas were still present on lower floors. The largest unburned areas seem to have been on the 93rd and 95th floors.

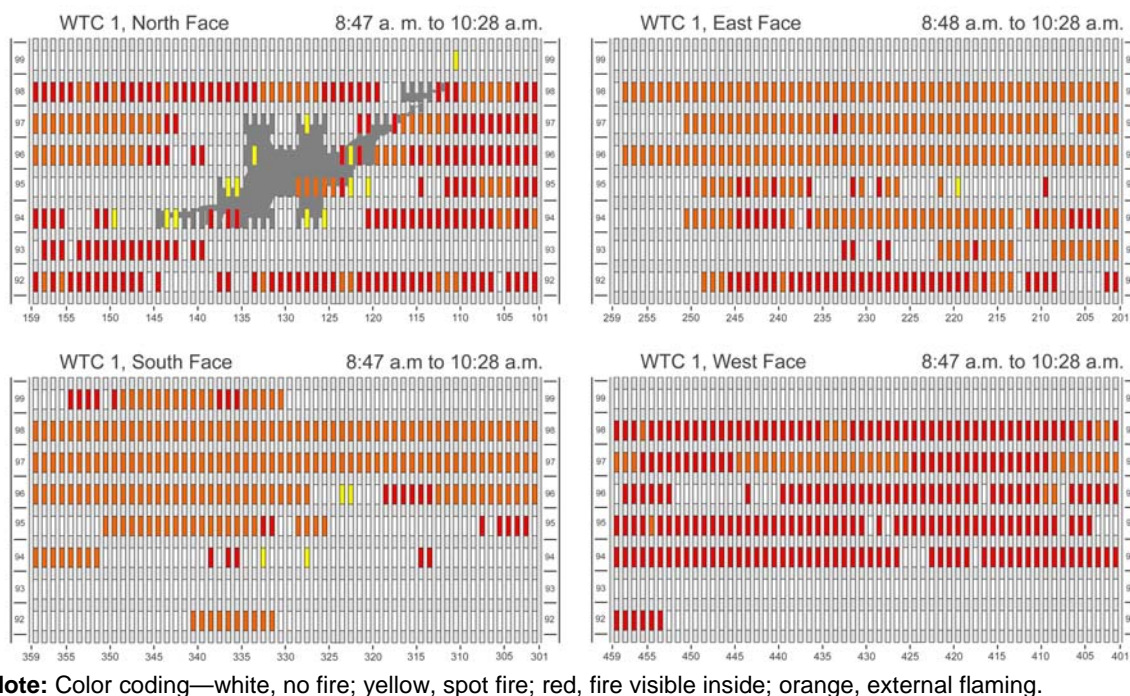


Figure 2–4. Maps of integrated fire observations between 8:47 a.m. and 10:28 a.m. for the four faces of WTC 1.

An interesting aspect of the fire behavior in WTC 1 was the variations in burning behavior observed on the different faces. Fires at most locations on the west and north faces of the towers burned without flame extension or release of large amounts of smoke from nearby windows. In many cases the fires appeared

to burn as relatively low-intensity distributed flames. The preponderance of red in the north- and west-face maps in Figure 2–4 reflects this type of burning. In contrast, the fires burning on the east and south faces most often generated external flames and heavy smoke flows at nearby windows as indicated by the façade fire maps for these faces. Various explanations for the different fire behaviors were considered. The most plausible is based on the effects of the prevailing wind. On September 11, 2001, the wind was striking WTC 1 from the northwest and then flowing down the north and west faces. This wind created positive pressures at the windows on these faces that tended to resist gas flows out of the tower. On the east and south faces the effect of the wind was the opposite, creating low pressure areas at the windows that tended to draw gases out of the building. The net effect of these pressure forces was a tendency for gases to flow internally on a floor, if a pathway was available, from the west and north faces to the east and south faces. Such internal flows provide a plausible explanation for the observed differences.

This summary focused on the time variation of the fire distributions and intensities observed in WTC 1. NIST NCSTAR 1-5A also includes detailed time lines for window condition on the various floors and faces of WTC 1. Generally, as the fires spread into new areas, window glass in the immediate vicinity would break out. As a result, the number of open windows continuously increased. This, in turn, increased the amount of outside air available to support the fires burning inside. The total number of windows that were broken open by the aircraft impact and subsequent fireballs was estimated to be 236, with the majority located on the north face where the aircraft impact occurred. By the time of tower collapse this number had increased more than five-fold to 1,312, with roughly equal numbers on each face. This increase in the number of open windows provided an additional 12,470 ft² of ventilation area.

Summary of Observed Fire Behavior in WTC 1

There was a significant difference in the fire behavior on the different faces of the towers. Fires at most locations on the west and north faces of the towers burned without releasing large amounts of smoke or flames from nearby windows. In many cases the fires appeared to be distributed fires that burned at relatively low intensities. (Three major exceptions to this were: early north face fires to the east of the impact cavity on the 96th and 97th floors and the west face of the 97th floor, the fires that developed within rooms along the facades, and the fire that developed on the west face of the 104th floor following the collapse of WTC 2.) By contrast, the fires burning on the east and south faces often generated heavy amounts of smoke and external flaming at nearby windows. (Exceptions to this general behavior included fires that developed on the east face of the 92nd floor and on the east side of the south face on the 92nd and 94th floors.) The most plausible explanation for this difference is that the prevailing wind was striking WTC 1 from the northwest and then flowing down the north and west faces. This wind created positive pressures on the windows on these faces, pressures that tended to resist gas flows out of the tower. On the east and south faces the effect of the wind was the opposite, creating low pressure areas at the windows that tended to pull gases out of the building. The net effect of these pressure forces would be a tendency for gases to flow internally on a floor, if a pathway was available, from the west and north faces to the east and south faces. Such internal flows provide a possible explanation for the observed fire behavior.

The exceptions noted above for the north and east faces provided support for this explanation. When the early fires developed on the north and west faces, most windows on the 96th and 97th floors still had glass in place on the east and south faces. As a result, internal pathways connecting the openings on the high pressure and low pressure faces did not exist. The fire burning on the west face of the 97th floor abruptly

stopped releasing smoke and flames from windows on the face at 9:06:27 a.m., when it approached the south edge of the floor. Just prior to this time there had been a bright flash of fire from a southwest window on this floor. It is likely that this was the time when windows on the 97th floor opened on the south face, providing the required internal flow pathway. A similar explanation pertains to the fire behavior on the 104th floor. In this case, the fire developed only on the west face, windows on other faces were closed, and internal flows to the east or south faces were not possible.

Since interior walls were often able to act as effective firebreaks, they would also have been able to limit internal flows from open windows on the north and west faces to other open windows at the east and south faces on the same floor. As a result, the effects of positive pressure at windows within the room would be mitigated, and underventilated fires within the room would be expected to generate the external flaming that was sometimes observed.

Displaced windows, in large part, accounted for the air supply available to the fires. The displaced windows provide a second indicator of fire intensity in that most of these (other than those broken by the initial aircraft impact) were forced out by the fires.

2.3 EVIDENCE REGARDING WTC 2

2.3.1 Time Line for the First 10 Seconds

By the time United Airlines Flight 175 struck WTC 2 at 9:02:59 a.m., a large number of still and video cameras were trained on the WTC site. More than 25 video clips of the aircraft striking WTC 2 from all four sides were included in the NIST visual database. All of these clips were placed on a common time line accurate to one video frame or 1/30 s, leading to the detailed chronology in Table 2–2. The window numbers were estimated based on observed locations relative to the width of a face and are generally accurate to ± 1 window.

As in the case of WTC 1, fuel-rich aerosol was expelled from WTC 2 and ignited to form multiple fireballs. Figure 2–5, cropped from a video shot from the east-southeast, shows the nascent fireballs and dust clouds as they appeared 1.2 s following the collision of the aircraft with the tower. Multiple small fireballs that had developed on the east face rapidly coalesced into a single fireball that reached nearly across the entire face. Less fuel appeared to have been expelled from the south face than from the east and north faces. No dust clouds or fireballs were observed on the west face.

By 4.3 s after the impact, the fireball appearances had changed significantly. Burning occurred at heights well above where the plane struck, and the fireballs became more spherical, with the fireball on the east face being considerably larger than the one on the south. Large amounts of dust, sheets of paper, and larger debris were falling below the fireballs. Burning on the south face seems to have been concentrated more on the west side with little flame evident in the cloud toward the east. Figure 2–6 shows intense fire covering nearly the entire plume on the north face. The highlighted areas are two large pieces of aircraft debris that passed through the building.

Table 2–2. Time line for events immediately following the plane strike on WTC 2.

Time (s)	Observation
0	Aircraft struck WTC 2
0.03	Bright orange flash seen from the aircraft body in the vicinity of the tower wall, only apparent for one frame
0.17	Puff of dust appears on the 81 st south face near a window
0.20	Aircraft disappeared completely inside the tower
0.23	First appearance of damage and dust on the 82 nd floor east face
0.26	Additional damage and dust appeared on east face of the 82 nd floor
0.30	Damage and dust appeared on the east face 81 st floor
0.40	Initial damage and dust appeared on the northeast corner of the 81 st floor
0.50	Large object exited north face in vicinity of intersection of 81 st and 82 nd floors
0.50	Damage and dust appeared on the east face of the 81 st floor
0.56	Fire appeared on the east face in the dust plume in the vicinity of window on the 82 nd and spread rapidly through the plume
0.56	Damage and dust appeared on the north face of the 79 th floor
0.59	Fire appeared on the south face in dust plumes located in vicinities of windows on the 79 th and 81 st floors
0.59	Fires appeared on the east face in other dust plumes on 81 st and 82 nd floors and expand rapidly
0.59	Damage appeared on the southern edge of the east face
0.63	Aluminum panel damaged on the southeast corner of the 82 nd floor
0.63	Flames appeared in 14 windows on the east face of the 83 rd floor
0.63	Line of fire covering 11 windows on the north face of 81 st floor
0.66	Fires expanded on the north face covering 28 more windows on the 80 th through the 82 nd floors
0.66	Fire appeared outside of the north face as observed from the east
0.66	Fire appeared in a dust plume on the south face
0.86	Damage appeared at windows on the 78 th floor
0.89	Dust cloud appeared at upper level of mechanical equipment room vents on north face of 76 th floor
0.92	Line of fire covering 8 windows on the 79 th floor appeared
0.99	Dust clouds appeared on upper and lower levels of the mechanical equipment room vents on the east face of the 75 th and 76 th floors
1:02	Damage appeared near window on the 80 th floor
1:09	Line of fire appeared in 2 windows on the 80 th floor
1:2	Three distinct fireballs visible outside the north face
4.3	Buoyancy carried fireballs upward, and their burning was above the impact floors; extensive debris was falling below the fireballs
6.5	Flames reached their maximum extension
8.7	Significant reduction in extent of visible flames in the fireballs
11	Fireballs extinguished



Figure 2–5. The nascent fireballs and dust clouds formed on WTC 2 1.2 s after the aircraft struck WTC 2.



Figure 2–6. Photograph of the towers recorded from the north-northeast 4.3 s after the aircraft struck WTC 2.

The fireballs continued to expand and rise for several more seconds before receding. Videos indicated that the fireball created on the east face lasted 11 s, that on the north face lasted 10 s, and that the small fireball on the south face lasted about 8 s. An analysis similar to that for WTC 1 indicated that less than one sixth of the jet fuel burned immediately within the building. Three previous estimates (McAllister 2002, and two in Baum and Rehm 2005) found that about 10 percent to 25 percent of the total jet fuel burned outside WTC 2. Since most of the fuel that formed the fireballs came from the starboard fuel tank, this suggested that 20 percent to 50 percent of this fuel burned externally with another few percent consumed inside the building. The remainder of the fuel was left behind in the tower following the initial fire. Almost all of the fuel in the aircraft's port fuel tank was also inside, primarily on the 78th and 79th floors. There was no visual evidence that the fuel from the port tank fuel burned in the short term.

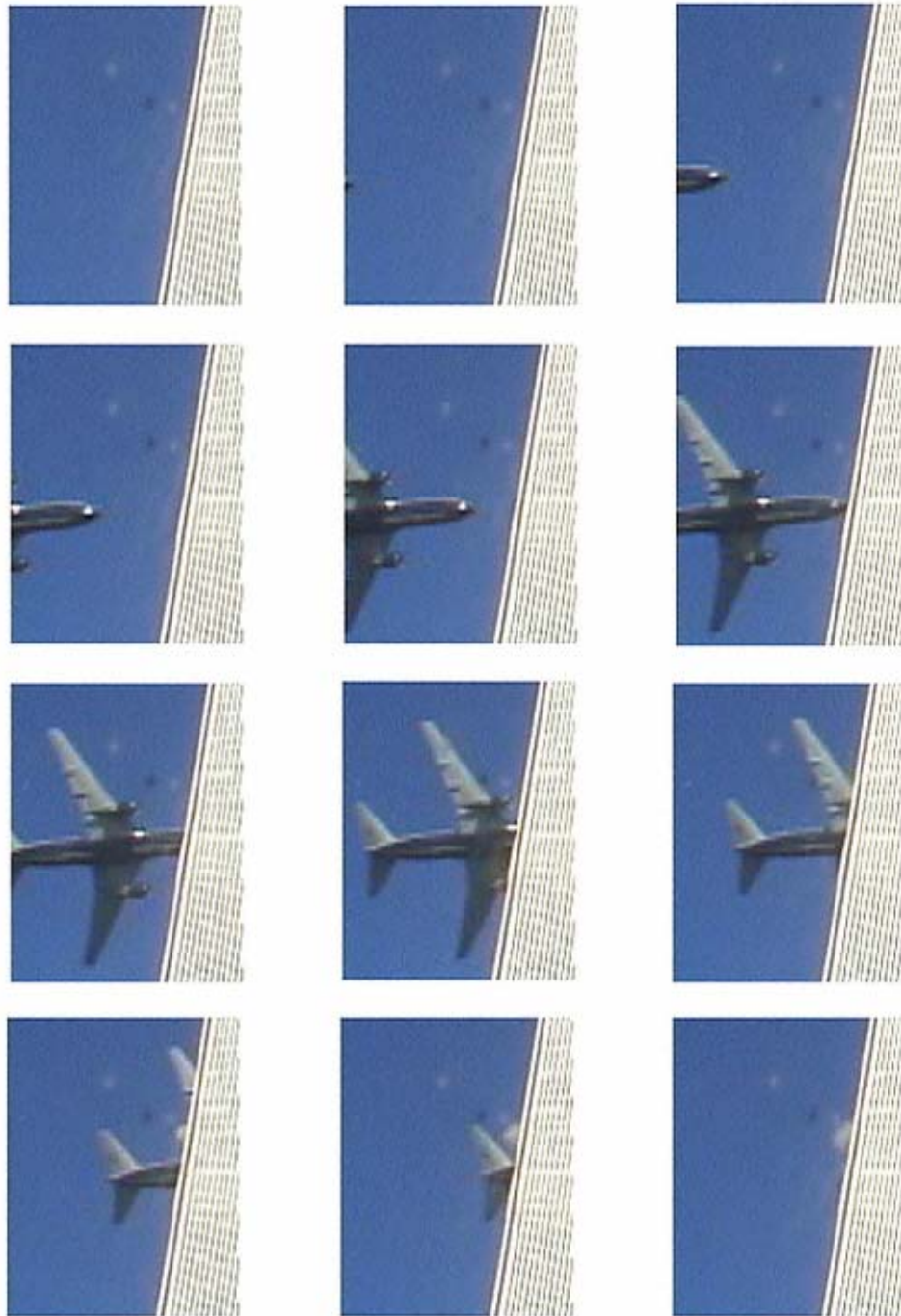
2.3.2 Estimated Aircraft Speed

Figure 2–7 is a series of cropped video frames that show the aircraft approaching WTC 2 and disappearing inside. In each digital frame, NIST determined the separation of the nose and tail from the point where the aircraft passes out of sight behind the corner of the building. Figure 2–8 shows the pixel locations of the nose and tail of the aircraft as a function of time. The lines are virtually parallel, indicating that the tail did not slow as the aircraft entered the building. The time between when the nose and tail passed the reference location was 0.194 s. Since the length of the fuselage was known to be 155.0 ft, the speed was estimated to be 799 ft/s (545 mph). An uncertainty estimate based solely on the uncertainty in the determined time difference yielded a value of ± 18 mph with 95 percent confidence. A more sophisticated motion analysis (NIST NCSTAR 1-2A) generated a value of 542 mph ± 24 mph.

2.3.3 Determination of Primary Oscillation Period

Close examination of the stable video revealed a perceptible movement of WTC 2 after it was struck by the aircraft. The building rocked back and forth, much like a pendulum, for many minutes. The stable nature of a video shot from the east allowed a detailed analysis of the north-south and torsional (twisting) motion of WTC 2 to be performed using image analysis of the Moiré patterns. Figure 2–9 shows the position of a location on the tower on the 70th floor as a function of time. A large increase in the motion of the tower followed the aircraft impact and slowly decreased after that. The peak amplitude of the movement in the north-south direction was determined to be 12 in. ± 1 in. at the 70th floor, which extrapolated to a value of 20 in. ± 3 in. at the roofline. Frequency analysis of the results revealed the fundamental north-south mode to have a period of 11.4 s, a torsional mode with a period of 5.3 s, and two higher frequency modes with periods of 3.9 s and 2.2 s. All periods were determined to an accuracy better than ± 0.1 s. The period of the fundamental mode was consistent with the expected range based on measurements of similar frequencies in WTC 1 (NIST NCSTAR 1-2). Similar measurements using a short video shot from the north yielded an amplitude of 12 in. ± 2 in. for the east-west motion, with a period of 5.3 s.

A moiré pattern is an optical effect that develops when objects having sets of lines are viewed simultaneously. In the case of this video, the lines correspond to the vertical rows of windows and columns on the tower and the vertical rows of pixels in the camera. In effect, the interactions of the lines allow motion to be followed with finer resolution than is available in the image.



© 2001 Scott Myers

Figure 2–7. Sequential cropped frames taken from a video showing the aircraft approaching WTC 2. The frames are separated by 33.3 ms.

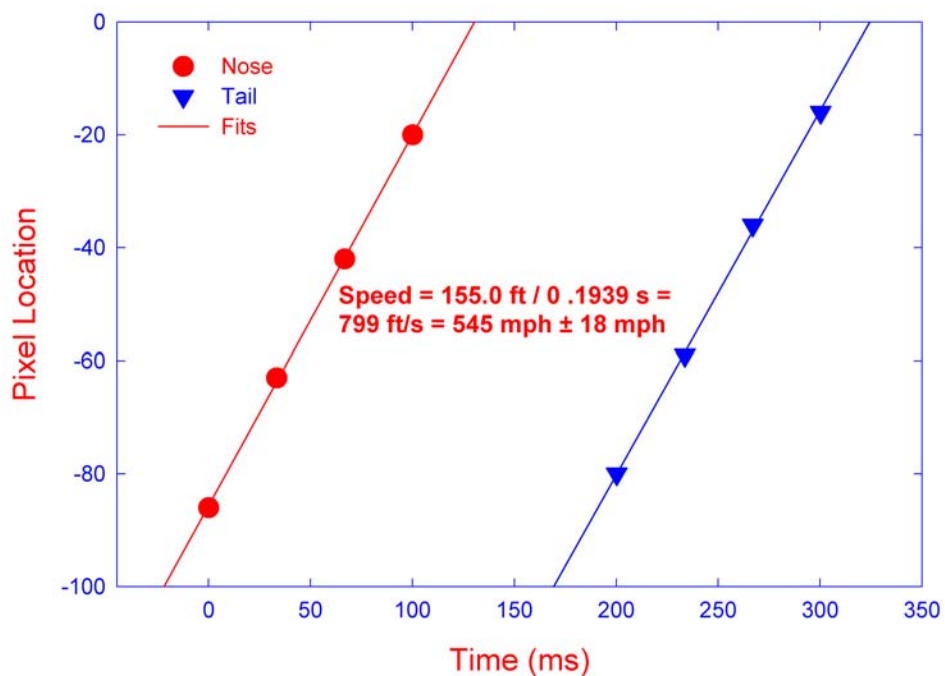


Figure 2-8. Plots of pixel locations for the nose and tail of the aircraft that struck WTC 2 as a function of time taken from the images shown in Figure 2-7.

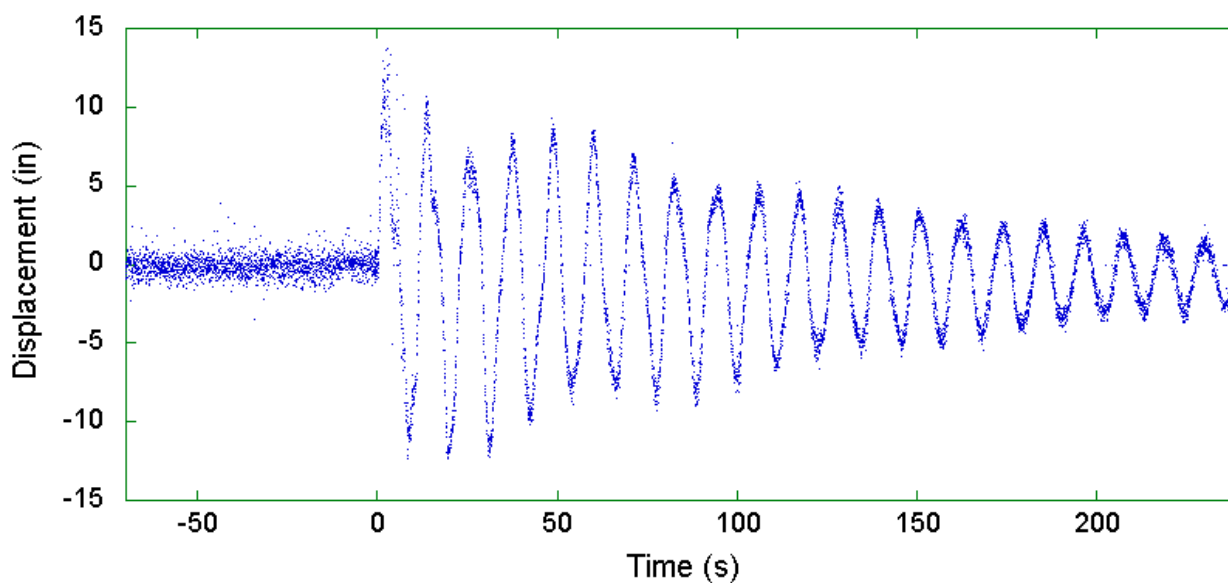


Figure 2-9. Displacement of the left-most window line on the 70th floor of WTC 2 as a function of time, determined using Moiré analysis.

2.3.4 Observed Impact Damage

When the aircraft struck WTC 2, it disappeared into the tower leaving a hole shaped like the aircraft. Very shortly after this a large cloud of debris and burning fuel exited the tower from the strike location, obscuring the strike point. As the fireball rose and the dust cloud cleared the hole in the building became visible once again.

A summary of the observed damage to the south face indicated:

- The nose of the aircraft struck well east of the center of the face. The aircraft was headed slightly to the east of perpendicular at the point of impact.
- The impact damaged the 77th floor through the 85th floor. The left wing tip marked the spandrel located below the 78th floor slab and the right wing marked column 404 on the 85th floor.
- Windows near the plane strike location were removed. A few of the windows further away were blown out by the overpressure generated by the initial fireball formation within the building.
- Portions of the aluminum cladding that formed the curtain wall for the building were partially or completely removed at locations close to the where the plane struck.

There was a great deal of debris piled on the right-hand side of the opening created by the plane. This debris along with the depth of the opening indicated that floors in this area were partially collapsed by the collision. There was insufficient information from the photographs to determine the exact areas over which the floor collapses occurred or their extent inside the building. Visual evidence suggested that at least some of the concrete in the floors was pulverized during the collision.

The largest areas of damage to the east façade were to the 80th, 81st, and 82nd floors. The body of the aircraft struck the first two of these; the third was where the majority of fuel from the starboard fuel tank was dumped. Much less damage is apparent on the 79th floor, where most of the fuel from the aircraft's port tank should have been released.

- Substantial areas of the aluminum curtain wall on the 80th and 81st floors were pushed out and partially removed.
- There were large piles of debris at the northeast corner of the 80th and 81st floors. It is likely that a large fraction of this debris was derived from the aircraft since its body impacted on these two floors. This suggested that either the debris was reflected from the core or that the plane was moving toward the east when it struck the tower, since the nose struck near column 421 on the south face. **I**t is likely that one of the aircraft's engines passed through this corner.

Large fires were ignited on the north face near the east side, making early observations of conditions in this area difficult.

The damage on the north face was inclined at an angle that roughly matched that at which the aircraft struck the tower on the opposite face. This suggested that debris from the aircraft tended to pass straight through the tower, perhaps being guided by the floor slabs.

- Significant areas of the aluminum curtain wall were removed, most prominently in a roughly rectangular area extending across 12 columns and covering the 80th, 81st, and 82nd floors. This was where the nascent fireball was first observed. Very little fire was observed in this area following the fireball and before the collapse of the tower. As a result this area has been called the “cold spot.”
- Large piles of debris were evident, extending from the northeast corner about eight windows toward the west on the 80th and 81st floors. These were the same floors where piles were observed on the east face at the north edge, suggesting that the debris had essentially filled up the corners of the tower on these two floors. A third pile of debris could be seen on the 79th floor, extending roughly from column 231 to column 240. These windows overlapped an area where a distinct line of fire appeared on this floor 0.92 seconds after the plane strike.
- One perimeter column in the north face was severed just below the spandrel between the 81st and 82nd floors. The adjacent column was severely bent. This damage must have been the result of a large part of the aircraft passing through the tower.
- Several windows were missing on the 78th and 79th floors.
- Though aircraft and/or parts of the building exited the facade on the north face on the 78th floor at two locations, no fire was observed emanating from this floor.

2.3.5 Debris Expelled by the Aircraft Impact

- Several pieces of the aircraft passed all the way through the building and exited at high velocities from the north side. Most of these were relatively small, but at least two were of substantial size. One, a portion of one of the jet engines, exited the northeast corner of the 81st floor and landed roughly 1,500 ft from the north side of WTC 2. The other, a landing gear assembly, exited in the vicinity of window 253 on the 81st floor and damaged the roof of a building at 45 Park Place, over three blocks to the north. Assuming the exit locations were identified correctly, the engine component exited the building moving toward the east at an angle of roughly 17 degrees to the normal with the north face, while the corresponding angle for the landing gear was approximately 12 degrees.
- There was a great deal of small debris, such as crushed pieces of concrete, and flaming material spread over the plaza. This most likely fell primarily from the north face of WTC 2 since this side overlooked the plaza.

Following the aircraft impact on WTC 2, the debris field on the south side of the building was noticeably increased.

2.3.6 Fire Behavior Following the Aircraft Strike

NIST NCSTAR 1-5A contains façade maps that summarize the visual analyses of window condition, fires, and smoke for the four faces of WTC 2 as a function of time. The fire behaviors are summarized here.

Compared to WTC 1, there was relatively little fire spread in WTC 2 during the 56 min between the impact of United Airlines Flight 175 and the collapse of the tower. One approach for characterizing the fire spread in WTC 2 was to compare integrated façade maps for the entire period from 9:03 a.m. to 9:59 a.m. with the initial fire distributions shortly after the aircraft impact.

Similar to the analysis for WTC 1, changes in window condition were used as a rough indicator of fire spread. This is less valuable for WTC 2, because the number of windows opened by the aircraft impact and subsequent fireballs was much larger than for WTC 1, and the ratio of windows open at the time of collapse was only about 40 percent larger than at 9:04 a.m. (Table 2–3). This is far smaller than the corresponding increase in WTC 1, which exceeded a factor of 4.5. This large difference reflects:

- In WTC 2, there were more windows broken by the aircraft impact and subsequent fireballs, particularly on the east face.
- The time available for the fires to break windows in WTC 2 was less than for WTC 1.
- The early rates of the development of fires were much slower for WTC 2 than for WTC 1.

As a result of the small increase in ventilation area, the effect of changes in the number of open windows was much less important for the fire behavior of WTC 2 than for WTC 1.

Table 2–3. Summary of open windows observed on faces (78th through 84th floors) of WTC 2 at 9:03 a.m. and 9:58 a.m.

Face	Number of Open Windows 9:03 a.m.	Number of Open Windows 9:58 a.m.
North	78	159
East	222	258
South	133	196
West	0	7
Total	433	620

2.3.7 Observed Fire Behavior in WTC 2

The following discussion of fire behavior in WTC 2 is broken into four time periods of roughly 15 min each. This summary focuses on fire observations, but includes some relevant structural observations. Details of the fire behavior as a function of time are documented in façade maps describing fire, smoke, and window condition observations included in Appendices G to J of NIST NCSTAR 1-5A. Detailed discussions of the fire observations, with numerous supporting images of the tower, and other related details such as window breakage, smoke flow, hanging objects (which may have been dislodged floors) observations, and unusual intense burning phases are available in the report.

9:03 a.m. to 9:15 a.m.

As described earlier, immediately after the aircraft impact intense fires, located on piles of debris, were visible burning on the north face of the tower adjacent to (and within) the northeast corner on the 81st floor and just to east of the center of the face on the 79th floor. During the period, it became clear that flames were also present on the 82nd floor immediately above the fire on the 81st floor and on the 80th floor immediately above the fire on the 79th floor. All of these fires continued to burn intensely during the entire period, and there was little indication of fire spread on the north face. Flames were not visible in a large rectangular area, which has been designated the cold spot, lying between the two burning piles of debris on the east side of the north face. The cold spot extended over twelve windows on the 80th, 81st, and 82nd floors. Near the end of the period closer images revealed that a number of objects were hanging across windows in and immediately adjacent to the cold spot on the 80th and 81st floors. As discussed below with regard to the east face, one possible explanation for these hanging objects is that they are sections of floor slabs that have been dislodged from the outer wall and have settled down below the spandrels at the tops of the windows.

In the immediate aftermath of the aircraft impact, extensive fires were visible through open windows on the east face of the tower coming from the 81st, 82nd, and 83rd floors. On the two lower floors intense continuous fires were burning on debris piles that covered nearly one-fourth of the floor widths extending to the south from the northern edge. The fire on the 83rd floor was intense, with external flames, and covered roughly one-fifth of the tower width at a location slightly to the south of the face center. Much smaller fires were present at other isolated locations on the face. Very shortly after the aircraft impact a hanging object was visible draped across the tops of 18 82nd floor windows (i.e., nearly one-third of the face width) near the center. This hanging object was observed numerous times in later images. While it proved difficult to identify the object with certainty, the evidence suggests that it was a portion of the 83rd floor concrete floor slab that had been dislodged from the spandrel located above the 82nd floor and had settled downward several feet, where it could be seen through the windows. The fact that the hanging object was visible so shortly after the aircraft impacted suggests that it was dislodged at some point during the impact and subsequent fireballs. It is reasonable to infer that the separation of the 83rd floor slab from the spandrel may have resulted from the overpressure on the 82nd floor generated by burning aviation fuel. By 9:06 a.m., the intense flames burning on the south side of the 83rd floor were receding back into the windows and were less prominent than earlier. At the same time, a new area of fire was growing near the center of the southern half of the 82nd floor. By the end of the period the fire on the south side of the 82nd floor had spread north to cover numerous windows, while the fire on the 83rd floor was no longer visible. The fires on the north sides of the 81st and 82nd floors had died down to the point where intense burning was primarily occurring near the northeast corner.

Shortly after the aircraft impact, only relatively small isolated fires were visible on the south face on the 78th floor, located just to the right of the aircraft impact cavity, and the 79th floor, within the cavity. During the following 12 min, similar small fires grew around the aircraft impact cavity on the 80th and 81st floors. More significant fires appeared in the windows between the aircraft impact cavity and the eastern edge of the face on the 81st and 82nd floors starting around 9:07 a.m. Both areas were burning at the end of the period.

The west face of WTC 2 remained clear of smoke and fire until 9:10:29 a.m., when a plume of smoke appeared from a window on the south side of the 86th floor. This location was well above the floors with

observed fire. A likely explanation for the appearance of smoke at this time is that people trapped in the tower broke out a window and released smoke that had built up on this floor. This indicates that smoke was traveling upward through the tower. Several windows were open at this location at 9:15 a.m.

In summary, during this time period, the major visible fires were burning on the east and north faces of the tower. The most intense fires were on the 81st through 83rd floors, i.e., the upper portion of the floors impacted by the aircraft.

9:15 a.m. to 9:29 a.m.

Near the start of the period, an infrared image which provides an indication of the heat distribution of the WTC 2 façade was taken from the northeast. On the north face, strong heating was evident from the fires burning on the 79th and 80th floors and the 81st and 82nd floors. The cold spot stands out in the image because the area was close to the ambient outside temperature. Standard photographs and videos showed that the primary fire distributions on the north face did not change dramatically during the period. The fires in the northeast corners on the 81st and 82nd floors and near the center of the face on the 79th and 80th floors continued to burn intensely. Near the end of the period a relatively low intensity fire became visible on the 83rd floor near the eastern edge of the face. Smoke was observed coming from windows on the south side of the face on the 93rd, 103rd, and 105th floors, indicating that smoke had migrated to the top of the tower. These windows were most likely broken open by people at these locations.

The infrared image taken at the start of the period revealed strong heating across the entire width of the 81st floor on the east face, suggesting either that the fire observed on the north side of the face was heating the entire floor or that unseen fires were burning inside. Standard images showed that the fire burning on the south side of the 82nd floor was dying down somewhat while continuing to spread to the north. The fires in the northeast corner of the 81st and 82nd floors continued to burn intensely. A short-lived fire was present on the eastern edge of the 83rd floor. Most often there was no smoke flow from open windows on the face below the 82nd floor, but increasingly frequent short-lived puffs of smoke were observed from multiple open windows on the 79th, 80th, and 81st floors. Sometime between 9:18 a.m. and 9:26 a.m. a portion of the hanging object visible through the 82nd floor windows on the east face settled down further in the windows, revealing the plate-like structure that would be expected for a floor slab.

By shortly after 9:15 a.m. a new area of fire had grown on the 79th floor to the immediate east of the aircraft impact cavity on the south face, adding to the fires burning in the immediate vicinity of the cavity. The fire observed earlier on the 81st floor between the cavity and the east edge of the face was dying down, while the fire immediately above on the 82nd floor continued to burn intensely. This fire distribution changed little over the period. There were indications that smoke flows on the south face increased at the some of the times that smoke puffs occurred on the east face.

Early in the period smoke was observed flowing from windows near the center of the 107th floor on the west face as well as from the locations on the 86th floor seen earlier. The smoke flow from the 107th floor suggests that smoke had traveled to the top of the tower by internal pathways, and, due to its buildup, people on the floor chose to break out windows to reach fresh air. These two smoke flows were the dominant features for the west face during the period.

Minimal fire spread took place during this period. The fire distributions on the east face for the two periods appear quite different due to the rapid changes in the fires observed near the beginning of the first

period and the continued spread of the fire on the 81st floor, that initially appeared on the south side of the face to the north while going through a cycle of growth, intense burning, and decay. As during the initial time period, the largest fires were in the northeast corners of the tower on the 81st and 82nd floors and near the center of the north face on the 79th and 80th floors. These fires had been burning since the aircraft impact and were dying down very slowly.

9:29 a.m. to 9:45 a.m.

Compared to the two earlier time periods, the fire behavior was more dynamic and difficult to characterize during this time. A number of other related observations were made simultaneously.

Shortly after 9:29 a.m., an intense flame suddenly erupted on the north face from a window on the 83rd floor just above and to the right of the cold spot and quickly spread to cover several windows. Later a fire erupted on this floor several windows further to the west and again rapidly covered multiple windows. These fires were the first indication of significant fire spread on this face. Meanwhile, flames on this floor spread to cover most of the area between the east edge and the new fire area. Shortly after 9:30 a.m. there were indications that the fire on the 79th floor near the center of the face had also begun to spread to the west. The fires on piles of debris in the northeast corner and near the center of the face continued to burn throughout the period. Close-up photographs shot near the end of the period revealed that the appearances of the hanging objects observed earlier through windows in the cold spot had changed. At the earlier time two objects were visible on the 80th floor, but now the lower object had apparently disappeared, while the second had dropped down lower. A similar change had taken place on the 81st floor.

Observations on the east face for the period were complex. The fire near the center of the 82nd floor continued moving toward the north, eventually approaching the north edge. Meanwhile, the fires in the northeast corner on the 81st and 82nd floors continued to burn, with that on the 82nd floor growing more intense. Shortly after 9:30 a.m., heavy smoke started to flow from a group of windows located near the center of the northern half of the 79th floor where the glass had been in place minutes earlier, suggesting that a fire had recently grown in the immediate vicinity. Fire was later observed in this area in several images and was still present at the end of the period. Around this time, three people either tried to climb down or fell from a window on the south side of the 79th floor, providing a possible indication that conditions were rapidly deteriorating in the area. The unusual short-lived smoke puffs from windows on the face described earlier continued, apparently randomly, throughout the period. Some of these released sufficient smoke to briefly obscure the face. In some instances smoke was also pushed simultaneously from windows on the north and south faces. Another type of transient behavior was first observed starting around 9:35:45 a.m. Heavy smoke began flowing out of numerous windows over the face and was particularly heavy near the centers of the 79th and 80th floors. Unlike observed for the smoke puffs, intense flames were also visible coming from many of these windows and, instead of lasting only a few seconds, the heavy smoke and flames were present for just over a minute before they abated as quickly, seemingly, as they appeared. This roughly one-minute widespread release of heavy smoke and flames represents a distinct type of behavior from the short smoke puffs and more typical burning behaviors seen up to this time. This unusual event was not unique. Two similar releases of smoke and fire, each lasting roughly one minute, were observed during periods starting just before 9:40 a.m. and after 9:42 a.m. A photograph taken around 9:38 a.m. showed that the hanging object (possibly the 83rd floor slab) visible earlier through open windows on the east face had once again dropped further

down and that some intermediate portions had disappeared from view. The windows where the object first appeared below the 83rd floor spandrel had moved further toward the edges of the tower on both the north and south ends. Figure 2–10 shows a photograph of the east face taken just before 9:45 a.m. during a period when there was very little smoke flow from the face. Closer inspection reveals that the columns near the center of the east face on the 80th and 81st floors were bowed inward. Similar bowing was identified in other images starting as early as 9:22 a.m.

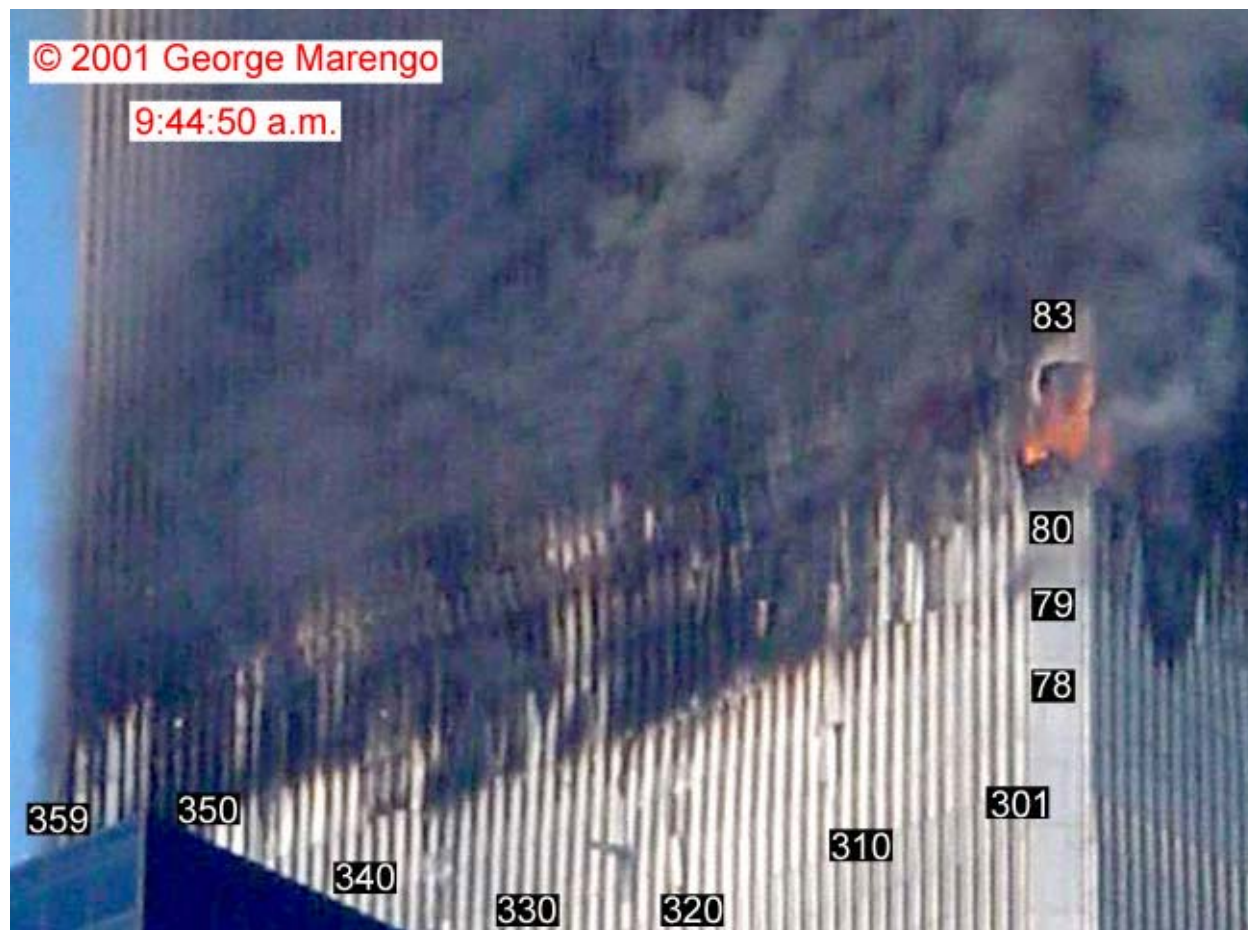


Figure 2–10. Photograph was shot from the northeast, showing east face of WTC 2 at 9:44:50 a.m. The original intensity levels have been adjusted, and column and floor numbers have been added.

On the south face, several relatively low-intensity fires continued to burn on multiple floors around the aircraft impact cavity. The fire on the 82nd floor located between the cavity and the eastern edge was still burning. Near the start of the period a small fire became visible near the center of the 83rd floor. Roughly half way through the period smoke began to flow and flames became visible on the 80th floor near the eastern edge. A view of the upper part of the tower revealed heavy smoke flowing from numerous windows on the 105th floor just to the west of face center. This was another location where people likely broke open windows.

On the west face, the number of open windows with smoke flow continued to increase, with smoke now observed on the 84th, 86th, 88th, and 107th floors. Smoke was also visible at the top of the tower next to the

southwest corner. This smoke appeared to be flowing from a location on the lower level of the mechanical equipment room on the 108th and 109th floors, where there was a nearby fresh air intake for the 107th floor observation area, suggesting that the smoke was back flowing from the 107th floor. There was still no indication of fire burning on this side of the tower.

In summary, during this period, new areas of fire appeared on the 79th and 83rd floors of the north face. Extensive new areas of fire were also present on the 79th and 80th floors of the east face. It should be remembered that a significant fraction of the observed fire on these floors was associated with the three roughly one-minute-long periods of heavy smoke flow from these floors.

9:45 a.m. to Collapse of WTC 2 at 9:58:59 a.m.

Near the start of the period several small fires were observed for the first time near the center of the cold spot on the north face at the 81st and 82nd floors. Fires elsewhere on the face were generally dying down at this time. During the period, the fire burning on the 79th floor continued to spread to the west. By the time of collapse, the flames were approaching, but had not yet reached, the west face. Around 9:54 a.m. a fire grew just to the west of the cold spot on the 82nd floor and began to spread westward, covering eight windows by the time of collapse. The fire that had earlier spread in the same direction on the 83rd did not appear to migrate further. A small spot fire was observed near the center of the 84th floor, suggesting that the fire on the 83rd floor had spread upward. Close-up photographs and videos during the period revealed a distinct outward bulge of the steel columns in the vicinity of the debris pile near the center of the 79th floor. Just before 9:52 a.m., puffs of smoke and/or dust were expelled from multiple locations on the north face near the east edge. Almost immediately a bright spot appeared at the top of a window on the 80th floor four windows removed from the east edge, and a glowing liquid began to pour from this location. This flow lasted approximately 4 s before subsiding. Many such liquid flows were observed from near this location prior to the collapse of the tower. Several were accompanied by puffs of dust and smoke that were now occurring frequently. The composition of the flowing material can only be hypothesized, but it is considered likely that it was molten aluminum that came from aircraft debris located immediately above on the 81st floor and had been heated by the fire burning on that floor. Shortly after 9:53 a.m. the fire that had been burning on the eastern edge of the 81st floor since the aircraft impact suddenly died down, revealing the windows above on the 82nd floor. A hanging object was visible through these windows that appeared to be a dislodged corner section of the 83rd floor slab. The hanging objects present in and near the cold spot were also visible in images taken during the period. At 9:58:59 a.m. WTC 2 began to collapse. Videos show that the only place flames were pushed out of windows on the north face was from the burning area near the western edge of the 79th floor.

A fourth short-lived (again roughly a minute) release of heavy smoke and flame from windows on the 79th and 80th floors of the east face occurred around 9:45 a.m. Three additional, somewhat less intense, releases lasting similar lengths of time occurred around 9:47 a.m., around 9:52 a.m., and just before 9:56 a.m. Smoke puffs, similar to those seen earlier, occurred multiple times during the period. At the start of the period the fire located at the center of the northern half of the face on the 79th floor continued to burn vigorously, only dying down near the end. A similar burning area became visible on the 80th floor just to the south of the fire on the 79th floor around 9:55 a.m. Much of this area had been hidden up to this time by smoke coming from below. A substantial fire continued to burn on the 82nd floor near the northern edge of the face. The fire in the northeast corner of the 81st floor was generally gently burning, but would occasionally flare up. During the period, the position of the hanging object visible through

windows on the 82nd floor moved again, with the northernmost window where it first became visible shifting slightly to the north. A prominent feature on the east face during the period was the inward bowing of the outer wall. This can be seen clearly over the 79th to 82nd floors in Figure 2–11, which was taken less than a minute before the collapse started. During the 20 s prior to the collapse a large number of pieces of debris fell from the northern sides of the 80th and 81st floors. The falling debris coincided with a heavy flow of molten metal from the north face. When WTC 2 collapsed very little flame was expelled from the east-face windows. Based on observations elsewhere on the two towers, regions of intense burning would have been expected to generate short-lived jets of flames. Their absence suggests that large fires were not burning near the face at the time of collapse.



Figure 2–11. Cropped photograph of the east face of WTC 2 at 9:58:02 a.m. The intensity levels have been adjusted, and column and floor numbers have been added.

At the beginning of the period a number of small fires were visible on several floors of the south face at locations surrounding the aircraft impact cavity. Their positions suggest these were continuations of the slow spreading fires that had grown around the cavity shortly after impact. The fire that had grown earlier between the cavity and the east edge of the 82nd floor continued to burn gently. Around 9:48 a.m. a brief flash of flame was observed from a window to the west of the impact cavity on the 80th floor, and just before 9:53 a.m. a substantial amount of smoke was released from windows still further to the west. Shortly afterward flames were observed spreading across the floor at this location from east to west. By the time of collapse an intense fire was burning near the center of the western half of the 80th floor and extended over roughly one-fifth of the floor width. As WTC 2 began to collapse, the only significant flames pushed out of open windows on the south face came from this fire area.

Views of the west face during the period showed smoke flowing from open windows on the 84th, 86th, 88th, 91st, 105th, and 107th floors and from the southern edge of the mechanical equipment room on the

108th and 109th floors. There were no visible indications that fires capable of breaking out window glass had reached the west face of WTC 2 prior to the collapse.

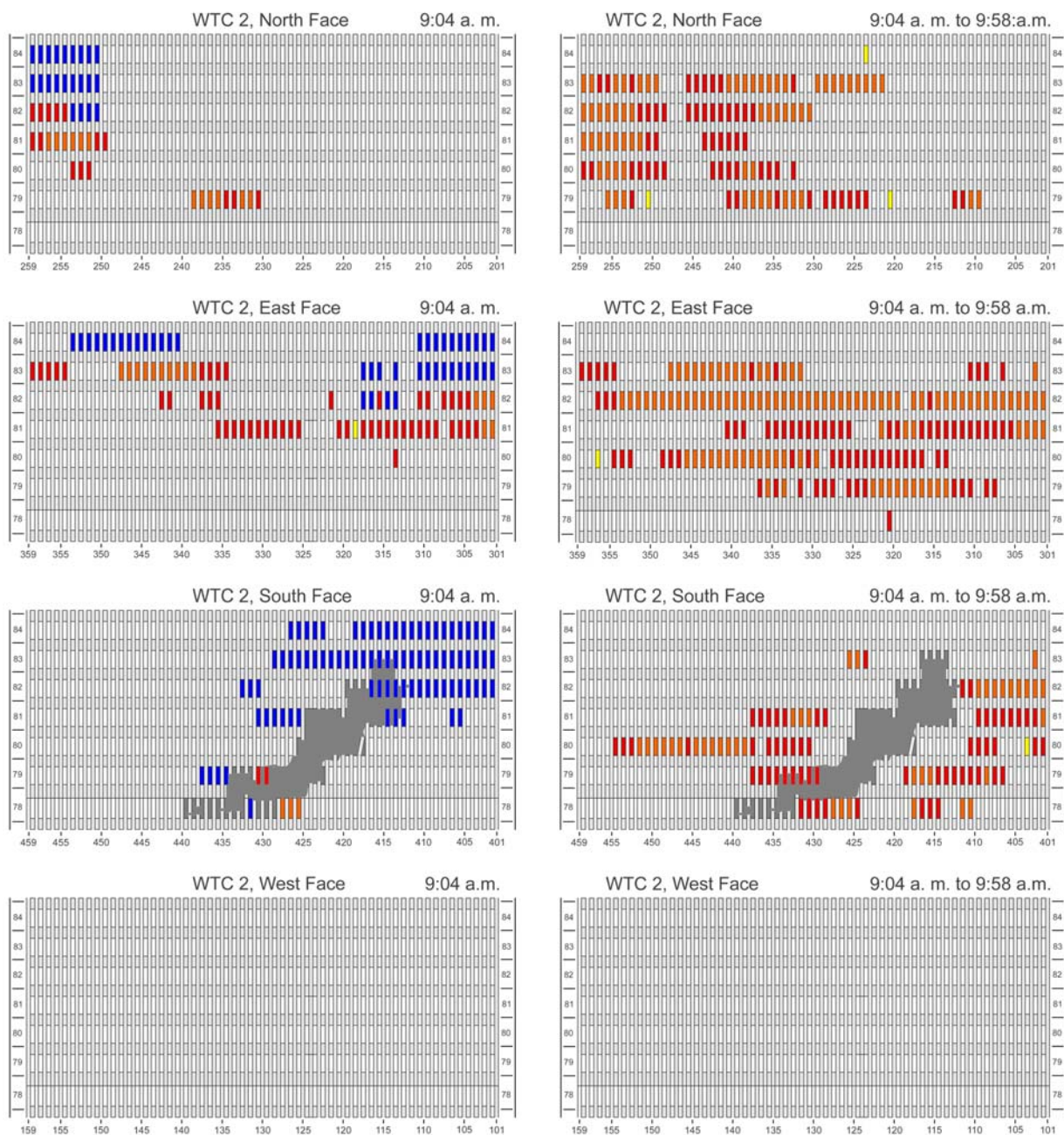
Many of the fires present during earlier periods were either no longer visible or were dying down during the final interval prior to the tower collapse. Some fire spread to the west has taken place on several floors on the north face. Areas with substantial fires include those on the north sides of the east face on the 79th and 80th floors (recall that the observed fires are combinations of sustained fires and short-lived flame releases) and the intense fire that grew on the west side of the south face at the 80th floor.

Summary and Additional Discussion of Observations for WTC 2 Fires

Compared to WTC 1, there was less observed fire spread in WTC 2, even when the differences in available time (102 min for WTC 1 and 56 min for WTC 2) are taken into account. Figure 2–12 compares WTC 2 integrated façade maps of fire observations for the entire 56 min period with initial fire distributions present shortly after the aircraft impact. Primary areas of fire growth and spread include the east side of the 83rd floor and locations to the west of the cold spot on several additional floors of the north face, much of the 81st floor and extensive areas toward the centers of the 79th and 80th floors on the east face, and areas on either side of the aircraft impact cavity on the south face, particularly to the west side of the 80th floor and to the east on the 81st and 82nd floors. The absence of visible fire suggests that substantial fires did not reach the west face of the tower during the available time.

Similar differences between WTC 1 and WTC 2 become apparent when changes in window condition (discussed in detail in NIST NCSTAR 1-6A) are considered. Recall that for WTC 1 the number of open windows following the aircraft impact (roughly 236) increased by more than a factor of five as a result of fire spread. For WTC 2 the number of open windows (estimated as 433) immediately following the aircraft impact was considerably larger, mostly due the fact that the aircraft struck toward the east side of the south face and caused extensive façade damage and window breakage along the east face and east side of the north face. When WTC 2 collapsed the estimated number of open windows was 620, having increased by less than 50 percent, reflecting the limited fire spread that had taken place.

A curious aspect of the fire behavior in WTC 2 was the presence of the cold spot on the north face, which covered three floors over a length equal to one-sixth of the face width. The existence of the cold spot implies that little fuel was available in the immediate vicinity to support burning. A number of possible explanations were considered for the absence of fuel. One is that the area was vacant and that there was limited fuel present prior to the aircraft impact. NIST is unaware of any information that supports such a conclusion. A second possibility is that the fireballs that exited through the area were so intense that they pushed most available fuel in the area to the sides or out through the opened windows. A third possibility is that the floor slabs, particularly on the 81st and 82nd floors, in the immediate area collapsed during the aircraft impact and fireballs, in effect, creating a cavity behind the cold spot. The available visual evidence both supports and argues against all three possibilities. NIST has concluded that insufficient information is available to allow a likely formation mechanism for the cold spot to be postulated.



Note: Blue represents windows where observations were not possible.

Figure 2–12. Maps of observed fire distributions on the four faces of WTC 2 shortly after the aircraft impact (near 9:04 a.m.) and corresponding integrated fire observations for the entire period between 9:03 a.m. and 9:59 a.m.

Additional unusual behaviors observed for WTC 2 included the correlated smoke puffs observed over large areas of the façade and the roughly one-minute periods during which the smoke flows increased dramatically, often accompanied by external flames. These events were usually most evident on the 79th and 80th floors of the east face, but could often be detected on other floors and faces as well. At least

65 occurrences of smoke puffs were documented along with seven times when the one-minute long smoke releases took place.

The evidence suggests that these smoke puffs resulted from pressure pulses generated within the tower and transmitted to other locations. It is considered likely that, while these pressure pulses were of sufficient magnitude to affect smoke flows over multiple faces and floors, they were much too small to affect the tower's structural components. For most of the smoke puffs, there was no visual indication of the event that generated the pressure pulse or its location. In a few cases, such as when molten metal poured from the tower, circumstantial evidence indicated that the puffs were associated with specific observed events.

The roughly one-minute-long periods of heavy smoke flow were easily distinguished from the smoke puffs due to their persistence and the presence of flames. The short-term release of large amounts of smoke along with external flaming over large areas of a building façade is not a typical building-fire behavior. Solid-fueled fires in buildings more typically go through the stages of growth, sustained burning, and decay observed elsewhere in both towers. Burning of isolated pools of aviation fuel deposited inside the building during the aircraft impact is one likely explanation. Given the likelihood that a large amount of aviation fuel from the aircraft's starboard fuel tank was spread across the 79th floor during the impact, perhaps the most noteworthy observation on the east face was the absence of large fires on the 79th (with the exception of the debris pile on the north face) and 80th floors for the initial 25 min of the fires. The fire behaviors during the short periods of heavy smoke release are those expected following the sudden ignition and rapid burn out of aviation fuel at interior locations within the tower. The identification of seven such occurrences suggests that, if the aviation fuel was indeed responsible, it had collected at multiple locations that separately ignited and burned.

Numerous visual observations suggest that important changes, which might have had structural relevance, were taking place in WTC 2 in the period following the aircraft impact until collapse. These observations included hanging objects, at least some of which, based on appearance, were likely locally dislodged floor slabs that had settled down to locations below the spandrel; at several locations on the north and east faces, changes in the positions of the hanging objects during the period; the occurrence of numerous pressure pulses identified by smoke and/or dust puffs generated over multiple windows and floors; the appearance of molten metal pouring from the tops of open windows; and bowing of the outer steel framework on the east face.

The general picture that emerges from the observations is that WTC 2 possibly underwent a prolonged series of subtle structural changes that began shortly after the aircraft impact and that these changes continued until the tower collapsed. Presumably, these changes occurred as the structure adjusted to the initial damage inflicted by the aircraft and associated fireballs and the additional deformation caused by the fires that subsequently developed. While there was similar direct evidence for structural changes in WTC 1 as for WTC 2, e.g., bowing columns, events, such as smoke puffs, that might be possible telltales for internal changes taking place within the tower, were considerably less frequent in WTC 1 than observed for WTC 2.

It has been noted that the fire events in WTC 1 and WTC 2 had different characteristics. These differences extended to human behavior, which provided additional indications about these differences. In WTC 1, people broke out numerous windows above the immediate floors that were burning and were often observed in open windows. While some windows were broken open in WTC 2, the locations were

limited and people were infrequently observed. Numerous people were observed falling from the upper floors on the four faces of WTC 1, while the three people observed falling from WTC 2 came from a single window on the east side of the 79th floor. These differences suggested that conditions on the upper floors in WTC 2 did not degenerate as quickly, nor become as dire, as on the upper floors of WTC 1.

In WTC 1 a large number of streamers were observed falling from the tops of windows. These were attributed to smoldering polyurethane that was originally located above the window head casings. In contrast, very few streamers were observed for WTC 2. The absence of streamers is likely due to the relatively limited fire spread that occurred in WTC 2 and because large areas of the aluminum curtain wall that contained the polyurethane insulation were removed by the aircraft impact and resulting fireballs.

2.3.8 Other Structural Changes

There was extensive overt impact-derived structural damage to the perimeter columns and floor systems visible in the photographs and videos. The nature and extent of this damage, its implications for the post-impact stability of the tower, and its use in corroborating the simulations of the aircraft impact are discussed in NIST NCSTAR 1-2, NIST NCSTAR 1-3C, and NIST NCSTAR 1-6. There were also indications that, as the fires progressed, WTC 2 underwent a series of subtle structural changes. Presumably, these changes occurred as the structure adjusted to the initial damage inflicted by the aircraft and associated fireballs and the additional deformation caused by the fires that subsequently developed. Observations of these changes included:

- Hanging objects. Some of these appeared to have been locally dislodged floor slabs on the north face (80th, 81st, 82nd, and 83rd floors) and the east face (83rd floor) that had settled down to locations below the spandrel of the floor below. They were located where the fireballs had been ejected from the building under pressure. The hanging objects changed positions between the initial observation and the tower collapse. Since the windows were not always visible, the exact times of the localized changes could only be estimated.
- Molten metal, presuming aluminum alloys that melt at 475 °C to 635 °C, pouring from the tops of open windows. A major instance occurred on the north side of the 80th floor at 9:52 and lasted 7 min. The sudden appearance of the flow at the top of the window was likely the result of the formation of a pathway from the 81st floor, where the aluminum presumably had pooled on top of the floor slab as it melted. This, in turn, suggested that the 81st floor slab sank or pulled away from the spandrel at this time. At one point the flow shifted one window to the east, indicating that the 81st floor slab in the vicinity might have been shifting.
- Bowing of the outer steel framework. Images of the east face of WTC 2 reveal that the perimeter columns were distinctly bowed inward as early as 9:21 a.m. This bowing appeared to be largest near the center of the face and to disappear near the edges. The extent and expanse of the bowing is discussed in NIST NCSTAR 1-3C.

2.4 REFERENCES

- Badrocke, M., and B. Gunston. 1998. *Boeing Aircraft Cutaways*. Osprey Publishing, Oxford UK.
- Baum, H.R., and R.G. Rehm. 2005. A Simple Model of the World Trade Center Fireball Dynamics. *Proceeding of the Combustion Institute*, Vol. 30, pp. 2247-2254.
- Forney, G.P., and K.B. McGrattan. 2003 *User's Guide for Smokeview Version 3.1: A Tool for Visualizing Fire Dynamics Simulation Data*. NISTIR 6980. National Institute of Standards and Technology. Gaithersburg, MD.
- Forney, G.P., D. Madrzykowski, K.B. McGrattan, and L. Sheppard. 2003. Understanding fire and smoke flow through modeling and visualization. *IEEE Computer Graphics and Applications*, vol. 23, p. 6-13.
- McAllister, T., ed. 2002. *World Trade Center Building Performance Study: Data Collection, Preliminary Observations, and Recommendations*. FEMA 403. Federal Emergency Management Agency. Washington, DC. May.

Chapter 3

BUILDING INTERIORS AND COMBUSTIBLES

3.1 DATA ON THE BUILDING INTERIORS

3.1.1 Focus

As was described in the prior chapter, the fires in the World Trade Center (WTC) towers were not stationary. They spread through the various tenant spaces, with the patterns and timing dependent on the availability of fuel and air for the combustion, as well as the layout and damage condition of the floors and walls.

In general, the tenants of the WTC towers occupied large, open spaces with few interior walls. Knowing the location and nature of those interior walls (partitions) was important to the reconstruction of the fires on September 11, 2001. The walls could have acted as fire barriers, delaying the exposure of structural components to the intense heat from the fires. The walls of perimeter offices or conference rooms could also have blocked the photographic views of fires in the building interior and kept flames and smoke from billowing out the windows.

Other features of the building interior layout could also have had an effect on the progress and impact of the fires:

- The nature and locations of any stairwells or other passages between floors. These could have provided a means for floor-to-floor fire spread.
- The nature and status of the ceiling tile systems. These could have provided a temporary but significant time delay for access of the hot fire to the floor membrane above. This is discussed further in Section 3.1.3.
- The general nature and magnitude of the office furnishings and any unusual combustibles (e.g., high density file storage areas, significant quantities of highly flammable items). This is discussed further in Section 3.2.
- Any significant modifications made within the ceiling (truss) space, especially anything that might have impacted the truss insulation.

The solicitation of this type of information on the tenant spaces was focused on those floors of the towers in which significant fires and physical damage were observed and those floors where fires were observed or might have existed unobserved (Table 3–1).

3.1.2 Floor Plans

The Port Authority reported that their copies of the architectural drawings for the tenant spaces were destroyed when the buildings collapsed. The National Institute of Standards of Technology (NIST) staff

then requested that tenant companies provide architectural drawings of their space at the time of the most recent renovation. The requests were also for information regarding the furnishings. As shown in Table 3–1, NIST obtained floor plans for a large fraction of the floors of interest in the two buildings. Discussions with Port Authority property managers, tower occupants, architects, and product manufacturers provided additional information, including estimates of the similarity of layouts of floors, for which no information was available, to others in the towers. However, despite the quality of the drawings and verbal descriptions obtained by NIST, there was no way to ascertain the degree of accuracy, e.g., of the locations of interior walls, as of the morning of September 11, 2001.

Some general features of the layouts of these focus floors emerged:

- As expected, most of the floors were very open.
- For multi-tenant floors the demising walls between the companies generally were of gypsum board over steel studs. The opaque walls between the tenant spaces and the core areas generally reached from the floor slab below to the floor slab above.
- Tenant space interior walls were of similar construction, but generally ran from the floor slab to just above the drop ceiling. These could also have resisted the passage of fire. However, the space bounded by the upper concrete floor slab and the drop ceiling formed a plenum that could have extended across the full area of a given floor. The hot upper layer generated by the fire effluent could then have spread floor-wide, unlike the case where there were demising walls. The doors in these walls were not likely to have been fire-rated or to have had automatic closers. For modeling purposes, NIST generally presumed these to have been open. However, in some cases, the observed interrupted progress of fire across a series of windows could have been the result of a partitioned area with a closed door. There were some slab-to-slab walls surrounding sound-sensitive offices and conference rooms.
- The walls in the building core, including those separating the core from the tenant spaces, generally consisted of solid, slab-to-slab gypsum planks covered with gypsum board sheathing. Most of these walls were also part of the elevator, stair, air handling, and other shaft enclosures. These walls served as demising walls between the core and the occupant spaces.
- There were glass walls at the (core) entrances to some of the suites. In these cases, the wall behind the reception area was to have been a demising wall.
- Within the tenant spaces, large floor-to-floor openings that would permit the spread of fire or hot effluent were rare. The instances were the open staircases as noted in Table 3–1.
- The floor slab was generally carpeted; there were some cases of slightly raised floors for power and data cabling and of wood- or stone-covered areas.
- The drop ceiling systems, one for the tenant spaces and one for the core areas, were designed specifically for the WTC (see Section 3.1.3).

Table 3–1. Floor layout information obtained.

Building	Floor	Tenant	Damage ^a	Fires ^b	Material Received ^c	General Description of Tenant Layout
WTC 1	92	Carr Futures, empty		Y	FP (Carr), V	
	93	Marsh & McLennan, Fred Alger Mgmt.	Y	Y	FP, F, V	Marsh & McLennan occupied the south side only. Filled with workstations. Demising walls for the south facade to the edges of the core. Offices along the east side of the south core wall. Stairwell to the 94 th floor.
	94	Marsh & McLennan	Y	Y	FP, F, V	Generally open space filled with workstations. Offices and conference rooms around most of the perimeter. Stairwell to the 93 rd and 95 th floors.
	95	Marsh & McLennan	Y	Y	FP, F, V	Generally open space filled with workstations. Offices, conference rooms and work areas in exterior corners. Large walled data center along north and east sides. Separate stairwells, one to 94 th floor and another to the 96 th and 97 th floors.
	96	Marsh & McLennan	Y	Y	FP, F, V	Generally open spaced filled with workstations. Offices at exterior corners and middle of north and south facades. Some conference rooms on north and south sides of core. Stairwell connections to 95 th and 97 th floors.
	97	Marsh & McLennan	Y	Y	FP, F, V	Generally open space filled with workstations. Offices at exterior corners and in the middle of the north facade. Two separate stairways. One connected to the 95 th and 96 th floors; the other connected to the 98 th , 99 th , and 100 th floors.
	98	Marsh & McLennan	Y	Y	FP, F, V	Generally open spaced filled with workstations. Offices at exterior corners and middle of north and south facades. Some conference rooms on north and south sides of core. Stairway connected to the 97 th , 99 th , and 100 th floors.
	99	Marsh & McLennan	Y	Y	FP, F, V	Open space filled with workstations on the east side and east half of the north side. Offices at exterior corners and along south and west sides. Large walled area on west side of north facade. Stairway connected to the 97 th , 98 th , and 100 th floors.
	100	Marsh & McLennan		Y	FP, F, V	Generally open space filled with clusters of workstations. Offices at exterior corners. Stairway connected to the 97 th , 98 th , and 99 th floors.
	104	Cantor Fitzgerald		Y	V	Trading floor. Tables with many monitors.

Building	Floor	Tenant	Damage ^a	Fires ^b	Material Received ^c	General Description of Tenant Layout
WTC 2	77	Baseline	Y	Y	FP, V	Generally open space. Offices along east and west core walls. A few offices in each exterior corner of the floor.
	78	Baseline, 1st Commercial Bank	Y	Y	FP, V	West side open. Northeast quadrant walled. Offices along south side of east core wall. Offices along east side of south facade.
	79	Fuji Bank	Y	Y	V	
	80	Fuji Bank	Y	Y	FP, V	Generally open space filled with workstations. Offices or conference rooms at exterior corners and along south half of west facade. Large vault at southeast corner of core.
	81	Fuji Bank	Y	Y	V	
	82	Fuji Bank	Y	Y	V	
	83	Chuo Mitsui, IQ Financial	Y			Chuo Mitsui had half the area. Wide open space. No information regarding IQ Financial.
	84	Eurobrokers	Y		V	Open floor for trading. Tables rather than workstations. Perimeter offices.
	85	Harris Beach	Y		FP, V	Offices around full perimeter. Offices along east, west and south walls of core.

a. Floors on which the exterior photographs indicated direct damage from the incident aircraft.

b. Floors on which the exterior photographs indicated extensive or sustained fires.

c. Types of descriptive material received: FP: floor plan; F: documentation of furnishings; V: verbal description of interior.

The project staff computerized drawings of each floor, including the layout of the partitions, stairwells and other features that might affect fire spread. These became input to the fire modeling described in Chapter 4. These drawings are included in NIST NCSTAR 1-5F.

As the Investigation proceeded, NIST determined that a smaller number of floors (a) experienced fires that were of sufficient intensity, expanse, and duration to compromise significant numbers of structural elements, and (b) were in the vicinity of the observed collapse initiations. These floors were 92 through 99 in WTC 1 and 78 through 85 in WTC 2. These are hereafter referred to as the focus floors.

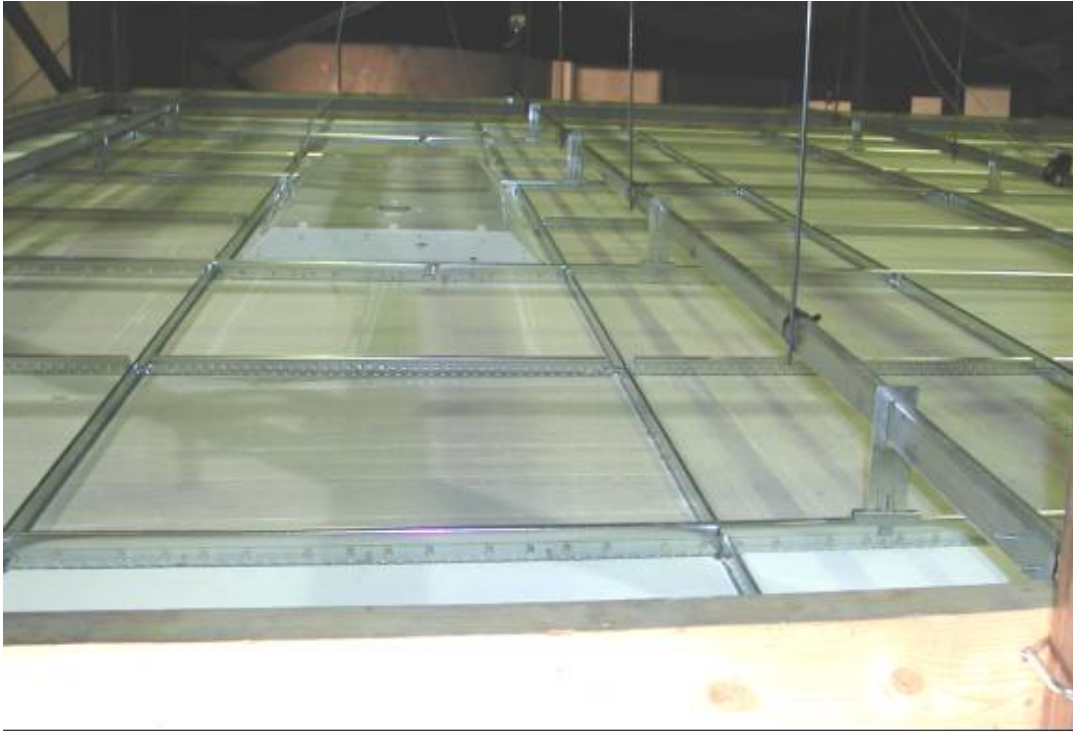
3.1.3 Ceilings

The condition of the ceiling tile system following the aircraft impact would have had a significant effect on the spread of the fires and their impact on the structural elements, especially the floor joists. The hot gases from a fire rise and form a hot layer across the top of a room. The temperatures in this layer could have exceeded 1,000 °C, well above the threshold temperature at which the strength of structural steels diminishes. However, as long as the ceiling tile system were intact, this layer would have formed *below* the floor joists, and the temperature in the upper “box” would have remained relatively cool for some time interval. This delay time is most often characterized by a fire resistance rating, obtained from a standard furnace test such as ASTM E 119 (ASTM 2000). Were a significant fraction of the tiles displaced from the framework, the hot flames from fires underneath would have bathed the floor system immediately. Further away, the hot upper layer formed from the fire effluent would have enveloped the floor trusses, rather than building from the drop ceiling down. It was thus deemed valuable to determine the condition of the ceiling tile systems in the regions where the fires existed and where their heat might have had structural implications. This determination consisted of measuring the response of the systems to shocks of different magnitudes, and then putting those results in the context of the shocks resulting from the aircraft impacts into the towers.

There were two different ceiling tile systems originally installed in the towers. The framing for each was hung from the bottom of the floor trusses, resulting in an apparent room height of about 2.6 m (8.6 ft) and an above-ceiling height of about 1.0 m (3.4 ft). Both sets of tiles were manufactured by Armstrong World Industries, Inc, specifically for the WTC (Fritz and Hough 2002).

- Tenant spaces: The PANYNJ originally specified Armstrong BF 803 tiles for the towers. These were 20 in. square, $\frac{3}{4}$ in. thick, lay-in tiles on an exposed tee bar grid system. Figure 3–1 is a photograph of a similar system. This was sold as a non-fire resistance rated system. The combustible content of the original tiles was estimated to be 13 percent to 15 percent by mass. Using ASTM E 84 (Test Method for Surface Burning Characteristics of Building Materials ASTM 2003), Armstrong determined the flame spread index as under 25 and the smoke developed index as under 50. The density of the tiles was approximately 1 lb/ft³ (16 kg/m³) (Fritz and Hough 2002). The ceilings were the responsibility of the tenants, and over the years many (if not all) tiles were replaced. Some of the replacement was with similar products by Armstrong and other manufacturers; some were replaced with alternative products such as gypsum board. The 20 in. tiles were manufactured only for the WTC towers and thus were no longer available.

- Core areas: The PANYNJ originally specified Armstrong BF 892 tiles. These were 12 in. square, 3/4 in. thick, mounted in a concealed suspension system (Fig. 3–2). This also was sold as a non-fire resistance rated system. The fire properties and material density were similar to the BF 803 tiles (Fritz and Hough 2002). Since 12 in. square tiles were more commonly manufactured, there is no definitive information on the specifics of any replacement tiles.



Source: NIST.

Figure 3–1. Top and bottom views of a ceiling system similar to that originally installed in the tenant spaces.



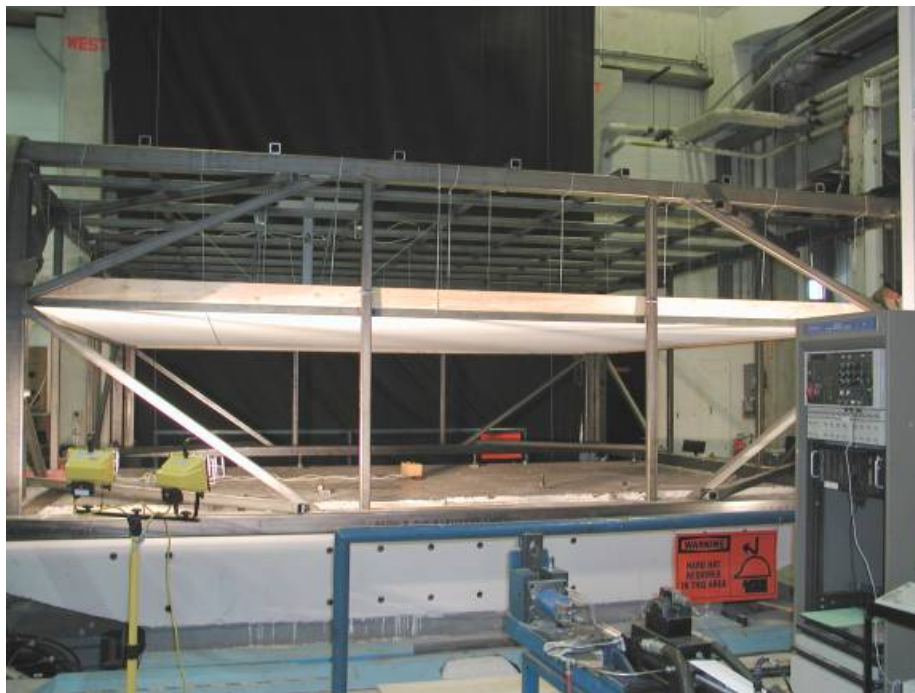
Source: NIST.

Figure 3–2. Bottom and top views of a ceiling system similar to that originally installed in the core areas.

Two independent estimates indicated that systems such as these might have stayed in place for approximately 10 min to 15 min in an ASTM E 119 type thermal environment if the grids were steel, perhaps for about 5 min if the grids were aluminum (Fritz and Hough 2002; Shipp 2002). When heated, the supporting grid would distort, and the tiles would shrink and fall out. Observations of the fires on September 11, 2001, and computer simulations of those fires indicated that the fires burned at least 20 min in most locations. The comparability of these times suggested that information regarding the integrity of the ceiling tile systems was pivotal to assessing the role of the floor truss assemblies in the eventual collapse of the towers.

Accounts of building occupants included mention that the impact of the aircraft resulted in extensive dislodging of ceiling tiles and damage to the framing system on many floors (NIST NCSTAR 1-7). Descriptions of the magnitude of the damage at the observers' locations and the spatial extent of the damage were neither quantitative nor comprehensive. Thus, additional information was needed in order to estimate where the ceiling systems were intact and where the heat from the fires might have impinged unabated on the floor truss assemblies.

Accordingly, a series of tests of ceiling tile systems was conducted using the earthquake simulator (“shaking table”) at the University at Buffalo of the State University of New York. A detailed description of the hardware, procedures, and outcome of these tests can be found in NIST NCSTAR 1-5D. Figure 3–3 shows the test platform, the test frame, and a ceiling tile system.



Source: NIST.

Figure 3–3. Test frame mounted on the shaking table at the University at Buffalo.

The data indicated that accelerations on the order of 5g would cause serious distress to the ceiling tile systems, most likely resulting in substantial displacement of ceiling tiles. Comparison of this result to the building accelerations obtained from dynamic modeling of the impact of the aircraft with the towers must take into account that these tests were not exact replications of the initiating events on September 11, 2001:

- The installed ceiling tile systems in the WTC towers had been in service for up to 30 years, and during that time, the buildings had been subjected to wind forces that swayed the towers. Several occupants have reported that high winds resulted in falling ceiling tiles (NIST NCSTAR 1-7). Thus, the frames were not in the new condition of the systems tested here.
- The boundary conditions in the test frame were not identical to the in-service boundary conditions in the towers at the times of the aircraft impacts. The ceiling tile system was far more extensive in the towers.

The estimated accelerations from the aircraft impacts were on the order of 100g (NIST NCSTAR 1-2). It is thus likely that numerous ceiling tiles were dislodged throughout the focus floors, a finding that is consistent with the multiple reports of severely damaged ceilings (NIST NCSTAR 1-7). When even a moderate fraction of the ceiling tiles are displaced, the hot fire smoke will quickly enter the exposed plenum, and thus in the modeling of the fires it was assumed that the ceiling tile system was absent.

3.1.4 Ventilation Paths

If the floors of the towers were airtight, a fire starting on a particular floor would have been limited to a size that would not likely have threatened the building:

- The volume of a floor was approximately $1.4 \times 10^4 \text{ m}^3$ ($4.8 \times 10^5 \text{ ft}^3$). The mass of air contained in that volume was $1.7 \times 10^4 \text{ kg}$ ($3.7 \times 10^4 \text{ lb}$); the mass of oxygen was $3.8 \times 10^3 \text{ kg}$ ($8.4 \times 10^3 \text{ lb}$). The heat release from combustion of typical combustibles is 13.1 MJ per kg of oxygen consumed (Huggett 1980). Only about half the oxygen could have been consumed, since that would have resulted in a level below which a fire cannot continue to propagate. Thus, a fire on this airtight floor would have generated about $2.5 \times 10^4 \text{ MJ}$.
- At a combustible fire load of 4 lb/ft^2 (Section 3.2.1), there would be approximately $7.3 \times 10^4 \text{ kg}$ ($1.6 \times 10^5 \text{ lb}$) of combustibles on a given floor. Were they wood-like in heat of combustion (heat of combustion approximately 20 kJ/g [Drysdale 2002]), they would have generated $1.5 \times 10^6 \text{ MJ}$, given sufficient oxygen. Since there was only enough oxygen to generate $2.5 \times 10^4 \text{ MJ}$, only about 2 percent of the combustibles would have burned.
- The peak heat release in the simulations of the fires (Chapter 4) was about 2,000 MW. Assuming the fires were almost instantaneously ignited by the jet fuel, at that burning rate, $2.5 \times 10^5 \text{ MJ}$ would have been generated in about 2 min. (If one assumed that the fire grew as a fast t^2 fire, a common design criterion (Alpert 2002), to the same peak heat release rate, $2.5 \times 10^5 \text{ MJ}$ would have been generated in about 20 min.)

Since the fires burned longer than this and since they thus consumed far more of the combustibles, the rate at which fresh air became available played a major role in determining the duration of the fires. The locations from which the air became available determined the direction of fire growth. In addition, the extent to which large openings existed between floors, those openings became paths for floor-to-floor fire spread.

Prior to the aircraft impact, only a modest flow of additional air would have reached the tenant space on any given floor because the windows were intact and sealed, there was no more than a single internal stairwell in any of the tenant spaces, the walls between the tenant spaces and the core area were demising walls, and there was at most a small amount of floor-to-floor leakage where the floors slabs met the exterior wall, through holes drilled in the floor for electrical cable, etc.

The core space contained relatively little combustible mass, and thus air supply in the event of a fire was not a concern.

At the time of the aircraft impact, these conditions changed markedly in each tower:

- Hundreds of windows were displaced by the impact (Tables 2–6 and 2–8). As the morning progressed, more windows were broken by both the fire and by occupants.
- The aircraft fuselage and the inner portion of the wings opened a large hole in the north facade through which they entered the building. The pressure wave from the jet fuel explosion and the larger fragments of the aircraft opened additional holes in the other three

faces of the building. This was described in Chapter 2 and in more detail in NIST NCSTAR 1-5A.

- The aircraft fuselage destroyed portions of the floor slabs (NIST NCSTAR 1-2). This is discussed further in Section 4.7.
- The aircraft debris opened large holes in the demising walls to the core and thus access to the elevator shafts, etc.

3.2 BUILDING COMBUSTIBLES

3.2.1 Nature of Combustibles

While much of the public attention has been focused on the jet fuel, most of this was combusted in only a few minutes. By contrast, typical office furnishings can sustain intense fires of at least an hour's duration on a given floor (see, e.g., Nelson 1989).

The most common layout of the focus floors was a continuous open space populated by a large array of workstations (also referred to as office modules or cubicles) (Table 3–2). The number of different types of workstations in the WTC towers is unknown and was probably large. However, discussions with office furniture distributors and visits to showrooms indicated that, while there was a broad range of prices and appearances, the cubicles were fundamentally similar. Each cubicle typically was bounded on four sides by privacy panels, with a single entrance opening. Within the area defined by the panels was a self-contained workspace: desktop (almost always a wood product, generally with a laminated finish), file storage, bookshelves, carpeting, chair, etc. Presumably there were a variety of amounts and locations of paper, both exposed on the work surfaces and contained within the file cabinets and bookshelves. These cubicles, as many as 200 or more per floor, were grouped in clusters or rows. Figure 3–4 shows the layout of the 97th floor of WTC 1.

As input to the fire modeling, it was useful to estimate the average fuel loading of the floors in the towers. This was done as follows:

- On a mass basis, the workstations were generally the dominant combustibles on the floors in WTC 1 where extensive fires were observed. For the fuel load calculation it was assumed that the entire tenant floor space was filled with workstations.
- The tenant space floor area (i.e., the total floor space minus the core area) was approximately 2,800 m² (30,000 ft²).
- There were approximately 200 workstations equivalents per floor. The workstations contained roughly 200 kg (400 lb) of combustible mass (NIST NCSTAR 1-5C). Paper in the bookcases and on the desktop could have been in the range of an additional 50 kg (100 lb). [Paper in the filing cabinets, while it might have been significant in mass, did not burn readily due to the limited oxygen available within the drawers.] Thus, the total combustible mass on a floor was about 5×10^4 kg (1×10^5 lb).
- The combustible fuel load in the tenant spaces then was approximately 20 kg/m² (4 lb/ft²).

Table 3–2. Use of space on focus floors in WTC 1.

Building	Floor	Number ^a			Other
		Cubicles	Conference Rooms/Work Areas	Offices	
WTC 1	92	103	10	22	Reception area
	93 ^b	29	1	1	Mail room, security office, waiting area
	94	170	7	33	Reception area
	95	166	3	15	Lunch room
	96	168	9	40	Lunch room, mail room
	97	215	8	21	Reception area, lunch room, mail room
	98	173	5	33	Reception area, lunch room, check printing room, copy room
	99	105	16	28	Reception area, large library, lunch room
	100	91	6	60	
WTC 2 ^c	80	> 250	> 5	>5	Large, heavy vault outside SE corner of the core. Data center at SW corner of the core.

a. Approximate; space has been assigned to the three categories based on furniture layout.

b. No furniture layout drawings available for the tenant who occupied most of the floor.

c. No furniture layout drawings available for floors 78, 79, 81, 82, and 83.

This combustible load was somewhat light compared to the two most recent prior studies. Culver (1978) reported survey results for fuel loads in general and clerical spaces of 32 kg/m² (6.5 lb/ft²) with a standard deviation of 21 kg/m² (4.4 lb/ft²). About 20 percent of this was due to interior finish, which was negligible in the WTC spaces. Caro and Milke (1996), in a smaller survey of office spaces, found the movable fuel loads to be 67 kg/m² ± 20 kg/m² (14 lb/ft² ± 4.0 lb/ft²). Over half of this was paper and books.

The detailed floor plan for the 80th floor in WTC 2 has a number of workstations similar to that on the focus floors of WTC 1. Since the occupancies on the remainder of the WTC 2 focus floors were similar, the team assumed that the combustible fuel loading was similar on these floors as well. In addition, based on discussions with people who had been in the towers, the team assumed that the fuel loading in the core areas of the focus floors was negligible.

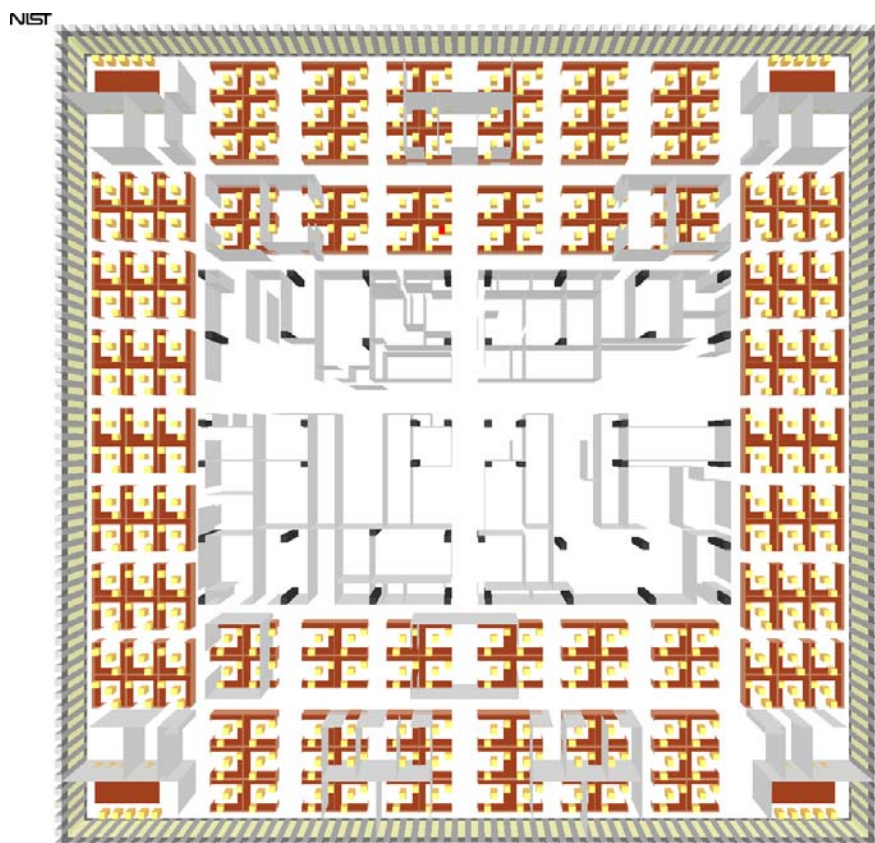


Figure 3–4. Furnishings and partitions layout of the 97th floor of WTC 1.

3.2.2 Flammability of Workstations

A series of experiments was conducted to guide the inclusion of workstation burning behavior in modeling the WTC fires (NIST NCSTAR 1-5C). The most important characteristic of the combustion is the heat release rate (HRR) of the fire. It dominates the growth of the fire and the concomitant hazards. (The mass loss rate (MLR), also measured, provides parallel information, since for a constant heat of combustion, the MLR and HRR are proportional.) Madrzykowski (1996, 1998) had measured the HRR behavior of workstations that were somewhat different from those studied here. He found the peak HRR values varied with such details as the number of privacy panels and the failure of a thermoplastic shelf support leading to a shelf collapse which spewed loose papers onto the fire immediately enhancing it substantially. Here, two different cubicle designs were combusted:

- A generic workstation, shown in Figure 3–5. A person from a company that supplied office furnishings to the occupants of WTC 1 suggested this layout and, as a frequent visitor to the WTC offices, provided information on the amount and distribution of papers and other office items (Fleck 2003). The workstation covered a footprint approximately 2.44 m (8 ft) square and was surrounded by privacy panels 1.22 m (4 ft) high. The panels had a steel and softwood frame and were covered on both sides with layers of fiberglass padding and perforated steel and a thermoplastic cover fabric.

- A workstation of a type used by Marsh & McLennan, designated the WTC workstation, shown in Figure 3–6. It differed slightly from the generic workstation, in that it had a different chair, privacy panels, and file cabinet fronts.



Source: NIST.

Figure 3–5. Photographs of the generic workstation.



Source: NIST.

Figure 3–6. Photographs of the WTC workstation.



The material make-up of the two workstations is summarized in Table 3–3. The thermophysical properties of both sets of cubicle materials (carpet, desktop, computer monitor, chair, privacy panel, and stacked paper) were determined using the cone calorimeter (ASTM 2003a) for input to the computational simulations. The results of these measurements are given in NIST NCSTAR 1-5C.

Table 3–3. Contents of workstations.

Component	Generic			WTC		
	Mass (kg)	Combustible Fraction	Combustible Mass (kg)	Mass (kg)	Combustible Fraction	Combustible Mass (kg)
Work surface	82.8	1.0	82.8	79.4	1.0	79.4
Paper and boxes	63.7	1.0	63.7	63.7	1.0	63.7
Kick plates and trim	7.1	1.0	7.1			
Computer keyboard	1.2	1.0	1.2	1.2	1.0	1.2
Waste basket	0.7	1.0	0.7	0.7	1.0	0.7
Carpet tiles and backing	38.0	0.9	34.2	38.0	0.9	34.2
Plastic doors for shelves				4.4 (est.)	1.0	4.4
Shelf ends	3.8	0.9	3.4			
Chair	19.4	0.8	15.5	22.4	0.8	17.9
Computer monitor	17.6	0.3	5.3	17.6	0.3	5.3
Computer processor	12.3	0.3	3.7	12.3	0.3	3.7
Wall panels	168.2	0.18	30.3 25.3 kg wood 5.0 kg fabric	89.2	0.23	20.5 15.4 kg wood 5.1 kg fabric
Bookshelf	8.3	0.1	0.8			
Filing cabinets	142.5	0.0	0.0	136.9	0.02 (est.)	2.7 (est.)
Total	557.1	0.45	248.7	465.8	0.50	233.7

In each of six tests, a single workstation was burned under a collector hood. The test plan (Table 3–4) included consideration of two factors that reflected:

- Occlusion of some of the surface by inert debris from the ceiling tile system or fractured walls. This was simulated using 15 cm by 30 cm (6 in. by 12 in.) pieces of inert calcium silicate board.
- More rapid ignition due to the presence of jet fuel (Jet A). Four liters of Jet A were sprinkled on the cubicle surfaces just before the beginning of a test.

Test 1 was a scoping test to ensure that the peak heat release rate would not overwhelm the test fixture and is not discussed further.

Table 3–4. Experimental test plan for single workstation fire tests.

Test	Specimen	Tiles	Jet Fuel
1	Half generic workstation	None	None
2	Generic workstation	None	None
3	Generic workstation	40	None
4	WTC workstation	None	None
5	Generic workstation	None	4 L
6	Generic workstation	40	4 L

As an example of the test results, the heat release rate curve from Test 2 is shown in Figure 3–7. The graph has been annotated to indicate the steps in the combustion of the workstations. Figure 3–8 is a sequence of photographs taken during Test 2.

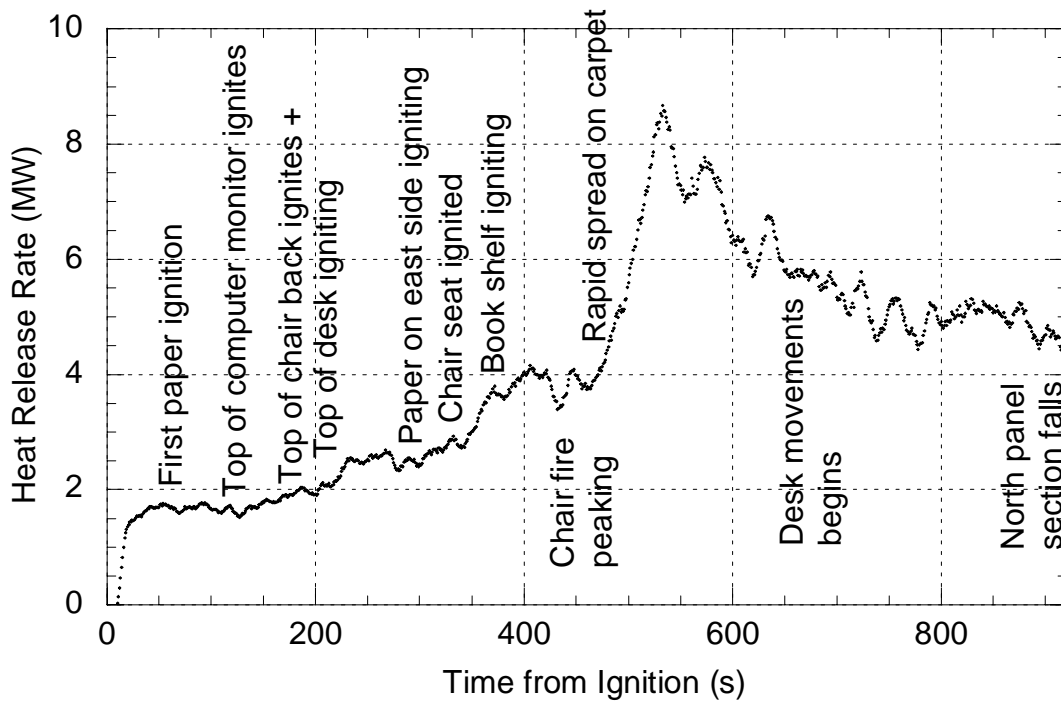


Figure 3–7. Annotated partial HRR curve from Test 2.



Source: NIST.

Figure 3–8. Photographs of a burning workstation at beginning of test, 165 s into test, near the peak heat release rate at 533 s, and at 965 s.

Table 3–5 summarizes the numerical results from the tests. The following observations emerged from comparison of the test results. These were features that the computational simulations needed to capture, in addition to the magnitude and shape of the HRR plots.

- The peak fire intensity from the half workstation was about two-thirds that of the full workstation. This was because the chair was present in both cases, and the inert steel file cabinets covered twice as much of the carpet in the second half of the workstation.
- The two workstations gave similar results.
- The ceiling tiles reduced the peak HRR in proportion to their coverage of the burning surfaces, both just under 15 percent.
- The Jet A sharply shortened the time to involvement of all accessible combustible surfaces, and thus the time to the peak HRR.

- The total heat release of approximately 3.9 GJ and mass loss of approximately about 200 kg were insensitive to the addition of jet fuel or inert material. Approximately 75 percent of the heat release and mass loss occurred over a period of approximately 20 min.
- There was essentially no interaction between the effects of the jet fuel and the surface coverage by inert materials.
- The ignition of the cubicle was facilitated by the presence of paper on the desktop, but was probably not sensitive to the mass of this paper. The total heat release from the burning cubicle would be sensitive to the mass of paper, both on the desktop and in the filing cabinets.
- A key step in reaching the peak was the flashover of the “compartment” under the desk.

Table 3–5. Key results from the workstation fire test burns.

Quantity	Test					
	1	2	3	4	5	6
Workstation	½ Generic	Generic	Generic	WTC	Generic	Generic
Tiles	N	N	Y	N	N	Y
Jet fuel	N	N	N	N	Y	Y
Peak HRR ^a (MW)	5.92/5.77	8.70/8.48	7.56/7.30	9.89/9.66	9.12/8.91	7.960/7.60
Time to peak (s)	490	530	590	510	160	200
Net peak HRR ^a (MW)	3.82/3.67	6.95/6.73	5.53/5.27	7.72/7.46	7.38/7.17	6.17/5.95
Peak MLR (kg/s)	0.197	0.308	0.263	0.420	0.336	0.293
Time to peak (s)	480	530	560	490	160	180
Net heat released (GJ)	1.20	4.05	4.13	2.93	3.60	3.74
Time interval ^b (s)	150 to 1,265	50 to 3,200	160 to 3,600	30 to 2,100	0 to 2,500	20 to 2,520
Total mass loss (kg)	69.1	205.0	213.6	173.6	200.2	205.3
Effective heat of combustion (MJ/kg)	17.4	19.8	19.3	16.9 ^c	18.0	18.2
FWHH ^d (s)		244	445		318	451
t (75 %) ^e		1,311	1,453		833	1,009
t _{ig} ^f (s) (item ignited)	39 (paper)	67 (paper)	56 (paper)	50 (paper)	90 (Jet A)	114 (paper)

- The first number is the calorimeter output; the second is a 10 s average about the absolute peak.
- The time interval applies to both the net heat released and to the total mass loss.
- There was some spillage of smoke in Test 4, which may partly account for the lower heat of combustion.
- Full width half height of net heat release rate curve.
- Time at which 75 percent of mass had been lost.
- Time of ignition of first object within workstation.

There were some features of the combustion that would be difficult for a simulation of current capability to capture:

- Since chairs of different designs (and thus different burning behaviors) could be fabricated from the same materials, the detailed fire behavior of the chair could not be inferred simply from the cone calorimeter data for the component materials.
- The chair fire rapidly collapsed to a pool fire on the floor whose reduced burning area meant a reduced HRR.
- The various paper piles developed a thick ash layer that would drive down their burning rate. Char formation on the desk surfaces drove down their burning rates.
- The desk surface collapsed, with separate sections doing so at differing times. The initial desk collapse probably did not greatly affect its burning rate, but ultimately what was left was a complex rubble pile whose burning would not be predictable from any knowledge of the original configuration coupled with cone calorimeter data.
- The wall panels collapsed at random times, inward and outward, typically rather late in the fire.

Thus, the further one went past the peak in the HRR curve, the less it would be predictable by a calculation that retained the original geometry. Fortunately, the major effects appeared to have occurred well after the desk surfaces collapsed and the time when contiguous workstations would have become ignited and dominated the heat release.

3.3 AIRCRAFT COMBUSTIBLES

3.3.1 Liquid Fuels

American Airlines Flight 11 (AA 11) departed with 34,500 kg (76,100 lb) of Jet A. At the time of impact with WTC 1, this was estimated to have been reduced to 30,000 kg (66,100 lb) (Barry 2003a). United Airlines Flight 175 (UA 175) departed with approximately 33,000 kg (72,800 lb) of Jet A. At the time of impact with WTC 2, this was estimated to have been reduced to 28,100 kg (62,000 lb) (Midgett 2003). In addition, a Boeing 767-200 aircraft carries 81 gal of hydraulic fluid (Nelson 2003).

3.3.2 Other Combustibles

Based on communications from the airlines and from Boeing, the two aircraft carried the solid combustibles shown in Table 3–6.

Table 3–6. Combustible contents of aircraft.

Category	AA 11 (WTC 1)	UA 175 (WTC 2)
Cabin materials (seats, galleys, lavatories, stowbins, linings, carpets, etc.) ^{a, b}	4,460 kg (9,830 lb)	4,460 kg (9,830 lb)
Windows ^a	200 kg (450 lb)	200 kg (450 lb)
Blankets, pillows, etc. ^c	400 kg (892 lb)	400 kg (892 lb) ^d
Passenger and crew carry-ons and clothing	1,110 kg (2,460 lb) ^c	660 kg (1,450 lb) ^{e, f}
Structural composites	2,270 kg (5,000 lb) ^{a, g}	2,270 kg (5,000 lb) ^{a, g}
Tires	1,130 kg (2,500 lb) ^a	1,130 kg (2,500 lb) ^a
Cargo bay contents		
Luggage	520 kg (1,150 lb) ^c	630 kg (1,390 lb) ^c
Cargo containers	[1,590 kg (3,500 lb) ^{i, j}]	[5,060 kg (11,100 lb) ^{h, j}]
Mail	2,040 kg (4,500 lb) ^c	2,740 kg (6,020 lb) ^h
Total solid combustibles	12,100 kg (25,800 lb)	12,500 kg (27,600 lb)
Jet A	30,000 kg (66,100 lb)	28,100 kg (62,000 lb)

- a. Nelson, M.D. 2003. The Boeing Company, Seattle, WA, memorandum to M. Rubin, National Institute of Standards and Technology, Gaithersburg, MD, September 29.
- b. Boeing gives the mass of cabin materials including wiring as 5,820 kg. Later in the memorandum, they cite the mass of wiring insulation to be 1,360 kg and that it is of very low flammability. This number assumes that nearly all the wiring was in the fuselage and subtracts the mass from the total cabin combustibles.
- c. Barry, D.T. 2003. Condon & Forsyth, LLP, New York, NY, memorandum to M.R. Rubin and M. Lieberman, National Institute of Standards and Technology, Gaithersburg, MD, August 12.
- d. Assumed to be the same as on AA 11.
- e. Midgett, J.T. 2003. United Airlines, Inc., memorandum to M. Lieberman, National Institute of Standards and Technology, Gaithersburg, MD, December 22.
- f. Assumes the crew carry-on mass (270 lb) was the same as AA 11.
- g. Boeing states that there are 2,270 kg of structural composites, without differentiating between those in the fuselage and those in the wings. The calculation here assumes that all of the mass was in the fuselage – an upper limit.
- h. Midgett, J.T. 2004. United Airlines, Inc., memorandum to M. Lieberman, National Institute of Standards and Technology, Gaithersburg, MD, January 23.
- i. Barry, D.T. 2003a. Condon & Forsyth LLP, New York, NY, memorandum to M.R. Rubin and M. Lieberman, National Institute of Standards and Technology, Gaithersburg, MD, October 31.
- j. The cargo consisted mainly of electrical equipment and seafood. Both are presumed to be nominally non-combustible.

The following estimation (Table 3–7) put the mass of the combustibles in Table 3–6 in context with the mass of combustibles already present within the towers along the entry path of the aircraft. The calculation assumed that all of the structural composite mass is in the fuselage – an upper limit. It also assumed that the combustibles from the two sources mixed. Thus, e.g., the make-up of combustibles ejected from the building was the same as remained within the building. From the estimates in the last row, it was clear that calculations of the fires in or near the impact zone had to include consideration of the combustibles from the incident aircraft.

Information from Boeing (Nelson 2003) mentioned that AA 11 carried 4 kg of oxygen in the crew compartment and 109 12-min oxygen generators and that UA 175 carried 2.6 kg and 102 12-min oxygen generators. The total mass of these is negligible compared to the mass of oxygen within a floor (3.8×10^3 kg, 8.4×10^3 lb, Section 3.1.4). The oxygen might have contributed to the intensity of the fireballs, but would have been consumed or dispersed well before the advent of the fires that eventually led to the collapse of the towers.

The 2003 Boeing memorandum also mentioned that the aircraft carried approximately 70 kg (150 lb) of halon 1301. If dispersed over the volume traced by the fuselage inside the buildings, the mole fraction would be four orders of magnitude lower than that needed to suppress a flame, 0.03.

Table 3–7. Importance of combustible contents of aircraft.

Category	AA 11 (WTC 1)	UA 175 (WTC 2)
Exterior width of fuselage ^a	5.03 m (16.5 ft)	5.03 m (16.5 ft)
Length of fuselage traverse	18 m (69 ft). Assumes that the aircraft impacted orthogonally on center and stopped within the core.	65 m (210 ft). Assumes that the aircraft impacted slightly to the east and at a slight angle to the east and reached the far side of the floor.
Floors entered by fuselage	95 & 96	80 & 81
Floor area traced by fuselage	180 m ² (1,940 ft ²)	650 m ² (7,000 ft ²)
Mass of combustibles in building on that floor space, assuming fuel load of 20 kg/m ² (4 lb/ft ²)	3,600 kg (7,800 lb)	13,000 kg (28,000 lb)
Mass of combustibles in the aircraft (Table 3–7)	12,100 kg (25,800 lb)	12,500 kg (27,600 lb)
Fraction of mass in aircraft entry path from aircraft combustibles	75 %	50 %

a. www.boeing.com/commercial/767.

3.4 INSULATION

3.4.1 Identification

The properties and presence or absence of thermal insulation used to retard the heating of structural elements in the WTC buildings could certainly have played a prime role in determining how long the structural elements resisted the fires on September 11. Table 3–8 (condensed from NIST NCSTAR 1-6) summarizes the types of sprayed fire-resistive materials (SFRMs) and where they were in use in the towers on September 11. In addition, most of the core columns were at least partially protected with box structures of gypsum wallboard.

3.4.2 Thermal and Mechanical Properties

NIST measured the cohesive strength of BLAZE-SHIELD DC/F and its adhesive strength to steel substrates with and without primer. These results are reported in NIST NCSTAR 1-6A. Combined with the information generated on the impact intensity of the aircraft (NIST NCSTAR 1-2) and estimates of the condition of the insulation prior to those impacts, these results enabled estimates of the degree of insulation that was not in place during the 102 min and 56 min that the fires burned in WTC 1 and WTC 2, respectively. The results became boundary conditions for the calculations reported in Chapter 5 of this report.

NIST also obtained samples of the two types of sprayed insulation and four types of gypsum wallboard and sent them to testing laboratories for determination of their thermal conductivity, density and heat capacity, all as a function of temperature from ambient. The sprayed material data were for 25 °C to

1,200 °C; the wallboard data were from 25 °C to 600 °C. The methodologies and data were also reported in NIST NCSTAR 1-6A and used in the calculations reported in Chapter 5 of this report.

Table 3–8. Types and locations of sprayed insulation on focus floors.

Building Component	Material
Floor Trusses	
Original	CAFCO DC/F
Upgraded	BLAZE-SHIELD II
Exterior Columns and Spandrels	
Column exterior faces	BLAZE-SHIELD DC/F
Column interior face	Vermiculite plaster
Core columns	BLAZE-SHIELD DC/F
Core beams	BLAZE-SHIELD DC/F

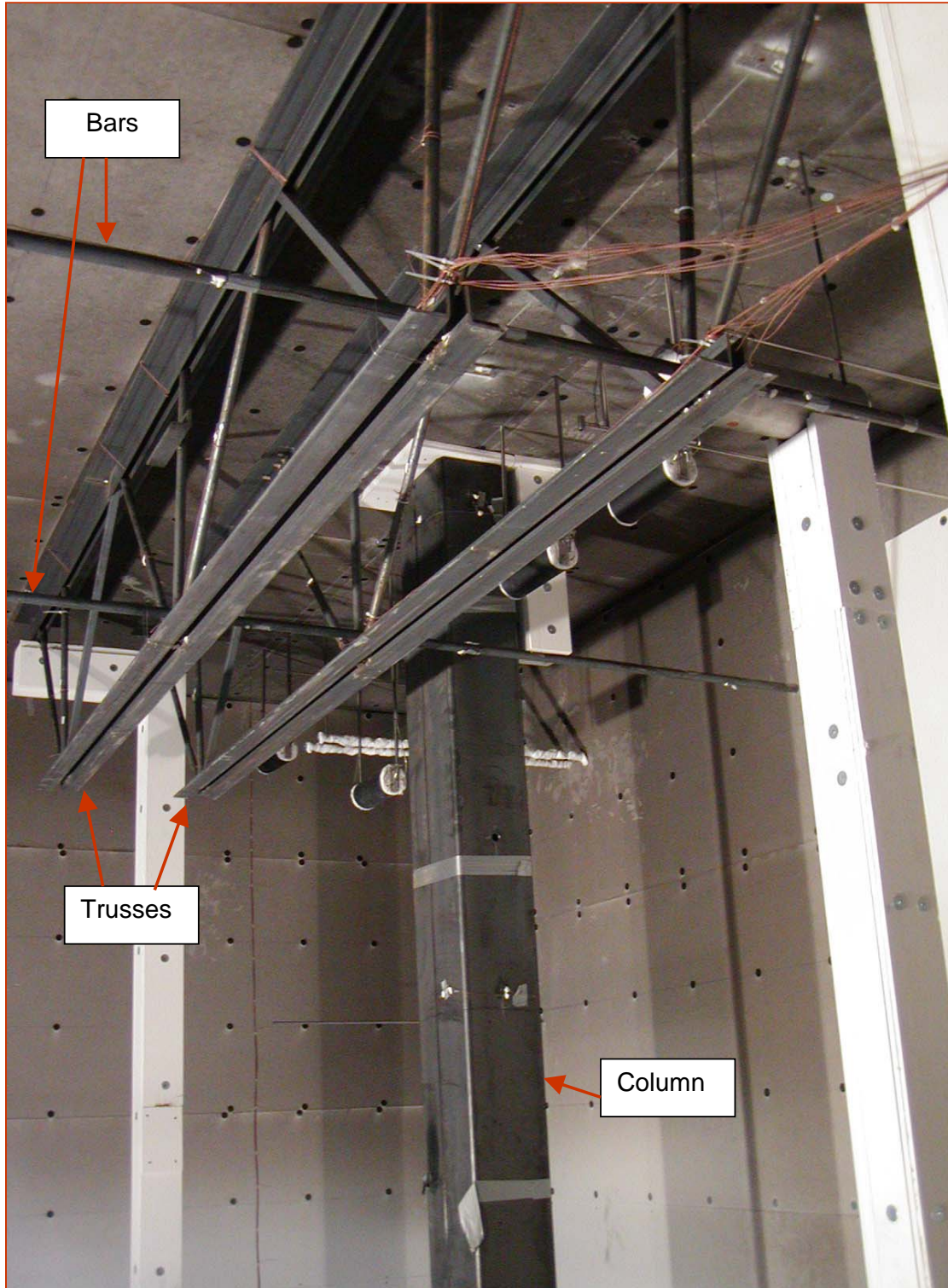
3.4.3 Thermal Behavior in Fires

The thermal protection afforded by SFRMs is typically obtained under steady and uniform heating conditions in a standard test furnace (ASTM 2000). Actual fires can reach high irradiances faster, are generally not isotropic, and may wane and re-grow before running out of fuel or being extinguished. From March 10 through 26, 2003, the Investigation Team conducted a series of experiments in the NIST Large-scale Fire Laboratory to obtain data on SFRM performance under realistic fire conditions. The results were then used to guide the fire modeling effort. A complete description of the tests and analysis of all the obtained data can be found in NIST NCSTAR 1-5B.¹

Within a large test compartment, assorted steel members were exposed to controlled fires of varying heat release rate and radiative intensity. The steel members were bare or coated with sprayed insulation of two thicknesses. The thermal profile of the fire was measured at multiple locations within the compartment. Temperatures were also recorded at multiple locations on the surfaces of the steel, the insulation, and the compartment.

In each of the six tests, the test subjects were one or two bars, two trusses, and a thin-walled tubular column. Depending on the test, these specimens were either left unprotected or were coated with BLAZE-SHIELD DC/F. The fibrous insulation was applied by an experienced applicator under a NIST contract who took considerable care to apply an even coating of the specified thickness. As such, the insulated test subjects represent a best case in terms of thickness and uniformity. Figure 3–9 is a view of the uncoated test subjects in the test compartment. Figure 3–10 shows some of the coated components.

¹ Extensive detail and additional data from these tests is provided in NIST NCSTAR 1-5B. To preserve continuity, only limited references have been inserted in the multiple sections of this report where the results from this test series are utilized. However, the reader should assume that unreferenced statements are supported by text in this reference.



Source: NIST.

Figure 3–9. Steel components in test compartment for Tests 1, 2, and 3.



Source: NIST.

Figure 3–10. SFRM-coated steel components prior to a test.

A description of the test series appears in Table 3–9. Table 3–10 shows the dimensions and variability of the sprayed insulation for Tests 5 and 6. A large set of thermocouples failed during Test 4, and those results are not discussed further here. The measurements were taken at numerous locations along the perimeter and length of each specimen using a pin thickness gauge specifically designed for this type of insulation.

Table 3–9. Test matrix for steel exposure fire tests.

Test	Measured Heat Release Rate (MW)	Fuel	Planned Insulation Thickness (mm)	Planned Test Duration (min)
1	2.0	Heptanes	None	15
2	2.4	Heptanes/toluene	None	15
3	2.0	Heptanes/toluene	None	15
4	3.2	Heptanes	Same as Test 5	15
5	3.0	Heptanes	See Table 3–11	50
6	3.0	Heptanes	See Table 3–11	50

Table 3–10. Summary of insulation on steel components.

Test	Item	Specified Thickness (mm)	Applied Thickness (mm)	
			Mean	Std. Deviation
5	Bar	19.1	23.0	5.5
	Column	38.1	41.0	3.0
	Truss A	19.1	26.9	7.3
	Truss B	38.1	40.5	8.2
6	Bar	19.1	25.3	4.6
	Column	19.1	21.4	3.5
	Truss A	19.1	26.0	6.9
	Truss B	19.1	25.6	6.9

Figure 3–11 shows typical temperature data obtained in the tests. These data were for Truss A (north) in Test 5. The thermocouple location notation is as follows: TU: Truss Upper Chord, TM: Truss Middle (Web), TL: Truss Lower Chord; 1 to 4: locations across the length of the test specimen; S: on the steel surface, I: on the outer surface of the SFRM; A: Truss A. From the figure, one can see that:

- The temperatures on the outside of the insulation rose sharply from the beginning of the test.
- The 19.1 mm (0.75 in.) insulation slowed the temperature rise and delayed reaching the peak steel temperature by almost an hour at all locations.
- The highest temperature reached at the steel surface was approximately 300 °C lower than the temperature at the outside face of the insulation material.

The curve patterns for the other steel specimens in the tests with insulated steel were similar in shape.

By contrast, Figure 3–12 shows the same plot for Truss A from test 3, in which the truss was not insulated and the fire was of shorter duration and lower intensity. The outer surface of the steel reached the targeted maximum temperature (just short of 600 °C) in about one third the time. This result was typical of the fire response of the uninsulated steel specimens in Tests 1 through 3.

This brief analysis indicated how large an effect intact SFRM played in extending the time for the protected steel to reach a temperature regime where it would lose a considerable fraction of its strength. Chapter 5 of this report contains further analysis of the temperature data from these tests. An appraisal of the expected condition of the SFRM prior to September 11 can be found in NIST NCSTAR 1-6A. Estimation of the damage to the SFRM from the aircraft impacts can be found in NIST NCSTAR 1-2.

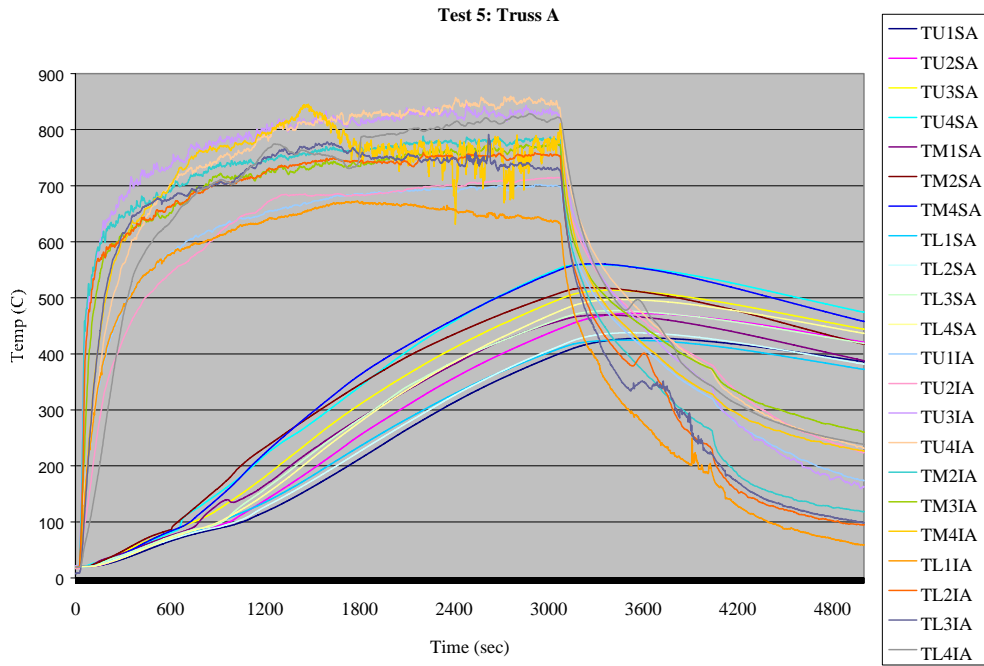


Figure 3-11. Temperature-time history for truss A in Test 5.

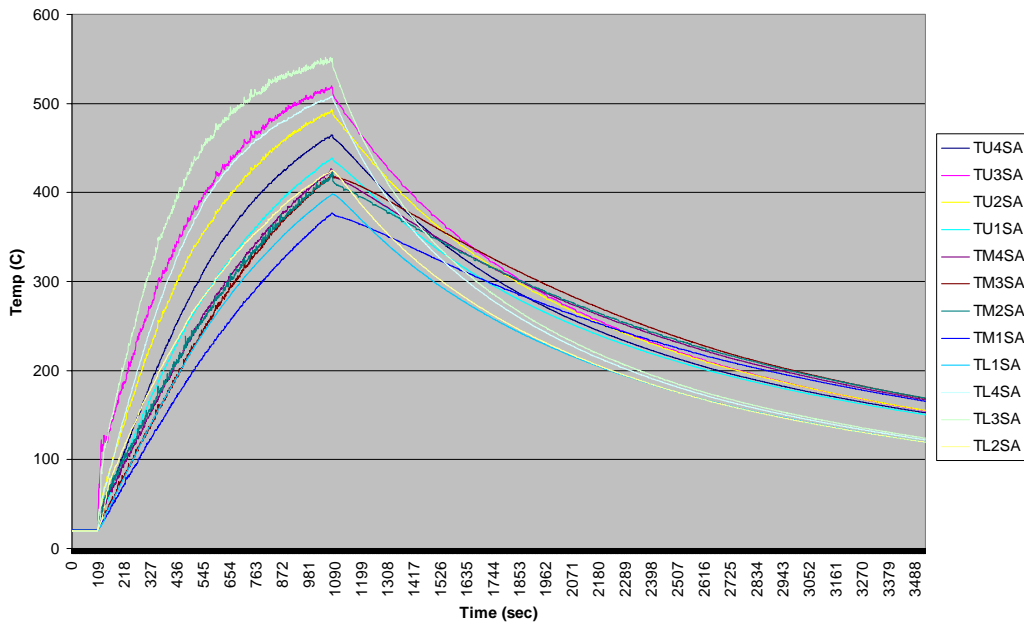


Figure 3-12. Temperature-time history for truss A in Test 3.

3.5 OTHER CONSIDERATIONS FOR THE FIRE RECONSTRUCTION

In reconstructing the fires of September 11, 2001, there were additional features that were considered:

- The aircraft damaged the risers, and no water was available for the sprinkler or standpipe systems (NIST NCSTAR 1-4).
- There was no action by building occupants that affected the course of the fires other than the breaking of windows on the fire floors (NIST NCSTAR 1-7).

3.6 REFERENCES

- Alpert, R.L. 2002. Ceiling Jet Flows, in DiNenno, ed., *The SFPE Handbook of Fire Protection Engineering*, NFPA International, Quincy, MA, p. 2-24.
- ASTM International. 2000. Standard Test Methods for Fire Tests of Building Construction and Materials, vol. 4.07. ASTM E 119-00a, *Annual Book of ASTM Standards*, West Conshohocken, PA.
- ASTM International. 2003. Standard Test Method for Surface Burning Characteristics of Building Materials, vol. 4.07. ASTM E 84-03, *Annual Book of ASTM Standards*, West Conshohocken, PA.
- ASTM International. 2003a. Standard Test Method for Heat and Visible Smoke Release Rates for Materials and Products Using an Oxygen Consumption Calorimeter, vol. 4.07. ASTM E1354-03, *Annual Book of ASTM Standards*, West Conshohocken, PA.
- Barry, D.T. 2003a. Condon & Forsyth LLP, New York, NY, memorandum to M.R. Rubin and M. Lieberman, National Institute of Standards and Technology, Gaithersburg, MD, October 31.
- Caro, T.C., and J.A. Milke. 1996. A Survey of Fuel Loads in Contemporary Office Buildings, NIST-GCR-96-697, National Institute of Standards and Technology, Gaithersburg, MD, September.
- Culver, C.G. 1978. Characteristics of Fire Loads in Office Buildings, *Fire Technology*, vol. 14, pp. 51-61.
- Drysdale, D.D. 2002. Thermochemistry, in DiNenno, ed., *The SFPE Handbook of Fire Protection Engineering*, NFPA International, Quincy, MA, p. 1-93.
- Fleck, D. 2003. Arenson Office Furnishings, NY, NY, personal communication to T.J. Ohlemiller, National Institute of Standards and Technology, Gaithersburg, MD.
- Fritz, T.A., and P.A. Hough. 2002. Armstrong World Industries, Lancaster, PA, personal communication to R.G. Gann, National Institute of Standards and Technology, Gaithersburg, MD.
- Huggett, C. 1980. Estimation of rate of heat release by means of oxygen-consumption measurements. *Fire and Materials*, vol. 4, pp. 61-65.
- Madrzykowski, D. 1996. Office Workstation Heat Release Rate Study: Full-scale vs, Bench-scale, Proceedings of Interflam '96, Interscience Communications, Ltd., London, pp. 47-55.

- Madrzykowski, D. 1998. Office Building Fire Research Program: An Engineering Based Approach to Fire Safety Design, Proceedings of the 5th Fire and Materials Conference, Interscience Communications, Ltd., London, pp. 23-33.
- Midgett, J.T. 2003. United Airlines, Inc., memorandum to M. Lieberman, National Institute of Standard and Technology, Gaithersburg, MD, December 22.
- Nelson, H.E. 1989. An Engineering View of the Fire of May 4, 1988 in the First Interstate Bank Building, Los Angeles, California. NISTIR 89-4061, National Institute of Standards and Technology, Gaithersburg, MD, March.
- Nelson, M.D. 2003. The Boeing Company, Seattle, WA, memorandum to M. Rubin, National Institute of Standards and Technology, Gaithersburg, MD, September 29.
- Shipp, P. 2002. U.S. Gypsum, Northbrook, IL, personal communication to R.G. Gann, National Institute of Standards and Technology, Gaithersburg, MD.

This page intentionally left blank.

Chapter 4

FIRE MODELING

4.1 INTRODUCTION

From the photographic evidence, the team was able to follow the progress of the fires at the periphery of the buildings. This provided a basis for estimating the heating of the perimeter columns, but not the core structure or the floor assemblies. Furthermore, there were times when assorted windows were blocked from view by smoke and debris clouds. What was needed was a set of three-dimensional, time-varying recreations of the thermal and radiative environment to which all the structural members in each tower were subjected from the time of aircraft impact until their collapses. These could only be obtained via computer simulations, and the computational model needed to feature:

- Resolution of the thermal environment, especially near the columns and trusses;
- Representation of the complex combustibles;
- Computation of fire progression across the large expanses of the World Trade Center (WTC) floors.

These requirements mandated the use of a computational fluid dynamics (CFD) model. The time frame of the Investigation favored the use of the Fire Dynamics Simulator (FDS), a CFD model with which the Investigation staff had extensive experience.

The accuracy of the predicted duration and spread of the fires at the plane of the windows could be assessed by comparison with the photographic evidence. The predictions of the fire behavior in the building interior were potentially subject to significant uncertainty. To estimate this uncertainty, the National Institute of Standards and Technology (NIST) conducted compartment fire tests at large scale (but still smaller than the acre-size fires that burned in the towers on September 11, 2001) and compared the results with the output from FDS simulations.

4.2 DESCRIPTION OF THE FIRE DYNAMICS SIMULATOR

FDS is a computational fluid dynamics model developed and maintained by the NIST Building and Fire Research Laboratory (BFRL). It solves numerically a form of the Navier-Stokes equations appropriate for low-speed, thermally driven flows with an emphasis on smoke and heat transport from fires. Under development at NIST since 1978, FDS was first publicly released in February 2000. Following is a brief description of the major components of FDS. Detailed information regarding the assumptions and governing equations associated with the model is provided in the FDS Technical Reference Guide (McGrattan 2004).

Hydrodynamic Model: The core algorithm is an explicit predictor-corrector, finite-difference scheme, second order accurate in space and time. Turbulence is treated by means of the Smagorinsky form of Large Eddy Simulation (LES).

Combustion Model: For most applications, FDS uses a mixture fraction combustion model. The mixture fraction is a conserved scalar quantity that is defined as the fraction of gas at a given point in the flow field that originated as fuel. The model assumes that combustion is mixing-controlled, and that the reaction of fuel and oxygen is infinitely fast. The mass fractions of all of the major reactants and products can be derived from the mixture fraction by means of “state relations,” empirical expressions arrived at by a combination of simplified analysis and measurement.

Radiation Transport: Radiative heat transfer is included in the model via the solution of the radiation transport equation for a non-scattering gray gas. The radiation equation is solved using a technique similar to a finite volume method for convective transport; thus, the name given to it is the Finite Volume Method. Using approximately 100 discrete angles, the finite volume solver requires about 15 percent of the total central processing unit (CPU) time of a calculation, a modest cost given the complexity of radiation heat transfer. Water and fuel droplets can absorb thermal radiation, and the absorption coefficients are based on Mie theory. This capability was exercised in the WTC simulations to describe the combustion of jet fuel.

Geometry: FDS approximates the governing equations on one or more rectilinear grids. Walls, floors, ceilings, and any other obstructions to the fluid flow must conform to this rectangular, three-dimensional grid.

Boundary Conditions: All solid surfaces are assigned thermal boundary conditions plus information about the burning behavior of the material. Usually, material properties are stored in a database and invoked by name. Heat and mass transfer to and from solid surfaces is usually handled with empirical correlations.

FDS is suited for a wide range of thermally driven fluid flow scenarios, including fire, both in the open (e.g., unconfined fire plumes) as well as within the built environment. To date, about half of the applications of FDS have been for design, and half for forensic reconstruction. Design applications typically involve an existing building or a building under design. A so-called “design fire” is prescribed either by a regulatory authority or by the engineers performing the analysis. Because the fire’s heat release rate is known, the role of the model is to predict the transport of heat and combustion products throughout the room or rooms of interest. Ventilation equipment is often included in the simulation, like fans, blowers, exhaust hoods, heating, ventilating, and air conditioning (HVAC) ducts, smoke management systems, etc. Detailed descriptions of the contents of the building are usually not necessary because these items are not assumed to be burning, and even if they are, the burning rate will be fixed, not predicted. Sometimes, it is necessary to predict the heat flux from the fire to a nearby “target,” and even though the target may heat up to some prescribed ignition temperature, the subsequent spread of the fire usually goes beyond the scope of the analysis because of the uncertainty inherent in object to object fire spread.

Forensic reconstructions require the model to simulate an actual fire based on information that is collected after the event, such as eye witness accounts, unburned materials, burn signatures, etc. The purpose of the simulation is to connect a sequence of discrete observations with a continuous description of the fire dynamics. Usually, reconstructions involve more gas/solid phase interaction because virtually all objects in a given room are potentially ignitable, especially when flashover occurs. Thus, there is much more emphasis on such phenomena as heat transfer to surfaces, pyrolysis, flame spread, and suppression. In general, forensic reconstructions are more challenging simulations to perform because they require more

detailed information about the room contents, and there is much greater uncertainty in the total heat release rate as the fire spreads from object to object.

Validation studies of FDS prior to the Investigation were aimed more on design applications than reconstructions. The reason is that design applications usually involve prescribed fires and demand a minimum of thermophysical properties of real materials. Transport of smoke and heat is the primary focus, and measurements can be limited to well-placed thermocouples, a few heat flux gauges, gas samplers, etc. Phenomena of importance in forensic reconstructions, like second item ignition, flame spread, vitiation effects, and extinction, are more difficult to model and more difficult to study with well-controlled experiments. Uncertainties in material properties and measurements, as well as simplifying assumptions in the model, often force the comparison between model and measurement to be qualitative at best. Nevertheless, current validation efforts, including those conducted for the Investigation, are moving in the direction of these more difficult issues.

4.3 FDS ACCURACY FOR FIRES OF KNOWN HEAT RELEASE RATE

The compartment spray burner fire tests described in Section 3.4.3 were designed to assess the accuracy of the fire model's predictions for scenarios in which the heat release rate (HRR) of the fire was prescribed. It was necessary to assess the basic transport algorithms within the model with calculations where the source of mass and energy was known before embarking on more complicated simulations of entire furnished compartments burning. The compartment was heavily instrumented so that all of the energy from the fire could be accounted for and reported in terms of conductive losses to walls, convective flux through openings, etc. Figure 4–1 displays a snapshot from an animation of one of the simulations. With the large number of measurements, it was possible to go beyond the traditional point-by-point comparison and discover why the model either over-predicted or under-predicted a given measurement. It was possible to compare the transport of energy, starting with the combustion of fuel, and ending with effluent exiting into a large hood. Based on these integrated quantities, discrepancies in heat flux and gas concentration predictions could be tied to errors in the overall energy budget, allowing for an assessment of the accuracy of various components within the model.

Prior to each of the tests, a prediction of the thermal environment in the compartment was determined using FDS. Following the tests, the prediction and experimental results were compared. Figure 4–2 compares measured and predicted gas temperatures at various elevations within the room during Test 5, in which an insulated steel truss section was exposed to a 3 MW fire for roughly 50 min. The complete set of test results and their analysis can be found in NIST NCSTAR 1-5E. The analysis of the data showed that FDS predictions of the compartment gas temperatures, major species concentrations, heat fluxes, wall temperatures, and flow velocities were within 10 percent of the measurements, an uncertainty that could be traced to the uncertainty in the measured heat release rate, an input parameter for the model. Exceptions were for near-field measurements of heat flux and wall temperature in the plume impingement region on the ceiling, and at the base of the fire on the floor. These predictions were within 20 percent of the experimental measurements and were largely due to simplifications of the spray burner geometry and in-flame fire physics. For the simulations of the WTC fires, the objective was to predict the upper layer gas temperatures from fires spread over a large area. Discrepancies in near-field phenomena were not expected to affect the large scale predictions significantly.

In these experiments, the “fire” was a heat source whose combustion properties were steady and well known. The comparison between experiment and calculation was thus a test of the fluid mechanics and heat transfer capability in FDS. The good agreement indicated that no changes were needed in these aspects of the model.

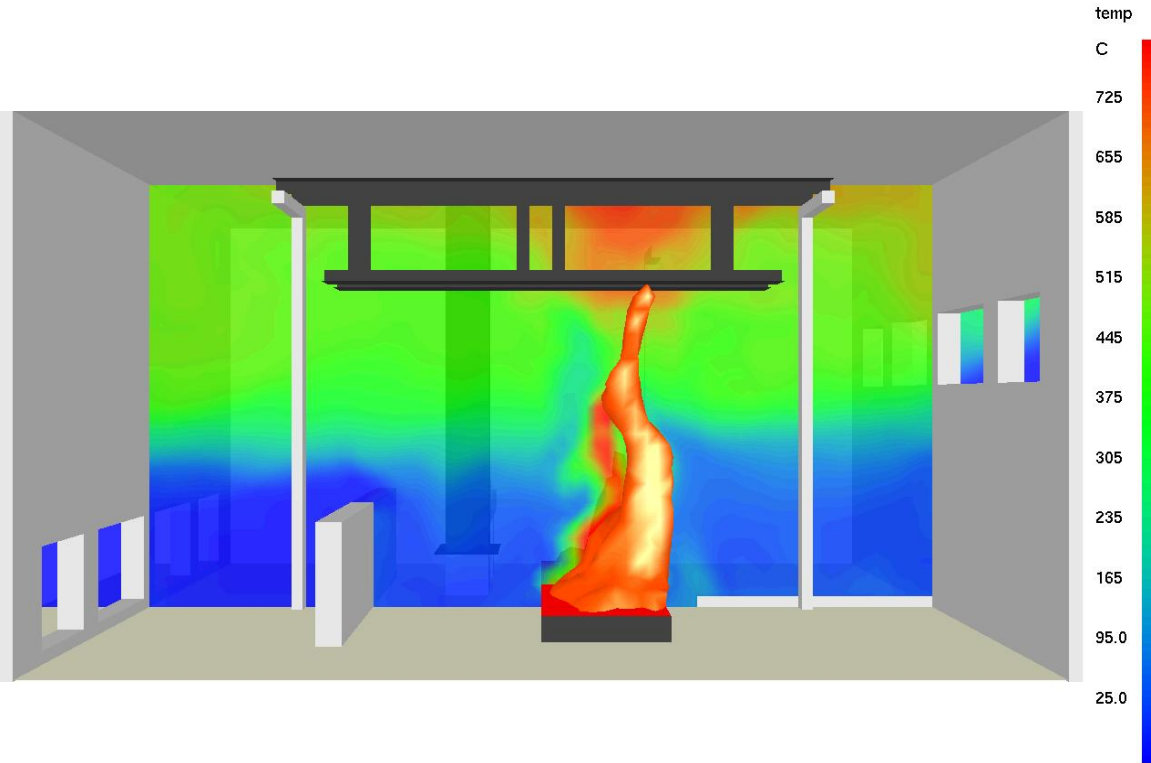


Figure 4–1. Simulated centerline gas temperatures in a spray burner test.

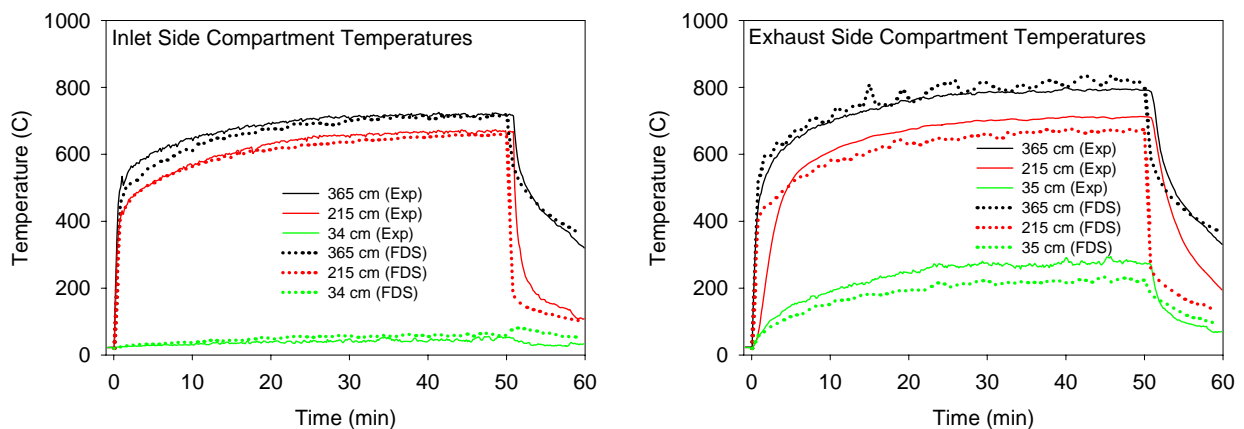


Figure 4–2. Comparison of predicted and measured gas temperatures at various heights above the floor, Test 5.

4.4 MODELING OF THE BUILDING COMBUSTIBLES

Following the completion of the initial spray fire experiments, the experimental program concentrated on the thermal properties of the office furnishings that constituted the bulk of the combustible fuel within the WTC buildings under study. Several types of office workstations typical of those used in WTC 1 and WTC 2 were purchased at area office supply stores. The thermal properties of the major materials making up the workstations were derived from bench-scale experiments (NIST NCSTAR 1-5C).

Briefly, cone calorimeter measurements at three different heat fluxes were performed for the carpet, desk (wood), computer monitor, chair, privacy panel, and stacked paper. For the simulations of the WTC fires, only the carpet, desk, and privacy panel data were used directly. The carpet and privacy panel were modeled as thermoplastics, that is, the burning rate was assumed to be proportional to the heat flux from the surrounding gases. The desk was modeled as a charring solid in which a pyrolysis front was assumed to propagate through the material, leaving a layer of char behind that insulated the material and reduced the burning rate.

The chair, computer, paper, and other miscellaneous items within the workstation were modeled as a composite material by lumping their mass together into large “boxes” and distributing them throughout the workstation. It is common practice in fire protection engineering to use surrogate materials for fire experiments, and this practice has been extended to numerical modeling. Over the years, simple, well-characterized combustibles have been developed that are representative of more complicated commercial products. For example, wood cribs are often used to represent ordinary combustibles found in residential or light industrial settings. Paper cartons with various amounts of plastic within are also used as surrogates for a wide range of retail commodities. One in particular is called the FMRC (Factory Mutual Research Corporation) Standard Plastic Commodity, or more commonly, Group A Plastic. This test fuel is often used in sprinkler approval testing at Factory Mutual and Underwriters Laboratories in the United States, and similar test fuels have been developed in Europe. In the late 1990s, FDS was used to simulate large scale rack storage fires to determine the effectiveness of the combined use of sprinklers, roof vents, and draft curtains (curtain boards). As part of this effort, a considerable amount of work was done to characterize the thermal properties of Group A Plastic (Hamins and McGrattan 2003). Because Group A Plastic has been shown to be fairly representative of fires fueled by a mixture of paper (cellulosic materials) and plastic, and because it has been used in numerous FDS simulations, it was decided to model the miscellaneous contents of the office workstations with a fuel similar to Group A Plastic.

Blind predictions of the single open workstation burns were made using the measured material properties, and then these properties were adjusted to match the results of the experiments. Thus, the single workstation burns served to *calibrate* the model. They were not intended as *validation* experiments. The results of the refined simulations of the various single workstation experiments are shown in Figure 4-3.

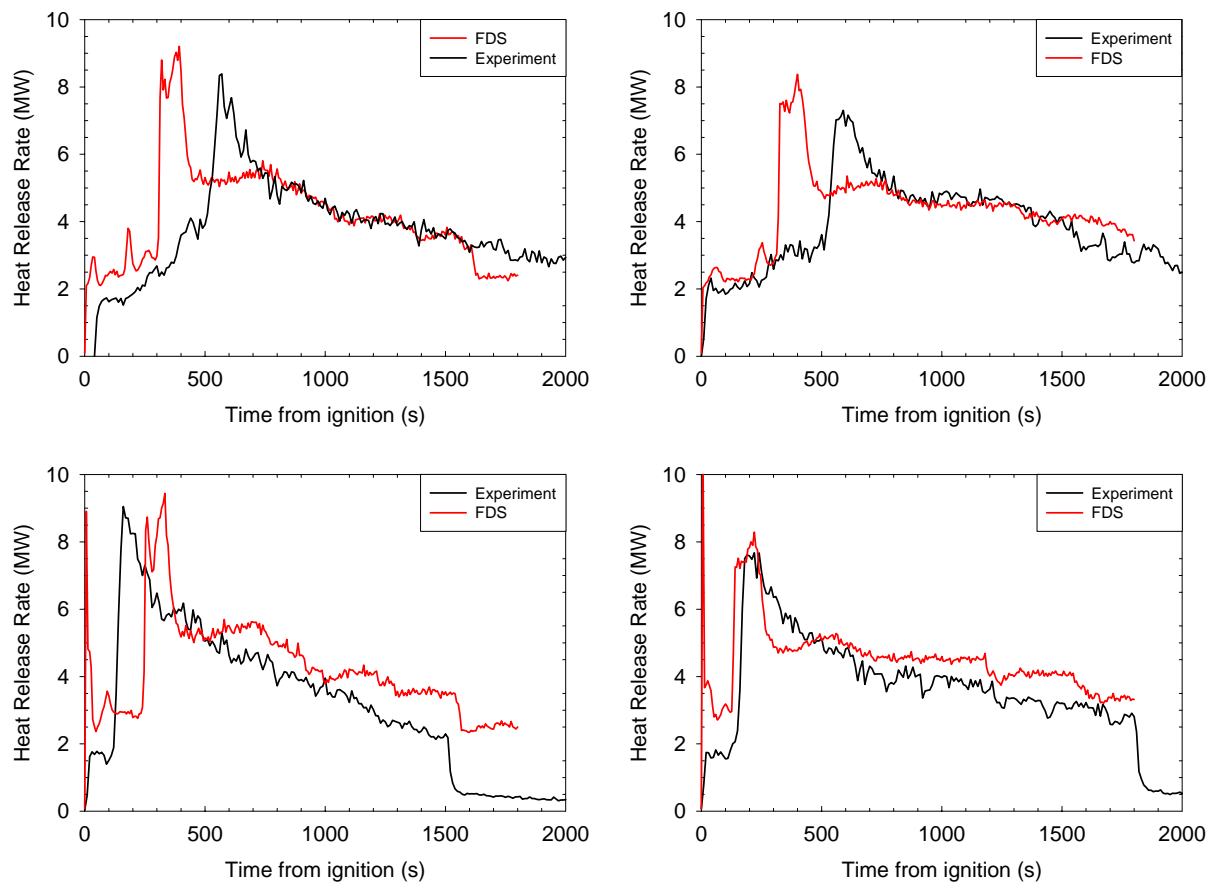


Figure 4–3. Heat Release Rates for the single workstation fire experiments. Clockwise from upper left: a single, undamaged workstation; a workstation with ceiling tiles added; a workstation with tiles and jet fuel applied; and a workstation with just jet fuel applied.

The workstation burns served to check that the assumptions made in modeling the workstation with the simplified fuel packages would produce reasonable results. All four simulations were successful in the major facets, within experimental uncertainty:

- The magnitudes of the peak HRR values were within 10 percent of the experimental values.
- The shape and magnitude of the subsequent, near-steady burning behavior were quite similar.
- The overall burning times were similar for the experiments and the simulations.
- The effect of the tiles in decreasing the peak HRR and on the subsequent burning behavior was captured correctly.
- The effect of the Jet A in increasing the peak HRR and on the subsequent burning behavior was captured correctly.

Some notes on the limitations revealed from the individual tests were:

- The peak HRR in the simulations without Jet A occurred sooner than in the experiments. In the experiment, the time to peak HRR was strongly influenced by the melting of the chair plastic onto the carpet. This level of detail was not captured in the numerical model, especially given the fact that the chair had been lumped together with various other combustible items.
- The simulations underpredicted the large reduction in the time to the peak HRR for the addition of Jet A. FDS consumed the Jet A immediately with relatively small effect on the growth of the heat release rate. For the actual fire, the ignition of the Jet A did not occur until about 120 s.

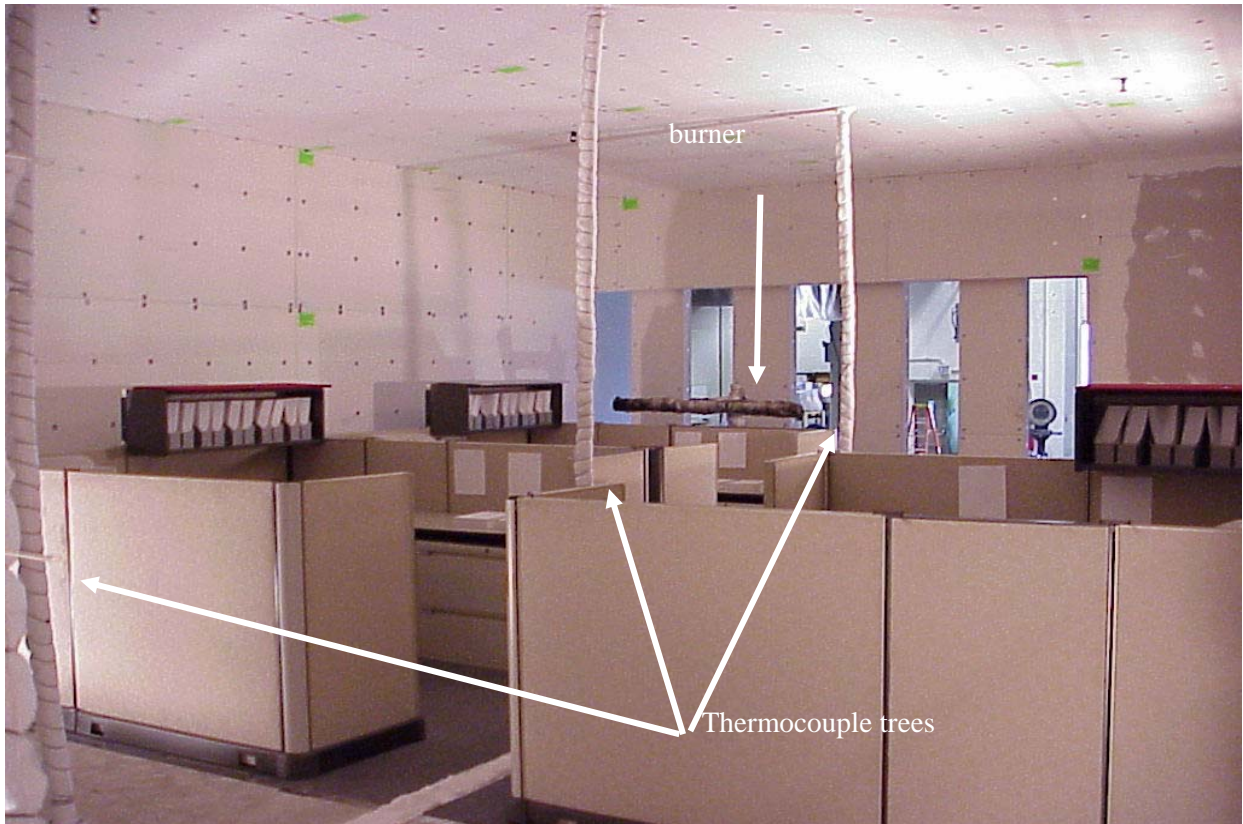
Overall, the chosen set of parameters and approximated component burning descriptions gave a reasonable description of the actual workstation HRR behavior and its dependence on the parameters (inert tile coverage and presence of Jet A). The localized differences between the simulations and experiments would become less important when many workstations were burning concurrently, as was the case in the large fires on September 11, 2001.

4.5 COMPARTMENT FIRE EXPERIMENTS INVOLVING WORKSTATIONS

Following the single workstation fire experiments and the accordant improvements in FDS, a series of large-scale experiments was conducted in the NIST Large Fire Laboratory between November 4 and December 10, 2003 (NIST NCSTAR 1-5E). The six experiments were designed to assess the accuracy with which FDS predicted the fire spread, heat release rate, and thermal environment in a large compartment in which multiple workstations were burning in a configuration characteristic of that found in the WTC buildings. Each test involved three workstations. Two of the workstations were contiguous, exemplifying a part of the type of cluster that existed in the WTC towers. The third workstation was separated from the other two by an aisle, representing a part of a second cluster. This array was to enable assessment of FDS's ability to replicate two different modes of cubicle-to-cubicle fire spread: direct flame impingement and radiative ignition from the hot ceiling layer. The nature of the tests is summarized in Table 4–1. Figure 4–4 shows the interior of the test room, and Figure 4–5 shows the “rubble” workstations prior to the start of Test 5.

Table 4–1. Test matrix.

Test	Ceiling Tiles	Jet Fuel	Burner Location	Workstations	Windows
1	None	None	Front	Intact	No
2	None	None	Front	Intact	No
3	Present	Present	Front	Intact	No
4	Present	None	Rear	Intact	No
5	Present	Present	Rear	“Rubble”	No
6	None	Present	Rear	Intact	Yes



Source: NIST.

Figure 4–4. View of the fire compartment before the start of Test 6.



Source: NIST.

Figure 4–5. Disassembled workstation burned in Test 5.

FDS simulations of each test were carried out before the test was conducted. Figure 4–6 and Figure 4–7 show pictures of an actual test and a corresponding simulation. Both the heat release rate and the compartment temperatures were compared.



Source: NIST.

Figure 4–6. Multiple workstation fire experiment.

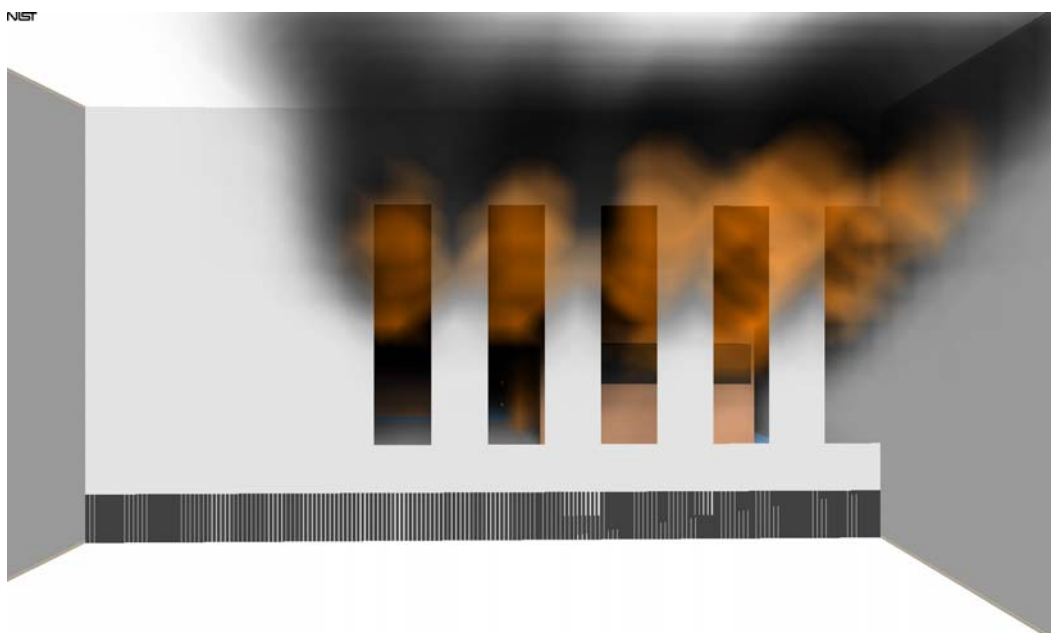


Figure 4–7. Coarse grid simulation of a multiple workstation experiment.

Figure 4–8 displays the upper layer temperature for Test 1 at four locations (clockwise from upper left: near window, between workstations, behind workstations, rear wall). The measured and predicted temperatures for all the tests were similar to those shown in Figure 4–8. Peak temperatures near the compartment opening were about 1,000 °C, decreasing to 800 °C at the very back of the compartment. The trend was captured in the simulations. The decrease in temperature was important because in the simulations of the WTC fires, the only basis of comparison was the visual observations of fires around the exterior of the buildings. It was important to demonstrate that the model not only predicted accurately the temperature near the windows, but also the decrease in temperature as a function of distance from the windows. The temperature predictions for the other tests were similar and are included in NIST NCSTAR 1-5E.

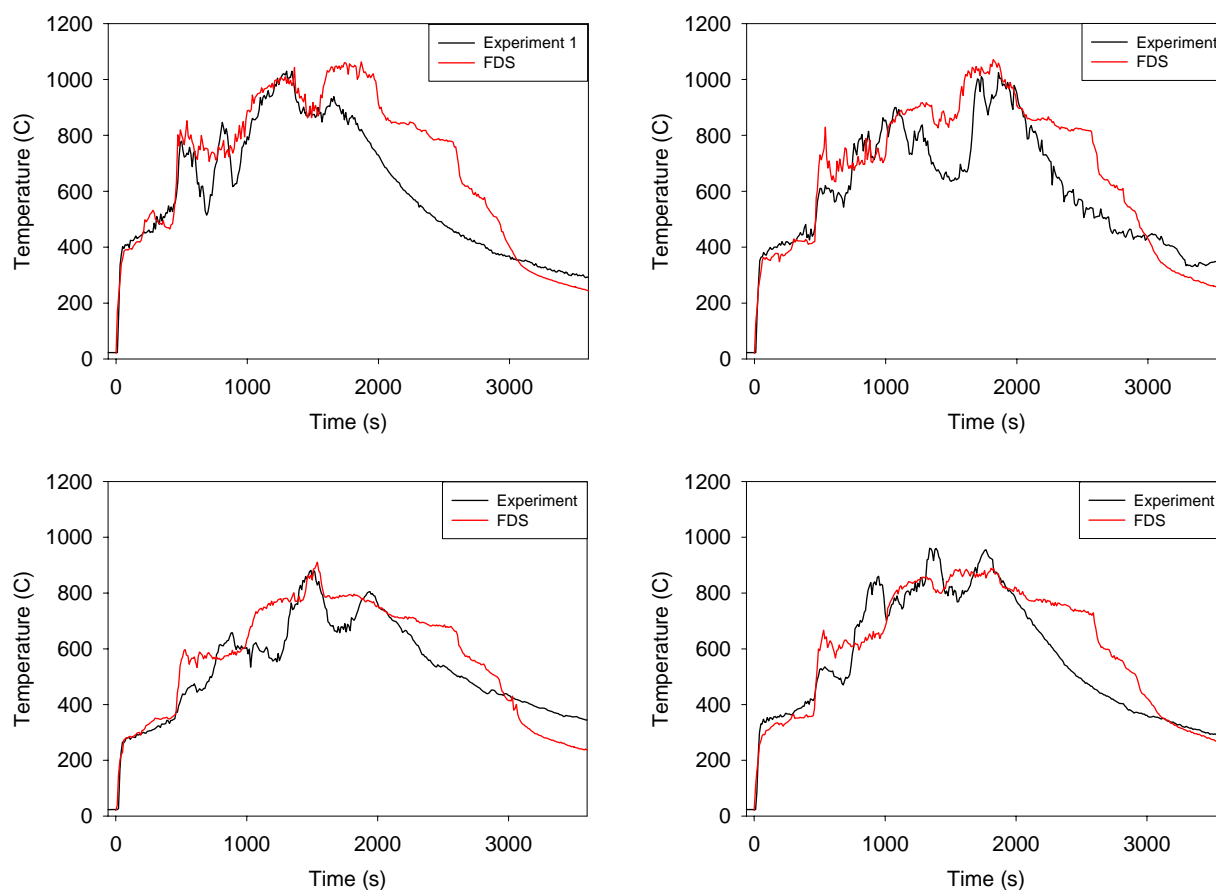


Figure 4–8. Upper layer temperatures at 4 locations, Test 1.

Figure 4–9 displays comparison plots of measured and predicted heat release rates.

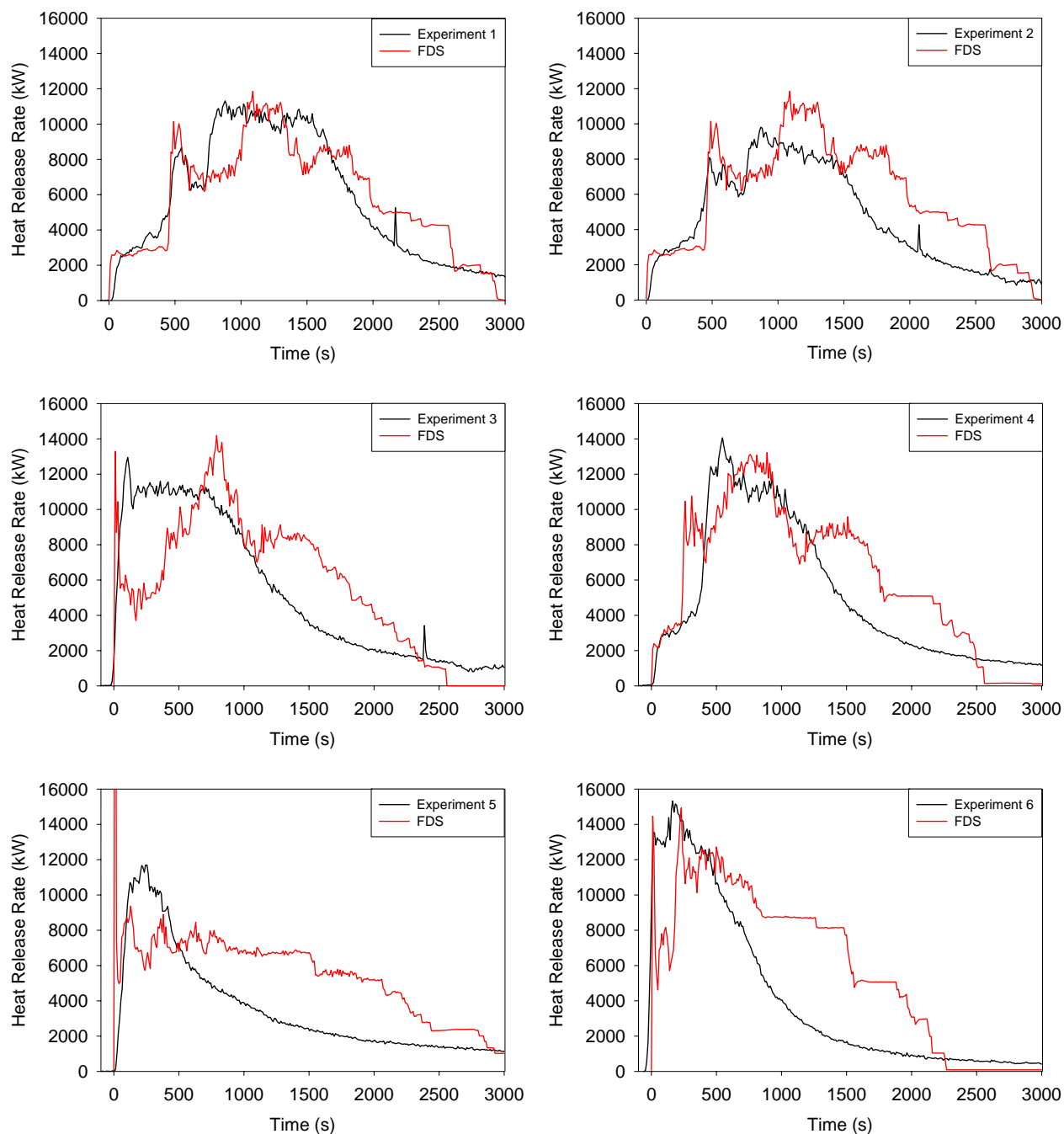


Figure 4–9. Heat Release Rates for multiple workstation experiments.

The agreement is quite good, albeit not perfect. For Tests 1 through 4 and 6:

- The predicted total heat release closely mirrored the measured value in each test. This was expected, since the heat release parameters were derived from the single workstation tests. Nonetheless, this was a confirmation that FDS was self-consistent.

- The broad shapes of the predicted and measured heat release rate curves were similar. FDS tended to underpredict the pre-peak behavior, overpredict the long-time slower burning period, and thus run out of fuel sooner than the actual tests. These effects were likely due to the simplified modeling of the complex thermoplastic combustibles.
- The spike at the start of the simulations of Tests 3, 5, and 6 was associated with the burning of Jet A. In the FDS mixture fraction model, the fuel burned immediately upon mixing with air, while in the experiment some Jet A had been absorbed by the furnishings and required more time to burn.
- The predicted times to half combustion of the workstations were, on the average, three minutes longer than the measured times.
- The predicted burnout times were, on the average, five minutes longer than the measured times.

Test 5 can be considered a calibration rather than a validation of the model. No free burns of collapsed single workstations had been performed. The mass loss from the rubblized cubicles was approximately half that of the assembled workstations. Thus, the burning rate for the simulation was reduced by the same factor, while retaining the same total fuel mass. The adequacy of the prediction suggested that this factor was a reasonable approximation for use in the reconstruction of the WTC fires in the regions where highly damaged furnishings were to be expected.

Figure 4–8 and Figure 4–9 were made using a 50 cm by 50 cm by 40 cm grid, the same as was used for the final WTC calculations. Results were similar with the 25 cm by 25 cm by 20 cm grid. The reason for the agreement was that the burning rate of the workstation assemblies was largely a function of the heat feedback from the hot upper layer. Given that the peak upper layer temperatures were similar in each case, the burning rates were similar. Note that the grid independence demonstrated in both the spray burner and the workstation fire simulations is not guaranteed for all applications of the fire model. Indeed, the simulation of small fires (relative to the overall compartment size) demands a much finer grid than the one used in the WTC Investigation because of the model's tendency to smear out steep gradients on coarse grids. However, if the fires are large enough to form a relatively uniform layer over an appreciable expanse of the compartment ceiling, the model is far less sensitive to the size of the grid cells so long as there are enough of them spanning the uniform regions. This was the case for all of the WTC simulations.

4.6 SUMMARY

From a modeling perspective, the objective of the simulations of the single and multiple workstation fires was to develop a simplified representation of the office furnishings found throughout the WTC, and then demonstrate that the fire model was capable of reproducing the thermal environment of a compartment filled with these furnishings. Because of the magnitude of the simulations of the building fires, the model of the workstation had to be fairly simple. However, because of the many uncertainties in the initial conditions of the fire simulations, the lack of detail in the model was not considered to be a problem. The model fires had similar growth patterns, peak heat release rates, decay patterns, and compartment temperatures. All agreed with measurements to within about 20 percent, an accuracy that was sufficient given the uncertainty in the state of the building and its furnishings following the impact of the aircraft.

In an assessment of the model, it was important to maintain perspective on the accuracy required to reconstruct the actual WTC fires. For fires that were sufficiently severe that they threatened the structural integrity of the building, many workstations burned concurrently. These workstations were at various stages of their combustion, and the aggregate burning of a large group of workstations would smear out features that were not precisely modeled.

4.7 REFERENCES

- Bryant, R., T.J. Ohlemiller, E. Johnsson, A. Hamins, B. Grove, W.F. Guthrie, A. Maranghides, and G.W. Mulholland. 2003. *The NIST 3 Megawatt Quantitative Heat Release Rate Facility - Procedures and Guidance*, Special Publication 1007, National Institute of Standards and Technology, Gaithersburg, MD, December.
- Hamins, A., A. Maranghides, A., and G.W. Mulholland. 2003. *The Global Combustion Behavior of 1 MW to 3 MW Hydrocarbon Spray Fires Burning in an Open Environment*, NISTIR 7013, National Institute of Standards and Technology, Gaithersburg, MD, June.
- Hamins, A., and K.B. McGrattan. 2003. Reduced-Scale Experiments on the Water Suppression of a Rack-Storage Commodity Fire for Calibration of a CFD Fire Model. *Fire Safety Science: Proceedings of the Seventh International Symposium*. International Association for Fire Safety Science, 457-468.
- Huggett, C. 1980. Estimation of the Rate of Heat Release by Means of Oxygen Consumption, *Fire and Materials*, vol. 12, pp. 61-65.
- McGrattan, K.B (Ed.). 2004. *Fire Dynamics Simulator (Version 4), Technical Reference Guide*. NIST Special Publication 1018. National Institute of Standards and Technology, Gaithersburg, MD, July.

This page intentionally left blank.

Chapter 5

HEAT TRANSFER MODELING¹

5.1 INTRODUCTION

Simulating the effect of a fire on the structural integrity of a building required a means for transferring the enthalpy generated by the fire to the surface of the structural members and then conducting the heat through those members. In the current Investigation, this meant mapping the time- and space-varying gas temperatures and radiation field generated by Fire Dynamics Simulator (FDS) onto and throughout the (insulated) columns, trusses and other elements that made up the WTC tower structures.

This process was made difficult for these large, geometrically complex buildings by the wide disparity in length and time scales that had to be accounted for in the simulations. Typical length scales ranged from 60 m, characteristic of the building, to 1 cm or 2 cm, characteristic of the details of structural components, to tens of cm, characteristic of the turbulent eddies in the fire effluent. Typical FDS time steps were of the order of ms, while the lengths of the fires burning in WTC 1 and WTC 2 were of the order of 100 min. Devising computation schemes to accommodate the finest of these scales while simulating the largest of these scales presented a software challenge in order to avoid extremely long computation times.

5.2 DESCRIPTION OF THE FIRE STRUCTURE INTERFACE

To overcome these difficulties, the National Institute of Standards and Technology (NIST) developed the Fire Structure Interface (FSI) (Prasad and Baum 2004). To use the FSI to generate the temperature distribution within structural elements exposed to a fire:

- The FDS-calculated gas phase temperatures served as boundary conditions for radiative and convective heat transfer to sub-grid scale structural components.
- A radiative transport model assumed that the local environment above and below each grid square on the surface of a structural member was divided into a hot, soot-laden upper layer and a cool, relatively clear lower layer whose contribution to radiative heat transfer was far lower than that of the upper layer. This “thermal column” was about 0.5 m². Assuming the two layers behaved as gray bodies (i.e., radiation properties independent of spectral wavelength), the upper layer temperature, absorption coefficient, and upper layer depth were computed at 30 s intervals and stored as an ASCII text file for computing the combined radiative and convective fluxes incident on the structural components.
- Explicit formulae for the radiative heat flux were obtained as a function of temperature, hot layer depth, soot concentration, and orientation of each structural element. These formulae

¹ Extensive detail of the material in this Chapter is provided in NIST NCSTAR 1-5G. Further references to this report are not inserted in order to preserve continuity of this text.

were used to generate realistic thermal boundary conditions for the coupled transient three-dimensional finite element code.

- Structural components in the hot layer were also subject to convective fluxes with bulk temperature values equal to the local instantaneous value of the temperature in the hot layer and an assumed convective heat transfer coefficient value of $25 \text{ W/m}^2\text{-K}$ (Eurocode 1994).
- The thermophysical properties of the steel and the insulation materials were obtained from NIST NCSTAR 1-3E, NIST NCSTAR 1-6A, and Taylor et al. (2003).
- The file was subsequently read into the ANSYS 8.0 (2004) finite element program, which generated the thermal distribution within the structural elements.

5.3 SENSITIVITY OF THE HEAT TRANSFER PROCESS

Prior to applying the FSI to the complexity of the fires of September 11, a number of computation experiments were performed to determine the sensitivity of the heating rates of structural element to the parameters in the simulations. These parameters included the presence and condition of insulation, the mass of the steel element, and the temperature of exposure.

One set of simulations involved immersing a typical core column in a constant temperature “furnace.” The presence and thickness of sprayed fire-resistive material (SFRM) was varied, as was the furnace temperature. Each experiment was terminated when the steel temperature reached a value at which significant loss of strength would have occurred (NIST NCSTAR 1-3). Figure 5–1 depicts the column. In the left-hand frame, the steel is in cyan and the SFRM is purple. The right-hand frame shows the thermal profile within the column later in the simulation. Table 5–1 shows the heating times for the various conditions. Only the simulations with damaged insulation showed any temperature gradient in the steel.

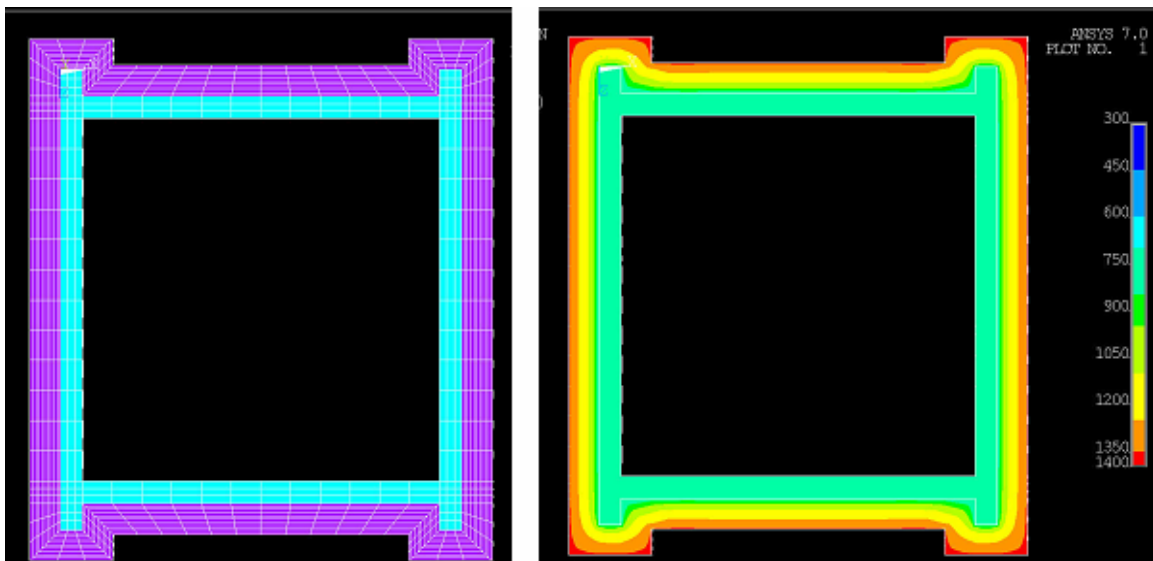


Figure 5–1. Finite element model of light box shape core column and temperature contours (Kelvin) at one instant in time.

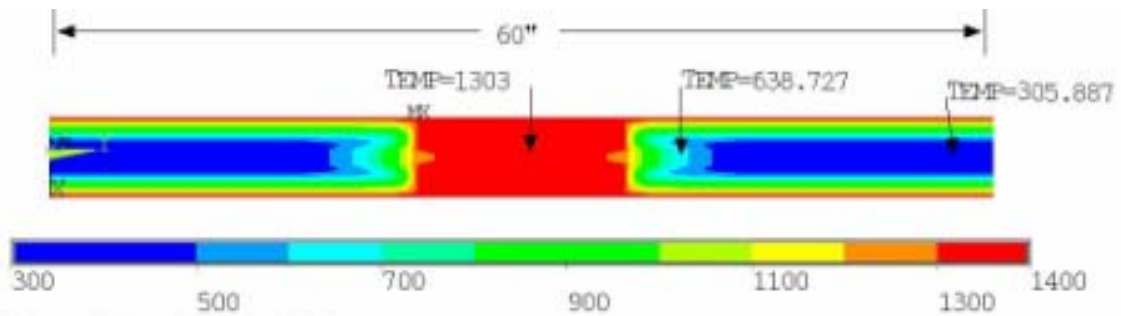
Table 5–1. Times (h) at which modeled columns reached target temperatures.

Insulation Thickness (in.)	Furnace Temperature/Final Steel Temperature, °C		
	700 °C/650 °C	900 °C/700 °C	1,100 °C/700 °C
	1,292 °F/1,202 °F	1,653 °F/1,292 °F	2,012 °F/1,292 °F
0	0.3	0.2	0.1
0.5	6.0	3.2	2.0
1.125	10.0	7.4	4.6
1.125, with 20 % Damage	6.6	4.5	2.2

Similar simulations with heavier columns resulted in significantly longer heating times. This was due to the larger mass of steel that had to be heated.

For both types of columns, the presence of even a thin layer of insulation led to heating times that were significantly longer than the times over which the towers remained standing after impact. The absence of SFRM led to heating times that were below the duration of fire exposure on September 11 (Chapter 6).

In another set of simulations, a 60 in. wide, 1 in. thick steel plate was inserted into a furnace at 1,100 °C. The thickness of the insulation was varied between 0 in. and 2.0 in. in ¼ in. increments; the standard deviation of the thickness was varied from 0 in. to 1.0 in., and a gap in the insulation was varied from 0 in. to 30 in. in 6 in. increments. Figure 5–2 shows the edge of the plate before and in the midst of the simulation. Figure 5–3 shows the rates of temperature rise at a location 6 in. from the right end of the plate. A dashed line at 600 °C is included in each plot for reference. For such a plate (which is as thick as the rods in the floor trusses), large variance in thickness and/or large gaps in the application led to short times to reach temperatures at which structural strength would have been compromised.

**Figure 5–2. Temperature rise (K) in a plate with a 12 in. gap in the thermal insulation.**

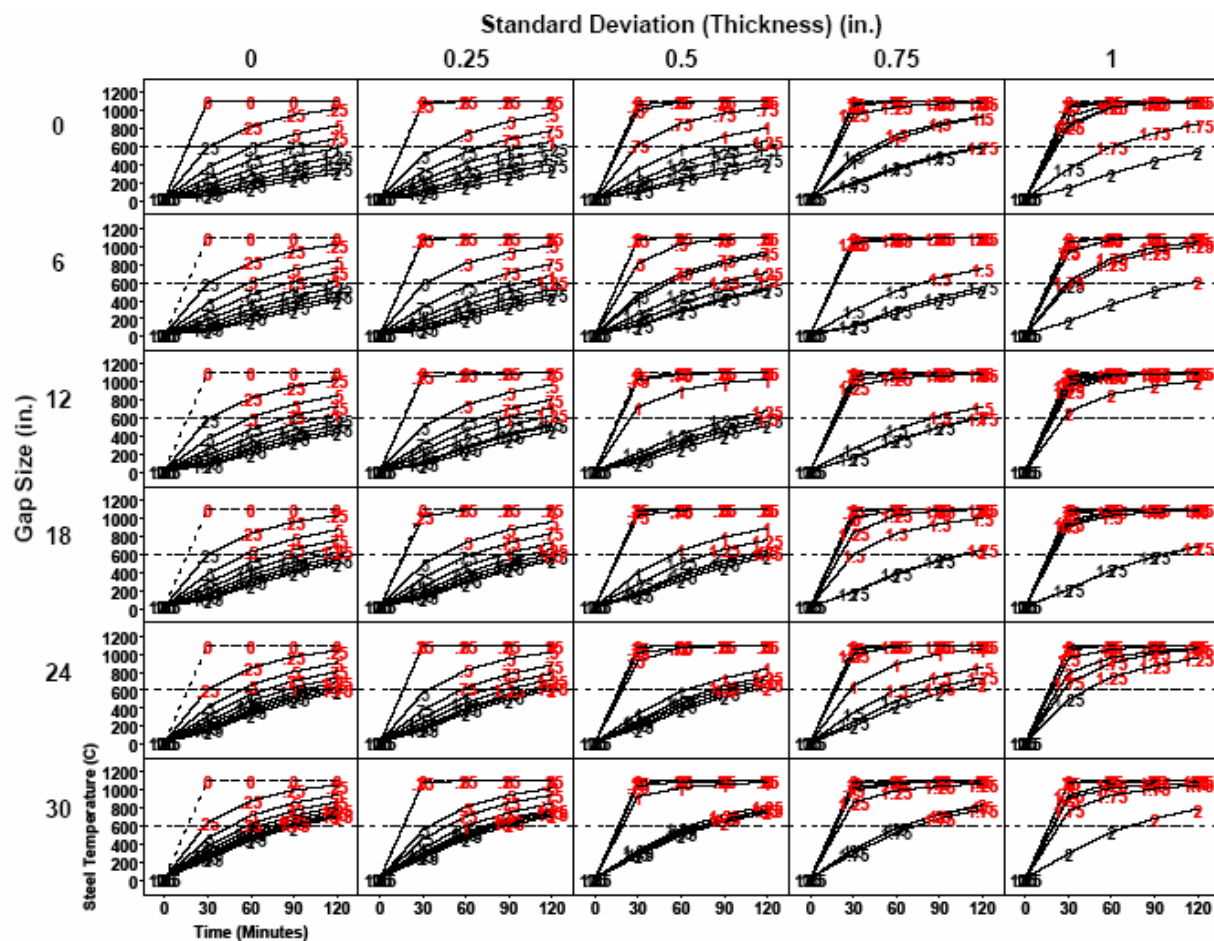


Figure 5–3. Rates of temperature rise in a 1 in. steel plate as a function of the length of a gap and the variability in the applied insulation for several insulation thicknesses.

5.4 ACCURACY ASSESSMENT OF FSI

As was done for FDS, it was necessary to establish the quality of FSI’s numerically predicted temperature profiles within insulated and bare structural steel components with the experimental measurements. This was done using data from the fire tests described in Section 3.4.3.

5.4.1 Rendition of Structural Elements

A sample of the types of grid structure used and data obtained is shown in Figure 5–4 for the steel rod depicted in Figure 3–17. The bar was also divided into 30 uniform divisions along its length. Figure 5–4 also shows the thermal profile of the rod well into Test 5 of the series. The thickness of the SFRM was 23.0 mm \pm 5.5 mm (0.91 in. \pm 0.22 in.) (Table 3–11).

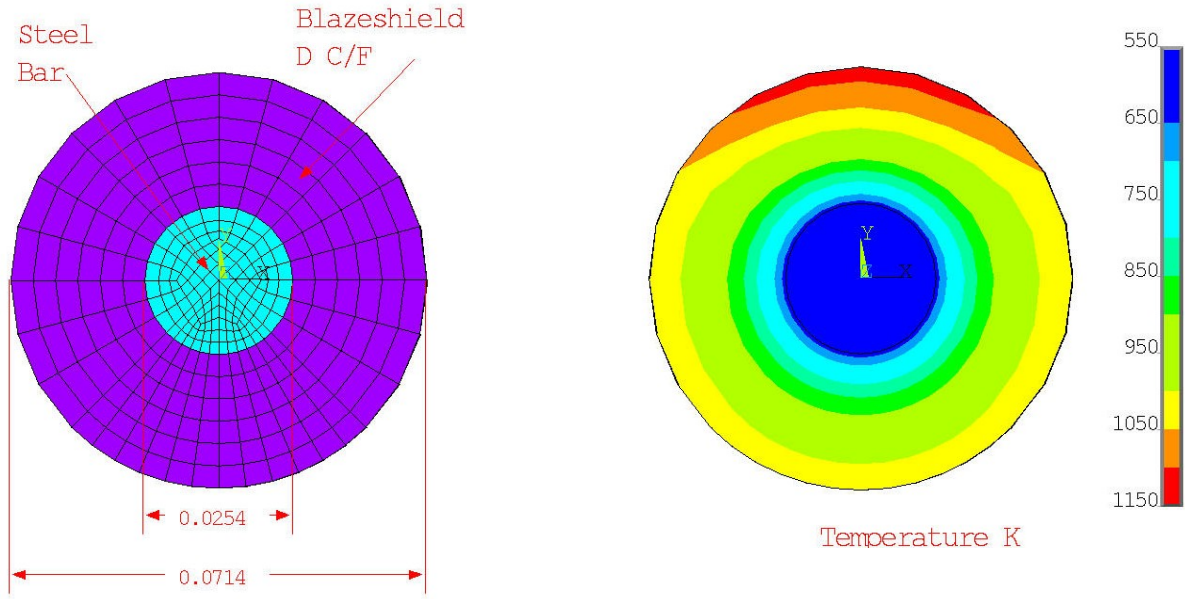


Figure 5–4. FSI grid structure of insulated steel rod (with dimensions in meters) showing the elements used to model the steel (in blue) and the SFRM (in violet), and the temperature contours after 2,000 s in Test 5.

Figure 5–5 shows the finite element structure used to model the thermal response of the column. A portion of the Marinite ceiling and floor were also included in the model in an effort to capture the radiative exchange between the column and these elements. The thickness of the SFRM was 25.3 ± 4.6 mm. Figure 5–6 shows a typical calculation for the temperature (in K) plotted as isocontours on the surface of the SFRM and the Marinite ceiling 2,000 s into the simulation of Test 5.

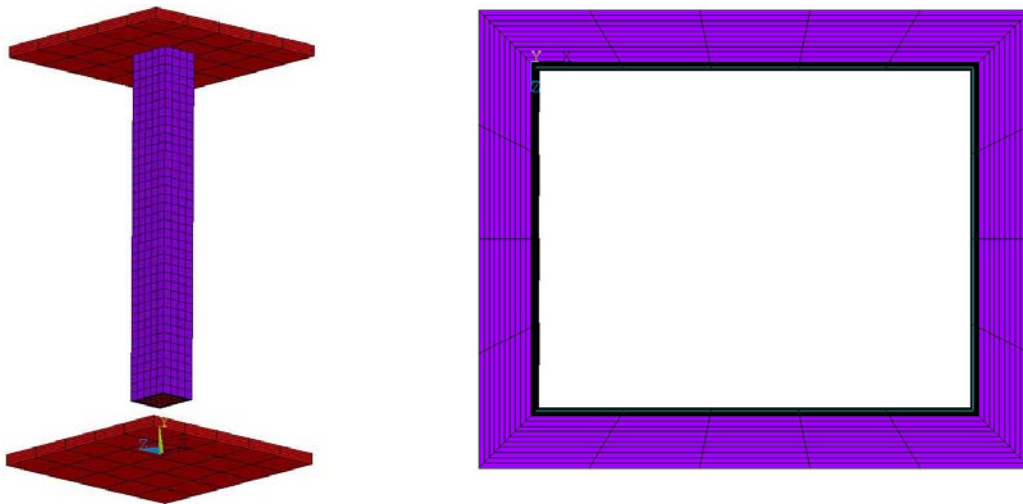


Figure 5–5. Perspective and top view of the finite element model of the steel column with SFRM.

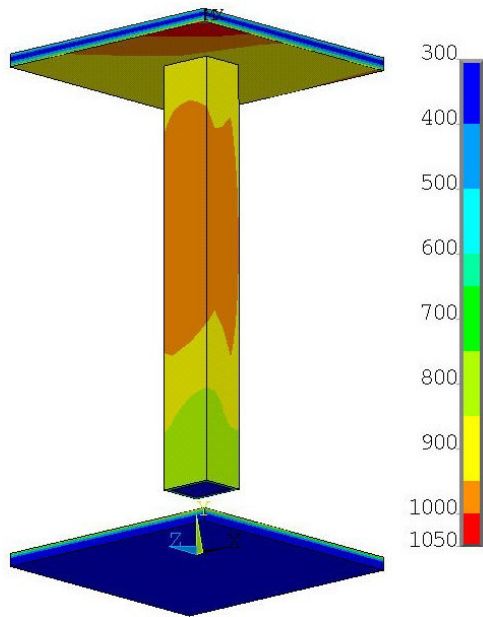


Figure 5–6. Temperature (in K) contours on the outer surface of the SFRM and the ceiling after 2,000 s in Test 5.

Figures 5–7 and 5–8 show the finite element representation of the truss used in the thermal analysis. Figure 5–9 shows a typical calculation of the temperature contours on the surface of the SFRM for Truss A 1,000 s into Test 5.

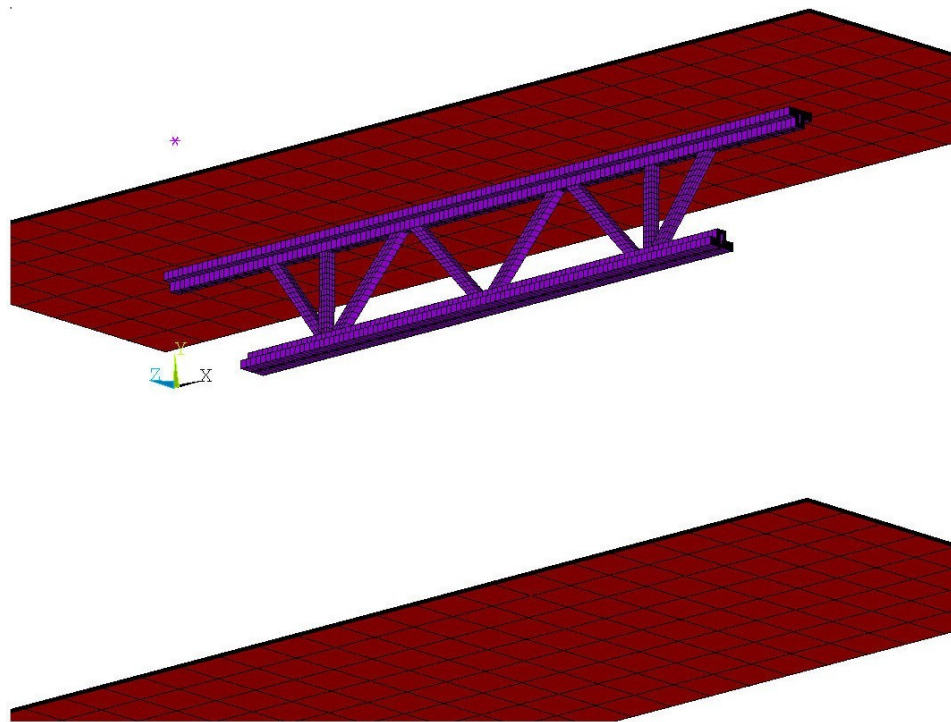


Figure 5–7. Finite element model of the insulated steel truss, the ceiling and the floor used in the thermal analysis of Test 5.

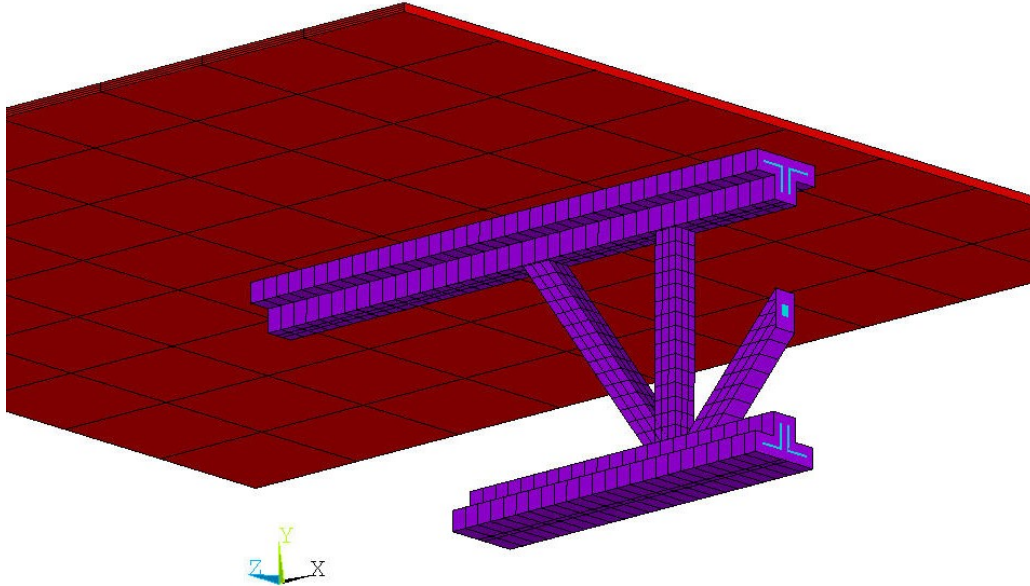


Figure 5–8. Finite element representation of the insulated steel truss (blue), the SFRM (violet), and the ceiling (red) used in the thermal analysis of Test 5.

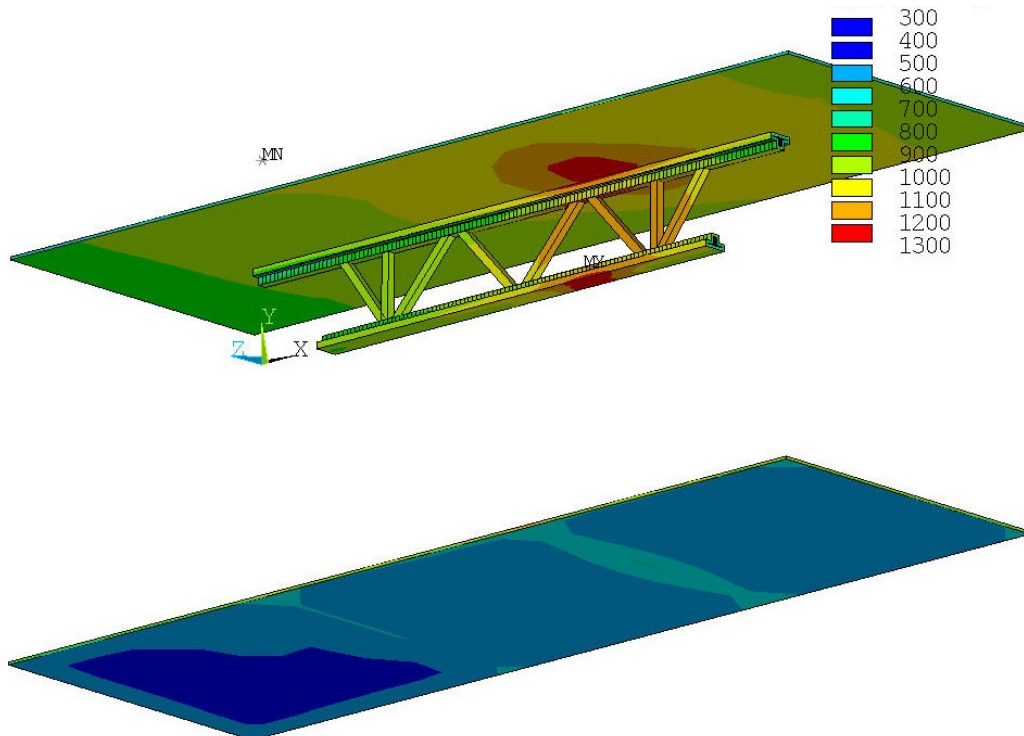


Figure 5–9. Temperature contours (in K) on the ceiling, floor and the surface of the SFRM on Truss A after 1,000 s in Test 5.

The following are comparisons of the FDS/FSI simulations with the experimental results from Test 1 (bare steel elements) and Test 5 (insulated steel elements). The comparisons between simulations and measurements focused on the peak temperatures attained by the insulation and steel rather than the amount of time it took to attain a particular temperature. This approach was taken because the peak steel and insulation temperatures varied widely from location to location and from test to test, making selection of a specific reference temperature impractical. In addition, the temperature rise in a given period of time was considered more important from the perspective of structural stability.

The quality of a simulation's replication of test results is determined by the uncertainty in the measurements (approximately 2 percent), the accuracy of the FDS computation of the thermal environment (approximately 10 percent greater near the asymmetric fire plume), and the accuracy with which the FSI transfers the fire-generated enthalpy to and throughout the test elements. While there were specific assessments of the first two components, the team did not have such data for the FSI. Thus, its accuracy was inferred from the overall agreement between the computation and the experimental data and knowledge of the uncertainties in the first two factors.

5.4.2 Test 1

In Test 1, bare structural steel elements were exposed to the heat generated by a nominal 2 MW spray burner. Figure 5–10 compares the simulation and experimental results for the west bar (Figure 3–16). The dimensions are measured from the north end of the bar. The general character of these results was representative of all of the tests.

- The shape of the simulated time-temperature results was similar to the measurements.
- For most locations, the absolute difference between the numerical predictions and the experimental data was less than 20 °C at any time. The agreement for the east bar (further from the fire pan) was within 10 °C. This was well within the combination of experimental uncertainty in the temperature measurements and uncertainty in the FDS simulations. (There were some locations where the difference was as large as 100 °C due to FDS not precisely predicting the asymmetry of the fire plume. These regions are not a true test of the accuracy of the FSI. As noted earlier, for the WTC fires that were severe enough to cause structural damage, the fire had a far wider spatial extent, and the calculation results will be less sensitive to the exact location of the fire plume.)

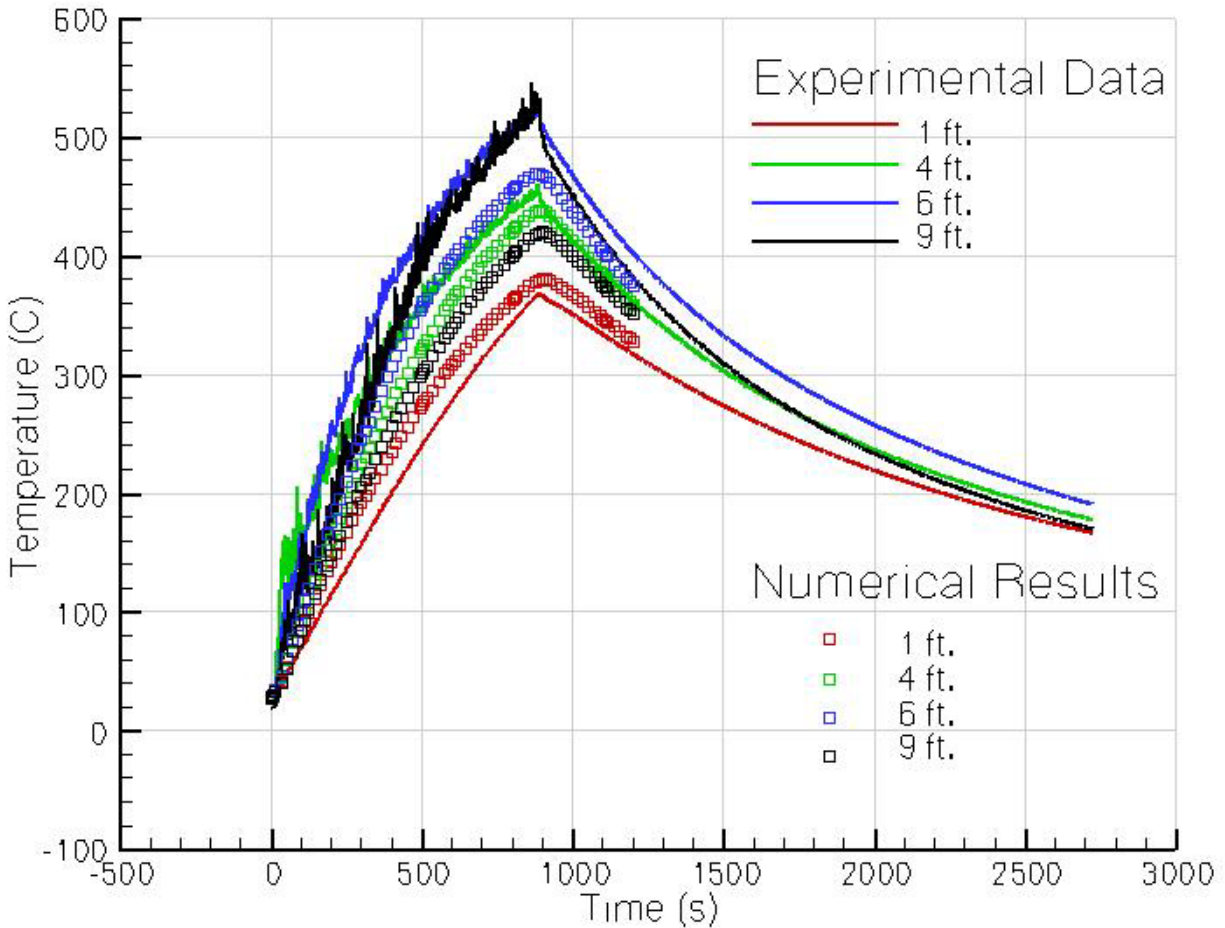


Figure 5–10. Comparison of numerical simulations with measurements for the steel surface temperature at four locations on the west bar in Test 1.

Figure 5–11 compares the numerical predictions with measurements of the steel surface temperature for locations on the north, south, east, and west faces of the bare column during Test 1 at 3.69 m above the floor. The west face of the column faced the air inlet to the compartment. The highest predicted and measured temperatures occurred on the south face of the column.

For most locations, the relative differences between the measured and simulated peak temperatures were less than 5 percent, although for some locations the differences were as large as 10 percent. The latter generally occurred just before the fuel flow was stopped at 900 s after ignition. These were all well within the combined uncertainty in the temperature measurements and in the FDS simulations. There was a very large disparity on the south face immediately after the start of the test when the temperatures were still relatively low, but the rate of temperature change was large. These results are discussed in terms of model and measurement uncertainty below.

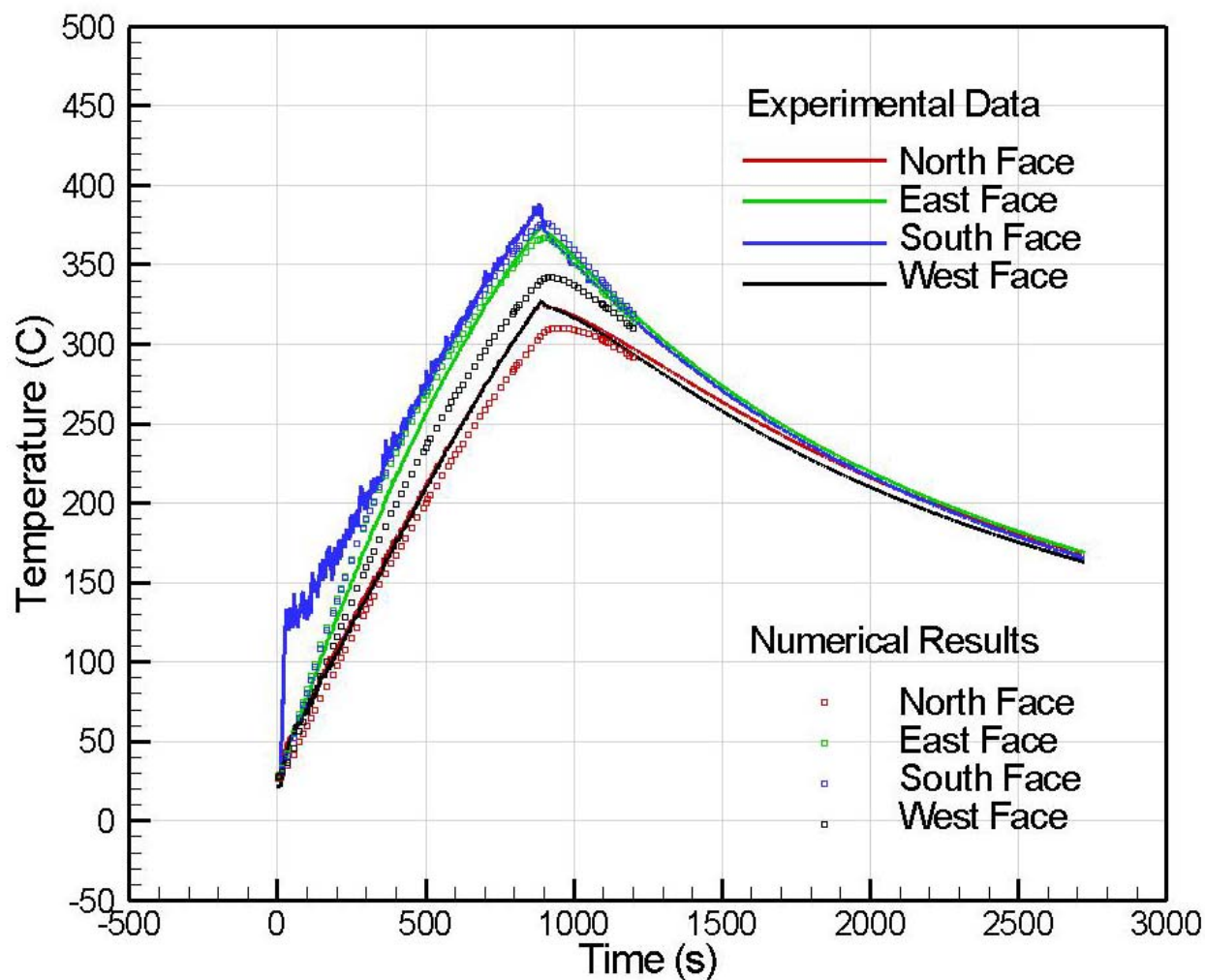


Figure 5–11. Comparison of numerical simulations with measurements for the steel surface temperature at four locations 3.69 m above the floor on the column in Test 1.

Figures 5–12 and 5–13 are representative of the comparison of calculated and measured temperatures on the surfaces of the north truss during Test 1. The four locations were along the length of the lower chord of the truss in Figure 5–12 and the upper chord in Figure 5–13. For most locations, the maximum difference between the measurements and the simulations was less than 10 percent, which typically occurred when the fuel flow was stopped. For a small number of locations, the difference was as large as 27 percent.

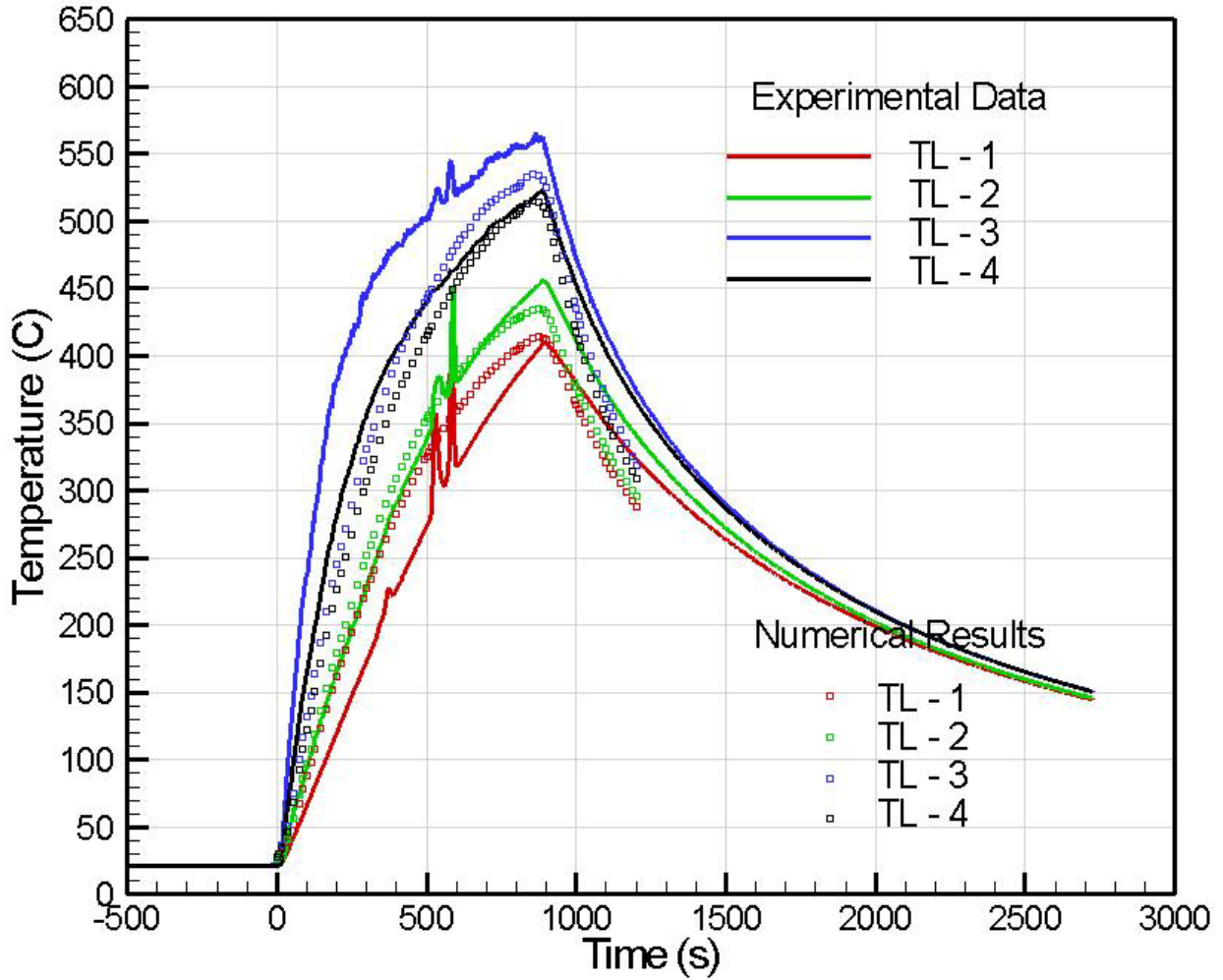


Figure 5–12. Comparison of numerical simulations with measurements for the steel surface temperature at four locations 2.89 m above the floor on the north truss in Test 1.

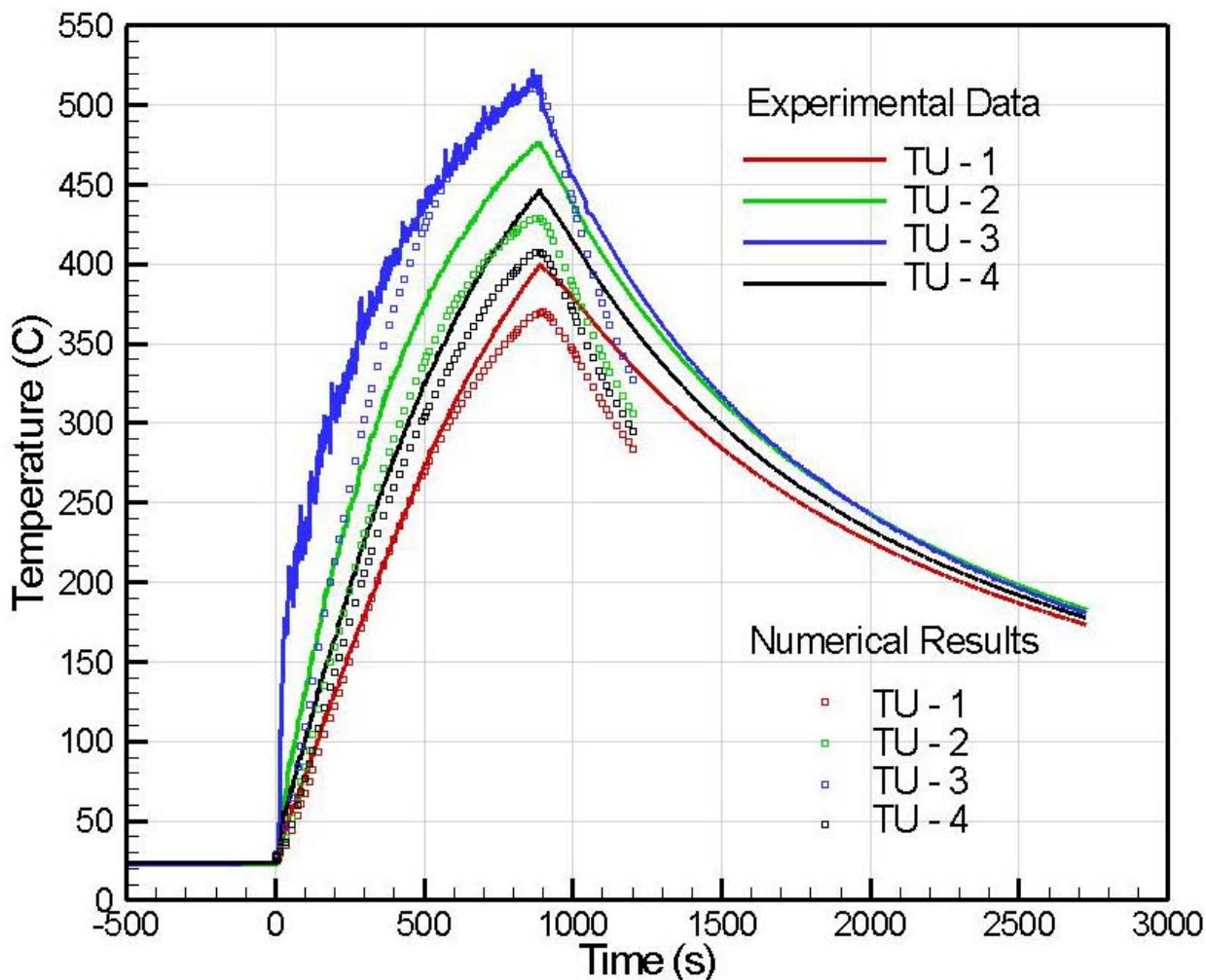


Figure 5–13. Comparison of numerical simulations with measurements for the steel surface temperature at four locations 3.70 m above the floor on the north truss in Test 1.

In summary, the simulations of the surface temperatures on the exterior surfaces of the bare steel elements were within the accuracy of the measurements and the FDS-computed thermal environment. The isolated cases where the disparity was large were apparently due to limitations in the FDS predictions.

5.4.3 Test 5

Test 5 exposed SFRM-coated structural steel elements to the heat from a nominal 3 MW spray burner. Figures 5–14 through 5–19 parallel the above figures, presenting comparisons of the numerical simulations and the temperature measurements for various locations on the outer SFRM and steel surfaces of the insulated elements. These plots are typical of those for other locations.

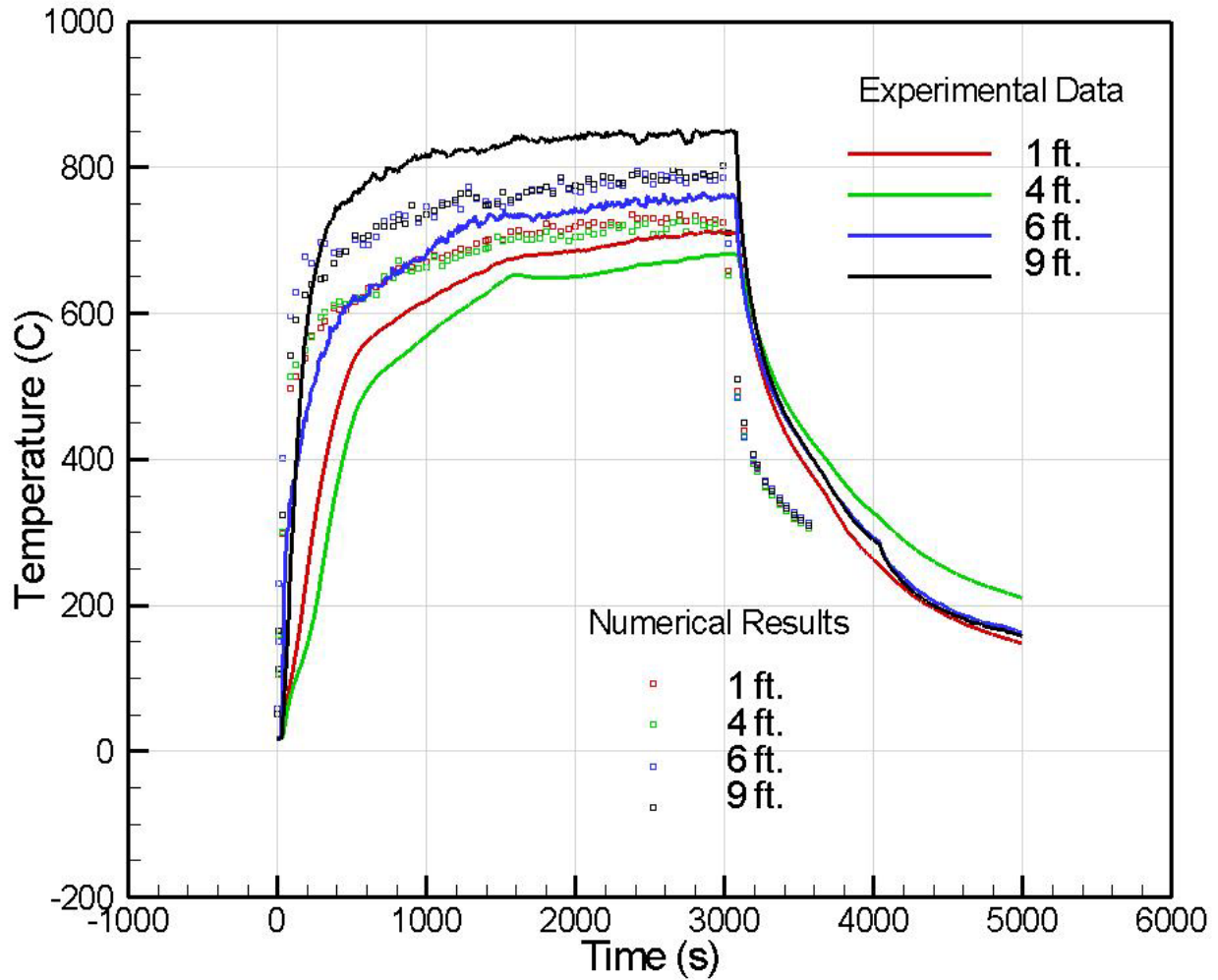


Figure 5-14. Comparison of numerical simulations with measurements for the temperature of the SFRM surface at four locations on the insulated bar in Test 5.

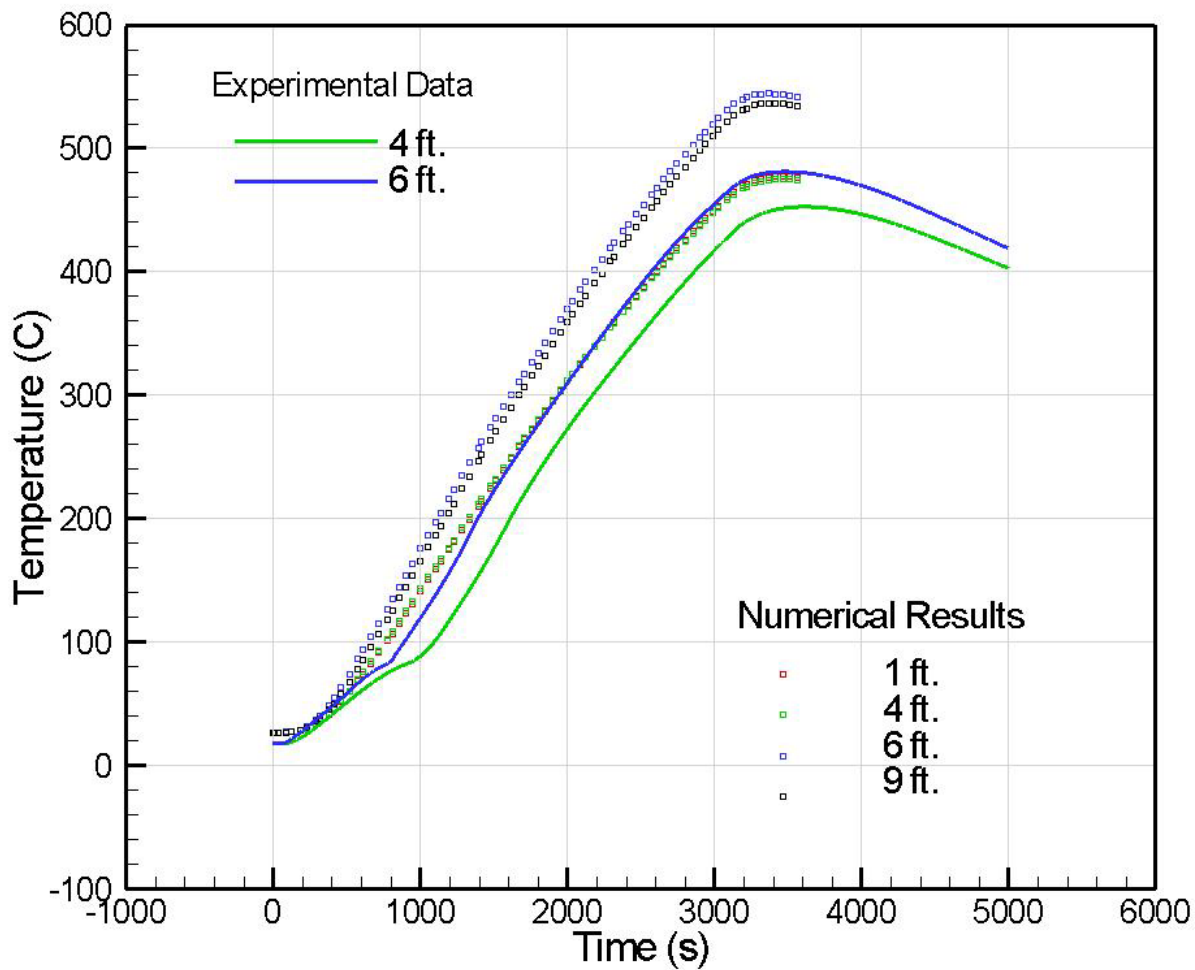


Figure 5–15. Comparison of numerical simulations with measurements for the temperature of the steel surface at four locations on the insulated bar in Test 5.

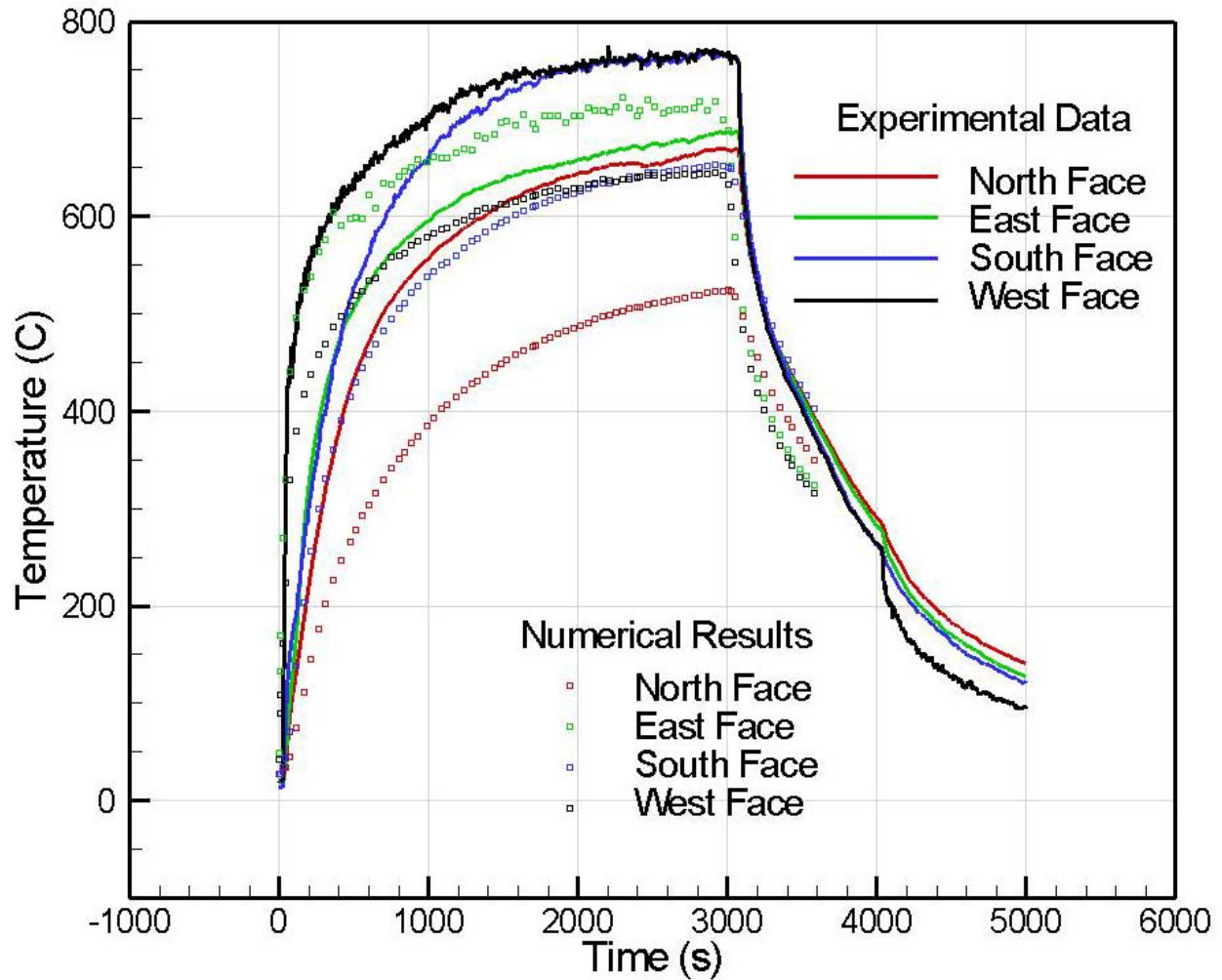


Figure 5–16. Comparison of numerical simulations with measurements for the temperature of the SFRM surface at four locations 3.69 m above the floor on the insulated steel column in Test 5.

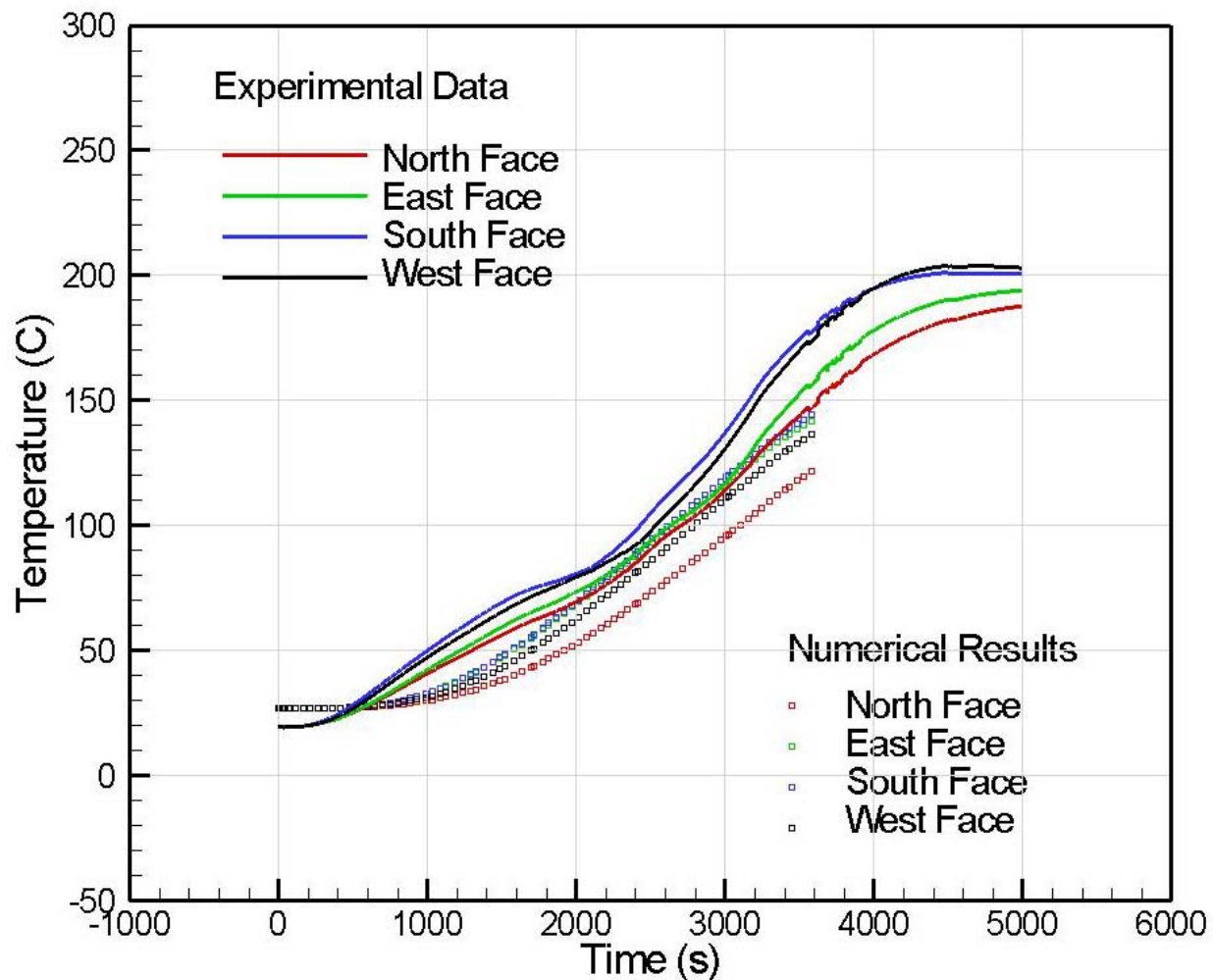


Figure 5–17. Comparison of numerical simulations with measurements for the temperature of the steel surface at four locations 3.69 m above the floor on the insulated steel column in Test 5.

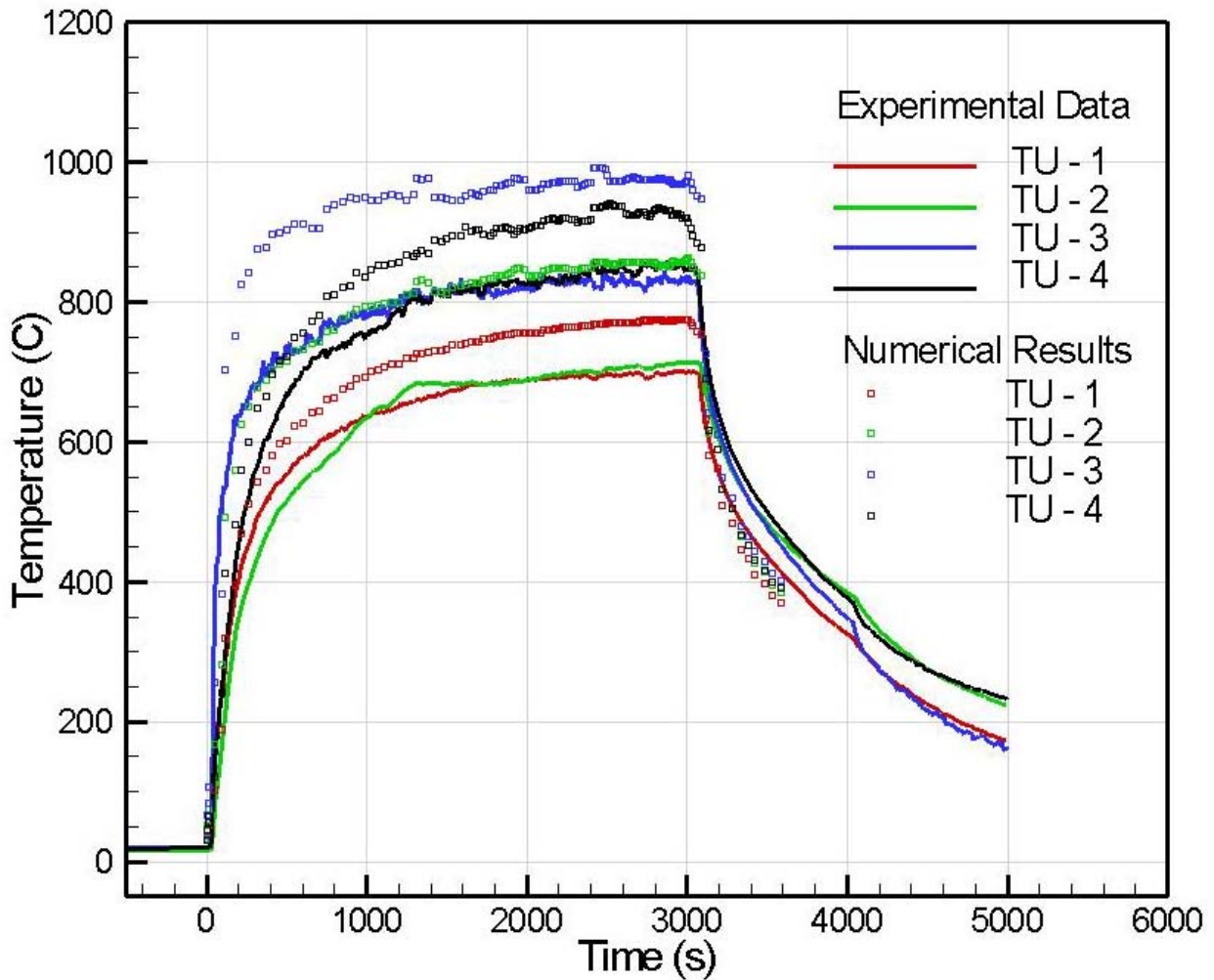


Figure 5–18. Comparison of numerical simulations with measurements for the temperature of the SFRM surface at four locations 3.70 m above the floor on the north truss in Test 5.

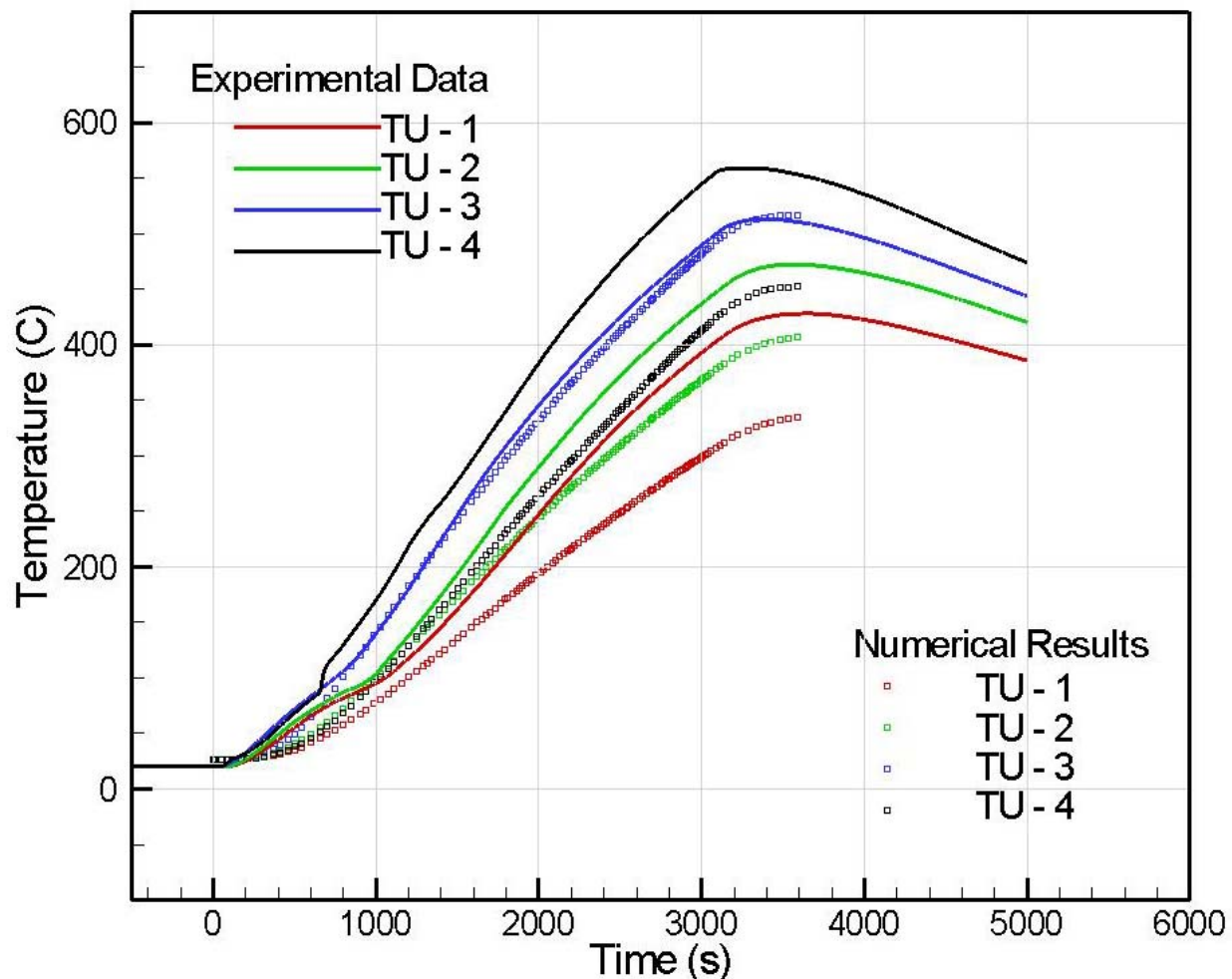


Figure 5–19. Comparison of numerical simulations with measurements for the temperature of the steel surface at four locations 3.70 m above the floor on the north truss in Test 5.

Examination of this set of graphs indicated the following:

- The temperatures at the surface of the SFRM rose more rapidly than did the temperatures at the surface of the bare steel elements. This follows from the far lower thermal conductivity of the SFRM than of the steel.
- FSI captured the significant decrease in the rate of temperature rise on the steel surface when the SFRM was present.
- The times to the peak temperature (or a near-plateau) were predicted to within the order of a minute in all cases. Where the curves were not yet peaked when the test ended, the curve shapes were quite similar.
- The agreement between the simulations and the measured temperature values at the outer surface of the SFRM was generally within 10 percent during the steady burning period

(i.e., after approximately 1,000 s). The largest deviation was for the temperatures on the north side of the column in Test 5. This was due to the FDS underprediction of the asymmetry of the fire plume which was close to the column.

- For the bar and the column, the maximum difference between the measurements and the simulations of the bare steel surface temperatures was less than 15 percent, which generally occurred shortly after the fuel flow was stopped. For the north truss, the maximum difference between the measurements and the simulations was typically less than 20 percent. At one location, however, the temperature difference was as large as approximately 30 percent. The reason for the magnitude of this difference appeared to be due to subtleties associated with predicting the exact location of the flame as mentioned previously. Other reasons for the differences between the numerical simulations and the temperature measurements are discussed below in terms of the uncertainty in the measurements and a sensitivity analysis of the model.
- For the bar, the quality of the predictions of the SFRM surface temperatures and the steel surface temperatures with and without SFRM was the same. This indicated that for a simple geometry, the FSI was not adding significant uncertainty to that from the temperature measurements and the FDS simulations.
- For the more complex column and truss, the disparities were about an additional 15 percent higher.
- The computations more frequently underpredicted the temperatures.

The FSI calculations were sensitive to:

- The fire heat release and the resulting upper layer temperatures. A sensitivity study showed that a 10 percent increase in the heat release rate led to a 20 percent increase in the steel surface temperature at the hottest locations.
- The proximity of the structural components to the fire. FDS did a better job predicting the heat flux to locations far from the fire, because the size, spatial extent, and precise location of the fire had less influence on the results.
- Variability in the thickness of the SFRM. The calculations assumed that the mean value was uniform throughout. As applied, the SFRM had a coefficient of variation that ranged from 0.17 to 0.27 for the bars, columns, and trusses. A 25 percent decrease in the thickness of the SFRM increased the steel temperatures by approximately 10 percent. In these tests, the local SFRM thickness on some sections of the bars was smaller than the mean by as much as 45 percent. This indicates that the variation in the calculated steel surface temperature was as much as 20 percent simply from uncertainty in the SFRM thickness.
- The thermal conductivity of the SFRM. Typical uncertainty in the determination of thermal conductivity using ASTM tests was ± 6 percent for materials similar to the BLAZE-SHIELD SFRM (NIST NCSTAR 1-6A).

5.5 SUMMARY

The FSI added little to the overall uncertainty in the simulation of the temperatures at the outer surfaces of bare steel elements and the surfaces of SFRM and, more importantly, at the SFRM-steel interface. On the average, the numerical predictions of the steel surface temperature were within 7 percent of the experimental measurements for bare steel elements and within 17 percent for the insulated steel elements. The former was determined to result from uncertainty in the heat release rate in the fire model. The increase in the latter was attributed to model sensitivity to the SFRM coating thickness and thermal conductivity.

Even modest application of insulation to the heavier steel provided significant thermal protection for exposure durations longer than the duration of the fires in the WTC on September 11. For thinner steel, the presence of gaps and high thickness variation in the applied insulation can lead to problematic heating rates of the steel.

5.6 REFERENCES

ANSYS, Inc. 2003. ANSYS Release 8.0 Documentation.

Eurocode 4. 1994. Design of Composite Steel and Concrete Structures, ENV 1993-1-2: General, EC4, Rules - Structural Fire Design. European Committee for Standardization, Brussels, Belgium.

Harmathy T.Z. 1983. *Properties of Building Materials at Elevated Temperatures*, paper NRCC-20956 (DBR-P-1080), Division of Building Research, National Research Council, Ottawa, Ontario, Canada, p. 72, March.

Prasad, K. and Baum H., 2004. *Coupled Fire Dynamics and Thermal Response of Complex Building Structures*, Proc. 30th Symposium International on Combustion, to appear.

Prasad, K., Baum, H., and Filliben, J.J. 2004. *Effect of Insulation on the Thermal Response of Structural Elements: A Sensitivity Study*, NIST Special Publication, in preparation.

Taylor, R.E., Groot, H., and Ferrier, J. 2003. *Thermophysical Properties of PVC, PE, and Marinite*, Report No. TPRL 2958, Thermophysical Properties Research Laboratory, Inc., April.

Chapter 6

SIMULATION OF THE WTC FIRES AND THERMAL ENVIRONMENTS

6.1 GENERAL

A substantial component of the Investigation into the World Trade Center (WTC) disaster was the four-step simulation of the sequence leading to the initiation of collapse:

1. The aircraft impact into the tower, the resulting distribution of aviation fuel, and damage to the structure, partitions, insulation materials, and building contents.
2. The multi-floor fires and the time-varying thermal environments they generated.
3. The transposition of these thermal environments onto the structural elements through both intact and damaged insulation.
4. The thermostructural response of the structural system and the progression of element failures leading to collapse initiation.

This chapter presents the results of the second and third steps.

6.2 FIRE DYNAMICS SIMULATOR SIMULATION ASSUMPTIONS AND VARIABLES

The aim of the Fire Dynamics Simulator (FDS) simulations of the fires in WTC 1 and WTC 2 was to replicate the major features of the fires: the rate of spread of the fires and the duration of fire activity in a given location. The visual evidence contained within the thousands of photographs and videotapes shot on September 11, 2001, was used to compensate, in part, for limited knowledge of the impact damage and interior contents.

Hundreds of preliminary calculations were performed to study the fire behavior. The simulations addressed fires on parts of a floor, single floors, and multiple floors. The objective of these preliminary simulations was to (1) assess the sensitivity of the many input parameters, (2) test the robustness of the numerical model during its development, and (3) gain insight into the physical phenomena that governed the growth of these fires. After this development phase, two final multi-floor simulations included variation of the influential parameters over plausible ranges. These two simulations, denoted as Cases A and B for WTC 1 and Cases C and D for WTC 2, used initial conditions provided by the impact analysis (NIST NCSTAR 1-2). Table 6-1 describes the salient features of Cases A, B, C, and D.

For each of the four cases, FDS was used to generate a time-dependent gas temperature and radiation environment on each of the floors.

Table 6–1. Values of WTC fire simulation variables.

Variable	WTC 1		WTC 2	
	Case A	Case B	Case C	Case D
Combustible Fuel load	20 kg/m ² (4 lb/ft ²)	25 kg/m ² (5 lb/ft ²)	20 kg/m ² (4 lb/ft ²)	20 kg/m ² (5 lb/ft ²)
Distribution of disturbed combustibles	Even	Weighted toward the core	Heavily concentrated in the northeast corner	Moderately concentrated in the northeast corner
Condition of combustibles	Undamaged except in impact zone	Displaced furniture rumbled	All rumbled	Undamaged except in impact zone
Representation of impacted core walls	Fully removed	Soffit remained	Fully removed	Soffit remained
Structural damage, NIST NCSTAR 1-2 Case	Base	More severe	Base	More severe
Insulation damage, NIST NCSTAR 1-2 Case	Base	More severe	Base	More severe

6.2.1 Assumptions and Fixed Parameters

- Floors: Eight floors were modeled in WTC 1 (92 through 99), and six floors were modeled in WTC 2 (78 through 83). The floors above and below were presumed to be at ambient temperature, since there was little or no fire activity observed. Each floor was modeled separately, since examination of the photographic collection indicated little evidence for floor-to-floor fire spread in the short times that the towers survived. Heat conduction through the floors was included.
- Floor layouts: As cited in Section 3.1.2 and Table 3–1, detailed floor plans were available for the eight modeled floors in WTC 1 and the 80th floor of WTC 2. For the remaining floors in WTC 2, the layouts were estimated from the architectural drawings of the core space and from recollections by The Port Authority staff and workers from the tenant spaces.
- Interior walls: The condition of the walls, whether intact or damaged by the aircraft debris, did not change during a fire simulation.
- Office combustibles (fuel load): The furnishings not in the debris path were assumed to be undamaged and were modeled as described in Section 4.6. Those furnishings deemed to be rumbled were assigned two-thirds the burning rate of the undamaged furnishings.
- Windows: During a simulation, each was removed at the time indicated in the compilation reported in NIST NCSTAR 1-5A.
- Other ventilation: Vertical shafts in the core area were incorporated as shown in the architectural drawings. For undamaged floors, all the openings to the core area were assumed to total 5 m² in area.

- Jet fuel: Based on the estimates reported in Sections 2.6.1 and 2.7.1 and the distribution of the Jet A among the impact floors, as shown in Table 6–1 from NIST NCSTAR 1-2B, it was assumed that 40 percent of the jet fuel was available for combustion on the impact floors. The thermal properties were assumed to be similar to JP-4 and JP-5, whose values were obtained from the SFPE Handbook.
- Aircraft combustibles: The mass was 12,100 kg (25,800 lb) for WTC 1, 12,500 kg (27,600 lb) for WTC 2 (Table 3–7).
- FDS computational grid size: Each floor comprised 128 by 128 by 9 cells. Each cell was 0.5 m in width and depth and 0.4 m in height.

6.2.2 Variables

The sensitivity of the output of single floor FDS simulations to five variables had been assessed previously (NIST NCSTAR 1-5F). There were two that affected the combustible mass (volume of jet fuel and density of office combustibles) and three that affected the availability of air for the combustion (fraction of core walls broken, air velocity in the core shafts, and the oxygen concentration of the air in the shafts). The most influential was density of combustibles; second was the extent of core wall damage. The other factors were secondary. In these simulations, most of the air for the fires came from the broken windows. As noted above, the location and number of broken windows were determined from the photographic evidence and were thus not variables.

Table 6–1 summarizes the differences between the two simulations for each tower. The following add additional detail on some of the variable parameters:

- It was assumed that the sprayed fire-resistive material (SFRM) prior to the impact was consistent with the as-built condition and characterized by a uniform equivalent thickness (NIST NCSTAR 1-6). If a structural element was found to be in the path of a debris field of sufficient intensity (NIST NCSTAR 1-2), all the insulation (SFRM and gypsum board) was deemed to have been removed.
- Damage to core walls: In Cases A and C, the walls impacted by the debris field were fully removed. This enabled rapid venting of the upper layer into the core shafts and reduced the burning rate of combustibles in the tenant spaces. In cases B and D, a more severe representation of the damage was to leave intact the top 1.2 m of the core wall. This "soffit" would maintain a hot upper layer on each fire floor. This produced a fire of longer duration near the core columns and the attached floor membranes.

6.2.3 Presentation of Results

The results of the FDS simulations of the perimeter fires were compared with the fire duration and spread rate as seen in the photographs and videos. Contour plots of the room gas temperature 0.4 m below the ceiling slab (in the “upper layer” of the compartment) were superimposed on profiles of the observed fire activity (from NIST NCSTAR 1-5A) for each floor at 15 min intervals (Figures 6–1 through 6–16 for WTC 1; Figures 6–17 through 6–28 for WTC 2). The results for the two Cases for a given tower are shown on facing pages for ready comparison.

- The results of the simulation as compared to observations on the following pages are shown every 15 min, with the exception of the last frame of WTC 1, which is shown at the time of collapse, 1 h 42 min past impact. There may have been considerable fire activity in between the consecutive plots included here.
- The stripes surrounding the image represent a summary of the visual observations of the windows, with the black stripes denoting broken windows, the orange stripes denoting external flaming, and the yellow stripes denoting fires that were seen inside the building.
- Fires deeper than a few meters inside the building could not be seen because of the smoke obscuration and the steep viewing angle of nearly all the photographs.
- The red regions of the contour maps represent numerical prediction of temperatures in the neighborhood of 1,000 °C, typical of a fully engulfing compartment fire. Such temperatures were measured during the multiple workstation experiments when the workstations were burning near their peak heat release rate and flames extended outside of the test compartment.

6.3 SIMULATION RESULTS FOR WTC 1, CASE A

6.3.1 Floor 92

In the simulation, there was no damage on this floor other than window breakage. The ignition of jet fuel in the northeast corner and air from broken windows led to sustained burning of the contents in that corner. The combustibles were consumed about 45 min after the aircraft impact, and the fires moved south along the east face (where they were stopped by a partition) and west along the north side of the interior core. There was a wall that blocked the fires from spreading directly to the north face.

Eventually, the simulated fires arrived at the north face about 15 min sooner than was observed in the photographs and videos. The fires never reached the south section of the floor because of various walls that obstructed their spread.

The general pattern of the simulated fires was consistent with the photographic evidence. However, the burning rates were faster than observed: the simulated fire in the northeast corner burned out faster than actually observed, and the simulated fire on the west grew faster. The actual fire on the east face moved slightly further to the south than in the simulation, suggesting that the wall location was incorrect or that the wall had been penetrated. If the latter, it was not clear what caused the fire to stop where it did.

6.3.2 Floor 93

As on the 92nd floor, the simulated fires began in the northeast corner, just under where the left wing of the aircraft dripped jet fuel through the damaged floor slab from the 94th floor. Consuming the combustibles in the northeast in about 30 min, the fires moved west along the north face and south along the east face.

The simulations over-predicted the intensity of the fires at the periphery of this floor. In the northeast corner, the actual fire broke windows and was visible some 45 min after the simulation showed the fire had moved on. The movement along the east wall was about 30 min ahead of reality, and there was a flare-up in the northeast corner at about 45 min after impact, both signs of overestimation of the initial

burning rate. The breaking of about 20 windows on the west side of the north face in the last 10 min indicated that there were interior fires or an overall build-up in the temperature of the gases. The observed window breakage along the south face in the last 10 min indicated the presence of a fire, but unlike the simulation, the fires had to have been away from the perimeter since they were not observed through the windows.

6.3.3 Floor 94

Floor 94 was directly impacted by the left wing of the aircraft, and a substantial amount of jet fuel was spread throughout the east side of the floor. Initially, severe fires were observed on the east face, and then steadily spread around the floor, with the heaviest activity in the end being in the southwest quadrant.

The simulation captured the movement of the fires reasonably well. The simulated fires burned vigorously in the northeast quadrant for the first 30 min. Then for the next hour, the fires moved at roughly the same rate as the real fires clockwise toward the southeast and counterclockwise toward the southeast. In some areas, the simulation shows the burning to be too close to the windows. The late fire on the south face was not seen in the photographs and videos.

6.3.4 Floor 95

The simulated fires started around the center of the north face where the fuselage of the aircraft hit. The fires then followed the pattern of window breakage. There was substantial fire activity predicted in the building core due to the extensive wall damage (NIST NCSTAR 1-2). The simulations suggested that air rising through the core mixed with the oxygen-starved fuel gases that were accumulating on this floor because of the relatively light exterior damage away from the impact zone. However, there was no evidence to confirm or deny the existence of vigorous fire activity within the core.

Taking into account the tendency to simulate burning too close to the windows, the overall pattern of the fires is reasonably consistent with the observations. The fire on the north side of the building was growing just before additional windows break there. The same is true for the fire on the middle of the east side. The early fire simulated on the south side is consistent, but burns too long or too close to the broken windows.

6.3.5 Floor 96

Floor 96 was directly impacted by the aircraft fuselage and inner wings. There was extensive damage to the core and internal walls. One simulated fire started to the east of the impact hole, spread southward along the east side of the building, and turned the corner to the south face. This behavior mimics closely the behavior of the actual fire. By contrast, the simulation overestimated the extent of the fire on the west face. The visual observations suggested that this fire originated in the south, not the impact area. The simulation is a fair rendition of the observations on the south side of the tower beginning about 15 min to 30 min after the aircraft impact. The model captured the delayed movement of the fires along the south face due to the presence of office walls.

6.3.6 Floor 97

The fuel-laden section of the right wing of the aircraft impacted this floor, igniting extensive fires. The southward movement of the fire on the west side is well replicated. The fire on the east, while burning too close to the perimeter, arrived at the southeast corner at roughly the same time as the observed fire.

6.3.7 Floor 98

The 98th floor, struck only by the empty outer length of the right wing, suffered minor damage. The simulation showed modest fire activity in the first 30 min, owing to the small amount of jet fuel distributed on the floor and the limited ventilation openings in the exterior and core. As large numbers of windows broke out, the simulated fires grew, following the observed time and perimeter flame patterns that eventually brought the heart of the fire to the southeast corner.

6.3.8 Floor 99

The 99th floor was impacted by the very tip of the right wing, and the window damage was minimal. The simulated fire activity was light and did not show any discernable trends, nor did it provide any clues to the late fire activity observed on the south face.

One point to note was the high temperatures in some of the elevator shafts. The late fire observed on the west face of the 104th floor might have started from accumulated fuel gases in the core shafts over the course of the first hour of fires below. The presence of fire in the shafts on the 99th floor in this simulation provided some support for this hypothesis, but no simulations were performed for floors higher than the 99th.

6.3.9 Observations

In the preceding descriptions, there were a number of instances where the fires burned too quickly and too near the windows. This resulted from the representation of combustion in the model. The burning occurred immediately wherever there was a flammable mixture of air and vaporized fuel. At the high temperatures and radiant fluxes generated by these fires, the furnishings were being “cooked” into generating large amounts of combustible vapors. The air supply was introduced through the windows. Thus, there was a tendency for the combustion to take place there, even if the burning furnishings were located somewhat closer to the interior.

6.4 SIMULATION OF FIRES IN WTC 1, CASE B

In general, the results of this Case were similar to those from Case A. This was because, in general, the size and movement of the fires in WTC 1 were limited by the supply of air from the exterior windows. Since the window breakage pattern was not changed in Case B, the extra and re-distributed combustibles within the building did not contribute to a *larger* fire, but they did delay the spread slightly because the fires were sustained longer in any given location due to the increase in combustible load.

- On the 92nd and 97th floors, the two Cases produced similar results.
- On the 93rd, and 96th, and 99th floors, the fires in Case B were slightly slower to develop.
- On the 94th floor, the fire on the east side was less intense for the first hour. The fire on the west was unchanged. The fire reached the south side later.
- For the 95th and 98th floors, the fires were similar for the first hour. Later, the fires in Case B were slower to develop, especially along the south wall.

6.5 SIMULATION OF FIRES IN WTC 2, CASE C

Simulating the fires in WTC 2 posed challenges in addition to those for WTC 1. The fires were largely on the east side of WTC 2. The aircraft, hitting the tower to the east of center, splintered much of the furnishings and plowed them toward the northeast corner of the building. Neither the impact study nor the validation experiments performed at the National Institute of Standards and Technology (NIST) could be completely relied upon to predict the final distribution, condition, and burning behavior of the demolished furnishings. In addition, only the layouts of the 78th and 80th floors were available to the Investigation, and the other floors were only roughly described by former occupants. As a result of these unknowns, the uncertainty in these calculations is greater than in those for WTC 1. To help mitigate gross differences between the simulations and the observables, NIST made floor-specific adjustments, based on the results of preliminary computations. These are noted below.

6.5.1 Floor 78

There was only light fire activity observed on the 78th floor, and this behavior is reflected in the numerical simulation. The impact analysis (NIST NCSTAR 1-2) predicted that a small amount of jet fuel was released on this floor. Given the modest number of window openings and the estimated light core damage, the numerical simulation of the fire did not predict any areas of significant temperatures. Most of the observed missing windows were broken out upon impact.

6.5.2 Floor 79

The simulation showed an early fire on the north face, ignited by jet fuel from the left wing tank of the aircraft. The fire spread to the west, supported by air rising through openings in the floor slab. The photographic evidence shows no fire and no broken windows on the west side of the building.

The simulation captured the fire in the northeast quadrant of the floor, but showed it burning too close to the façade and too intensely, burning out about 15 min too early.

Neither the simulation nor the photographic evidence indicate any fire activity on the south side, where the aircraft entered the tower.

6.5.3 Floor 80

Preliminary simulations of WTC 2 had shown far more fire activity on this floor than was observed. Consequently, the combustible load and the volatility of the furnishings were reduced to better match the observations. Even so, the simulation predicted a modest fire on the north side that moved west and then south with time. The movement to the west was too fast by about 15 min, and the actual fire did not have time to reach the west tenant space before the building collapsed.

The late fire that was observed to break out on the south face was not captured in the simulation. The source of the actual fire was unknown, but the breakage of windows after the 45 min time frame indicated that there likely was a fire toward the interior, perhaps having spread from the east.

6.5.4 Floor 81

Pictorial details showed an accumulation in the northeast corner of debris and combustibles that burned steadily and intensely until the building collapse. The aircraft impact modeling (NIST NCSTAR 1-2A) confirmed that the upper fuselage and right wing of the aircraft had plowed an appreciable amount of the combustible load of the east side of the floor into that corner. Accordingly, a heavy concentration of combustibles was assumed in the northeast corner. As a result, the predicted fire in the northeast corner is the dominant combustion on the floor.

The sharp western boundary of the fire for the first 45 min was due to a wall assumed in the floor plan. The coincidence of the wall and the observed window breakage for the first 30 min was merely fortuitous, since NIST did not have a detailed plan for this floor. Nothing in the simulations explained the absence of fires in the cold spot, the 10-window expanse toward the east of the north face of floors 80, 81, and 82 (Section 2.7.4).

The simulation predicted some burning in the southwest (where none was observed) and some in the north central (where a light amount was observed).

6.5.5 Floor 82

The observed fire activity on the 82nd floor was similar to that of the 81st floor. The simulated fires were similar as well because of similar assumptions of combustible load, floor plan, and initial jet fuel distribution.

6.5.6 Floor 83

The simulation predicted burning in the southeast quadrant that spread northward along the east section and turned the corner to head west along the north wall. The post-impact window breakage indicates that this pattern is accurate, but that the simulated fire spread more slowly, reaching the middle of the north wall about a half hour later than in the simulation. This delay resulted from a wall along the north side of the core that extended into the east part of the floor. (Inclusion of this wall this barrier was based on a recollection by a former worker on the 80th floor.)

6.6 SIMULATION OF FIRES IN WTC 2, CASE D

Unlike WTC 1, changing the combustible load in WTC 2 had a noticeable effect on the outcome of the simulation. Because most of the windows on the impact floors in WTC 2 were broken out by the aircraft debris and the ensuing fireballs, there was an adequate supply of air for the fires. Thus, the burning rate of the fires was determined by the fuel supply. In the Case D simulation, the office furnishings and aircraft debris were spread out over a wider area, and the furnishings away from the impact area were undamaged. Both of these factors enabled a higher burning rate for the combustibles. The following are results of the Case D simulations that differ from those in Case C:

- On the 78th floor, there was a fire in the southeast corner that burned out after half an hour.
- On the 79th floor, the simulated fires matched the observations more closely. The fire on the east side burned more intensely and reached the south face sooner. The higher fuel availability on the east side, combined with its proximity to the broken windows, slowed the fire spread to the west, where Case C showed burning that was not in the photographs.
- The simulation of the 80th floor also matched the observations more closely. However, neither simulation captured a fire on the west side of the south face that erupted just a few minutes prior to collapse.
- The fire on the northeast corner of floor 81 burned more intensely. The reduced burning on the west side was a closer match to the observables.
- The burning in the northeast corner of the 82nd floor was too intense and ran out of fuel too soon. The reduced burning on the west side was a closer match to the observables.
- The fire on the east side of the 83rd floor burned too intensely in the early stages, but reached the south face more realistically than Case C.

In general, the Case D simulations more closely approximated the observations in the photographs and videos. The comparisons suggest that the Case D simulations still predict burning too close to the perimeter, especially on the east side of the 78th, 79th, 81st, and 83rd floors. The assumptions in both Cases, necessitated by lack of knowledge of key input information, led to a greater uncertainty regarding the accuracy of the predictions in those regions where there is no corroborating evidence.

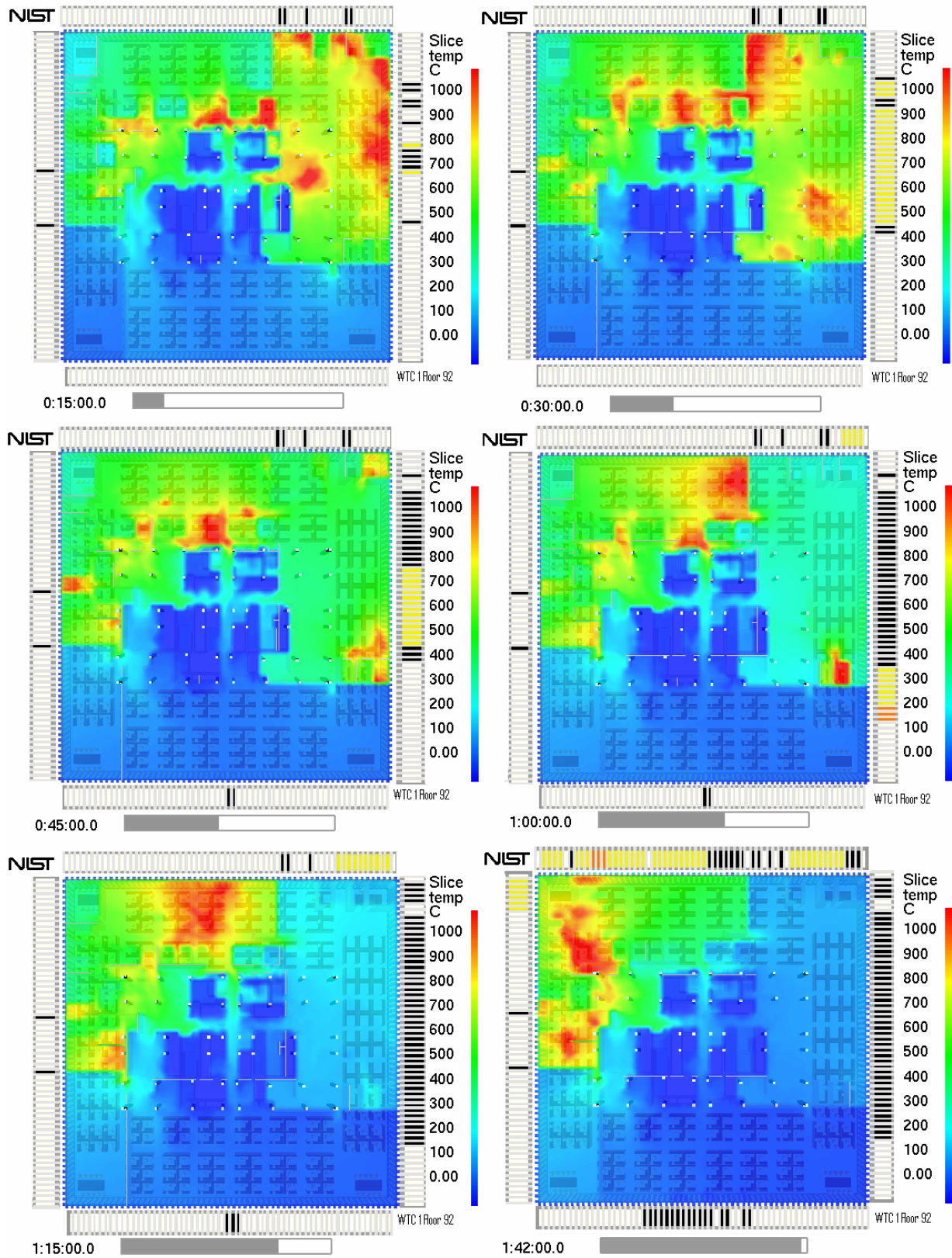


Figure 6–1. Simulated upper layer temperatures on floor 92 of WTC 1, Case A.

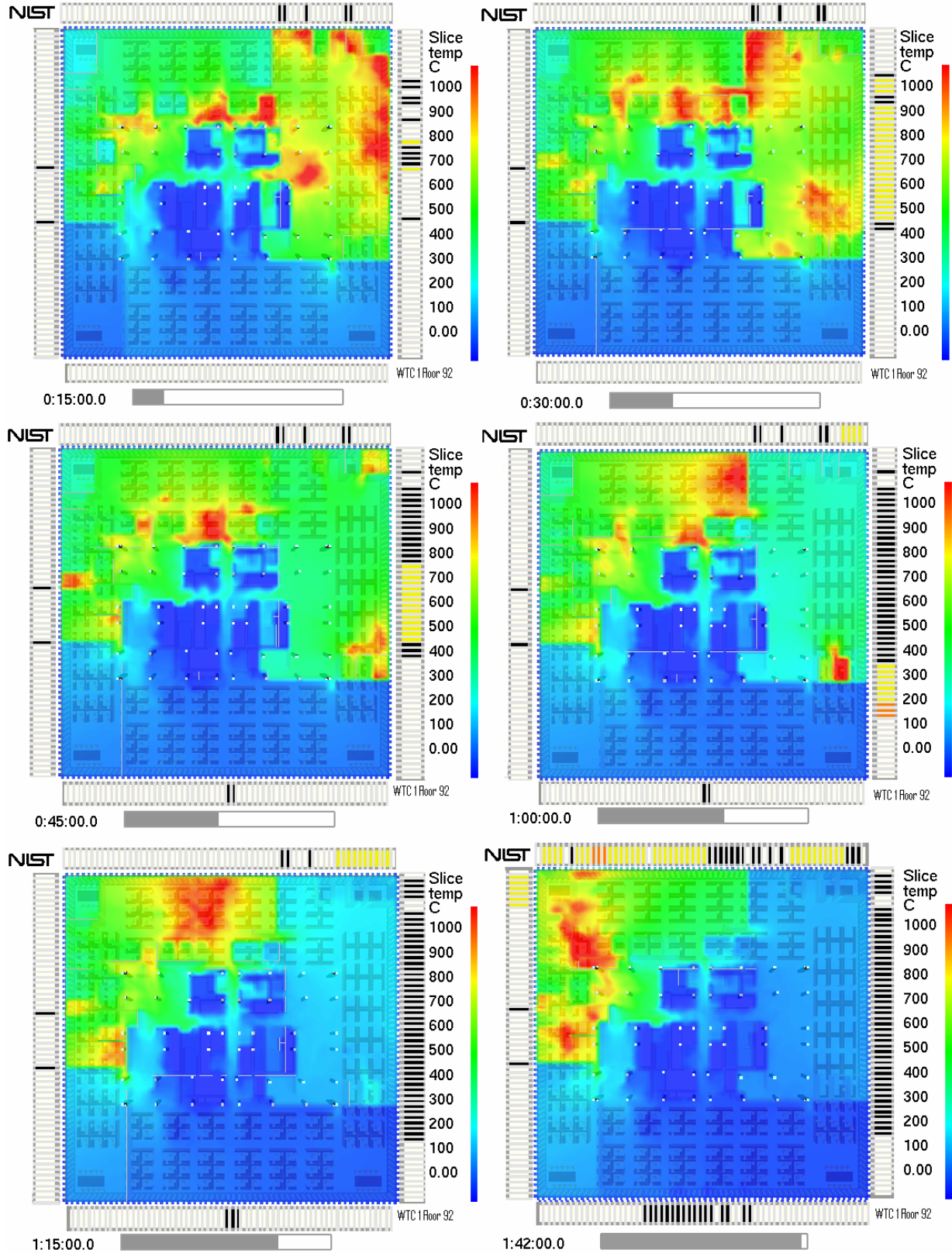


Figure 6–2. Simulated upper layer temperatures on floor 92 of WTC 1, Case B.

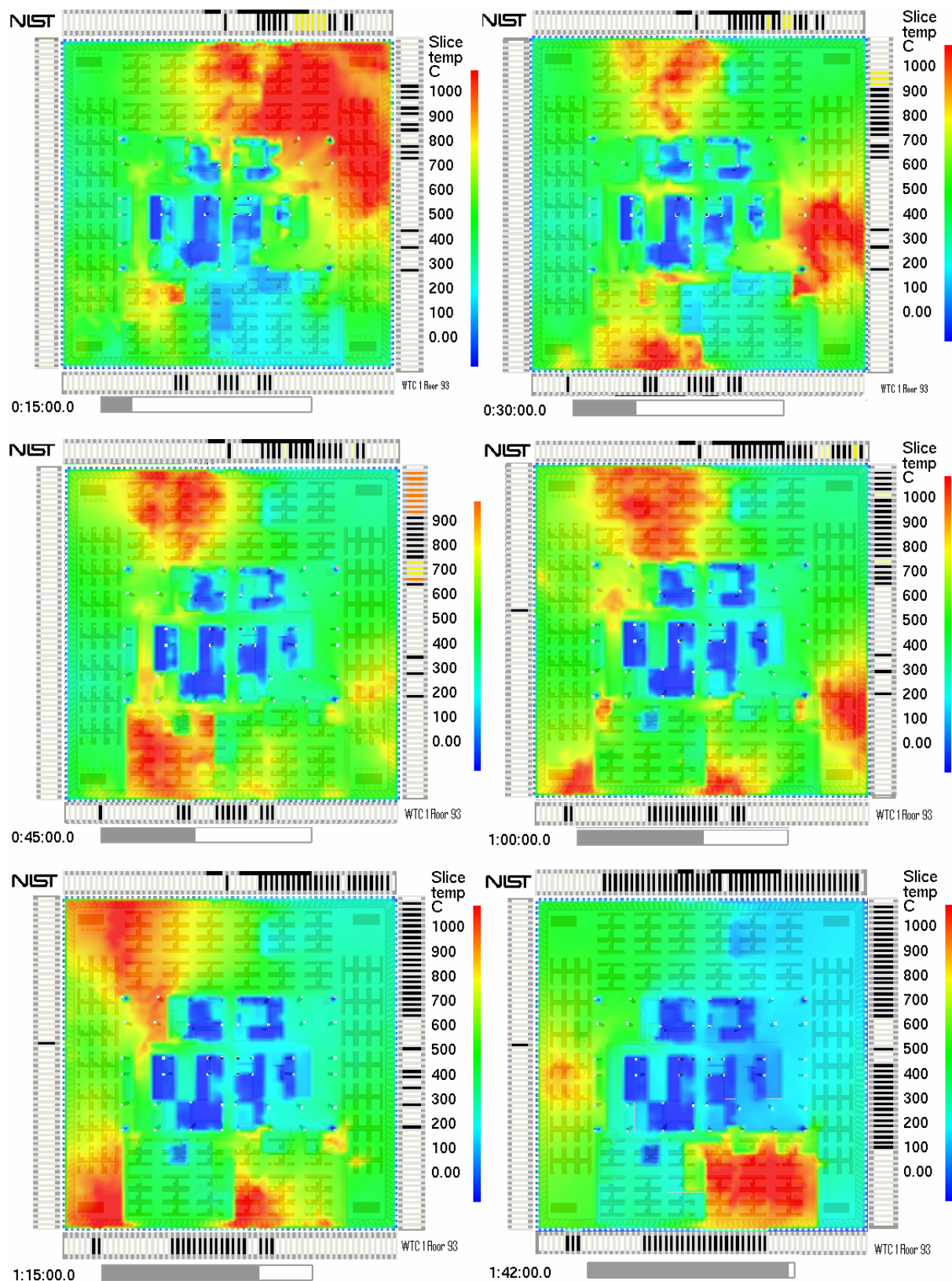


Figure 6–3. Simulated upper layer temperatures on floor 93 of WTC 1, Case A.

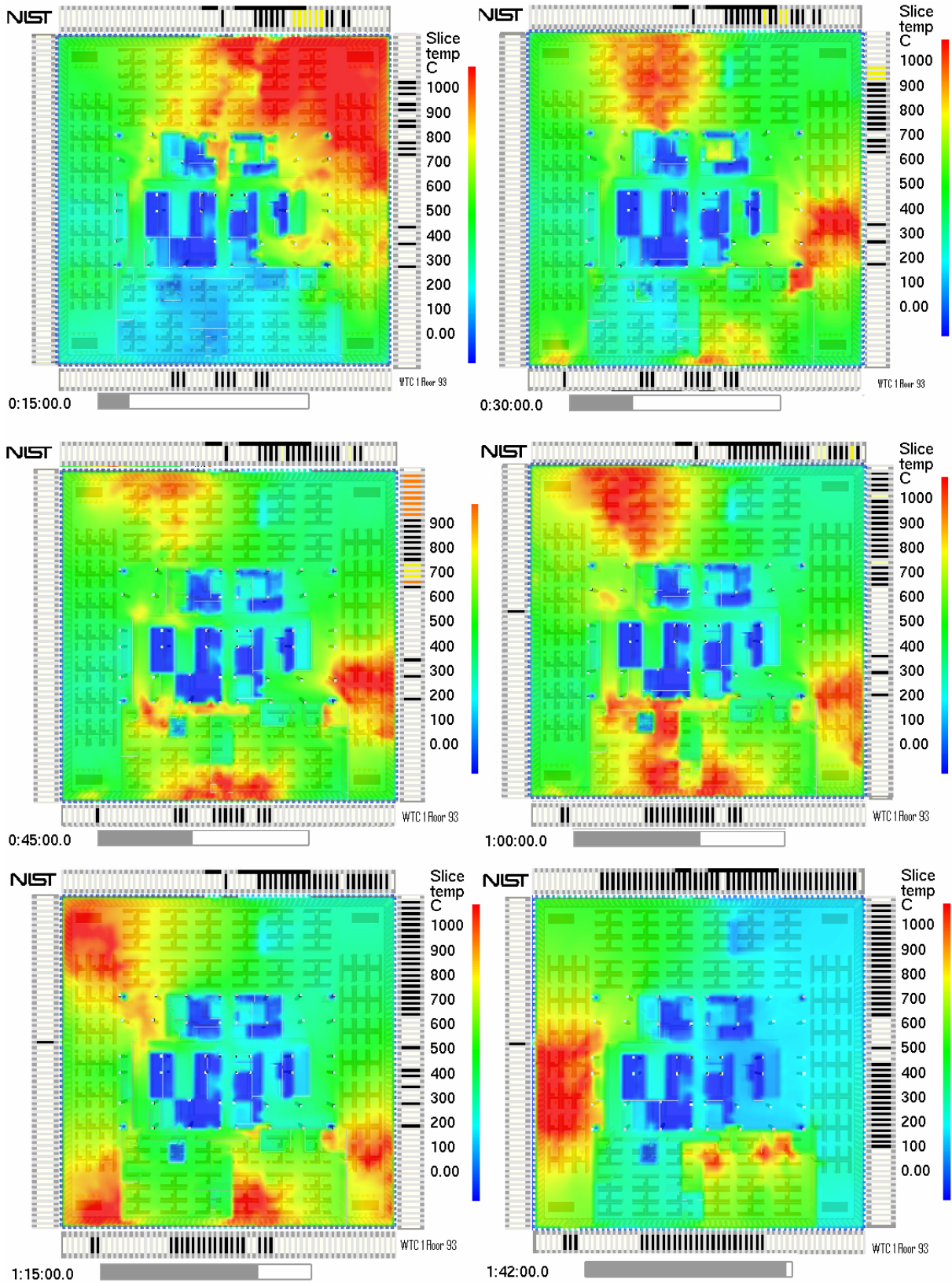


Figure 6-4. Simulated upper layer temperatures on floor 93 of WTC 1, Case B.

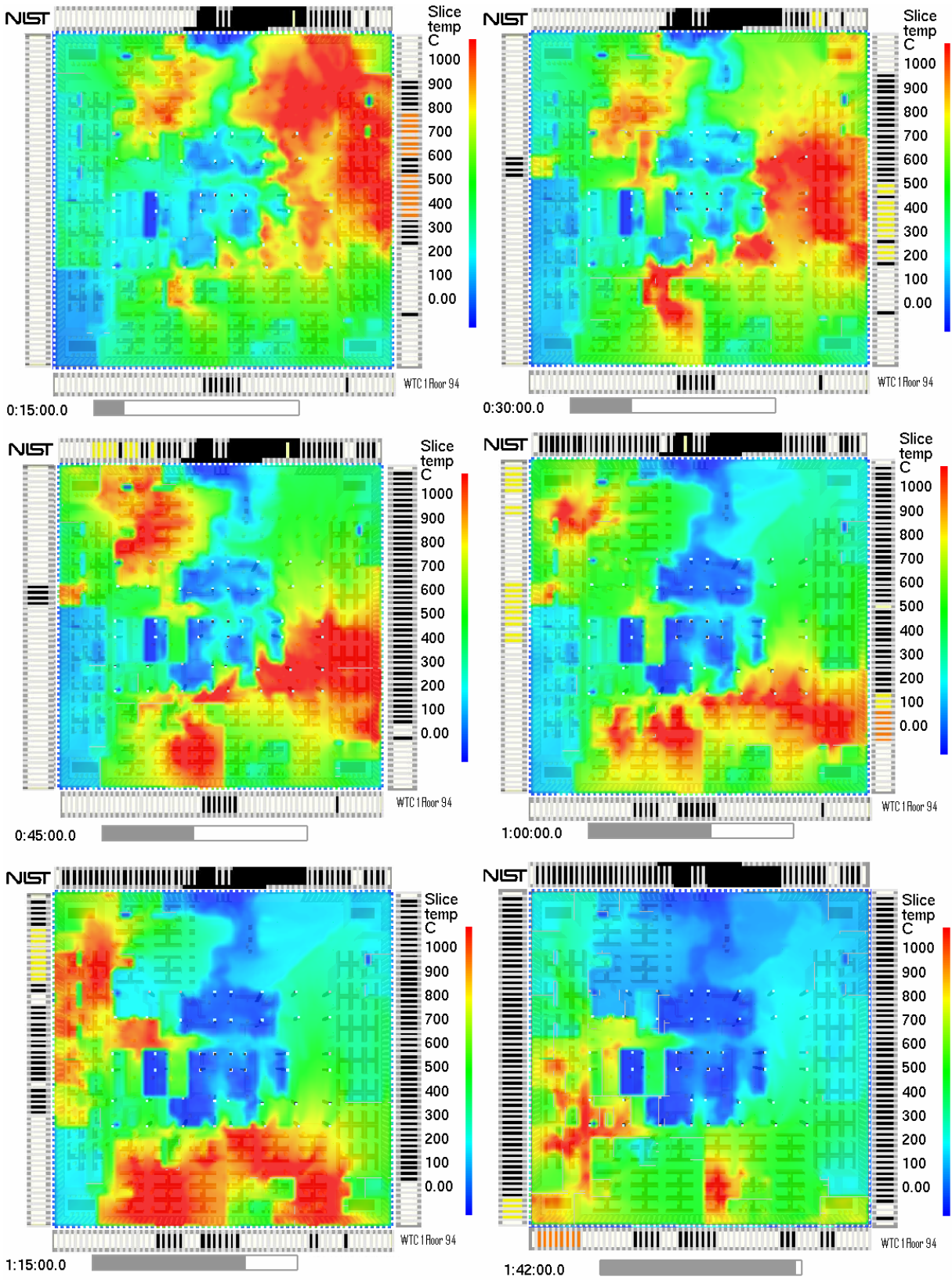


Figure 6–5. Simulated upper layer temperatures on floor 94 of WTC 1, Case A.

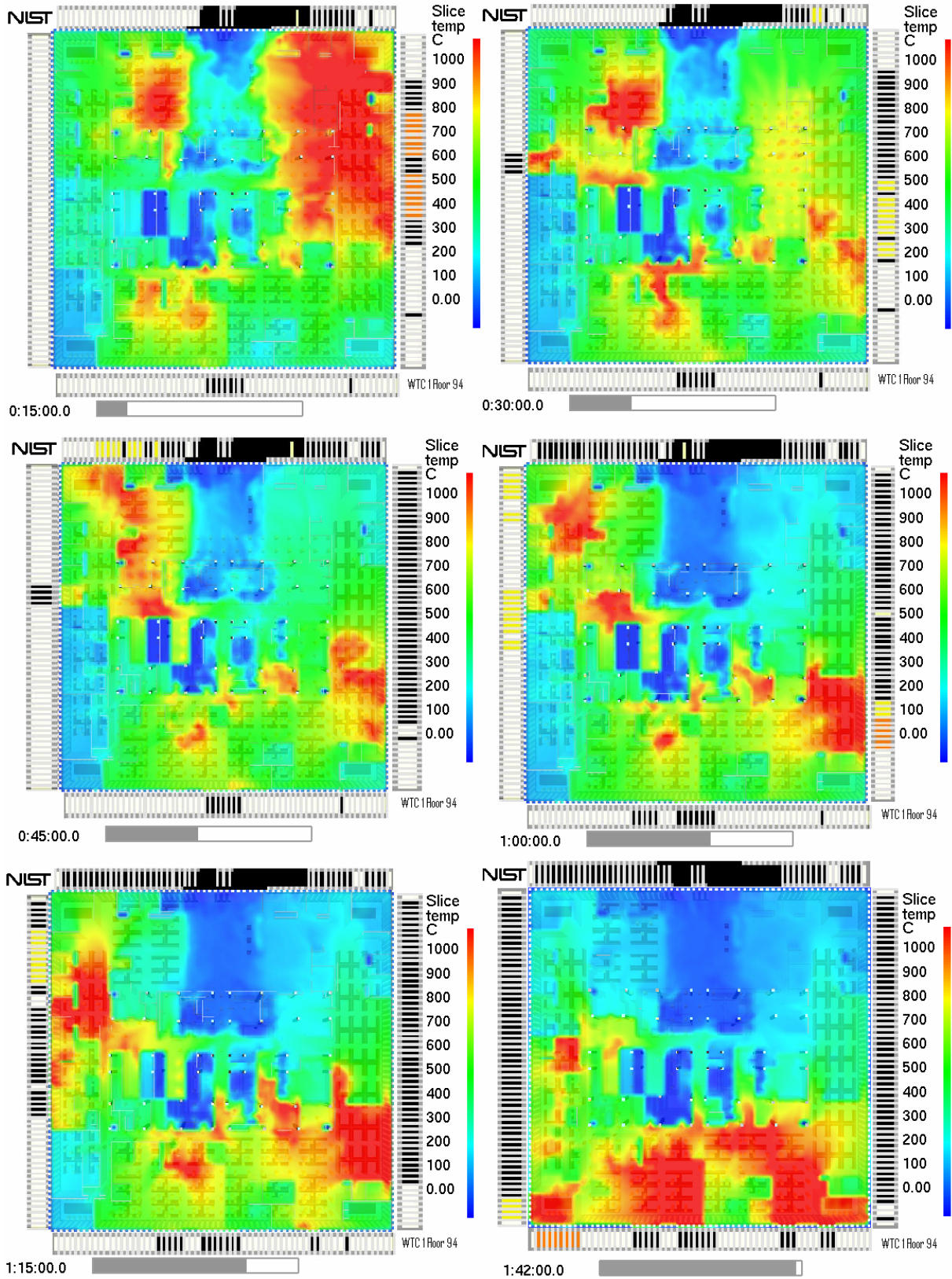


Figure 6-6. Simulated upper layer temperatures on floor 94 of WTC 1, Case B.

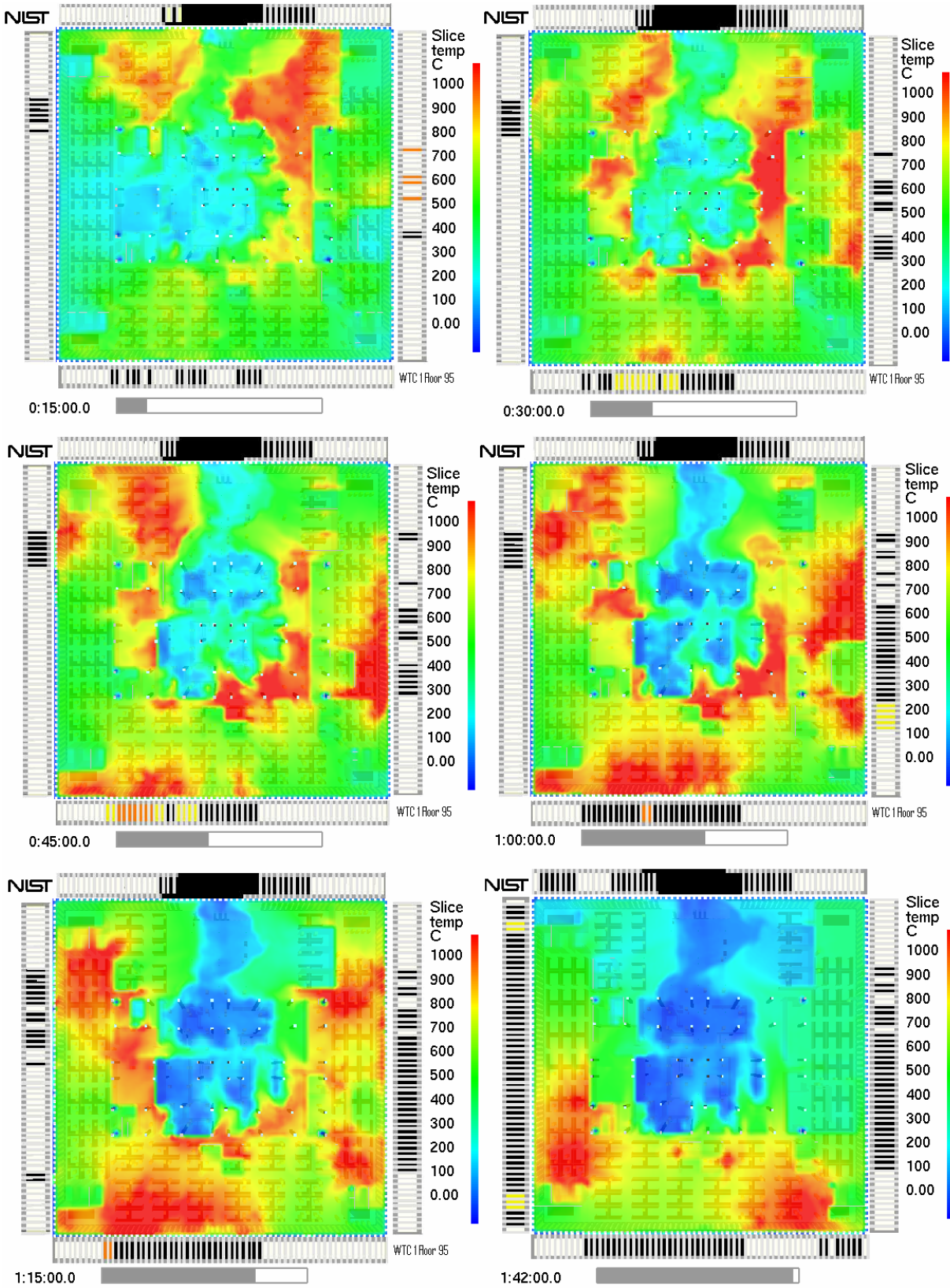


Figure 6–7. Simulated upper layer temperatures on floor 95 of WTC 1, Case A.

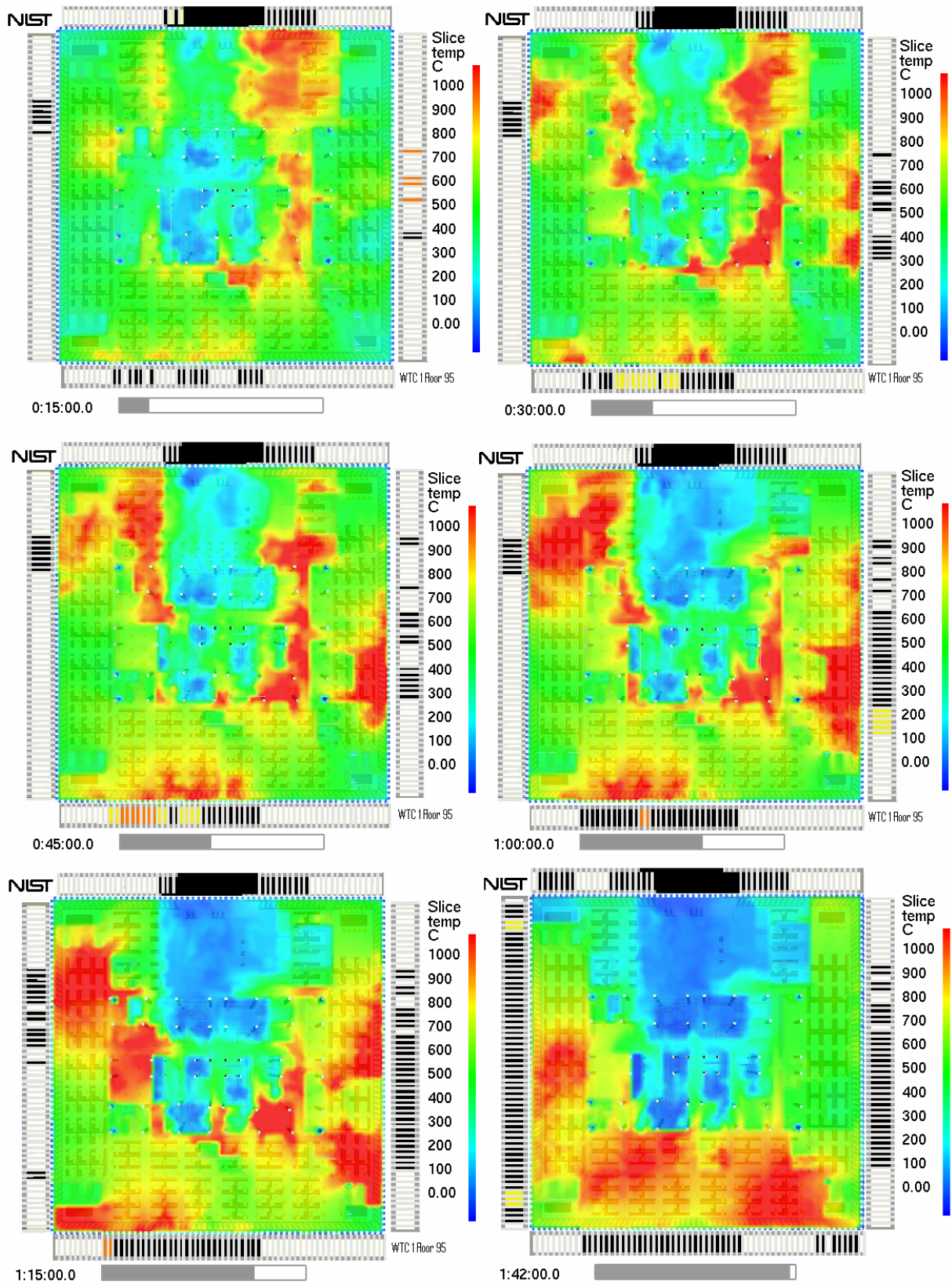


Figure 6–8. Simulated upper layer temperatures on floor 95 of WTC 1, Case B.

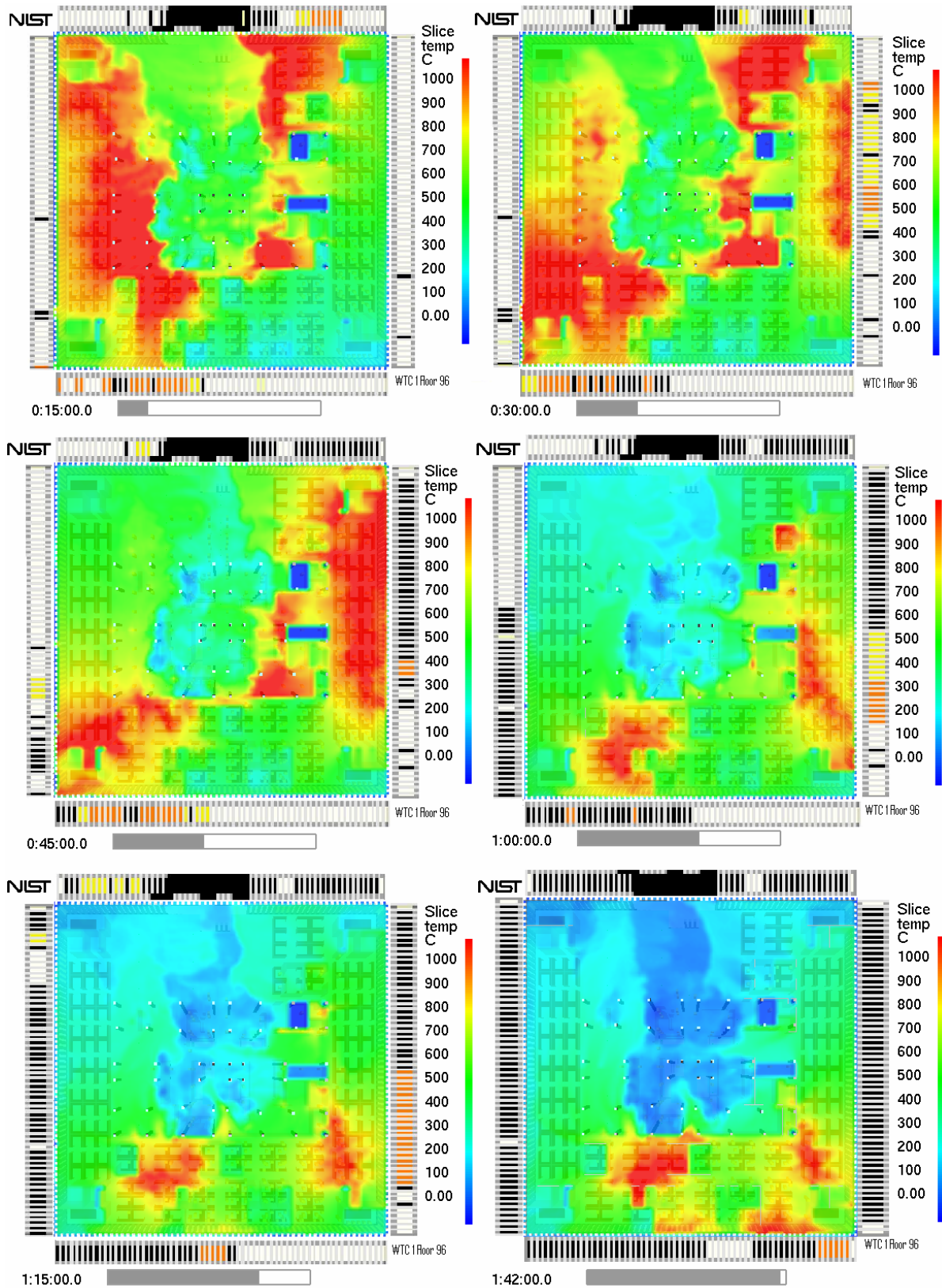


Figure 6–9. Simulated upper layer temperatures on floor 96 of WTC 1, Case A.

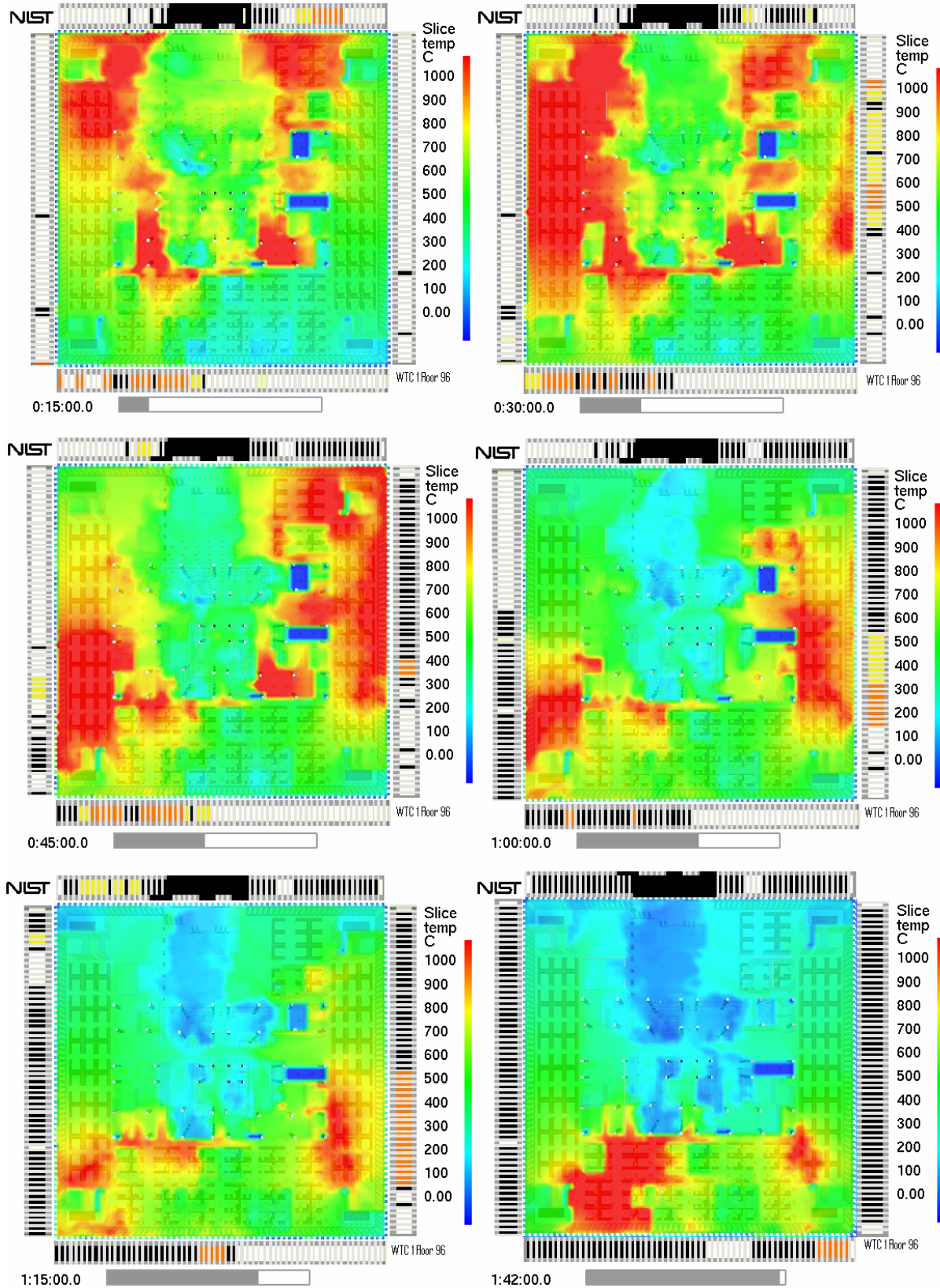


Figure 6–10. Simulated upper layer temperatures on floor 96 of WTC 1, Case B.

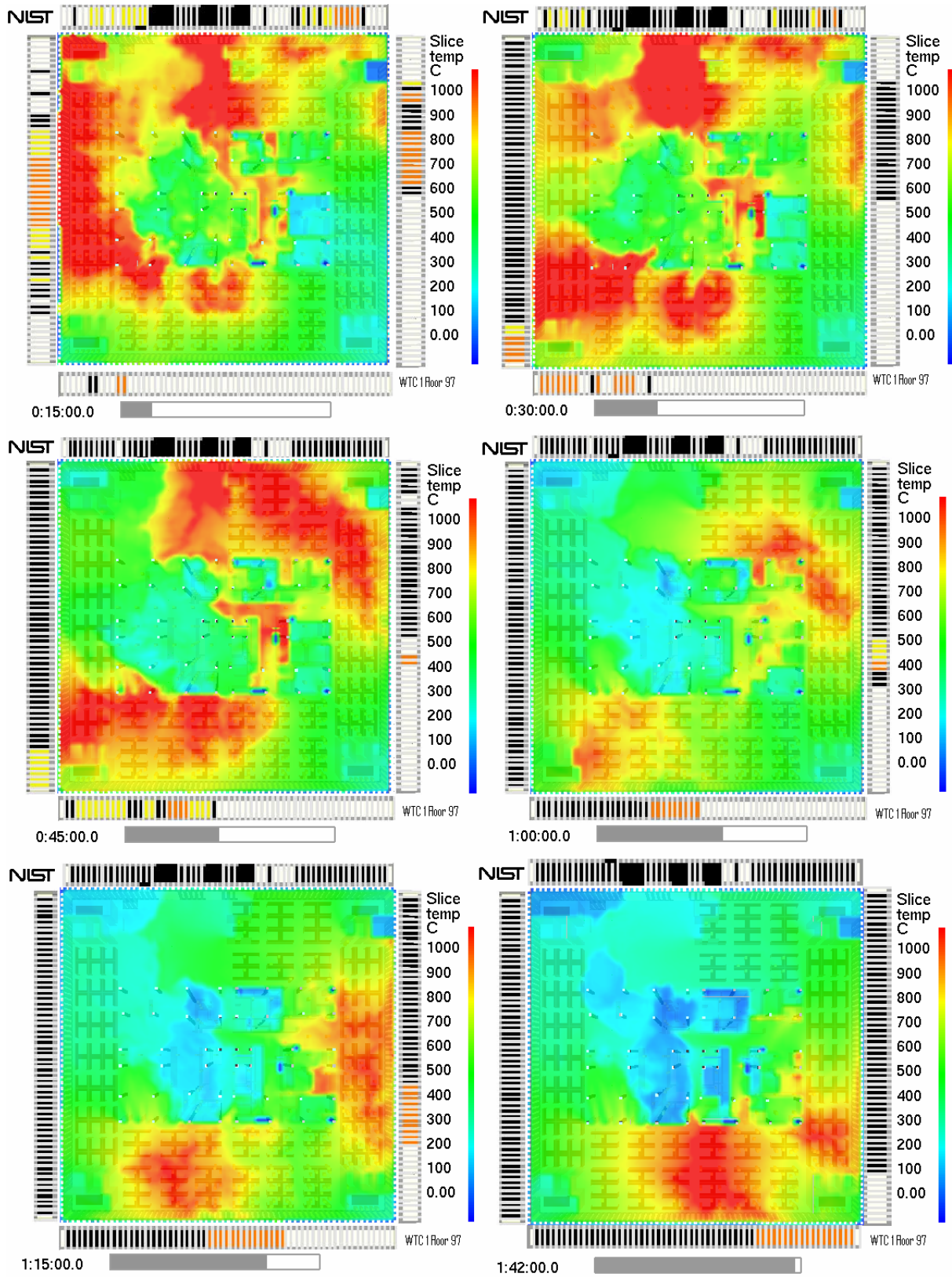


Figure 6–11. Simulated upper layer temperatures on floor 97 of WTC 1, Case A.

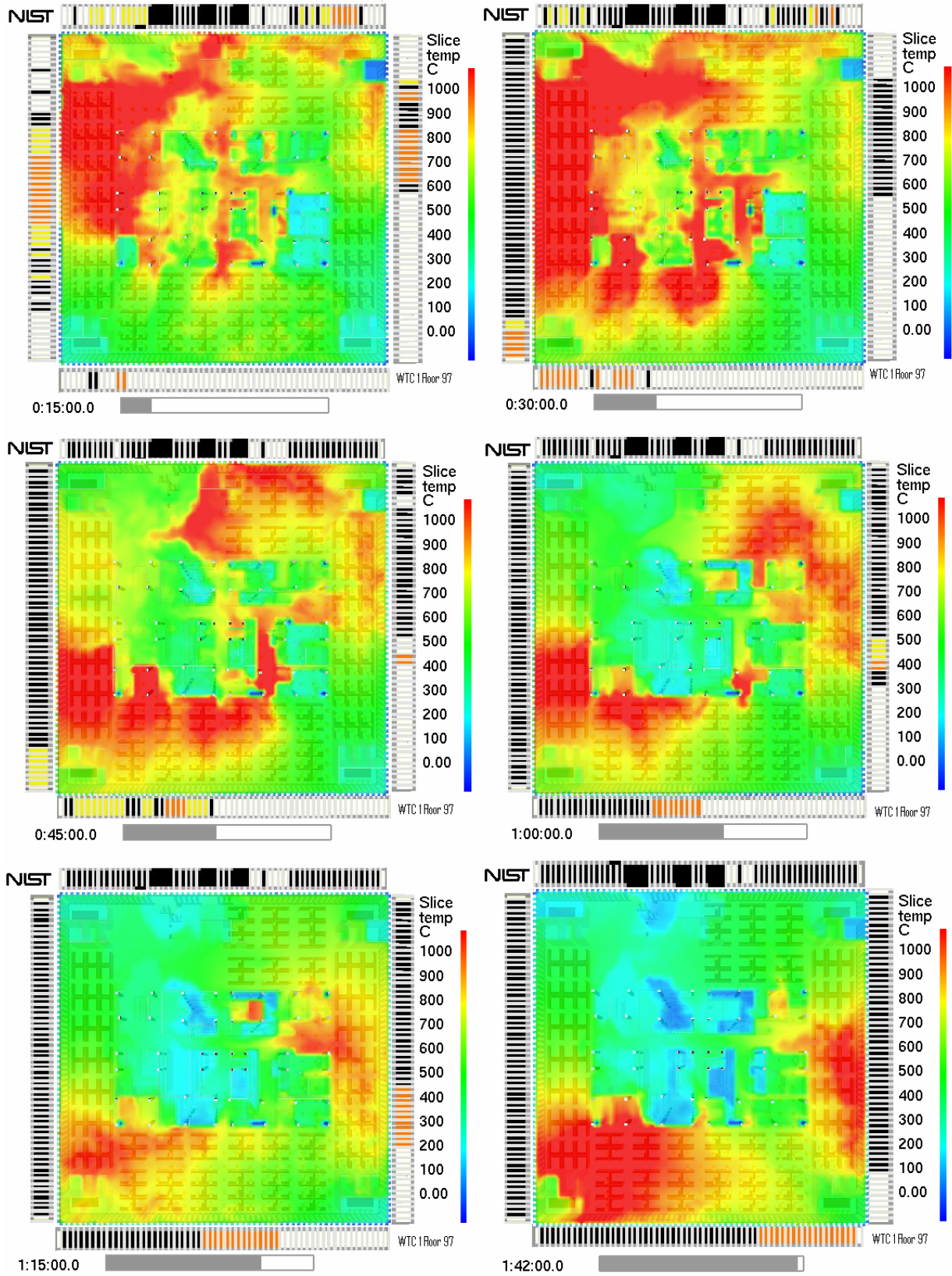


Figure 6–12. Simulated upper layer temperatures on floor 97 of WTC 1, Case B.

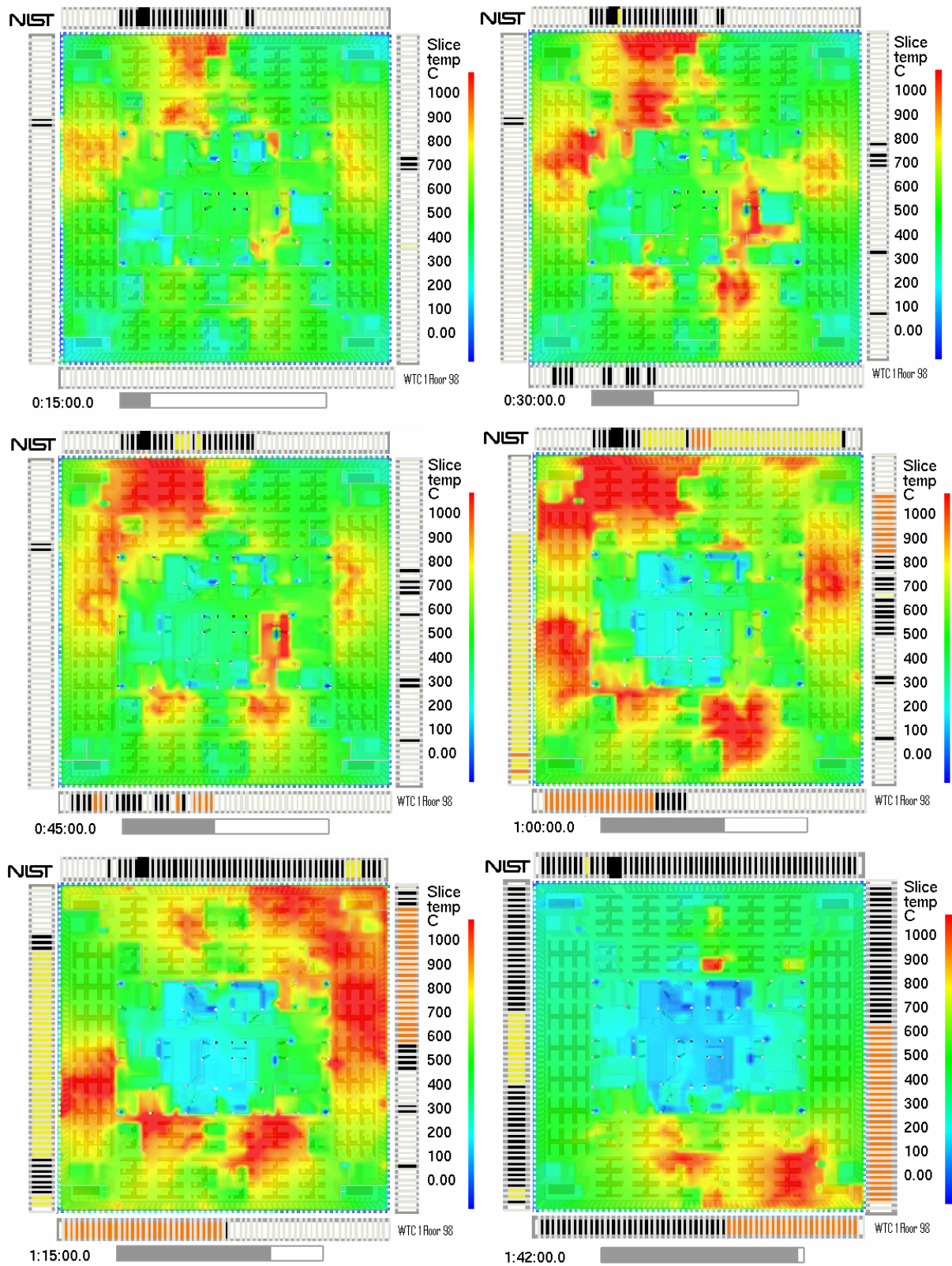


Figure 6–13. Simulated upper layer temperatures on floor 98 of WTC 1, Case A.

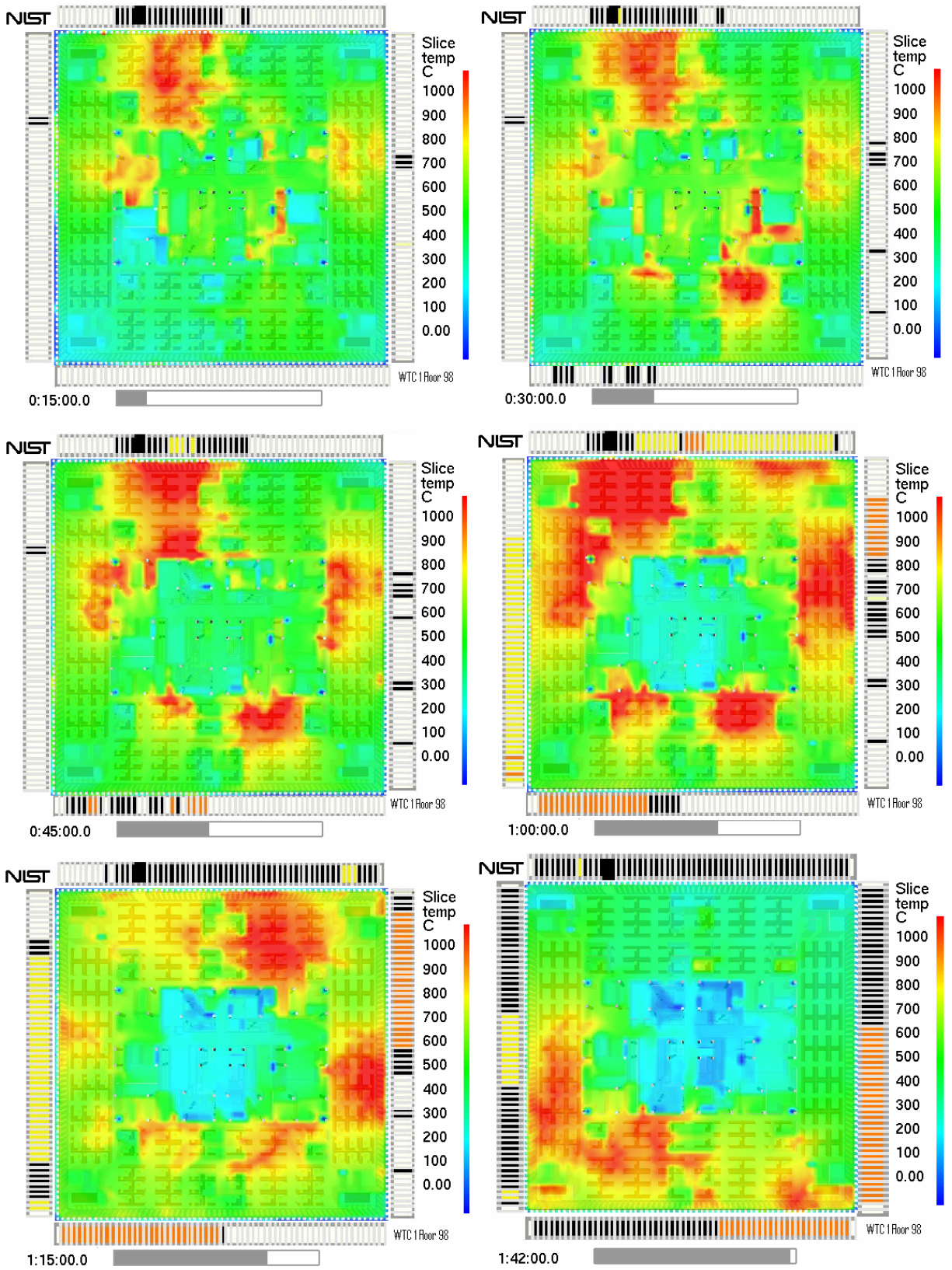


Figure 6-14. Simulated upper layer temperatures on floor 98 of WTC 1, Case B.

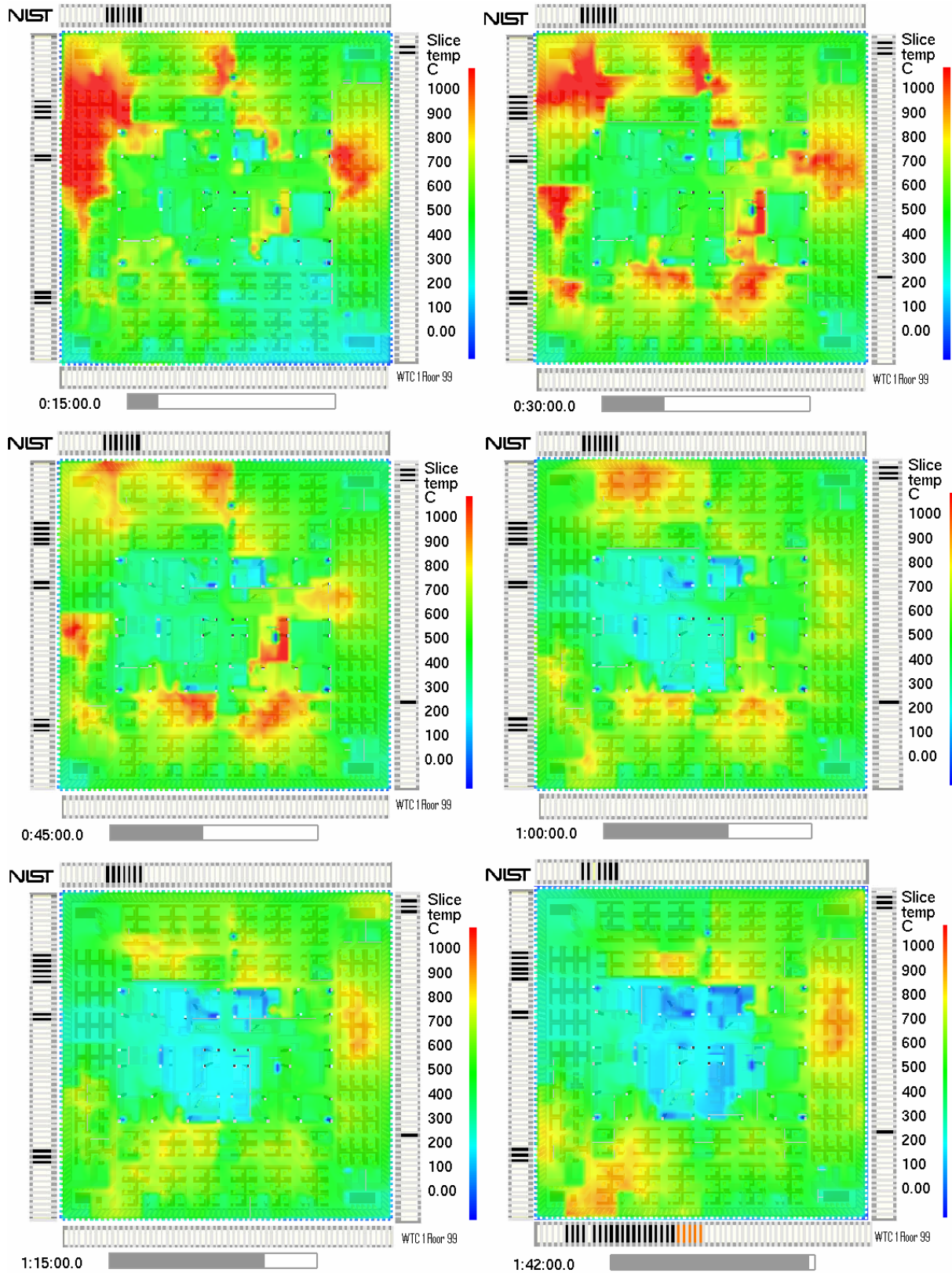


Figure 6–15. Simulated upper layer temperatures on floor 99 of WTC 1, Case A.

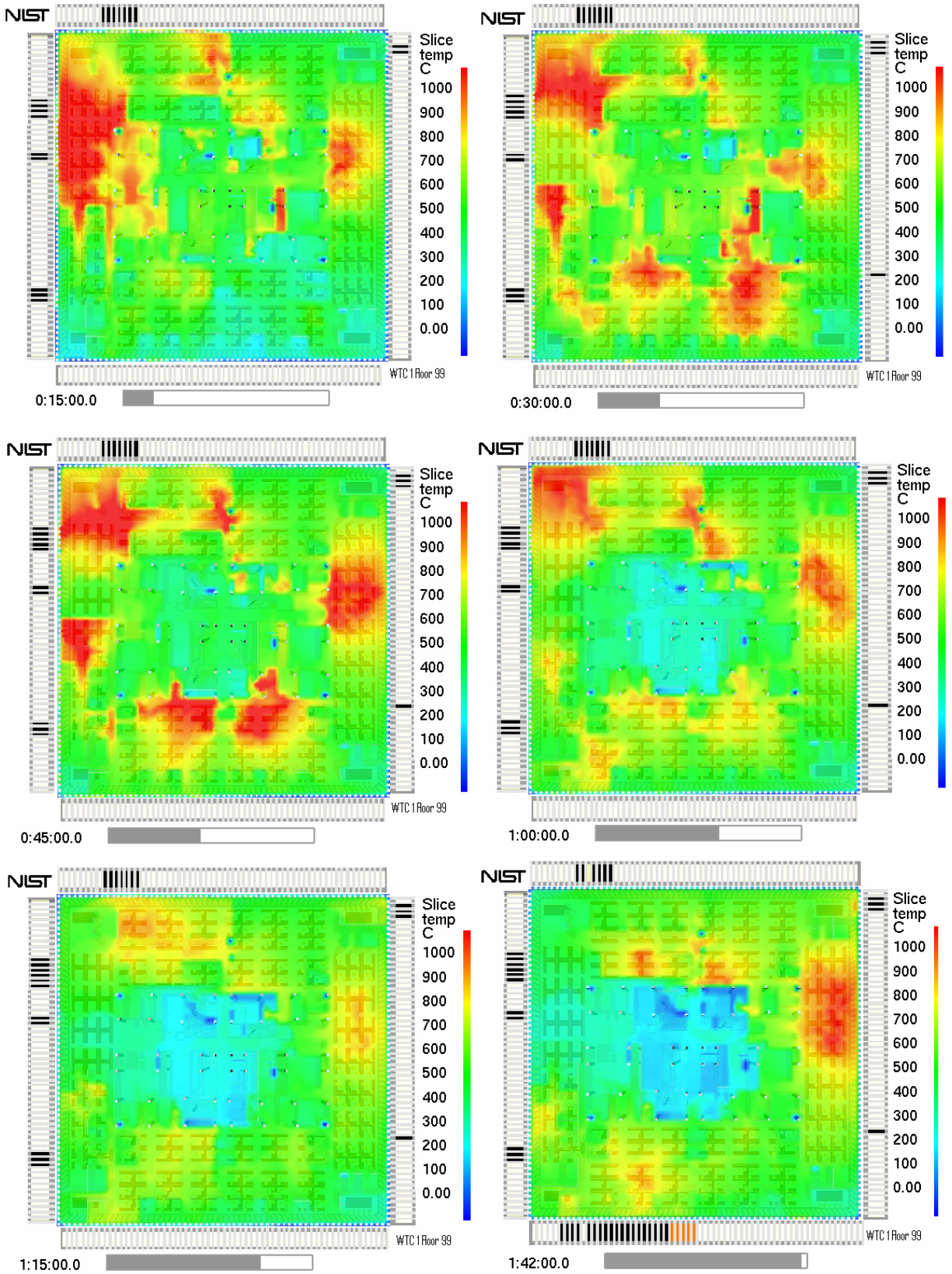


Figure 6-16. Simulated upper layer temperatures on floor 99 of WTC 1, Case B.

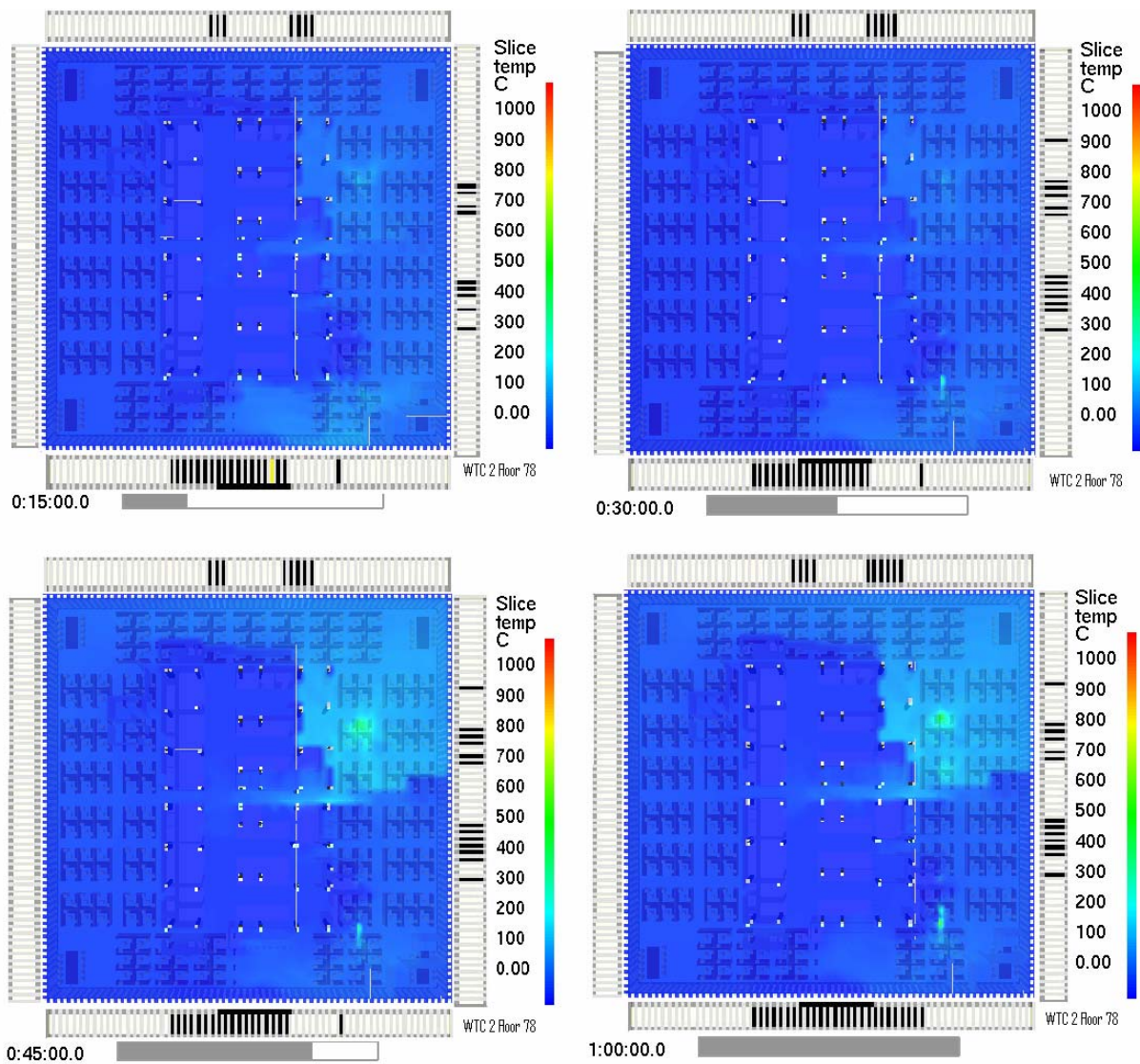


Figure 6–17. Simulated upper layer temperatures on floor 78 of WTC 2, Case C.

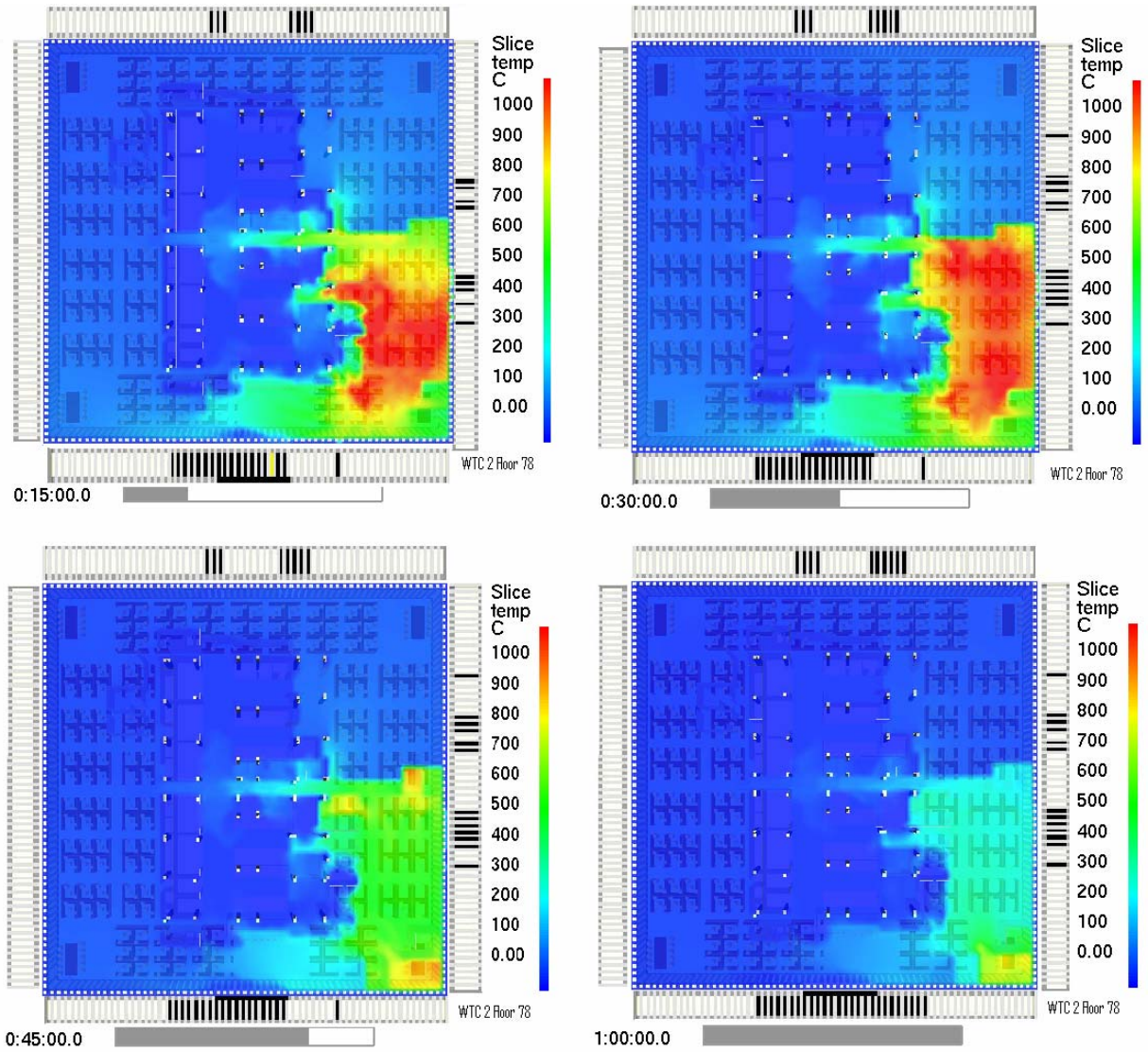


Figure 6–18. Simulated upper layer temperatures on floor 78 of WTC 2, Case D.

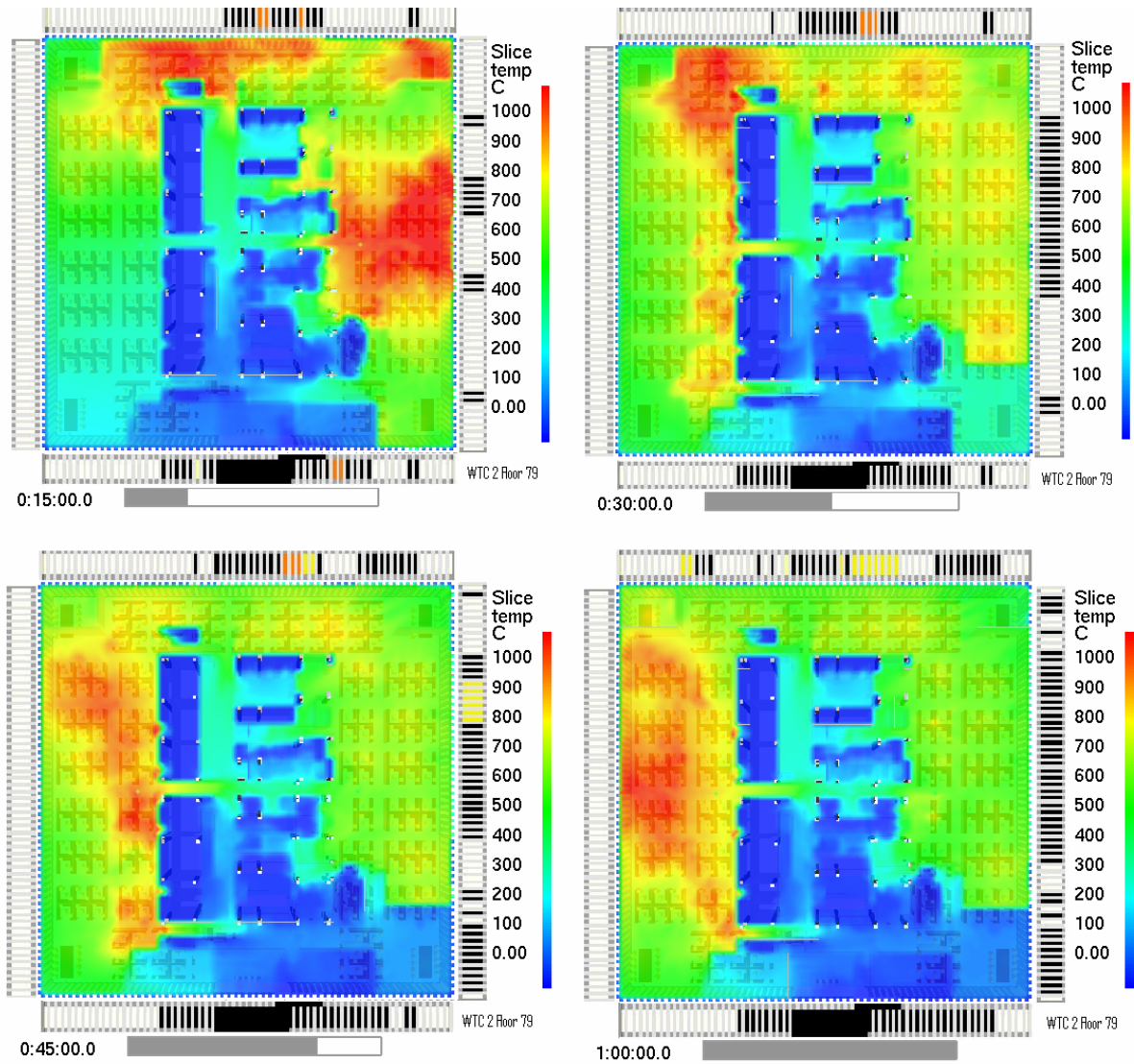


Figure 6–19. Simulated upper layer temperatures on floor 79 of WTC 2, Case C.

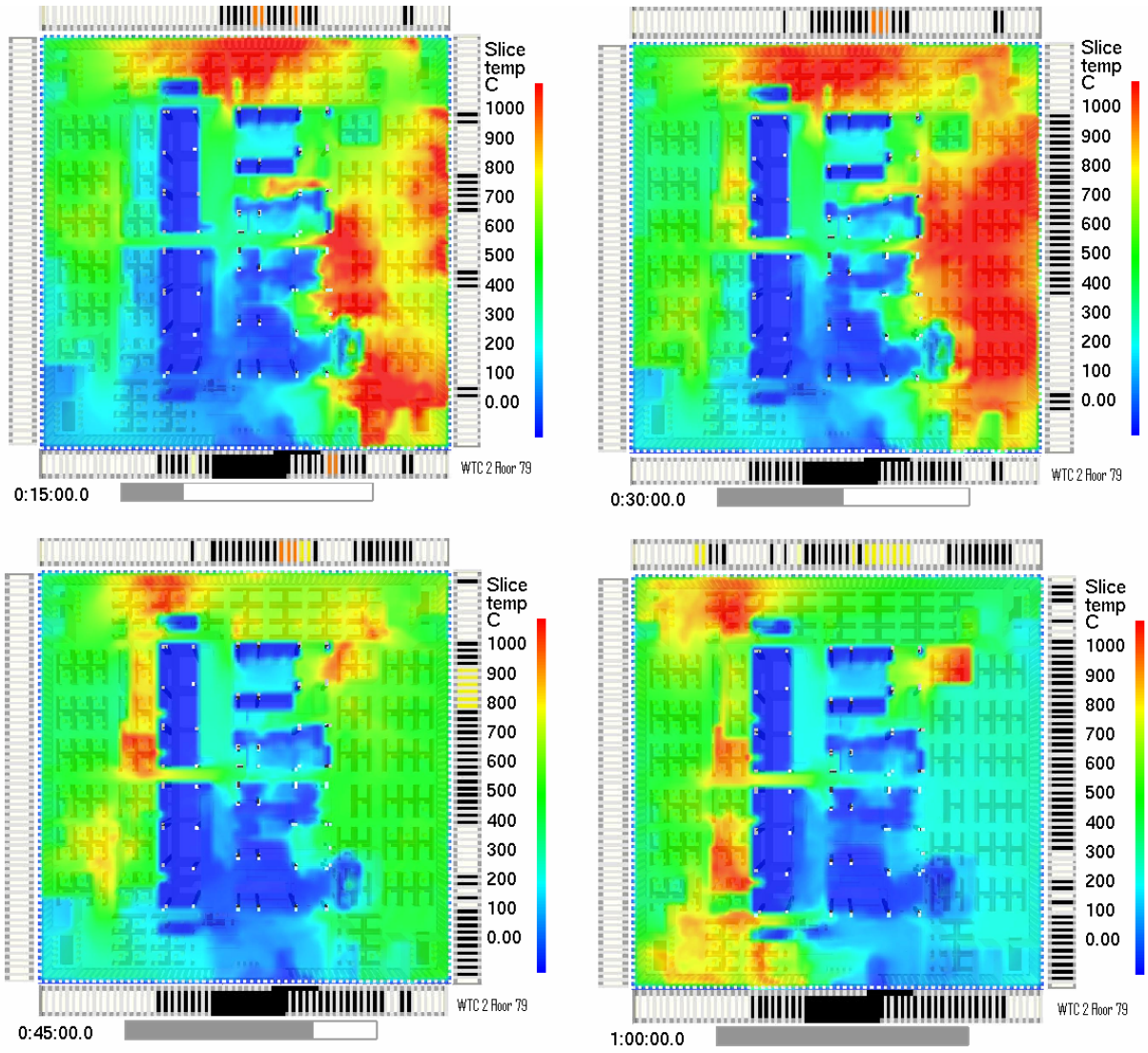


Figure 6–20. Simulated upper layer temperatures on floor 79 of WTC 2, Case D.

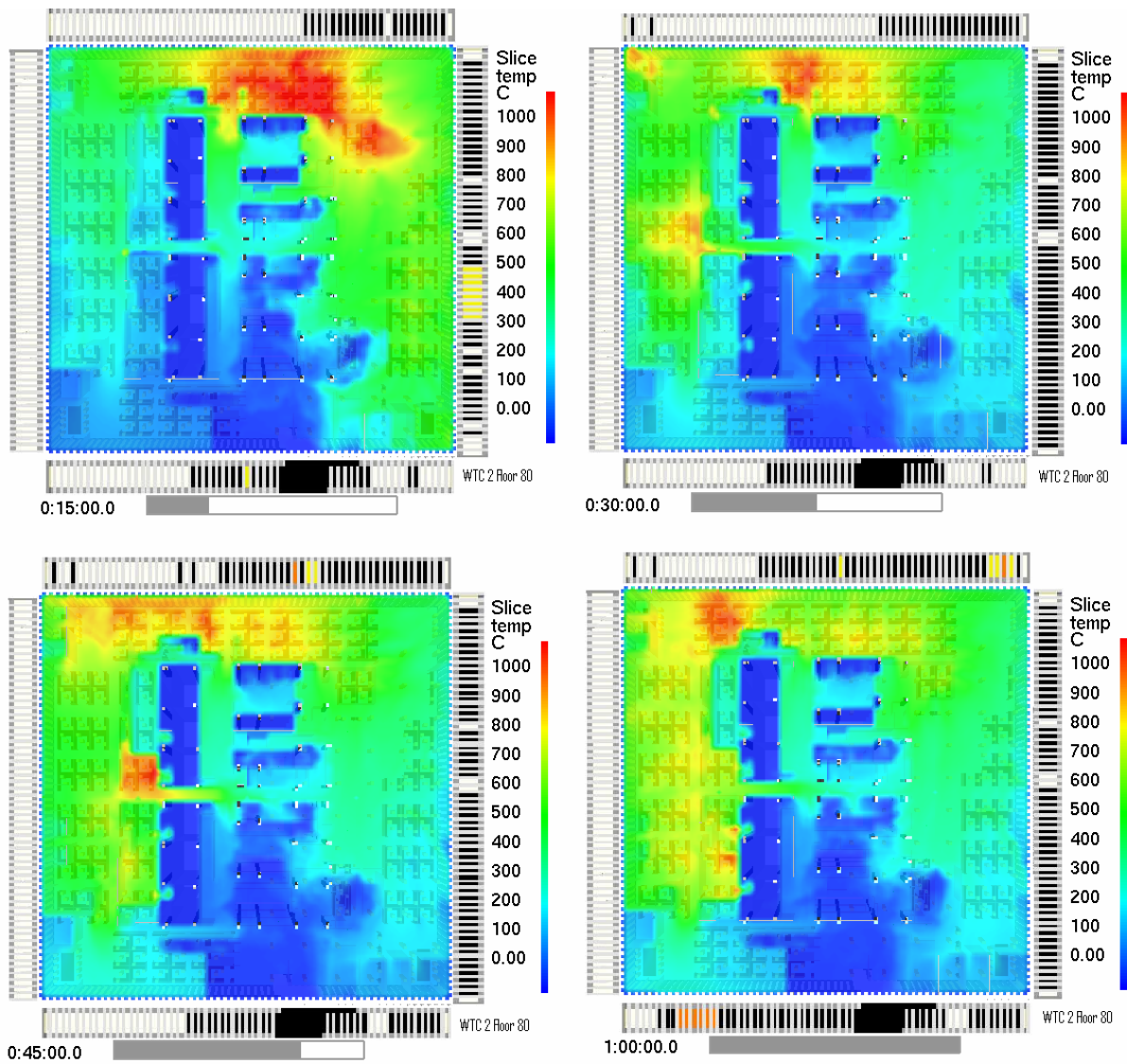


Figure 6–21. Simulated upper layer temperatures on floor 80 of WTC 2, Case C.

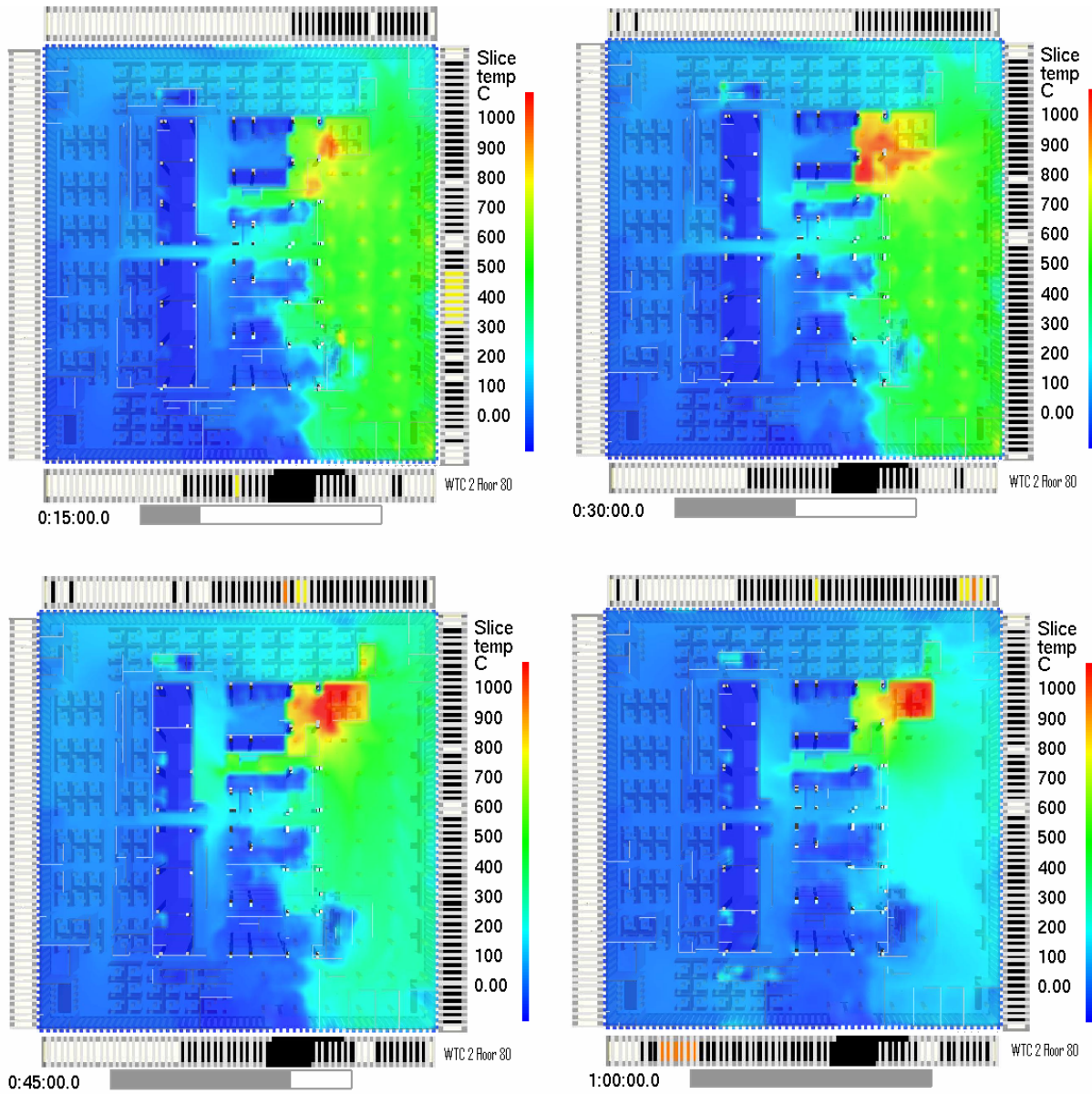


Figure 6–22. Simulated upper layer temperatures on floor 80 of WTC 2, Case D.

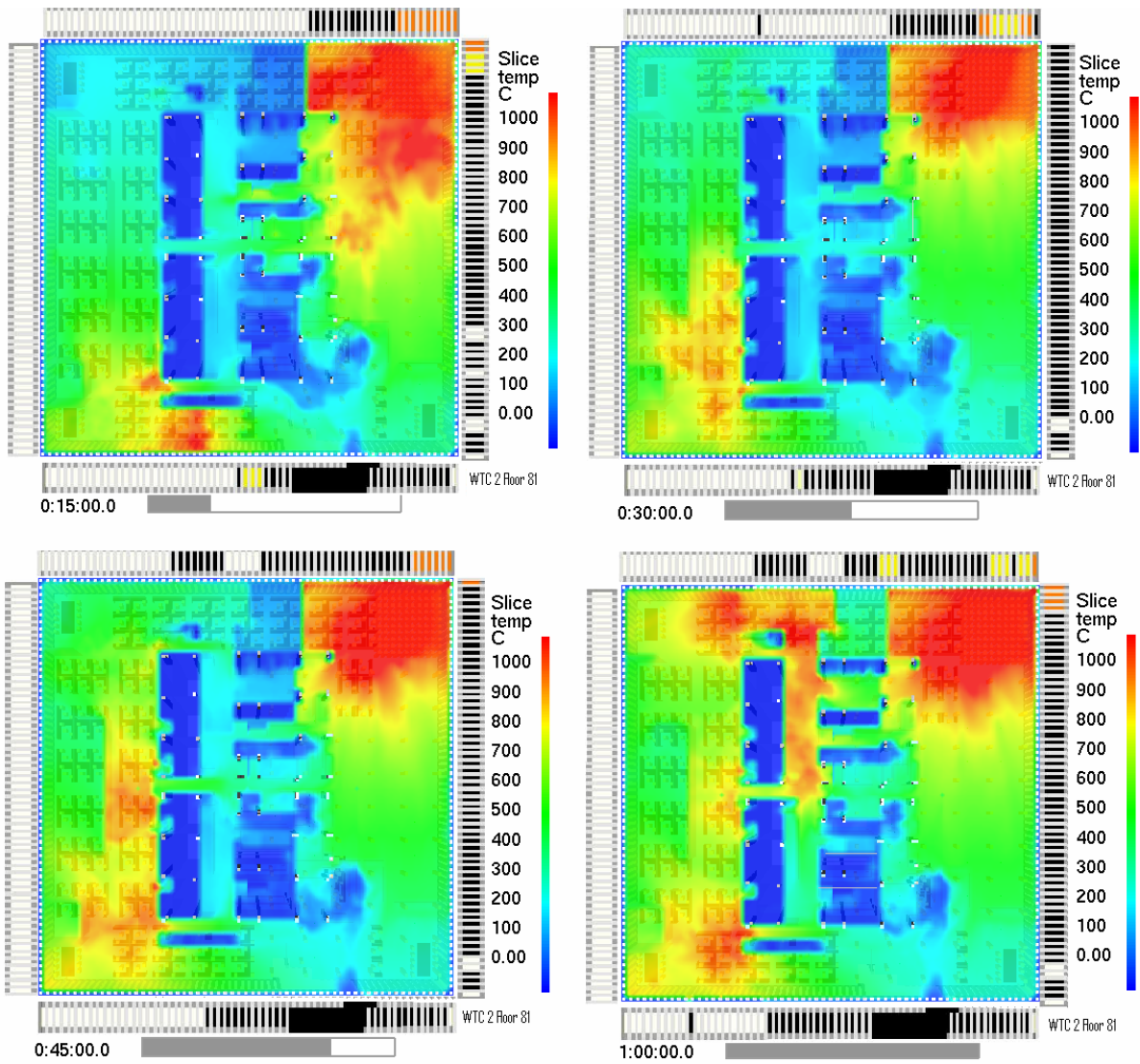


Figure 6–23. Simulated upper layer temperatures on floor 81 of WTC 2, Case C.

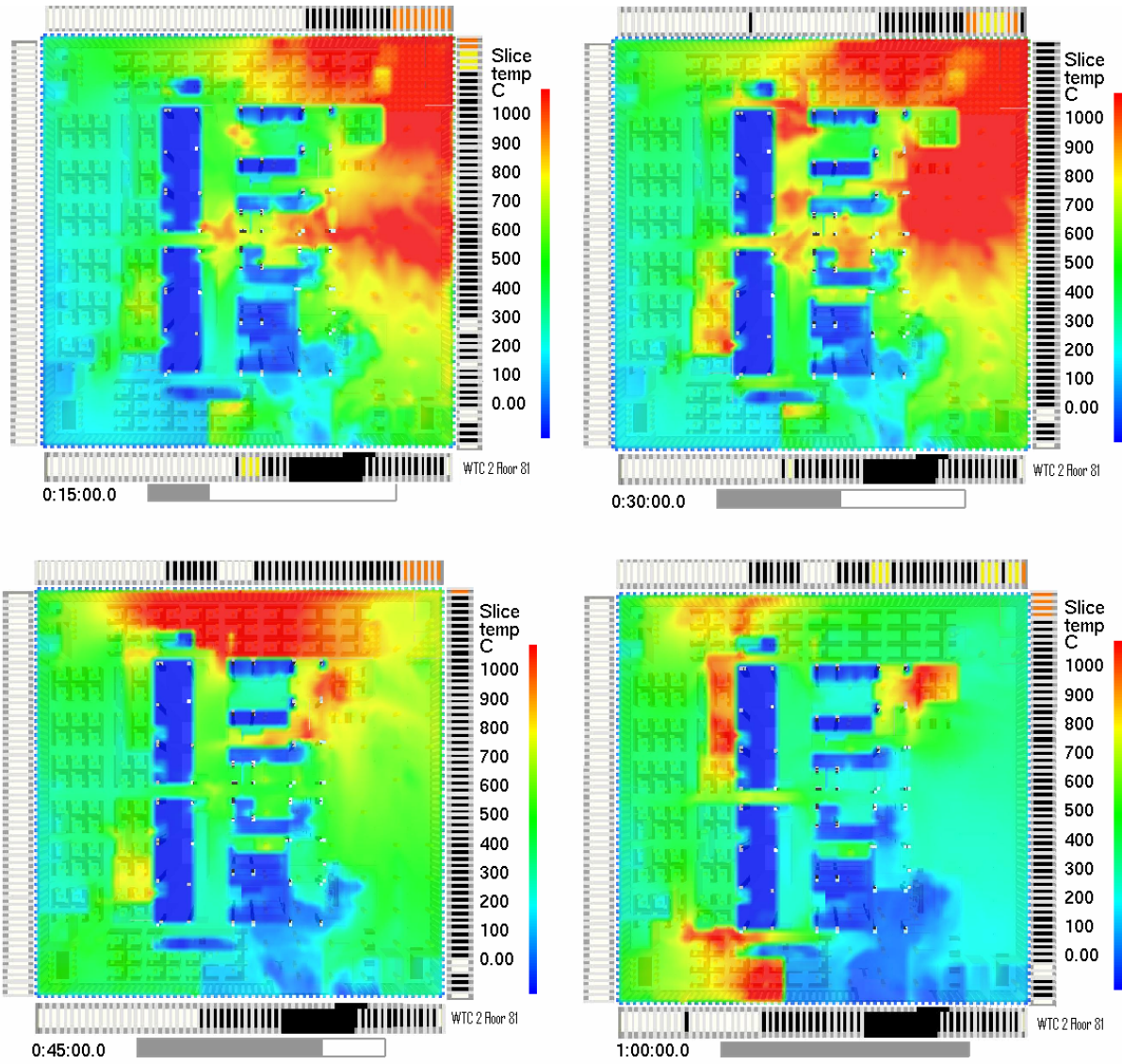


Figure 6–24. Simulated upper layer temperatures on floor 81 of WTC 2, Case D.

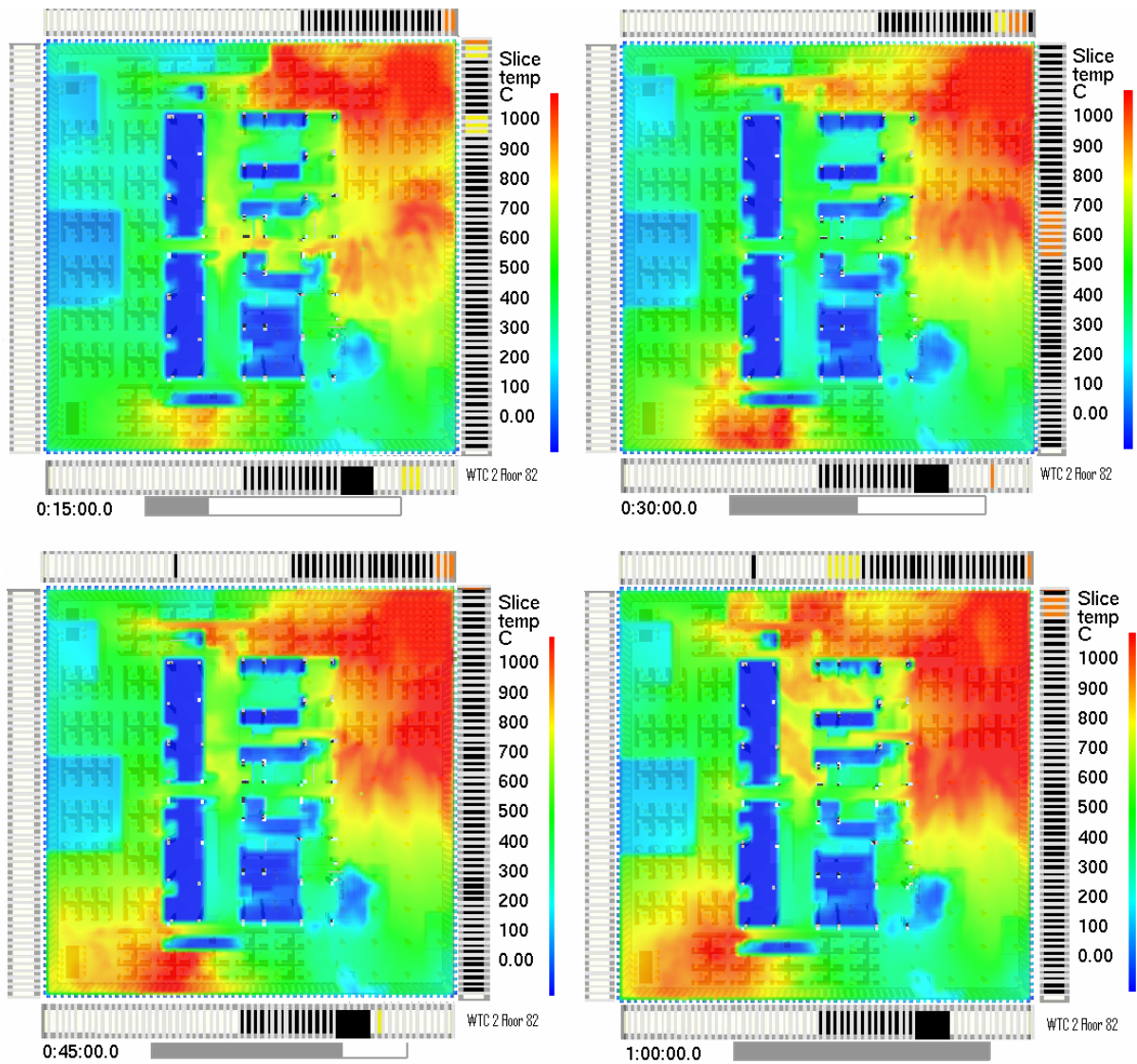


Figure 6–25. Simulated upper layer temperatures on floor 82 of WTC 2, Case C.

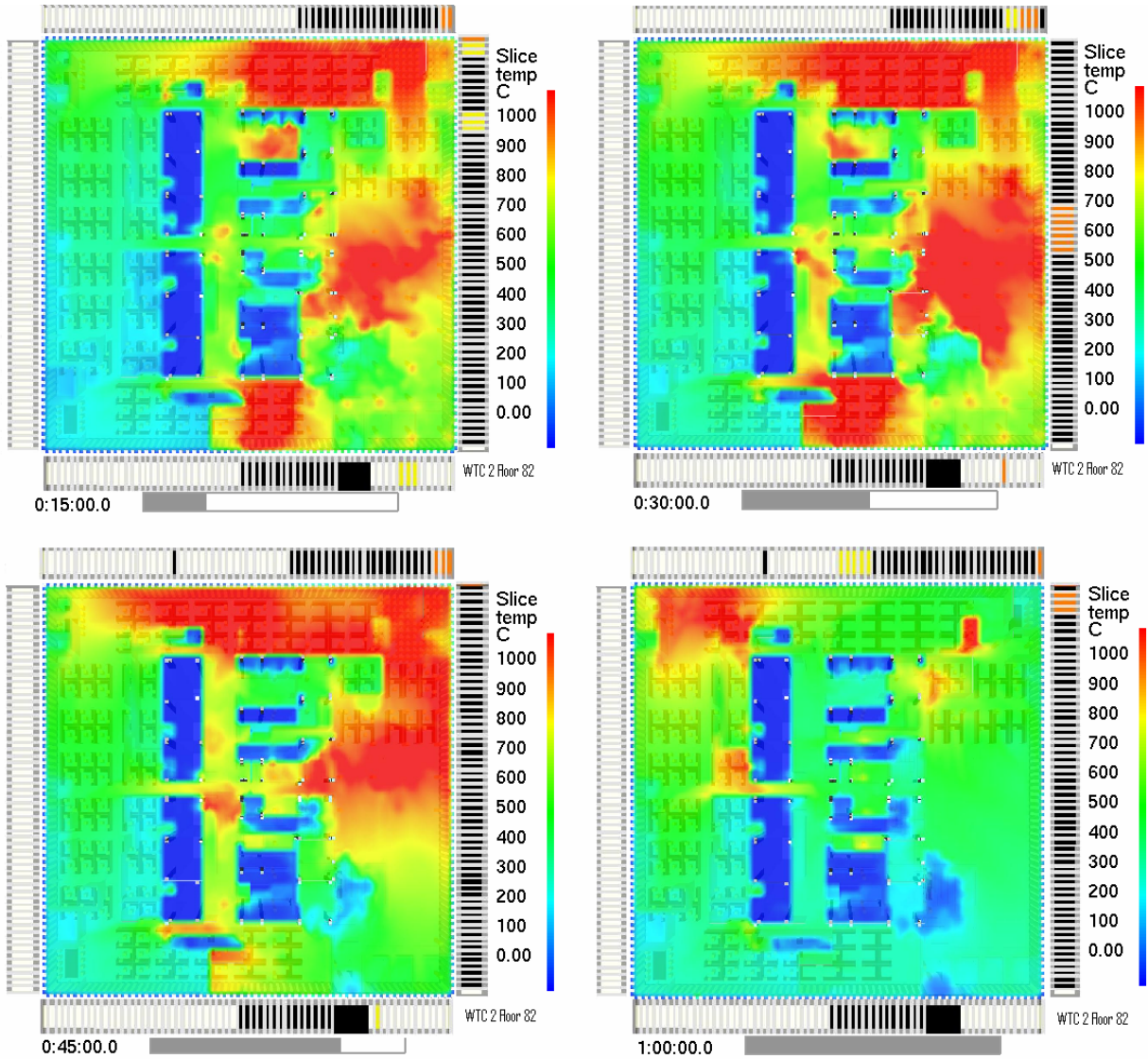


Figure 6–26. Simulated upper layer temperatures on floor 82 of WTC 2, Case D.

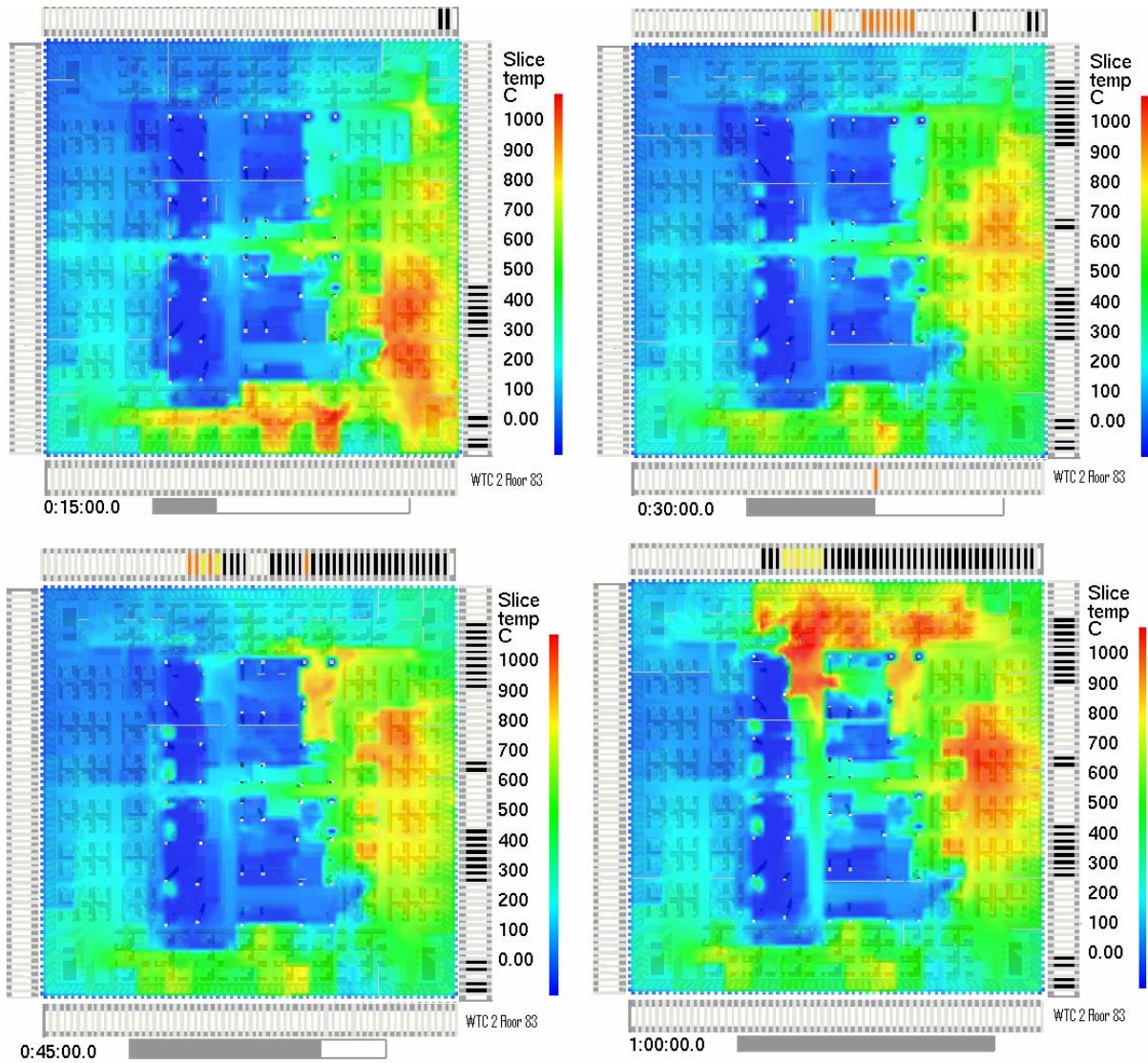


Figure 6–27. Simulated upper layer temperatures on floor 83 of WTC 2, Case C.

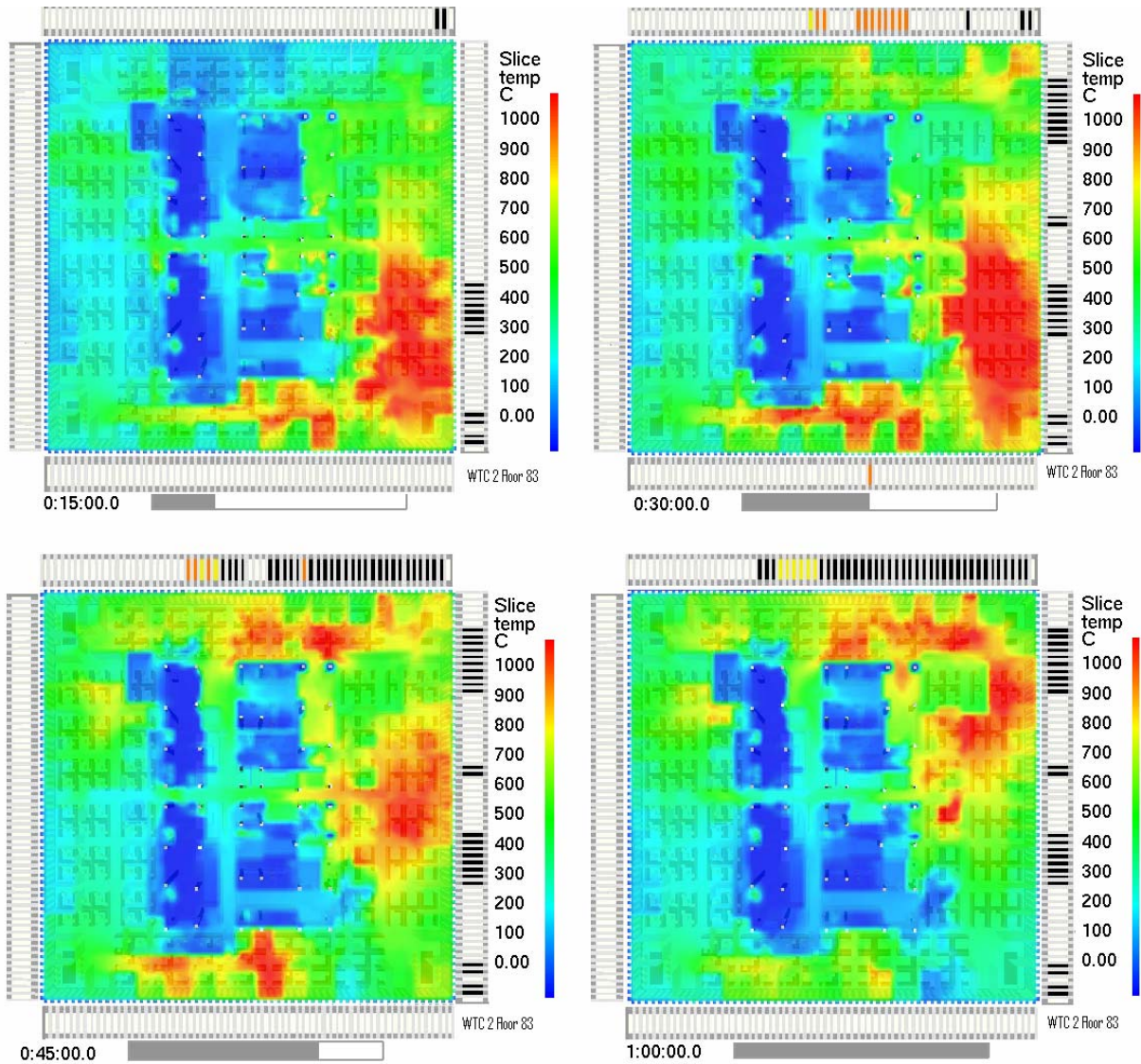


Figure 6–28. Simulated upper layer temperatures on floor 83 of WTC 2, Case D.

6.7 DISCUSSION OF FDS RESULTS

6.7.1 Fire Spread Patterns

The visual observations of the fire activity near the building exterior were the primary means of evaluating the accuracy of the numerical predictions. Although it was not possible to replicate all of the documented fire behavior (NIST NCSTAR 1-5A), the simulations captured the major trends of the fire activity in terms of spread and duration.

In WTC 1, much of the fire activity was initially in the vicinity of the impact area in the north part of the building, then it spread around the east and west faces, and was last observed to be concentrated in the south part of the building at the time of collapse, as depicted in Figure 6–29.

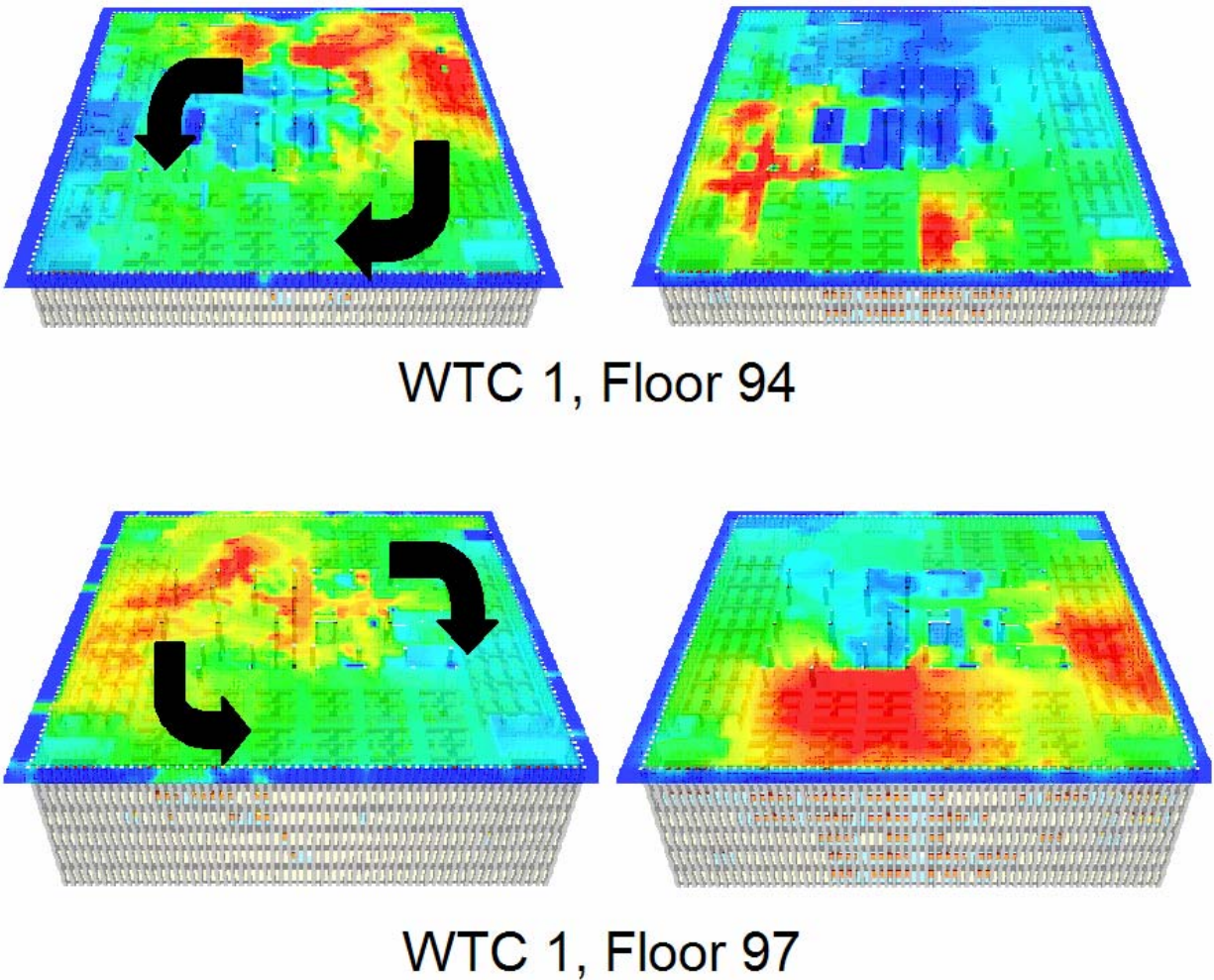


Figure 6–29. Direction of simulated fire movement on floors 94 and 97 of WTC 1.

The fact that the simulated fires encircled the building in roughly the same amount of time as the actual fires supported the estimate of the overall combustible load of 20 kg/m^2 (4 lb/ft^2). Simulations performed with higher loads required a proportionately longer amount of time to bring the fires around to the southeast because of the fact that the burn time was roughly proportional to the fuel mass in the oxygen-limited interior of the fire floors.

For WTC 2, relying mainly on Case D, there was less movement of the fires. The major burning occurred along the east side, with some spread to the north.

6.7.2 Fire Temperatures

It was clear from both the simulations and observations that the computation of some “average” gas temperature was not a satisfactory means of assessing the thermal environment on floors that were over $4,000 \text{ m}^2$ (1 acre) in area. Not only would the assumption of an average temperature have been inconsistent with the visual evidence, but it would also have led to large errors in the subsequent thermal and structural analyses.

The heat transferred to the structural components was largely by means of thermal radiation, which is roughly proportional to the fourth power of the gas temperature. The simulations and the visual evidence suggested that the duration of temperatures in the neighborhood of $1,000 \text{ }^\circ\text{C}$ at any given location on any given floor was about 15 min to 20 min. The rest of the time, temperatures were predicted to have been in the range of $400 \text{ }^\circ\text{C}$ to $600 \text{ }^\circ\text{C}$ on floors with active fires. To put this in perspective, the heat flux onto a truss surrounded by smoke-laden gases of $1,000 \text{ }^\circ\text{C}$ is approximately 150 kW/m^2 , whereas it is 20 kW/m^2 for gases of $500 \text{ }^\circ\text{C}$.

6.7.3 Global Heat Release Rates

Much of the information needed to simulate the fires as described above came from laboratory-scale tests. While some of these (NIST NCSTAR 1-5E) involved enclosures several meters in dimension and fires that reached heat release rates of 10 MW and 12 GJ in total heat output, they were still far smaller than the fires that burned on September 11, 2001, in the WTC towers. Figure 6–30 shows the heat release rates from the FDS simulations of the WTC fires. The peak plateau heat release rates were about 2 GW for WTC 1 and 1 GW for WTC 2. (These are quite similar to the preliminary estimates by Rehm et al. (2002), which were between 1 to 1.5 GW for each tower.) Integrating the area under these curves produced total heat outputs from the simulated fires of about 8,000 GJ from WTC 1 and 3,000 GJ from WTC 2. That adequate representations of disasters can be generated using data from experiments two orders of magnitude smaller is an indication of the capability within the fire research community.

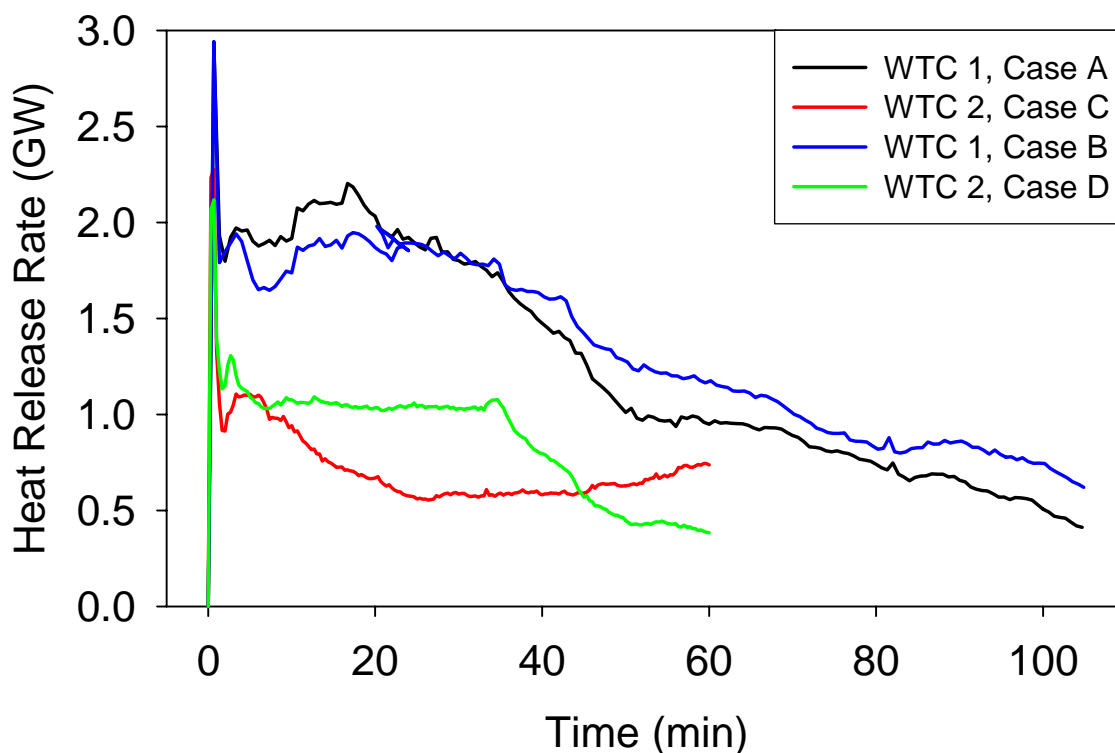


Figure 6–30. Predicted heat release rates for fires in WTC 1 and WTC 2.

6.8 DATA TRANSFER

The results of the FDS simulations were used in detailed calculations of the temperature histories of the structural components. The data from FDS was processed and used as boundary conditions for the finite-element calculation of the structural temperatures. Four quantities were transferred from FDS:

- The upper and lower layer gas temperatures, time-averaged over 100 s and spatially-averaged over 1 m. The upper layer gas temperatures were taken 0.4 m (one grid cell) below the ceiling. The lower layer temperatures were taken 0.4 m above the floor.
- The depth of the smoke layer, estimated from the vertical temperature profile using a simple algorithm that is described in the FDS User’s Guide (McGrattan 2004).
- The absorption coefficient of the smoke layer 0.4 m below the ceiling.

6.9 THERMAL RESPONSE SIMULATIONS

The FSI was then used to “map” these onto and within the structural elements. Based on the analysis summarized in Section 5.5, FSI was assumed to be nominally transparent in transferring the thermal and radiative environment to the building structure.

Table 6–2 lists the sources of data files for the four FSI transformations.

Table 6–2. Sources of WTC thermal response inputs.

Input	WTC 1		WTC 2	
	Case A	Case B	Case C	Case D
Structural damage, NIST NCSTAR 1-2 Case	Base	More severe	Base	More severe
Insulation damage, NIST NCSTAR 1-2 Case	Base	More severe	Base	More severe
Thermal and radiative environment to which the structure was exposed	FSI Case A	FSI Case B	FSI Case C	FSI Case D

All damage estimates were based on the aircraft impact simulations, with some confirmation of perimeter column damage from photographs and videos. Structural changes that occurred later, due to the fires, were not included. In the FSI computations, the concrete slab, trusses, or core beams identified as severed (NIST NCSTAR 1-6) were removed.

The thermal results presented in this chapter were transferred to Simpson, Gumpertz & Heger, Inc. (SGH), under a NIST contract, for analysis of the changes in structural performance that resulted from exposure to the fire environments (NIST NCSTAR 1-6D). The FSI calculations were performed at time steps ranging from 1 ms to 50 ms. Use of the resulting data set for structural analysis would have required a prohibitive amount of computation time. Thus, for each Case, the instantaneous temperature and temperature gradient for each grid volume was provided at 10 min intervals after aircraft impact. For WTC 1, there were 10 such intervals, ending at 6,000 s; for WTC 2 there were 6 intervals, ending at 3,600 s. The data files were in a format consistent with ANSYS 8.0.

Each floor in the FSI simulation provided thermal information for the floor assembly above. Thus, the lowest floor in the FSI simulations cannot be fully modeled. For WTC 1, the global thermal response generated by FSI included floors 93 through 99; for WTC 2, the included floors were 79 through 83.

The composite figures shown below depict visualizations of these snapshots of the external temperatures on the columns and floor structures. They are positioned to enable perception of the evolution of the temperatures from shortly after the aircraft impact until roughly the time of collapse. For space reasons, the presentations for WTC 1 omit the snapshot at 3,600 s.

6.10 GLOBAL THERMAL RESPONSE OF WTC 1, CASE A

Figures 6–31 through 6–44 depict the evolving temperatures on the columns and trusses. (NIST NCSTAR 1-6G also contains thermal plots of the floor slabs.) For ease of comparison, the equivalent drawings for Case B have been interspersed. In each case, the first sub-figure shows the north and east faces of the building for orientation.

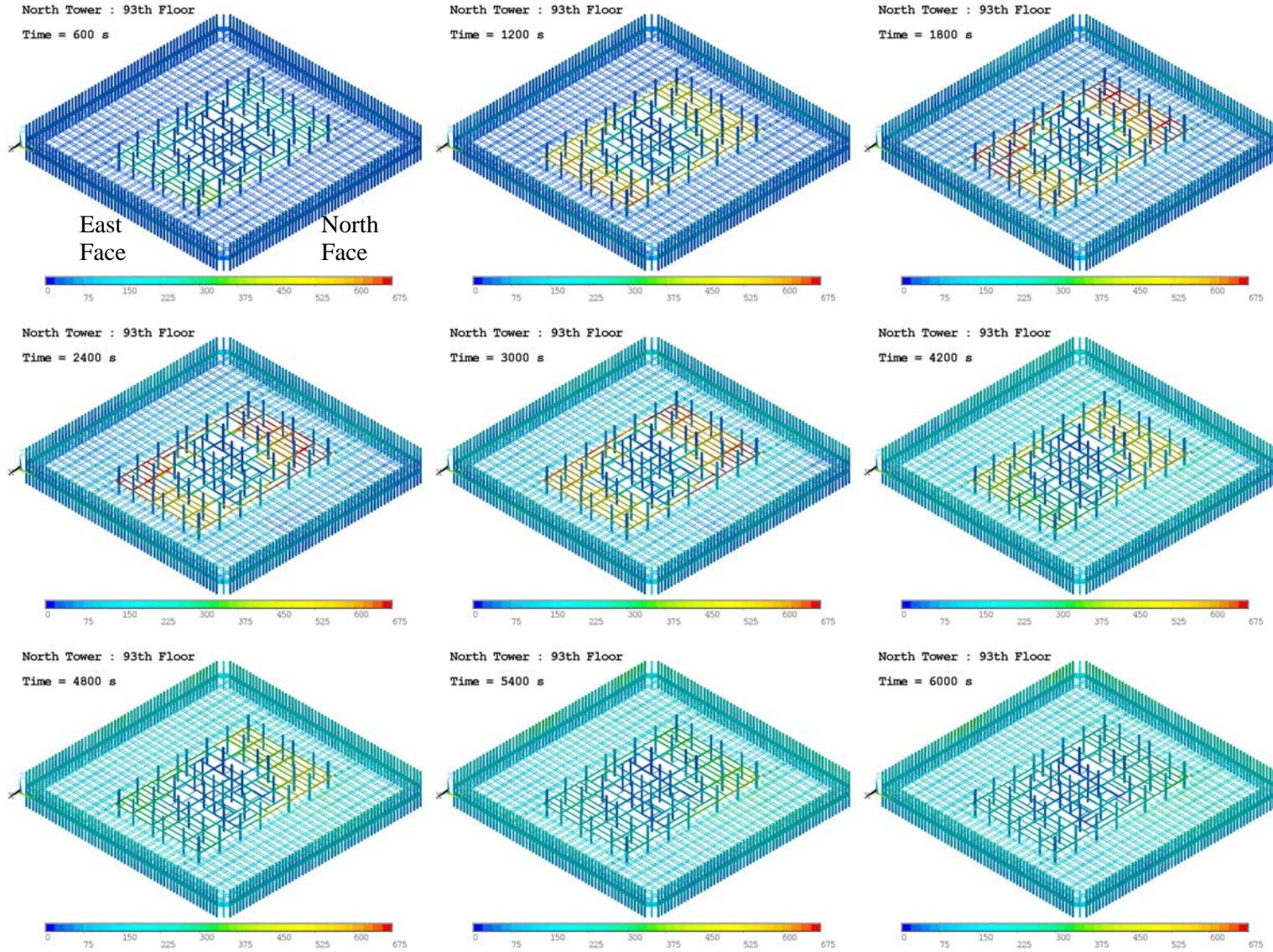


Figure 6-31. Thermal response of floor 93 of WTC 1, Case A.

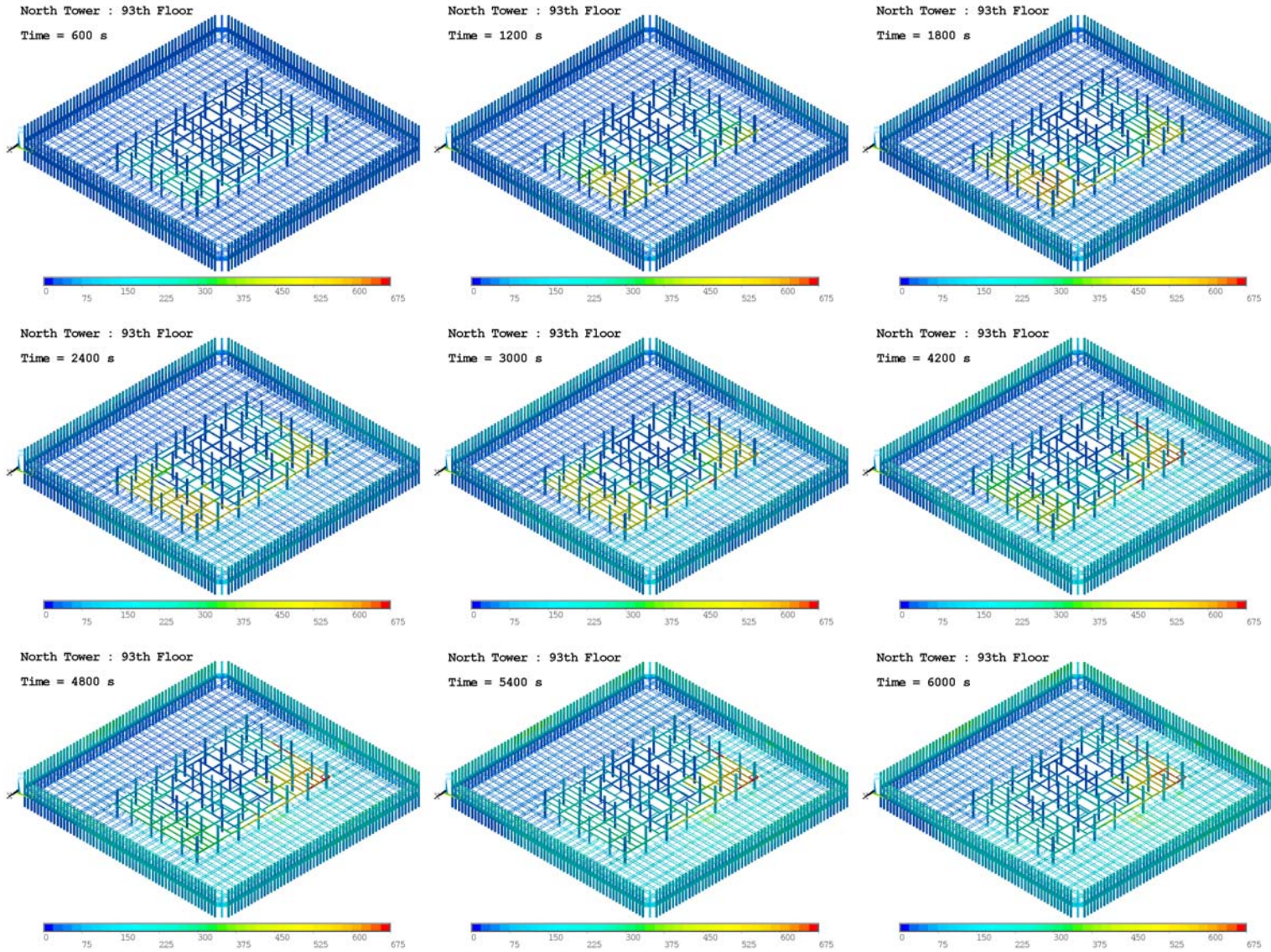


Figure 6-32. Thermal response of floor 93 of WTC 1, Case B.

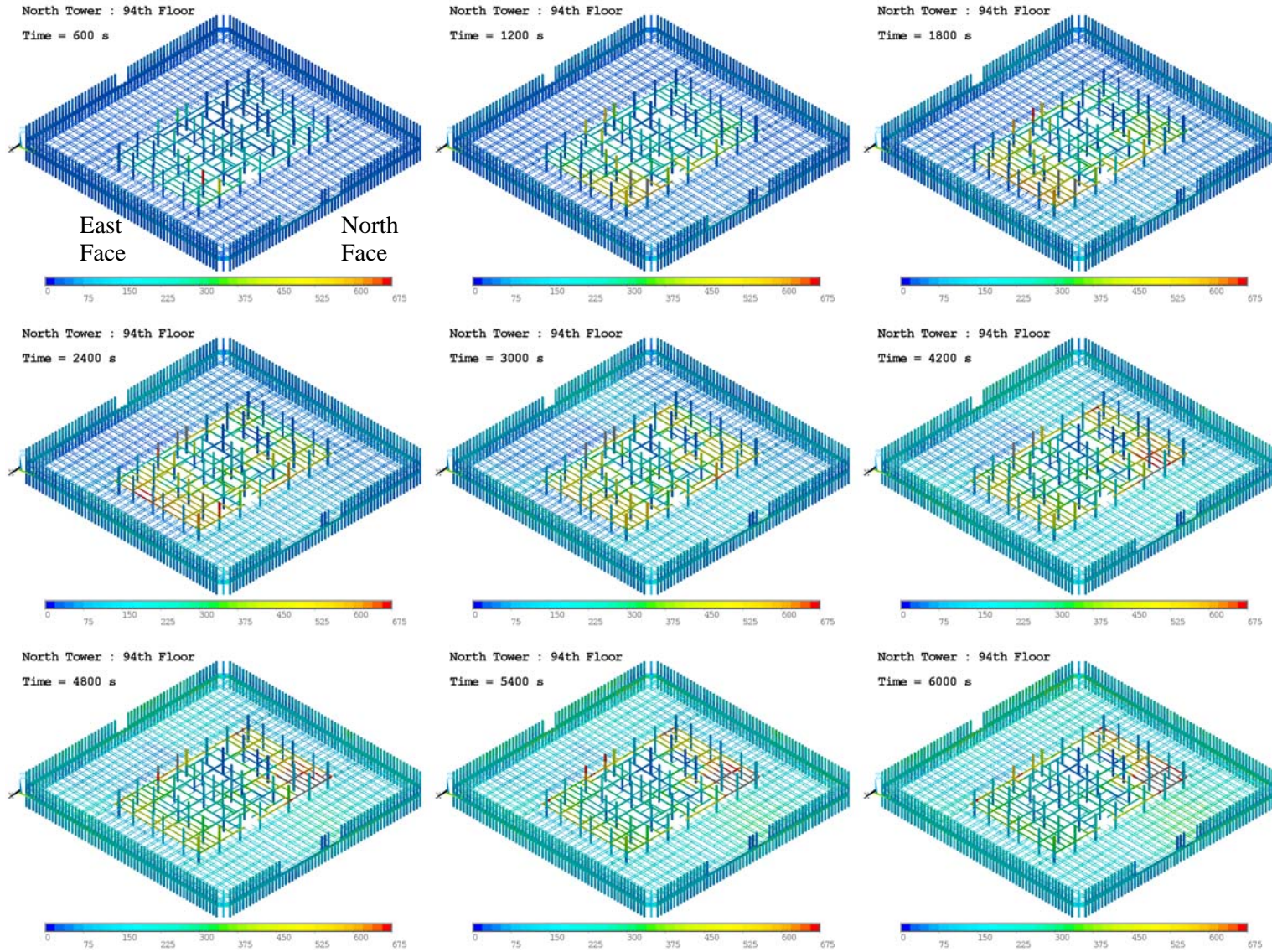


Figure 6-33. Thermal response of floor 94 of WTC 1, Case A.

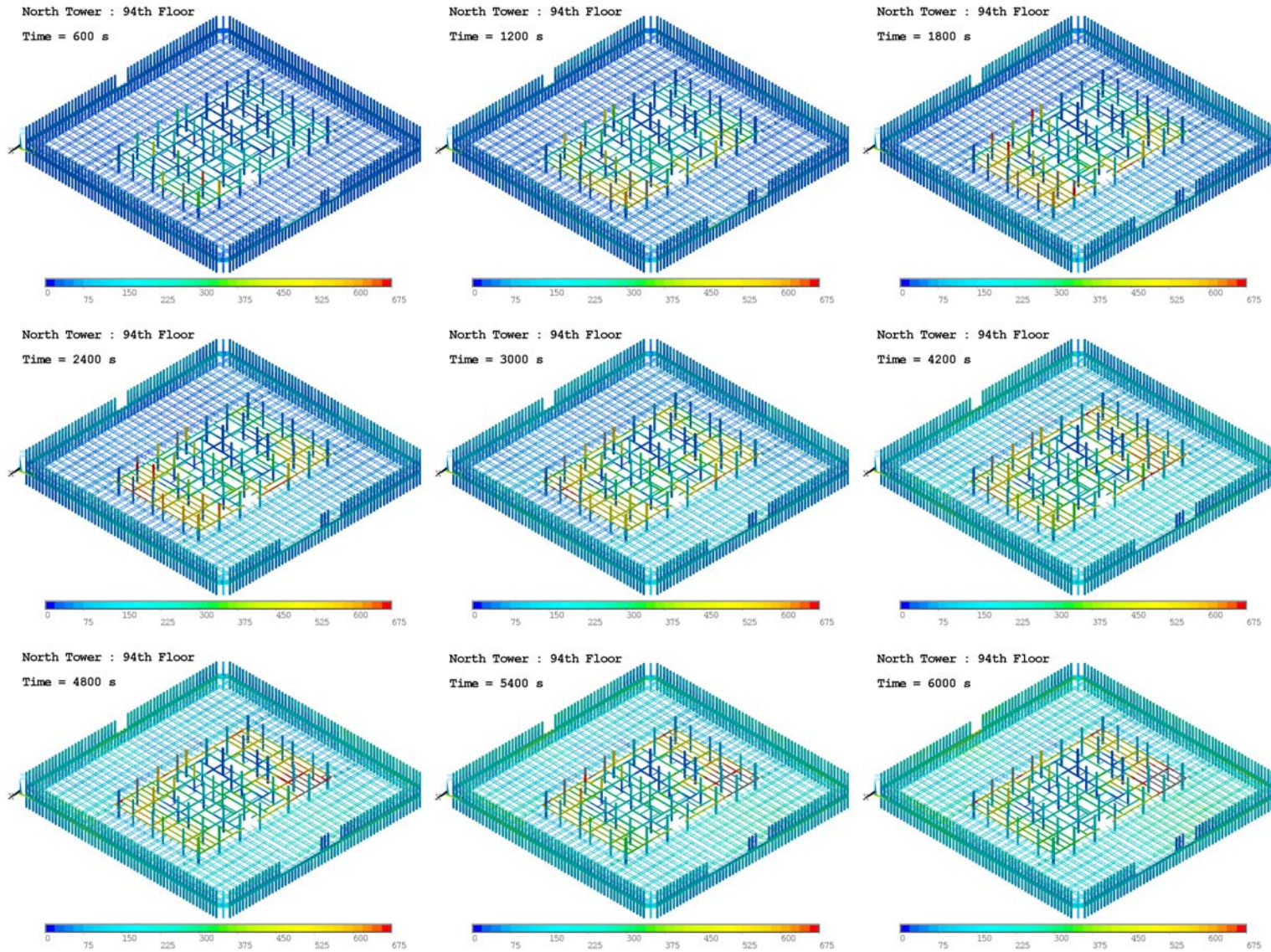


Figure 6-34. Thermal response of floor 94 of WTC 1, Case B.

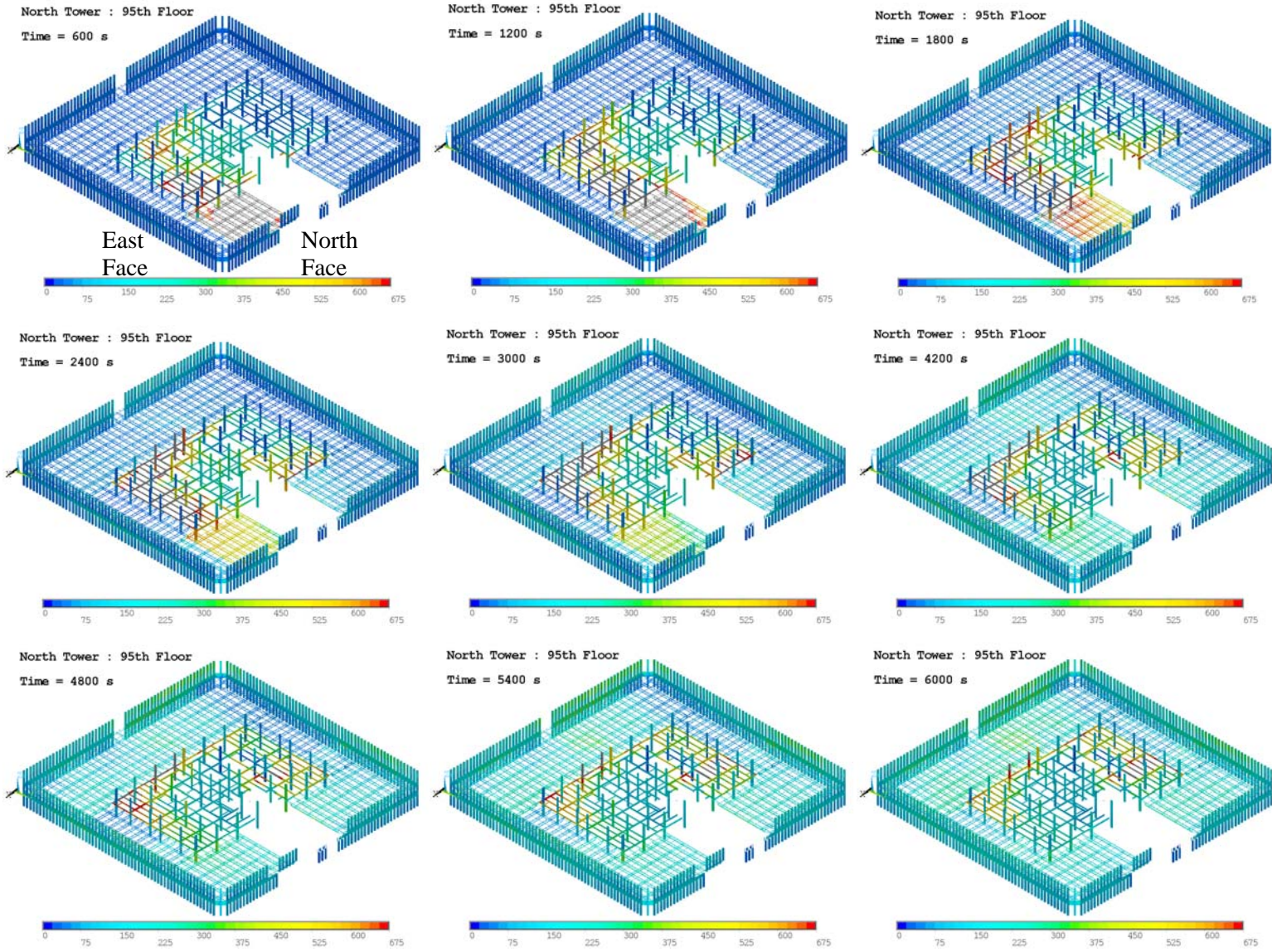


Figure 6–35. Thermal response of floor 95 of WTC 1, Case A.

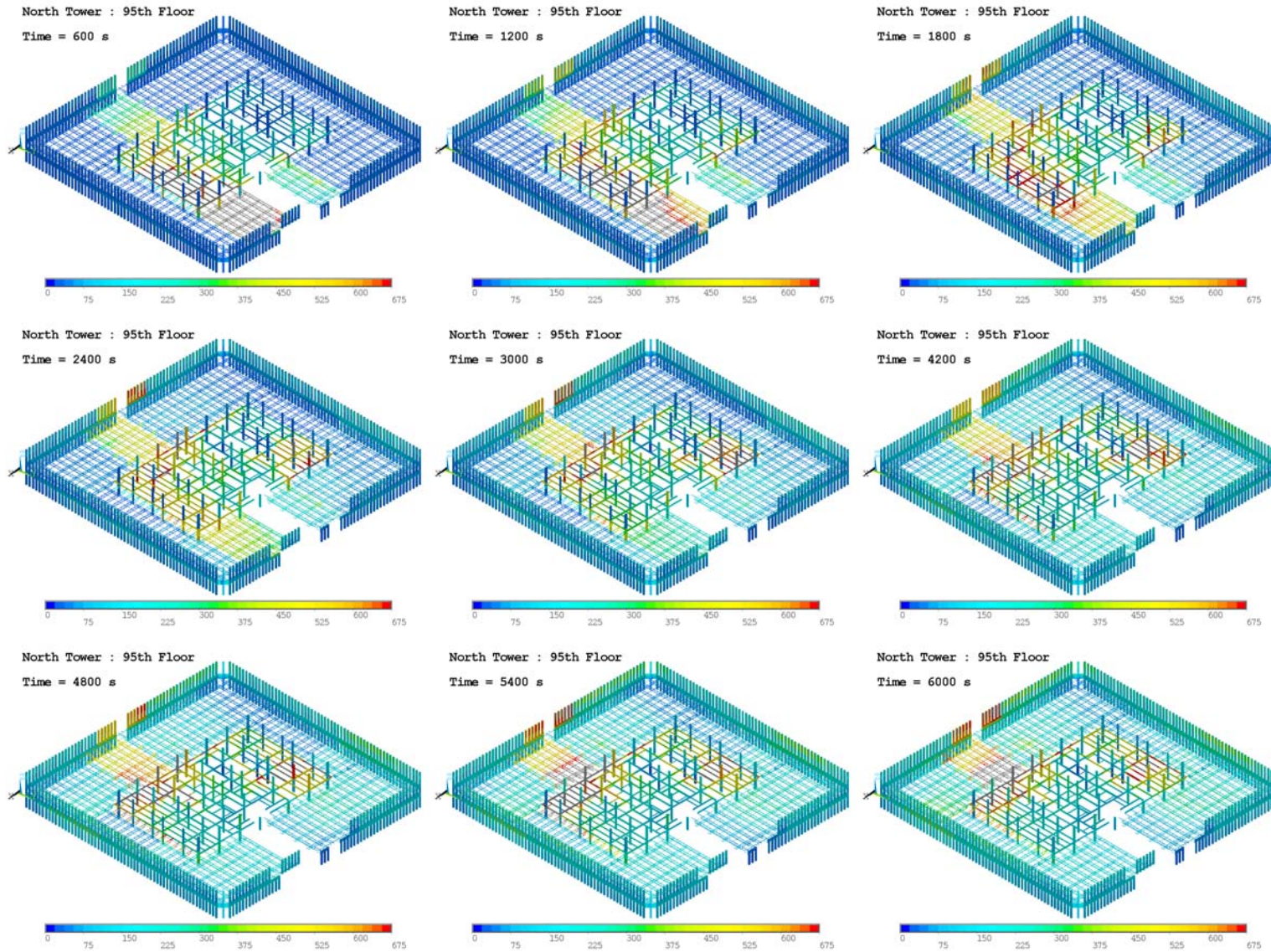


Figure 6-36. Thermal response of floor 95 of WTC 1, Case B.

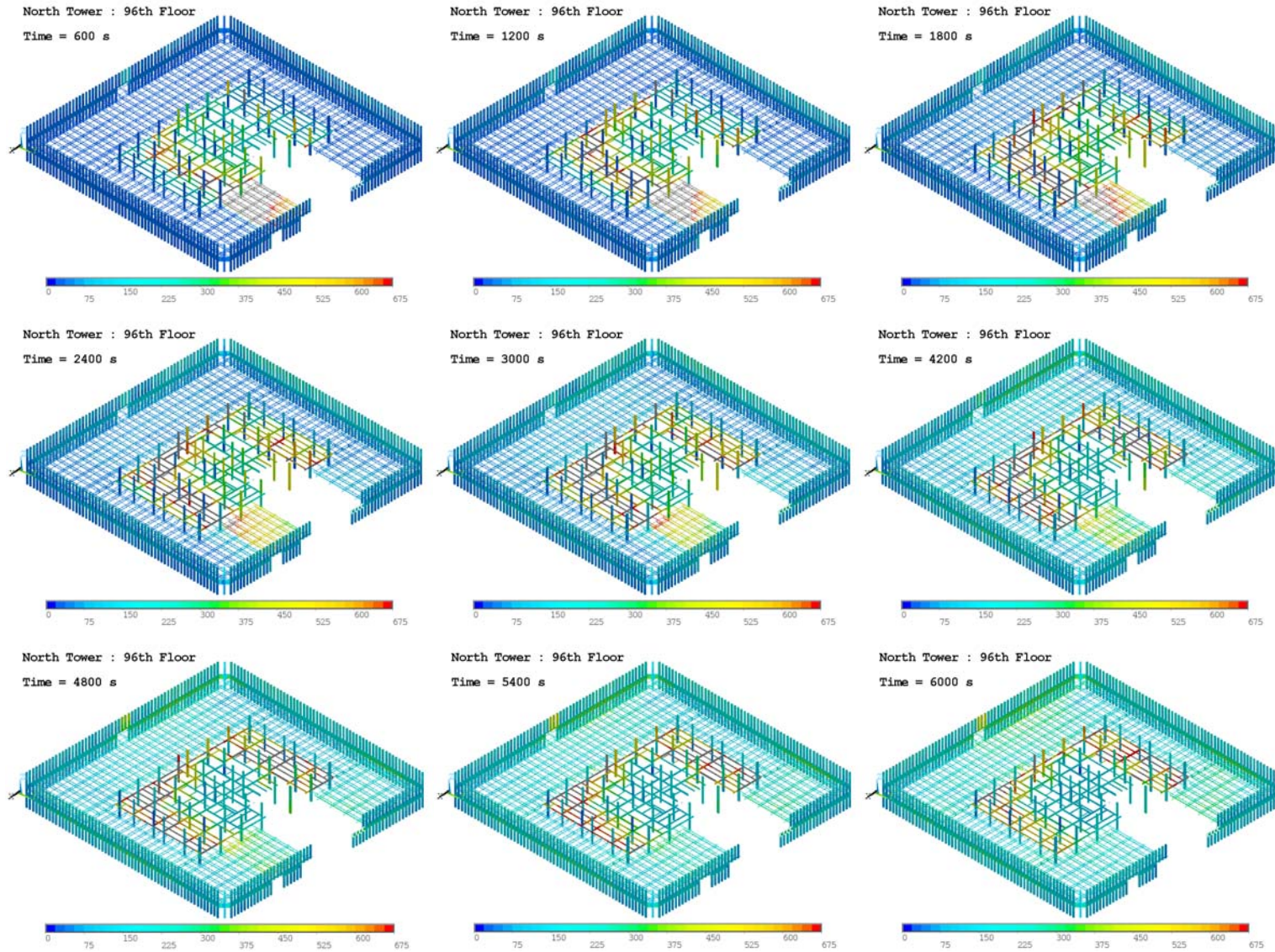


Figure 6–37. Thermal response of floor 96 of WTC 1, Case A.

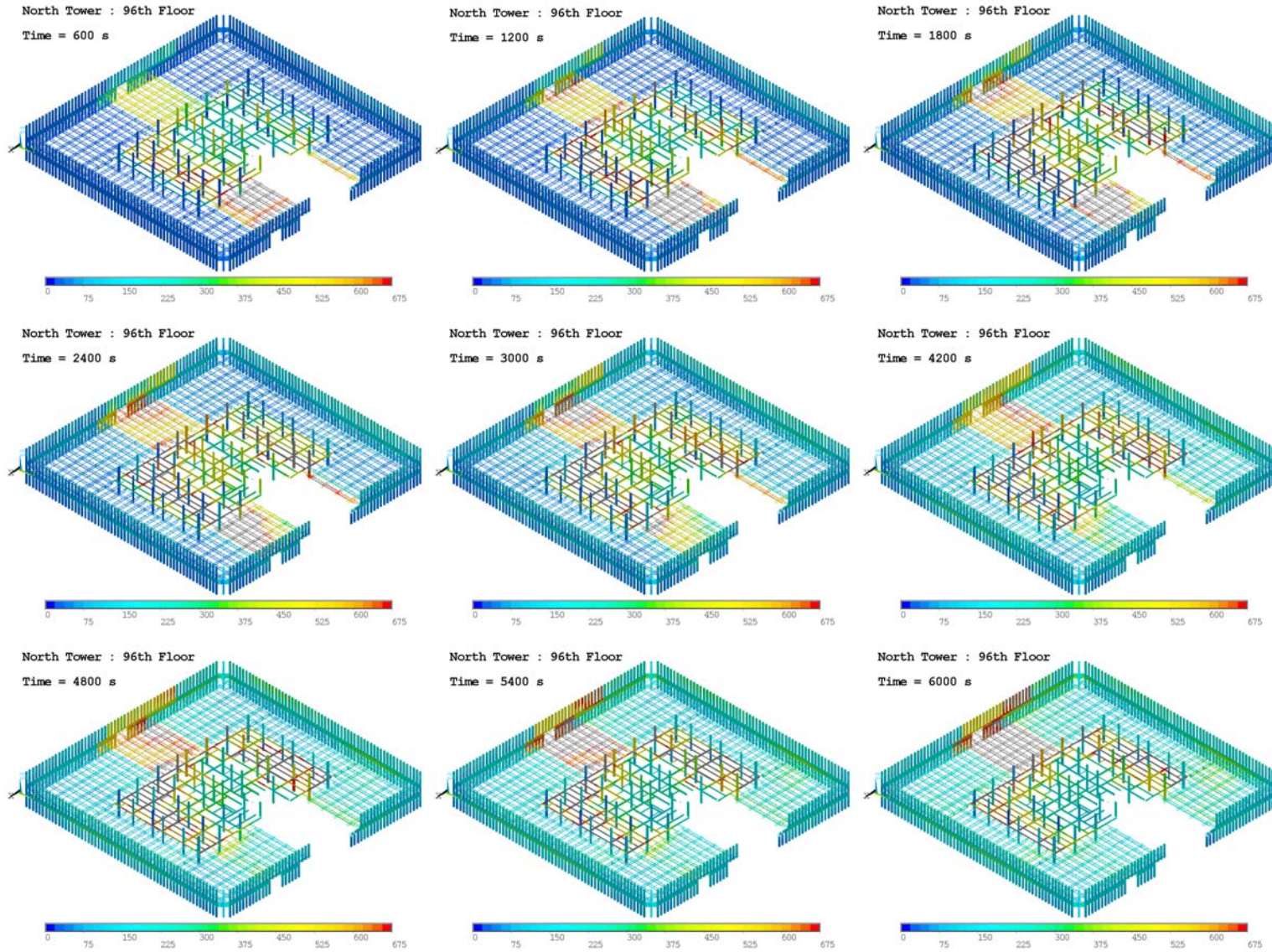


Figure 6-38. Thermal response of floor 96 of WTC 1, Case B.

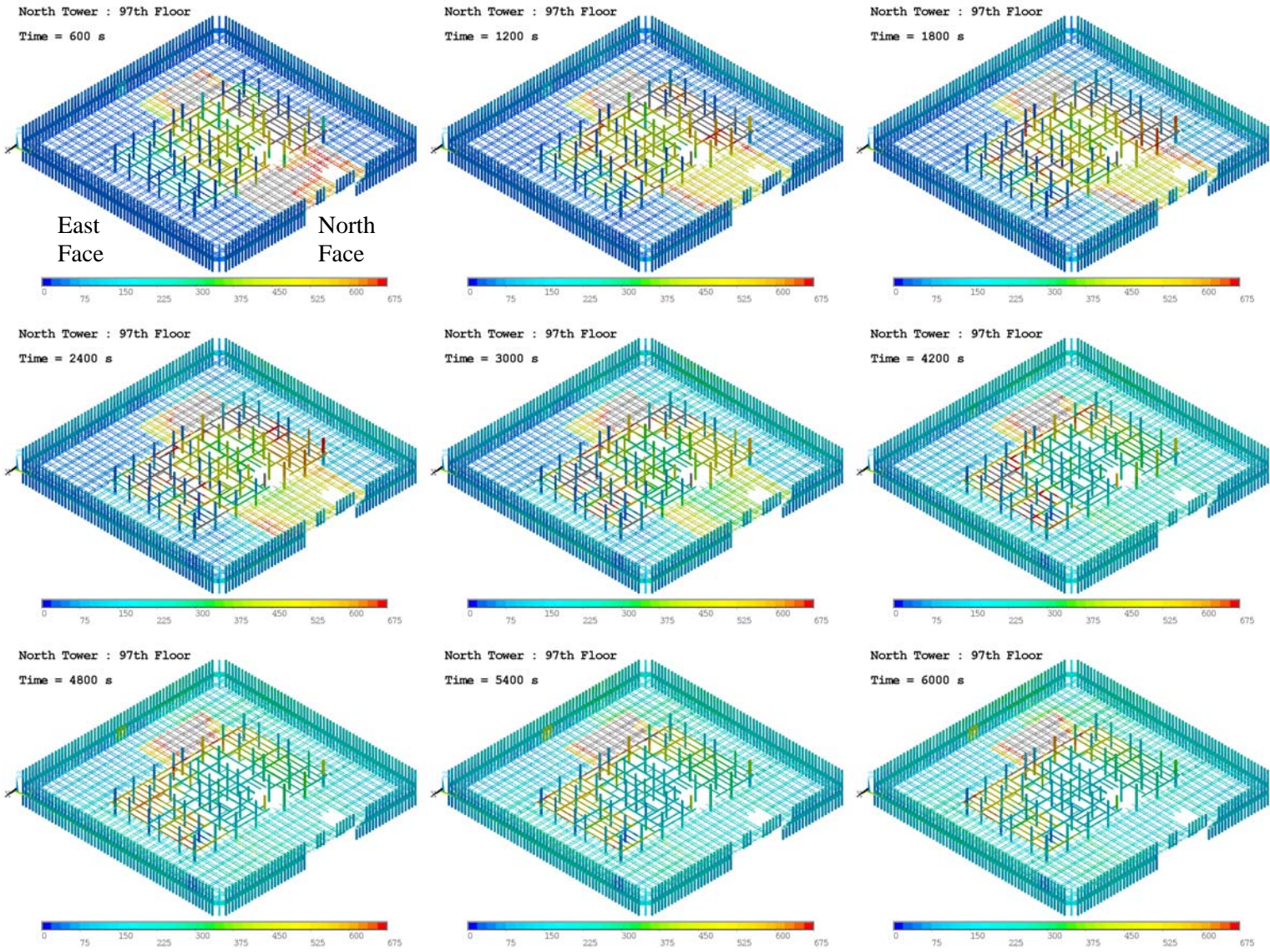


Figure 6-39. Thermal response of floor 97 of WTC 1, Case A.

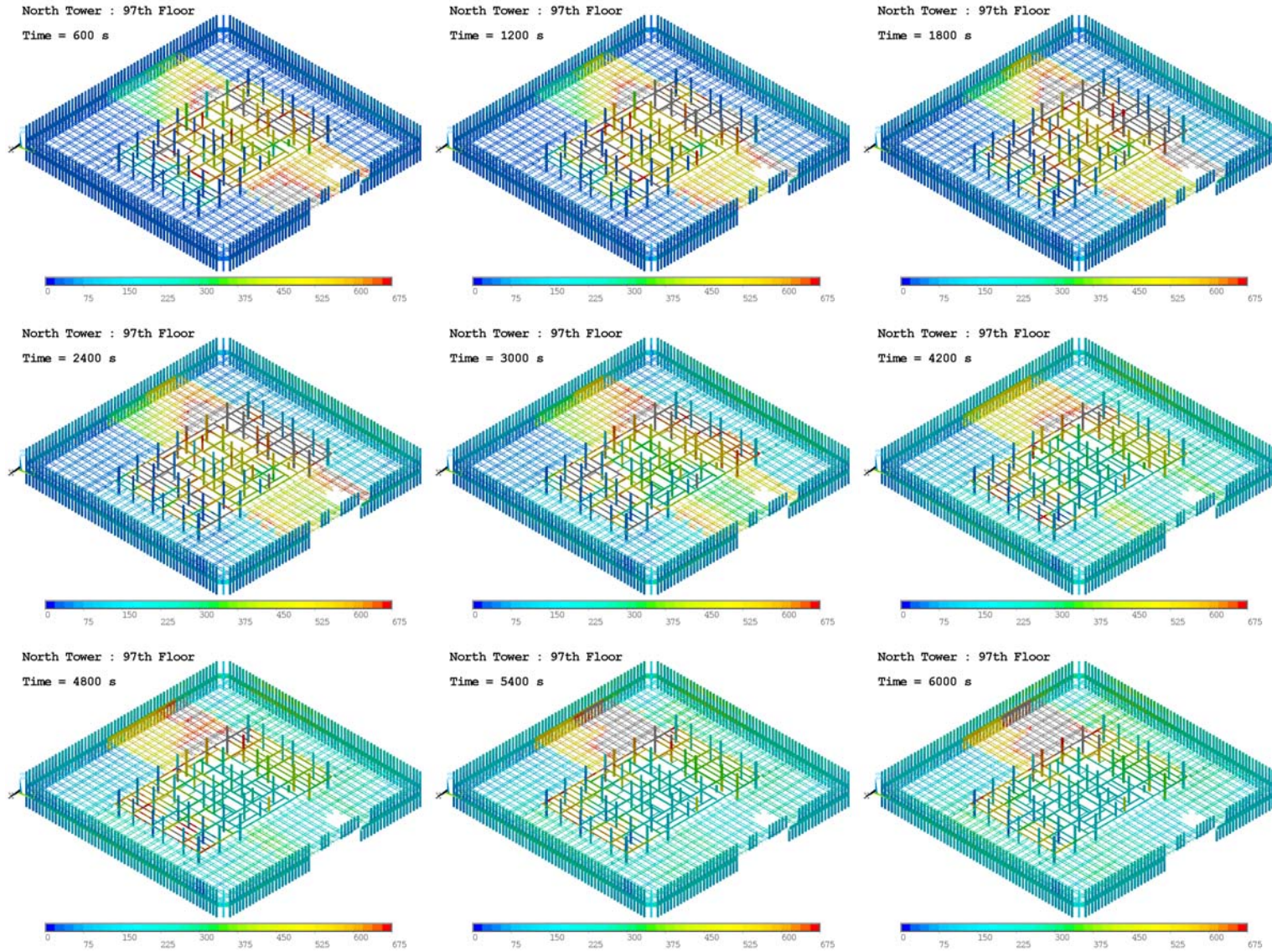


Figure 6-40. Thermal response of floor 97 of WTC 1, Case B.

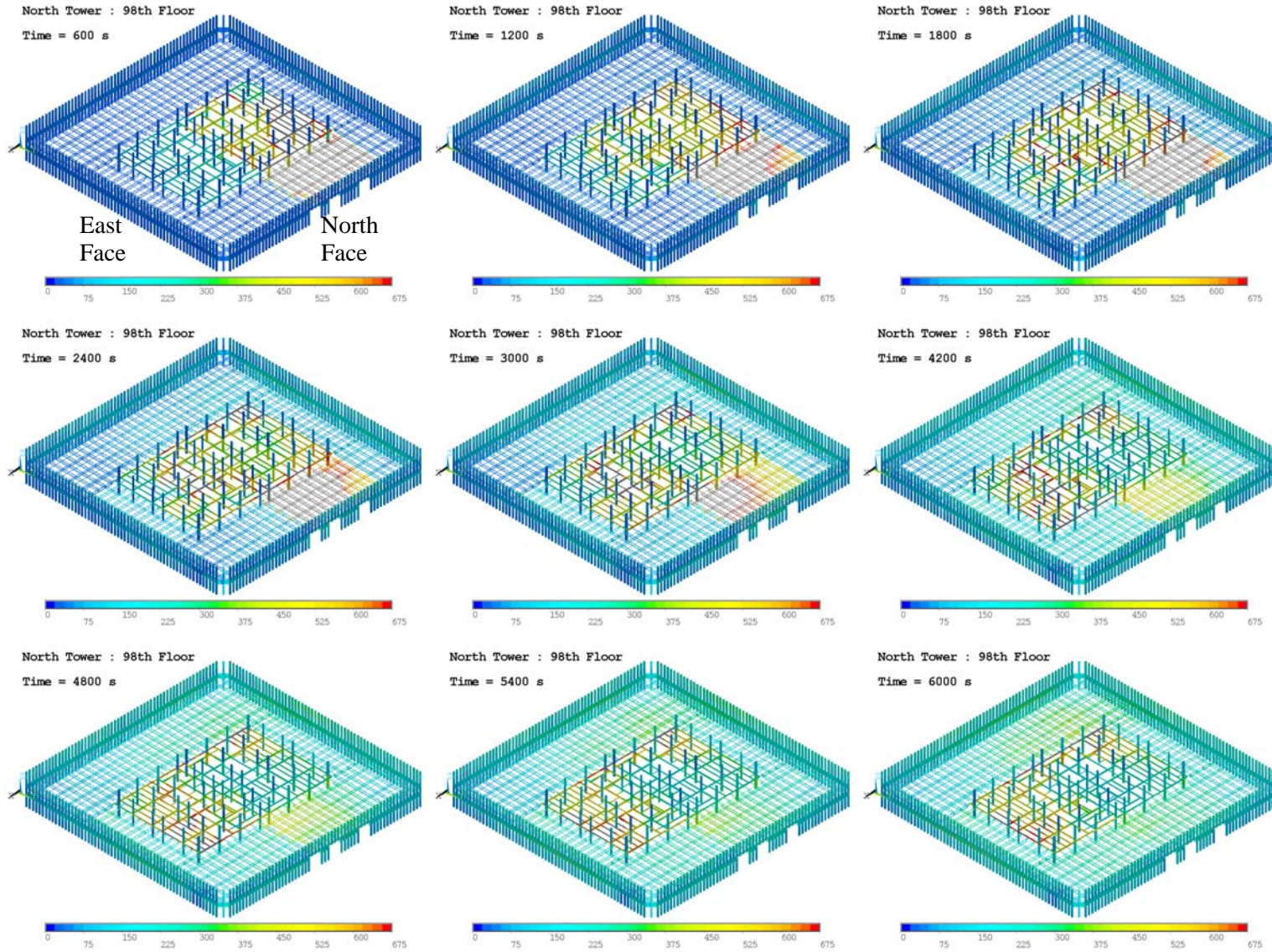


Figure 6-41. Thermal response of floor 98 of WTC 1, Case A.

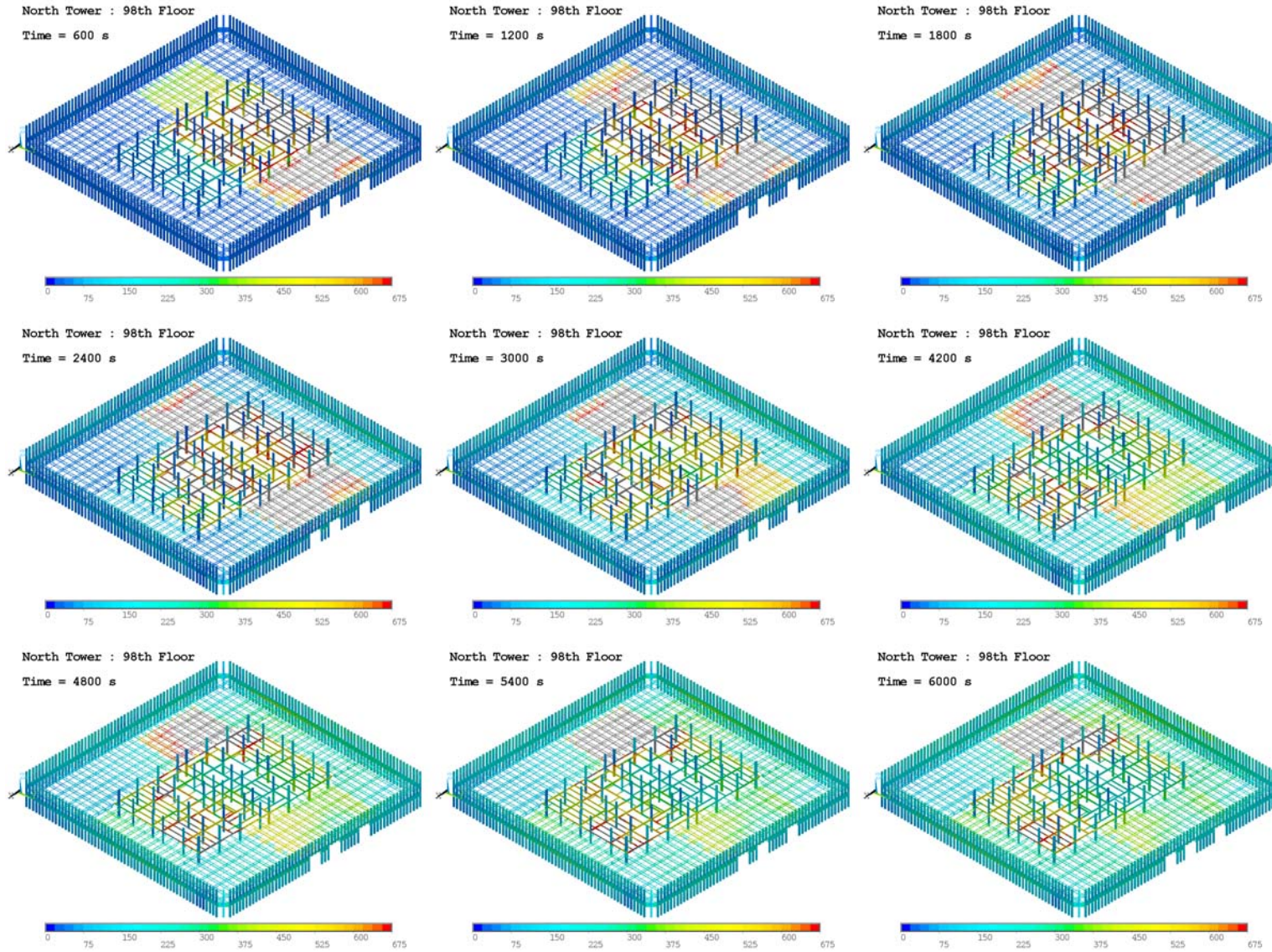


Figure 6-42. Thermal response of floor 98 of WTC 1, Case B.

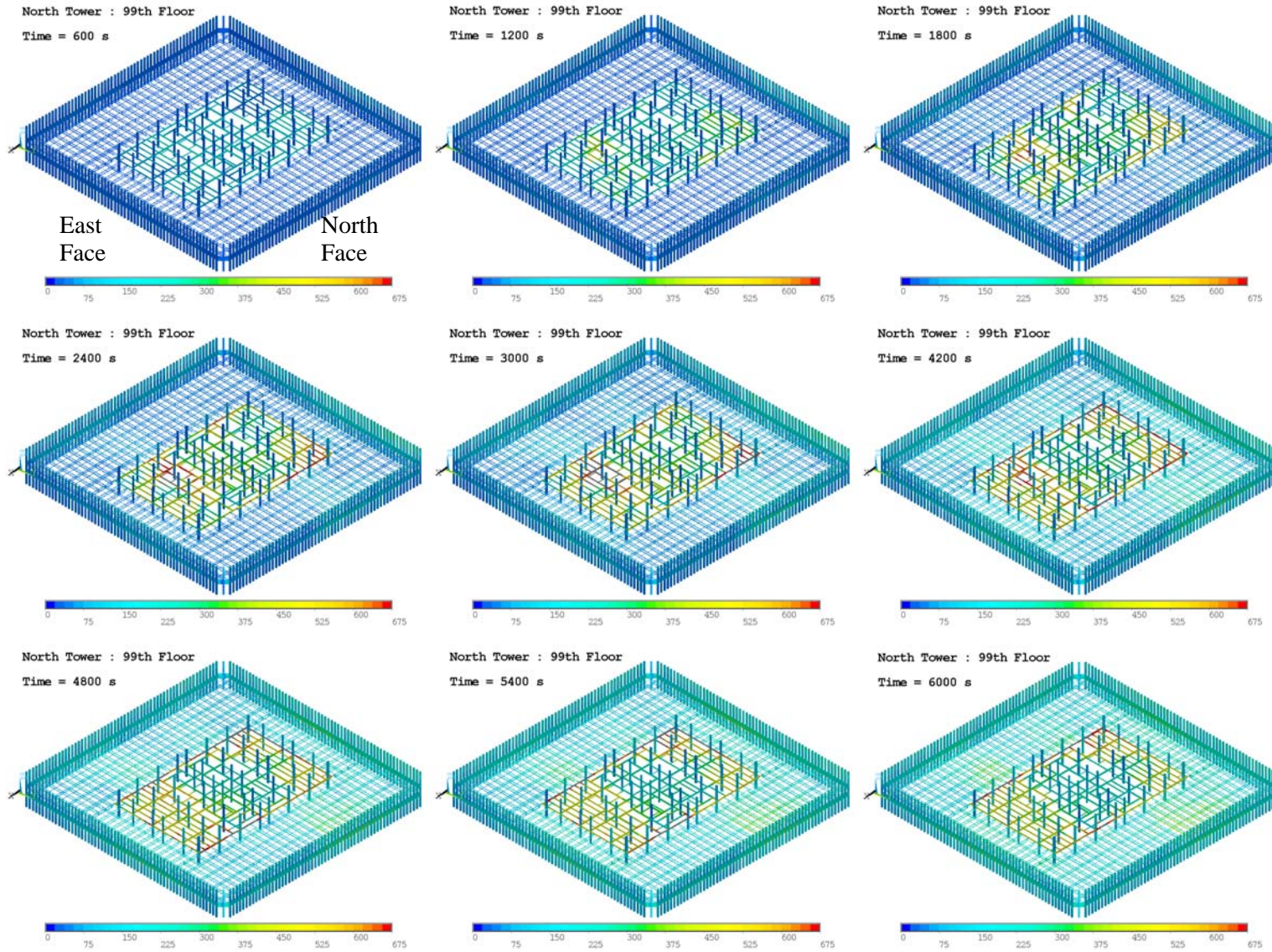


Figure 6-43. Thermal response of floor 99 of WTC 1, Case A.

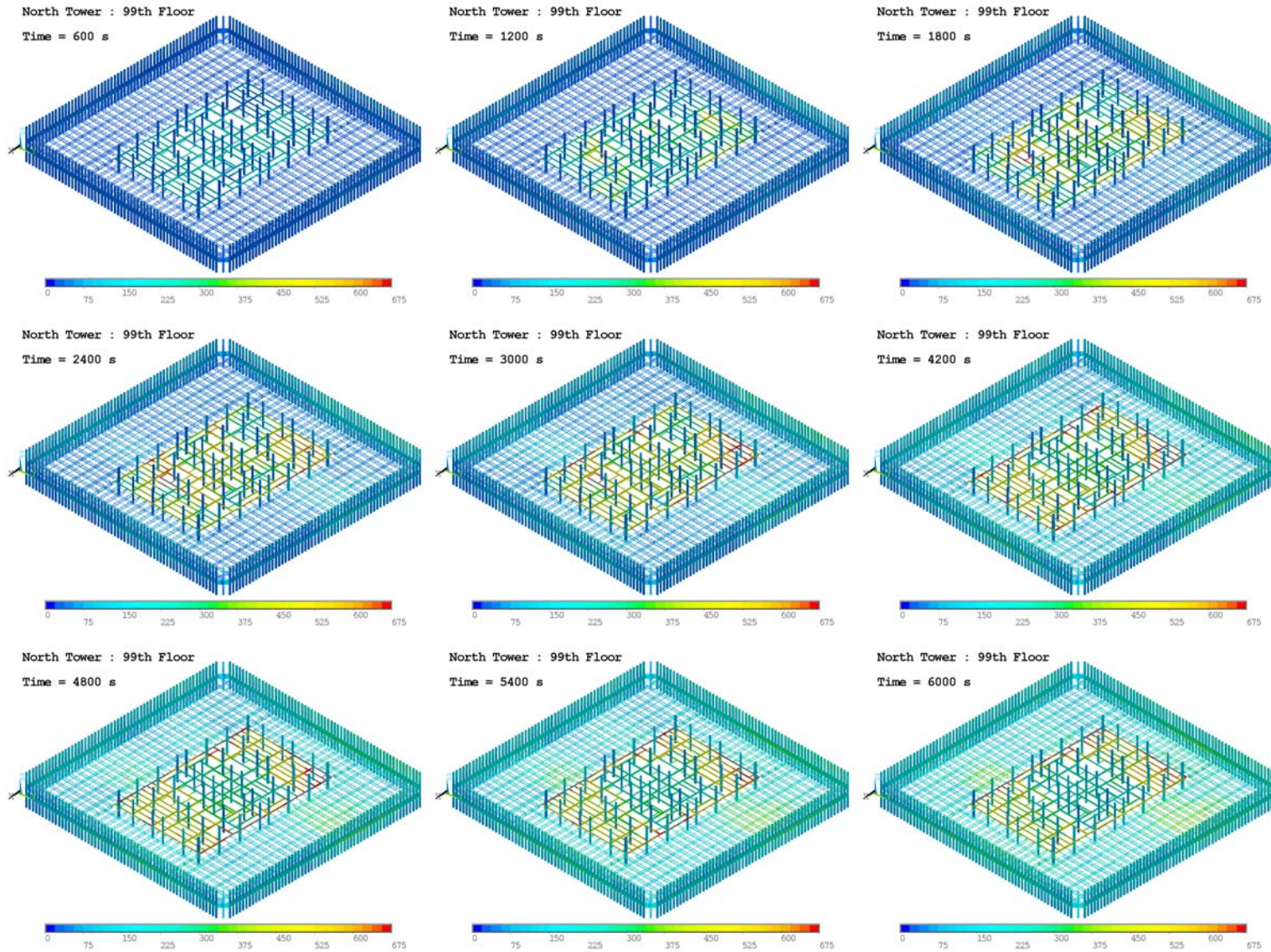


Figure 6-44. Thermal response of floor 99 of WTC 1, Case B.

6.10.1 Floor 93

There was no structural or insulation damage to the trusses, core beams, or perimeter columns on floor 92 or floor 93. Columns 504 and 605 were damaged structurally on floors 92 and 93, while column 705 was damaged on floor 93 only. There was no insulation damage to the core columns on these floors.

Since there was no insulation damage, the trusses and columns on floor 93 stayed relatively cool. The trusses had a mean insulation thickness of 2.2 in., which resulted in gradual heating of the entire floor system. The core beams were covered with 0.5 in. of insulation and, as a result, heated faster. This is illustrated by significant heating of the core beams at 1,800 s after impact. As the fire spread toward the south face of the North Tower, the core beams gradually cooled and showed relatively lower temperatures at 6,000 s after impact.

6.10.2 Floor 94

Figure 6–45 shows the structural and insulation damage to floor 94.¹

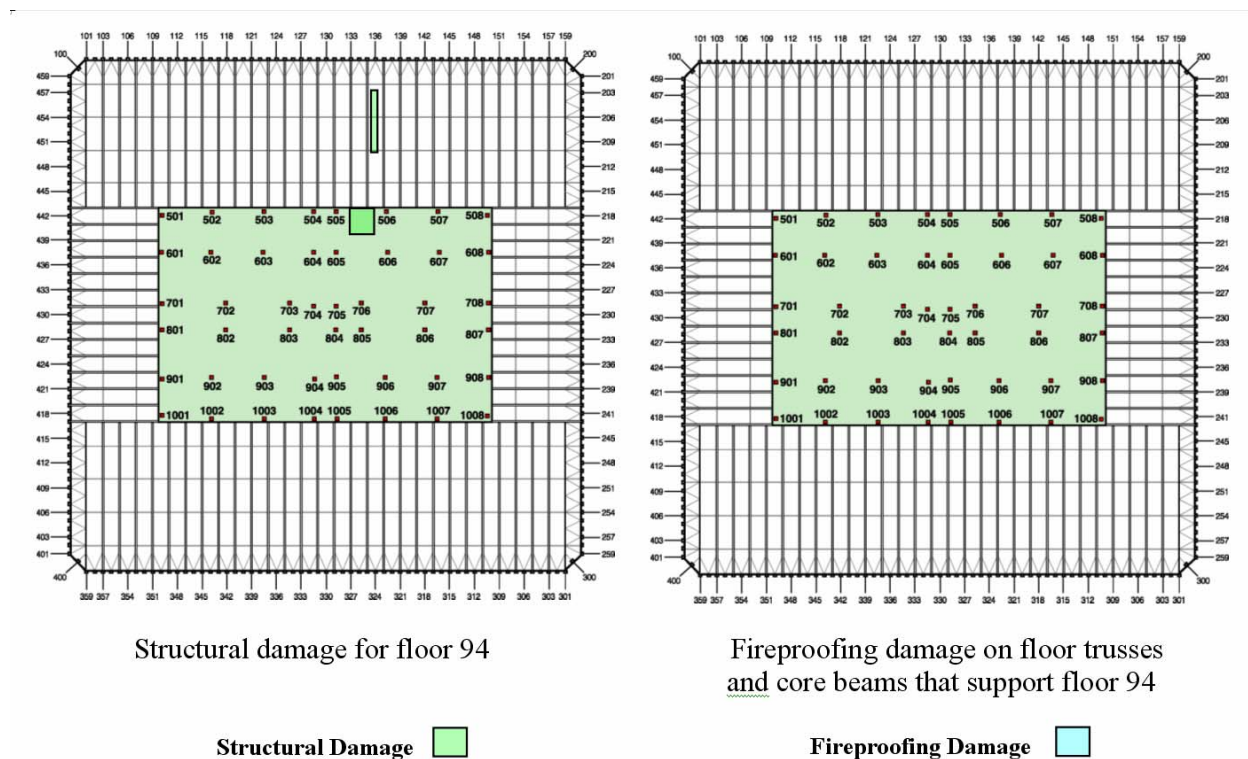


Figure 6–45. Structural and insulation damage to floor 94 of WTC 1, Case A.

The trusses supporting the slab on the 94th floor, with their insulation intact, stayed relatively cool, heating no more than 150 °C during the course of the simulation. The thinly insulated core beams were covered with 0.5 in. insulation and as a result, the core beams were heated significantly at 1,800 s and

¹ The damage graphics used in the thermal analysis are discussed in detail in NIST NCSTAR 1-6 and have been presented here for reference only.

2,400 s after impact and then began cooling. The core beams on the west face were heated by the fires on the 93rd floor below.

The thermal response of the perimeter and core columns was highly dependent on the state of the fireproofing and to a lesser extent on the fire growth and spread pattern. Since there was no insulation damage for the perimeter columns on the 93rd or the 94th floor, the temperature increases were moderate, reaching no higher than 200 °C to 300 °C.

The core columns exhibited a vast variation in steel temperature. Columns 501, 601, 701, 801, 901, and 1001 had intact insulation and stayed relatively cool in spite of fire activity in this region. Column 607 had intact insulation, but was relatively light in weight. It responded relatively quickly to an evolving fire in the vicinity, showing a very high temperature at 600 s after impact, cooling near 1,200 s after impact, and then increasing again at 3,000 s.

The core columns that had lost their insulation heated differently depending on their mass and fire exposure. Columns 1004, 1005, and 1006 reached the 500 °C to 600 °C range at 1,800 s and remained hot until the end of the simulation.

6.10.3 Floor 95

Figure 6–46 shows the structural and insulation damage to floor 95.

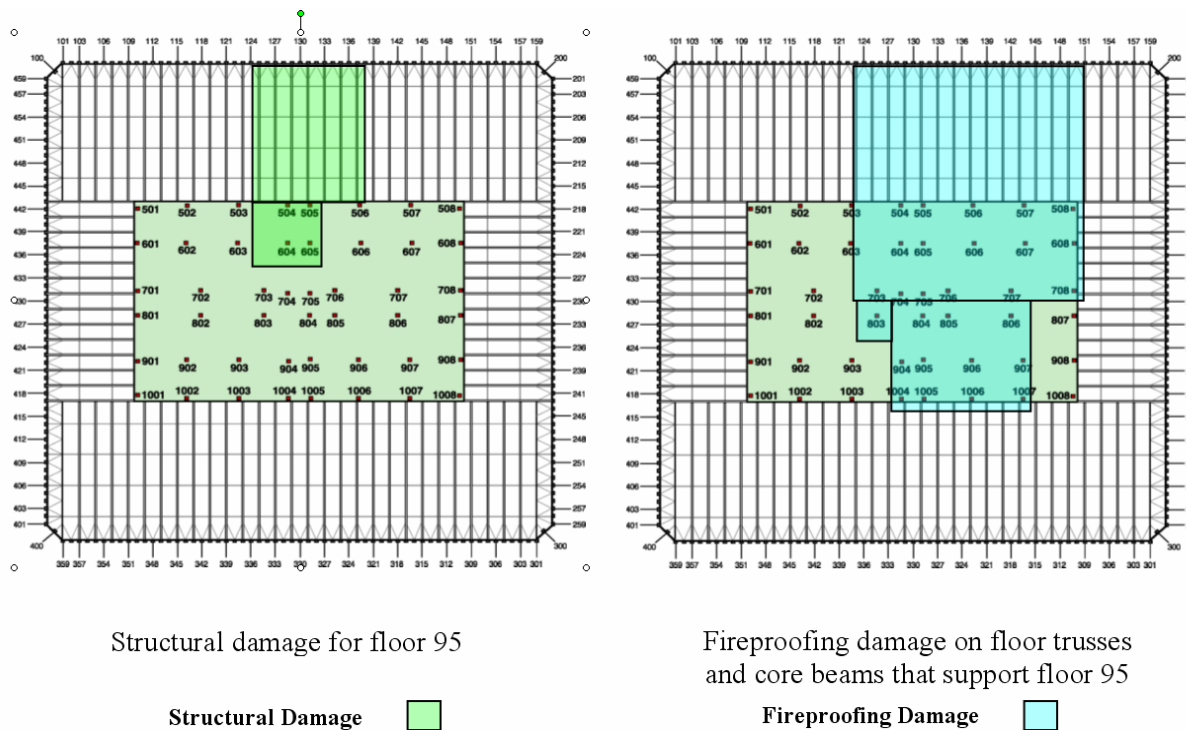


Figure 6–46. Structural and insulation damage to floor 95 of WTC 1, Case A.

There was extensive insulation damage to the trusses that supported the slab on the 95th floor, and those in the northeast heated rapidly. They cooled gradually as the fire moved southward.

The thermal response of the perimeter and core columns was highly dependent on the state of the insulation and to a lesser extent on fire growth and spread pattern. The west side core columns stayed cool, since their insulation was intact, while some of the core columns to the east and center showed rapid increase in temperature.

6.10.4 Floor 96

Figure 6–47 shows the structural and insulation damage to floor 96.

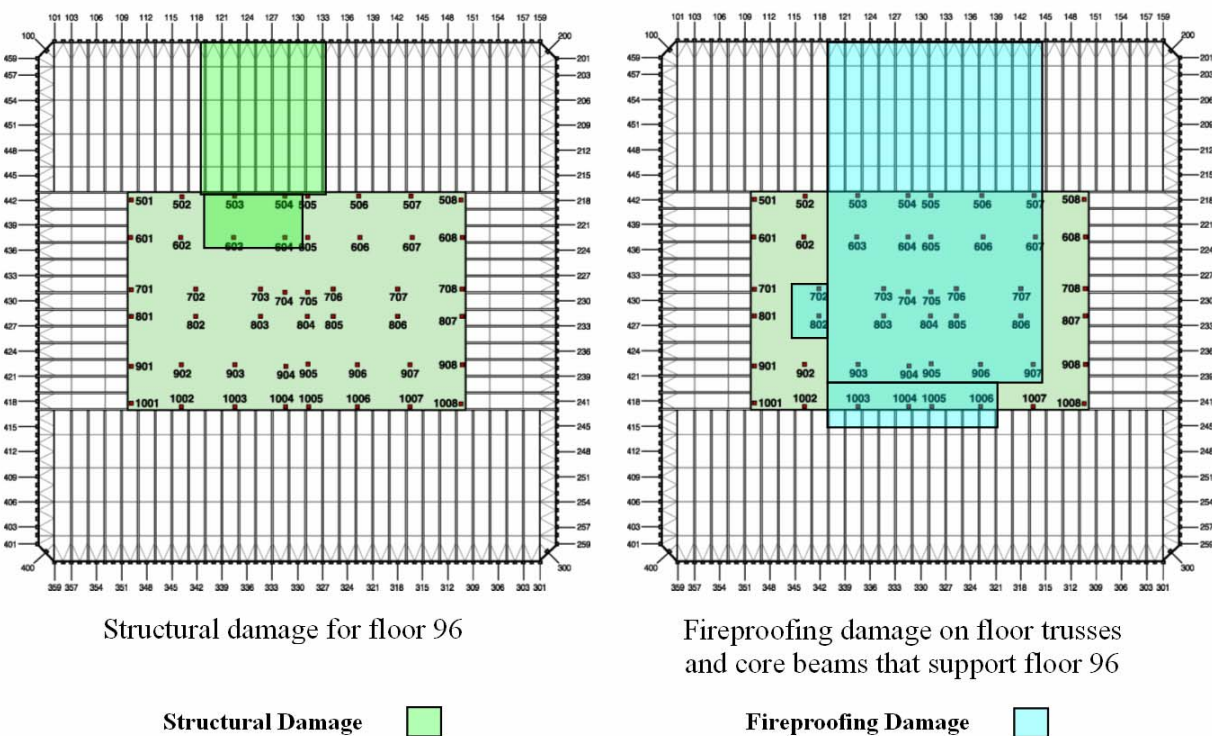


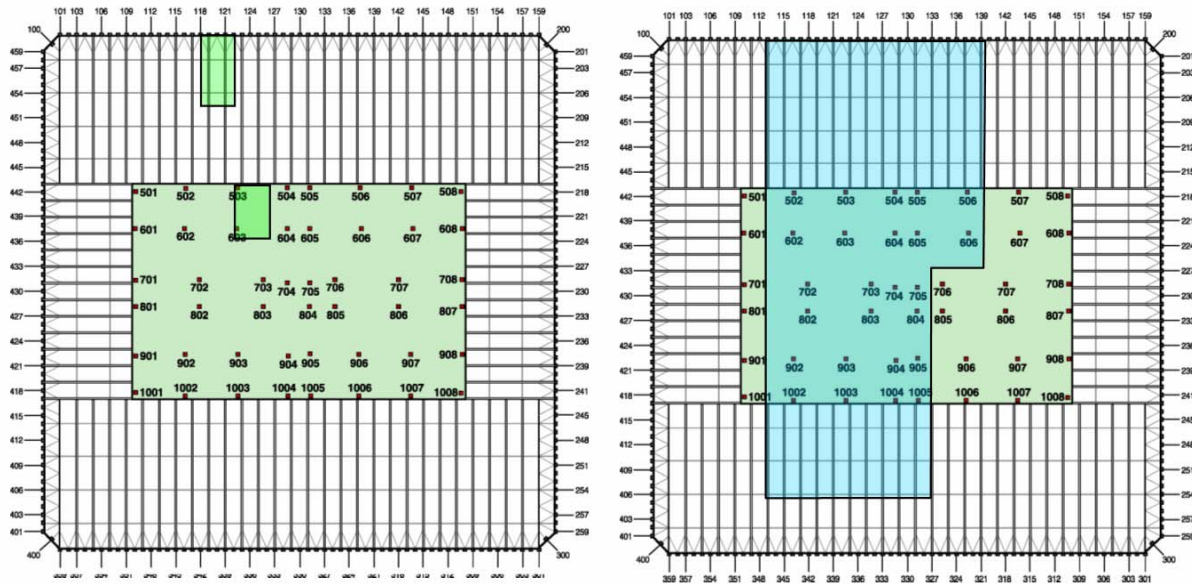
Figure 6–47. Structural and insulation damage to floor 96 of WTC 1, Case A.

The insulation-damaged trusses on the north face heated rapidly in the first 30 min after impact. They then cooled as the fire moved to the south. The fully insulated trusses at the west face only reached peak temperatures of approximately 150 °C.

The insulated perimeter columns on floor 95 heated only moderately. The insulated west side core columns stayed cool. The center core columns showed significant heating on the 96th floor because of lack of insulation, yet were relatively cool on the 95th floor where the insulation was intact.

6.10.5 Floor 97

Figure 6–48 shows the structural and insulation damage to floor 97.



Structural damage for floor 97

Structural Damage ■

Fireproofing damage on floor trusses and core beams that support floor 97

Fireproofing Damage ■**Figure 6–48. Structural and insulation damage to floor 97 of WTC 1, Case A.**

The west side of the core on floor 97 suffered extensive insulation damage, and this resulted in heating up of the core columns. Core columns on the east side of the core have their insulation intact and as a result stay relatively cool.

6.10.6 Floor 98

Figure 6–49 shows the structural and insulation damage to floor 98.

For the core columns, we observe higher temperatures on the west side, because of insulation damage and fire activity in this region. Some core columns indicated very high temperature below the concrete slab and relatively low temperatures above the slab. This was due to differences in insulation status and fire activity in the immediate vicinity of these columns on floors 97 and 98.

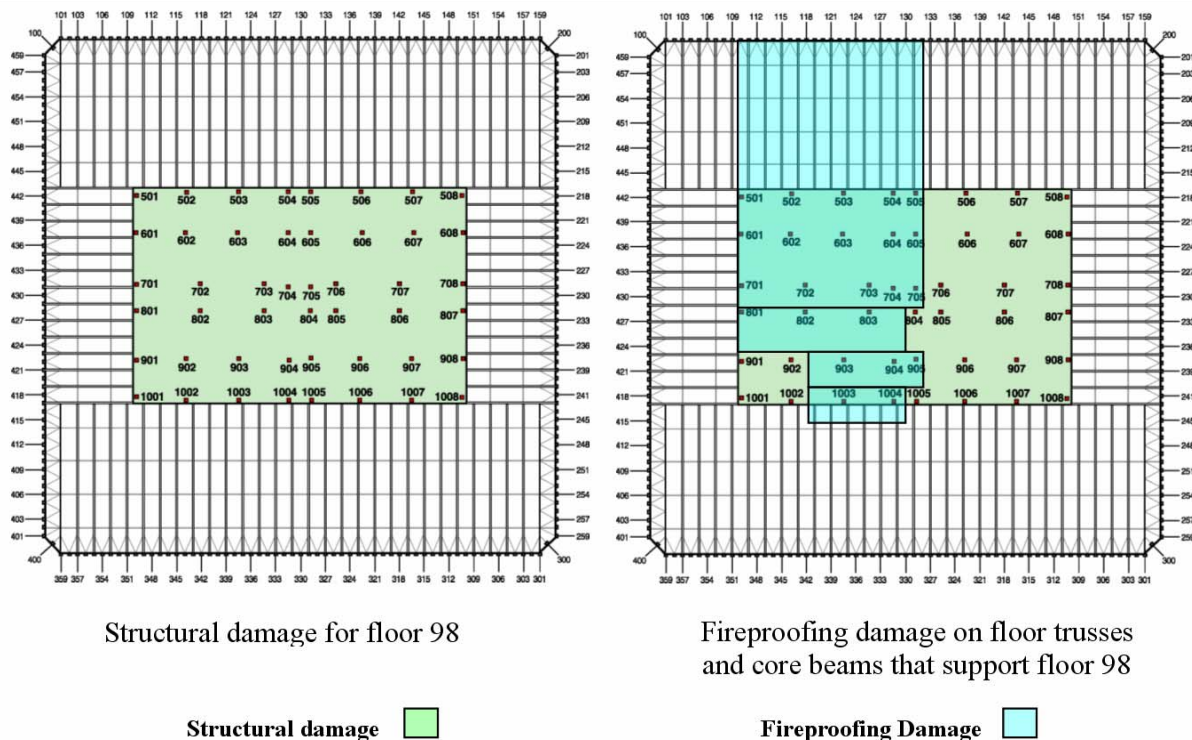


Figure 6–49. Structural and insulation damage to floor 98 of WTC 1, Case A.

6.10.7 Floor 99

There was no structural or insulation damage to the trusses, core beams, perimeter columns, or core columns. As a result, the structural temperature rises were modest.

6.11 GLOBAL THERMAL RESPONSE OF WTC 1, CASE B

As noted in Section 6.4, there was relatively little difference between the results of the two fire simulations. Thus, significant differences in the FSI output were generally due to changes in the damage patterns.

6.11.1 Floor 93

Neither case showed insulation or structural damage for floor systems due to aircraft impact. The truss system that supported floor 93 showed slightly higher temperatures for Case A compared to Case B. Core beams in the northwest corner showed higher temperatures for Case B at 100 min after impact, while in Case A, the core beams had cooled by the end of the simulation.

6.11.2 Floor 94

Core columns 1005 to 1007 in Case B showed higher temperatures compared to Case A at 20 min to 30 min after impact. The core columns on the east side indicated higher temperatures for Case B. The

thermal state of the perimeter columns and floor trusses was not significantly different. The core beams exhibited slightly higher temperatures in Case B compared to Case A at 100 min after impact.

6.11.3 Floor 95

The structural damage on the truss elements that supported floor 95 shifted toward the east face for Case B. The insulation damage on the trusses extended south of the core, which resulted in higher thermal loading on the floor trusses throughout the simulation. The perimeter columns in the south face showed higher temperatures for Case B due to more extensive insulation damage. A larger fraction of the core columns in Case B exhibited higher temperatures compared to Case A. The peak temperatures in the two cases were not very different, but in Case B, a larger fraction of the structural elements were heated.

6.11.4 Floor 96

There was more structural damage to core columns and a larger fraction of the core columns exhibited fire-induced heating. Case B showed higher temperatures on the trusses in the region south of the core. Insulation damage on the truss elements was more extensive for Case B. Truss elements south of the core reached 600 °C at 20 min after impact. Perimeter columns on the south face also exhibited higher temperatures due to more extensive insulation damage.

6.11.5 Floor 97, 98, and 99

Floor 97 showed differences similar to those on floor 96. The damage patterns were skewed towards the west face on floor 97. Extensive heating of the truss elements south of the core was observed for Case B. The core columns on the west face showed more heating in Case B compared to Case A. The differences between Case A and Case B for floor 98 were similar to those described for floors 96 and 97. Floor 99 in both cases stayed relatively cool during the entire simulation.

6.12 GLOBAL THERMAL RESPONSE OF WTC 2, CASE C

Figures 6–50 through Figure 6–59 depict the evolving temperatures on the columns and trusses. For ease of comparison, the equivalent drawings for Case D have been interspersed. The south face is in the upper left side of each drawing.

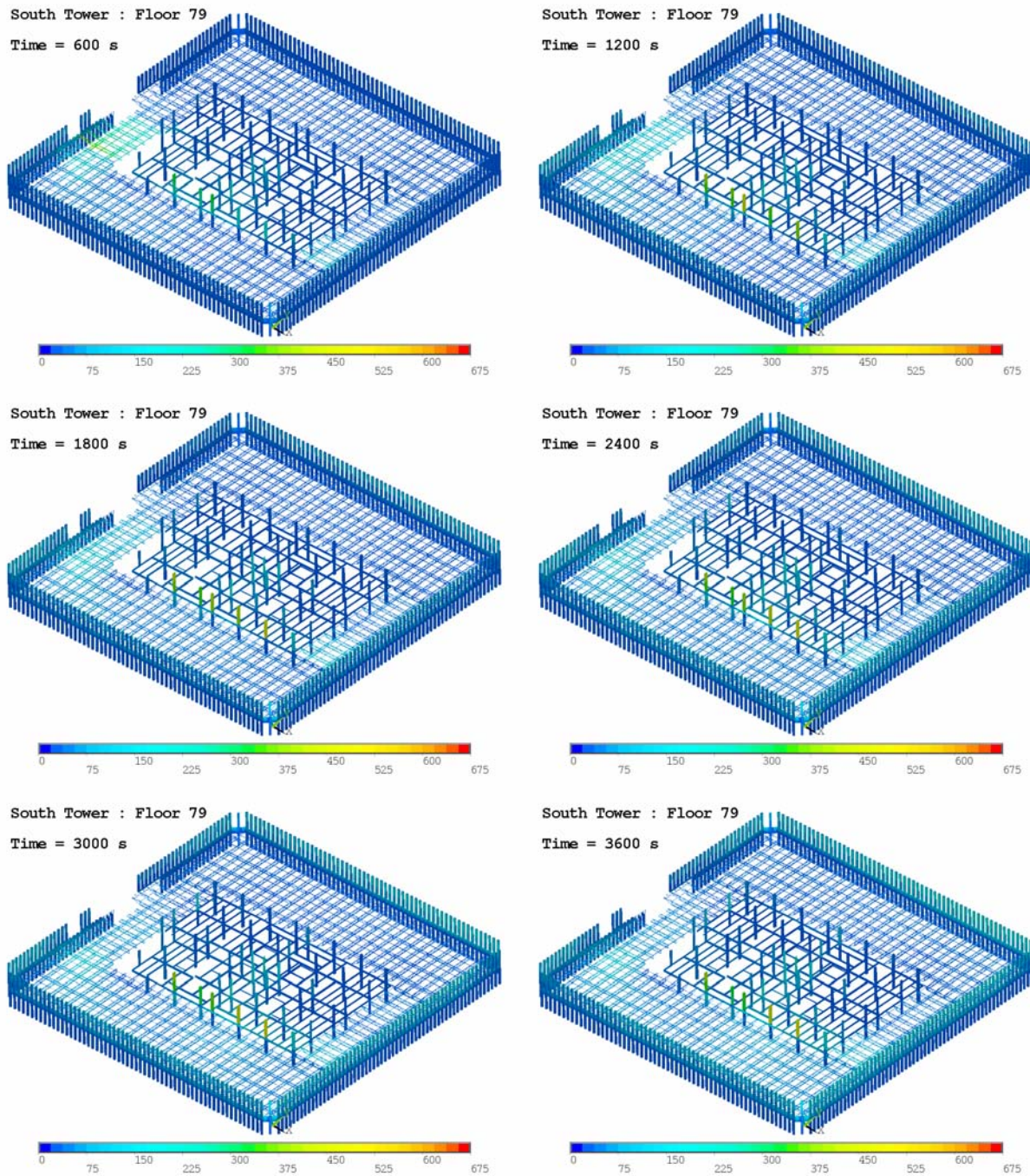


Figure 6-50. Thermal response of floor 79 of WTC 2, Case C.

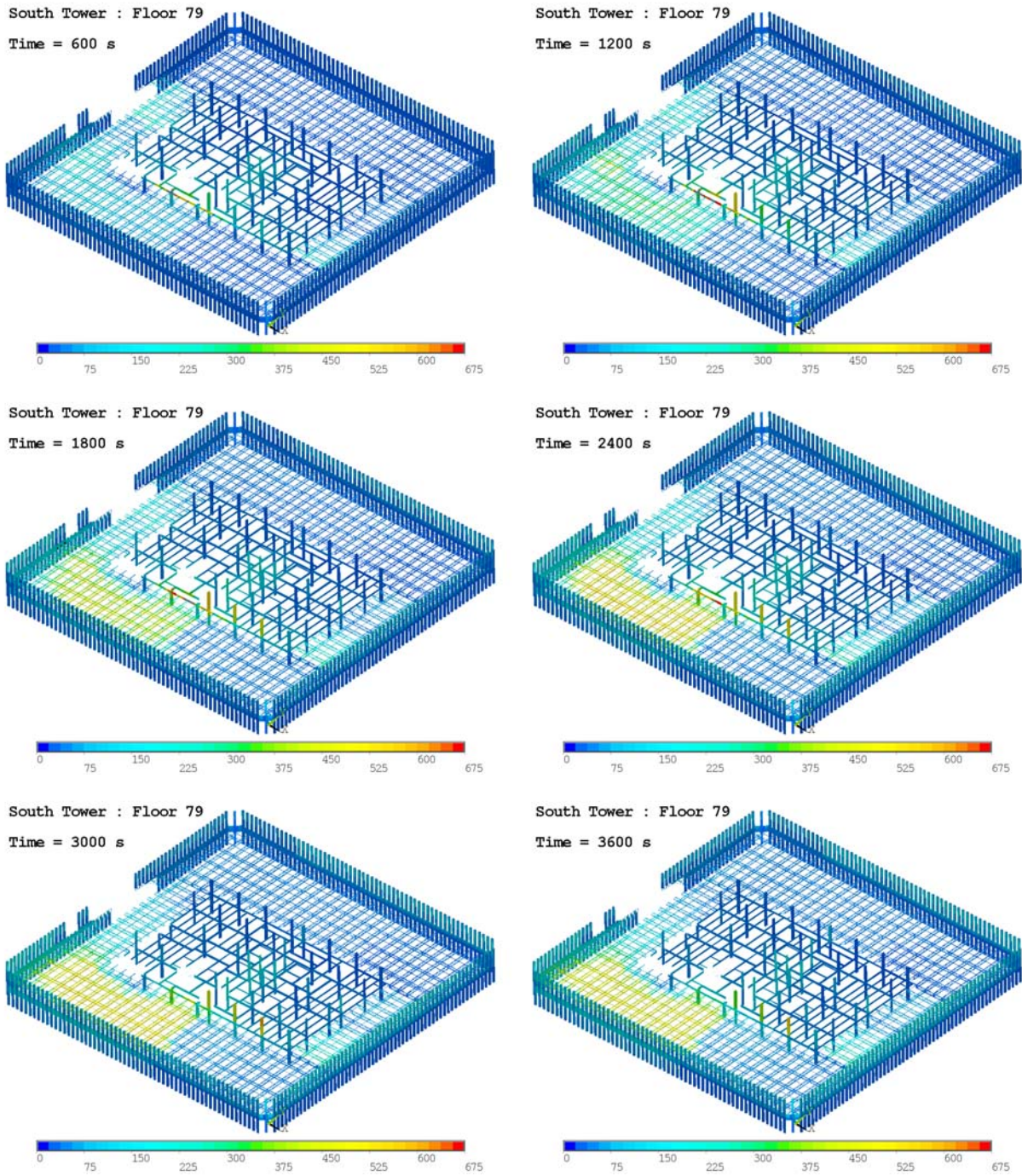


Figure 6-51. Thermal response of floor 79 of WTC 2, Case D.

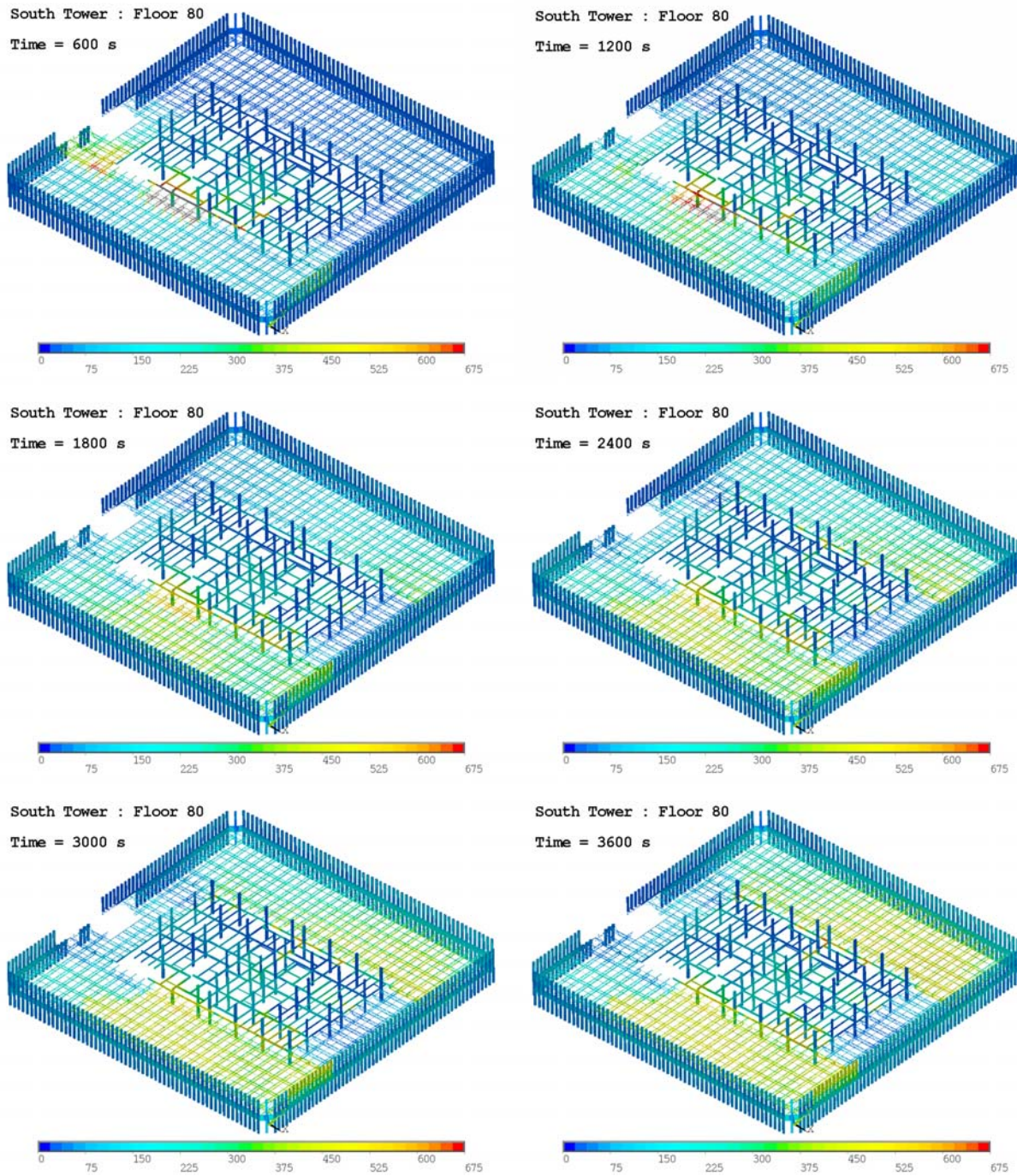


Figure 6-52. Thermal response of floor 80 of WTC 2, Case C.

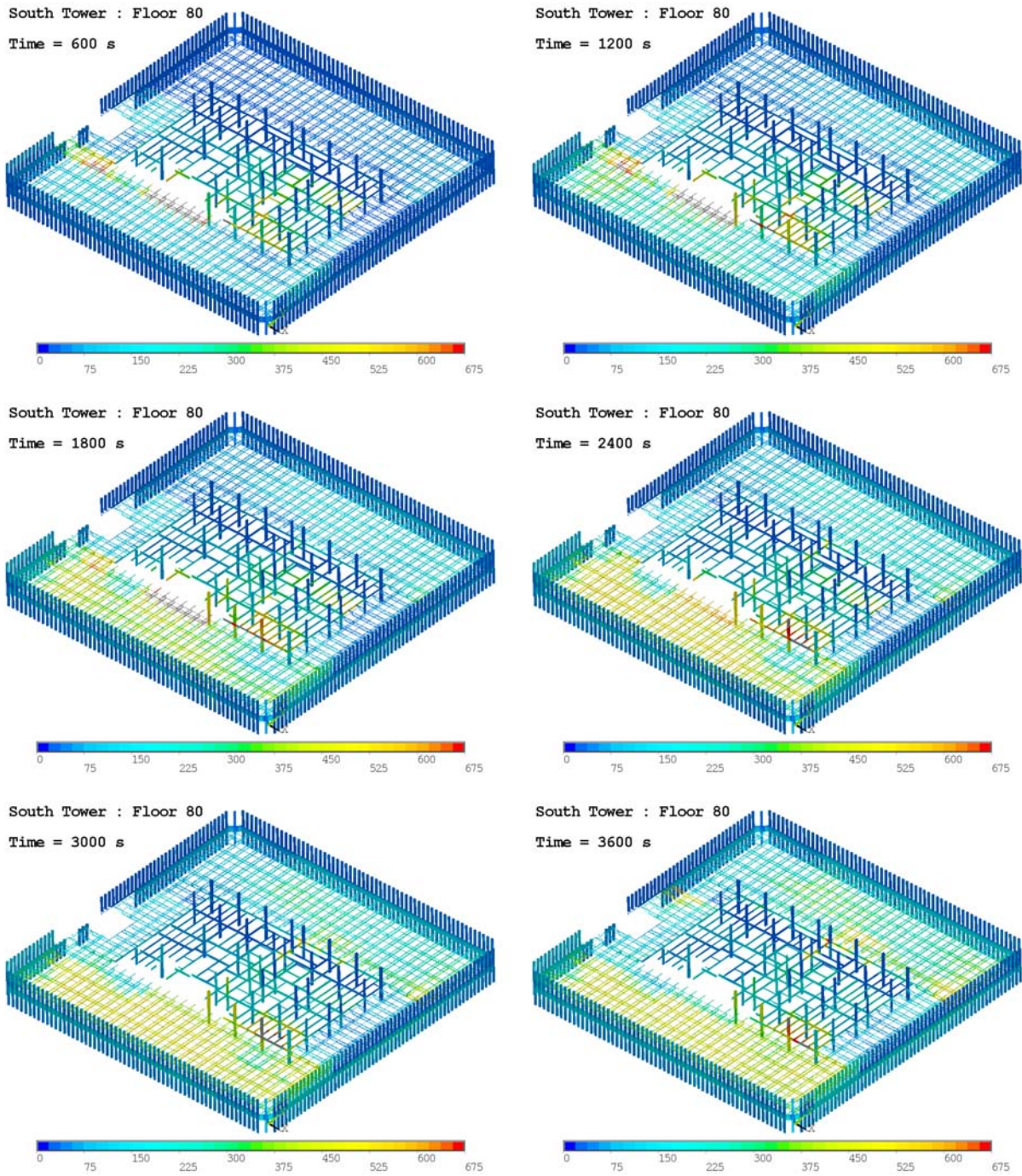


Figure 6-53. Thermal response of floor 80 of WTC 2, Case D.

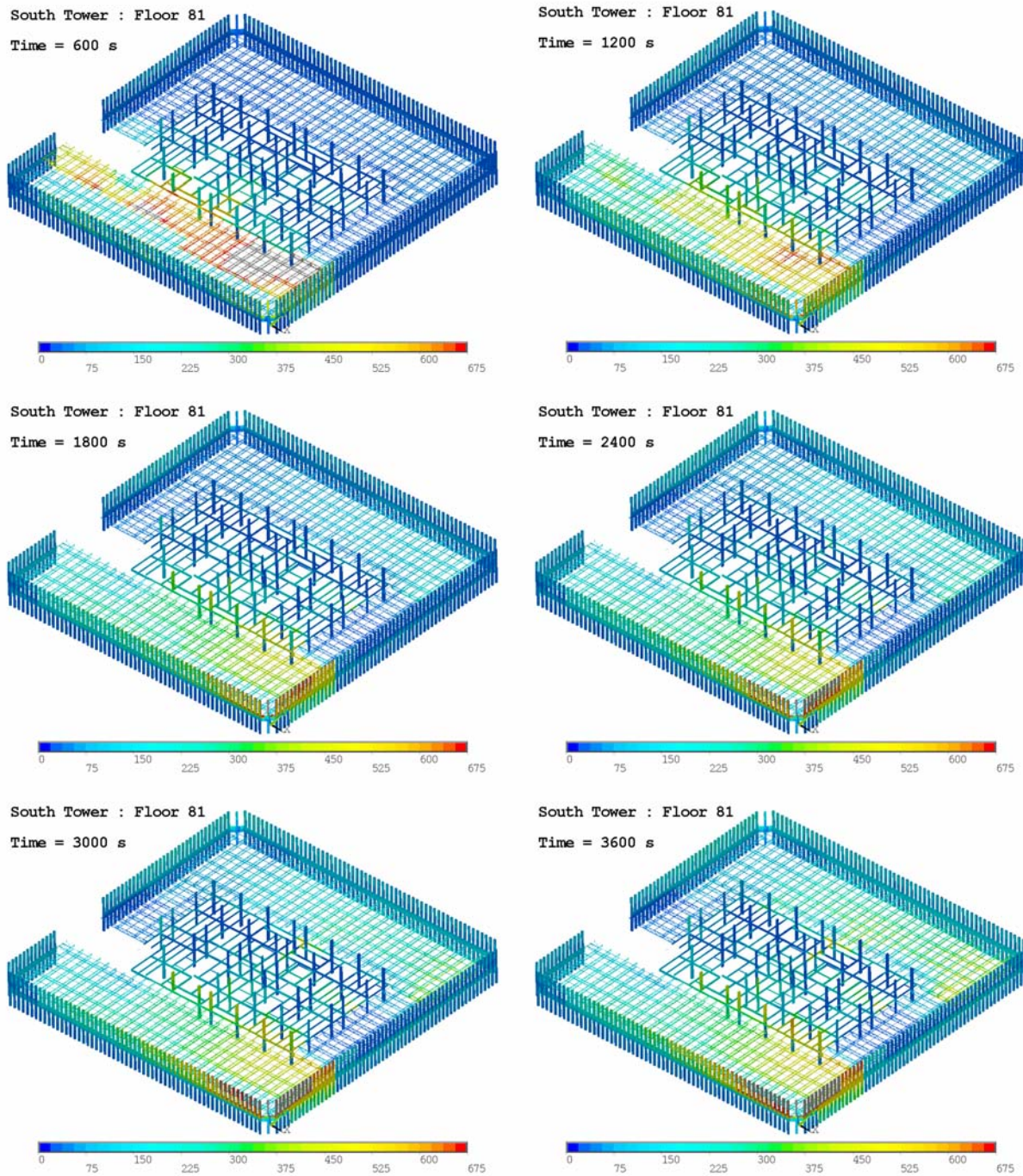


Figure 6-54. Thermal response of floor 81 of WTC 2, Case C.

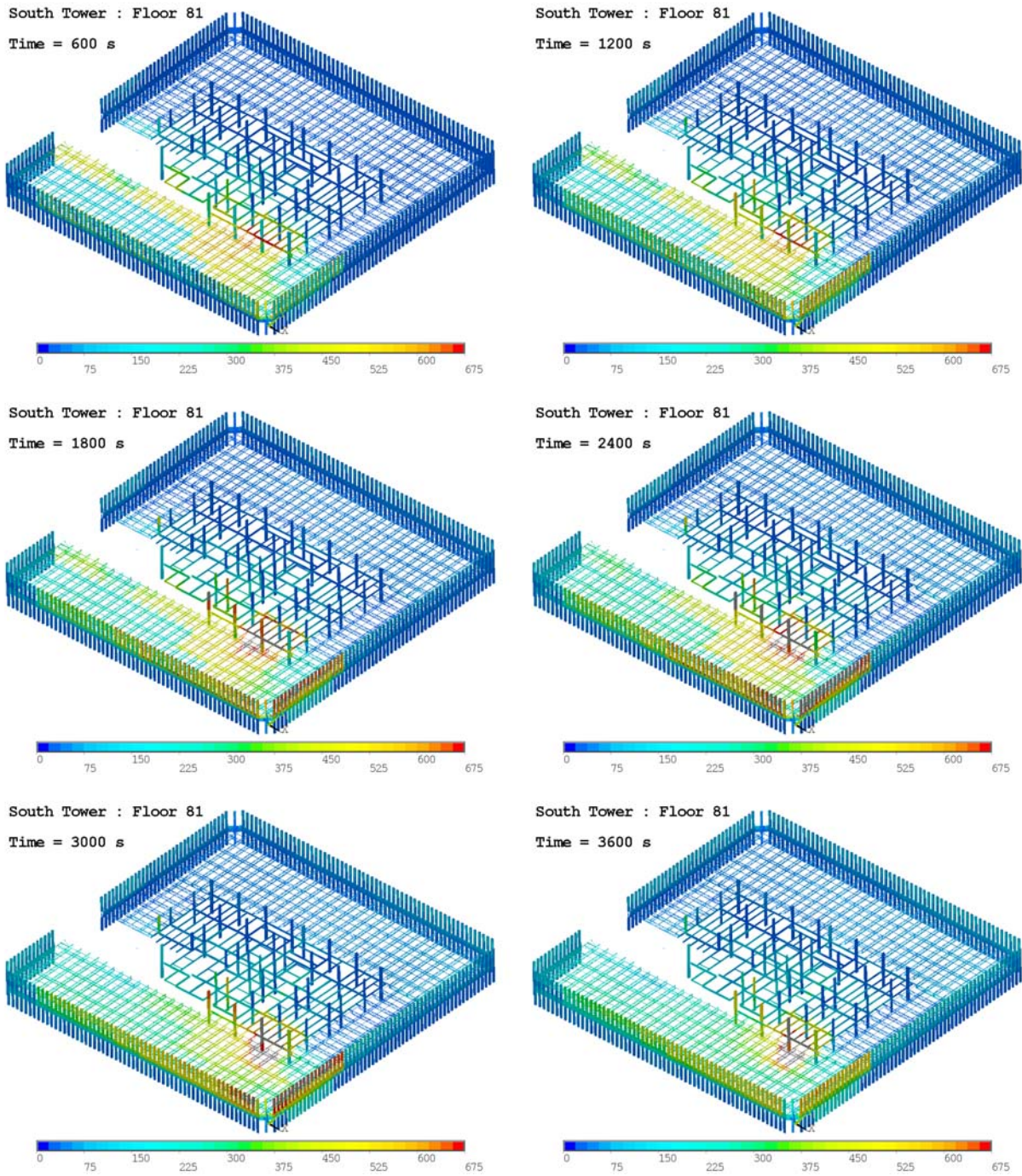


Figure 6-55. Thermal response of floor 81 of WTC 2, Case D.

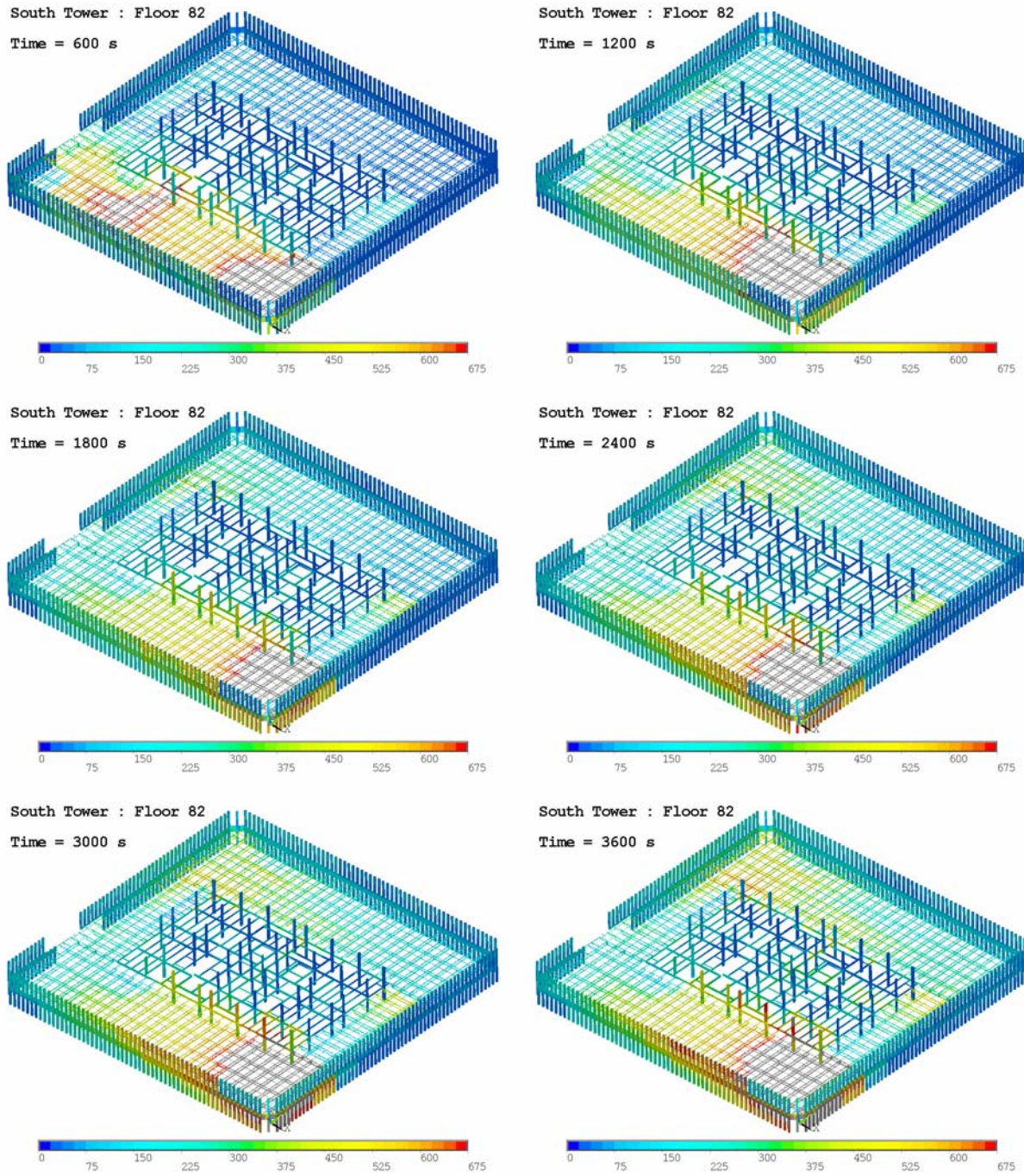


Figure 6–56. Thermal response of floor 82 of WTC 2, Case C.

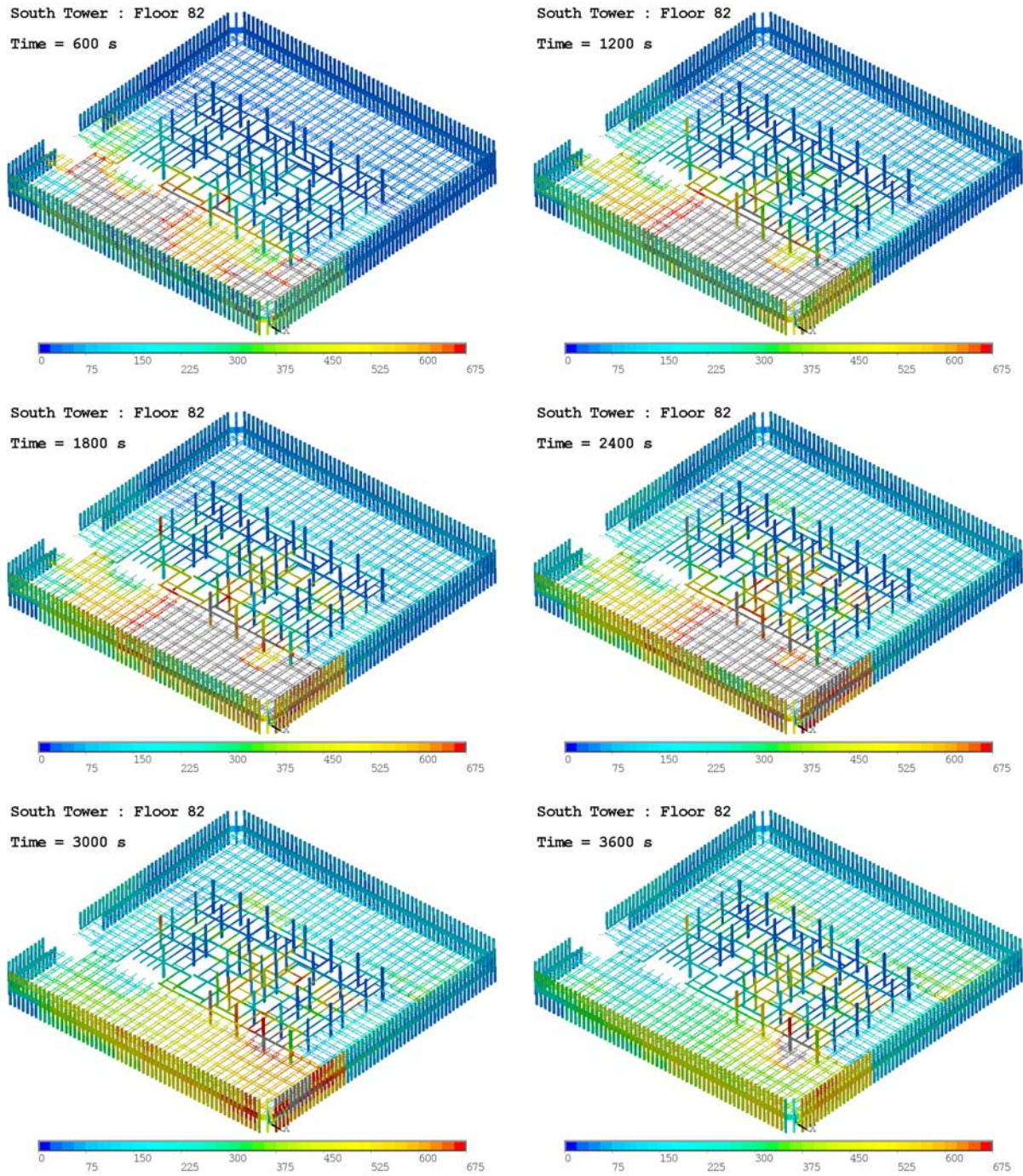


Figure 6-57. Thermal response of floor 82 of WTC 2, Case D.

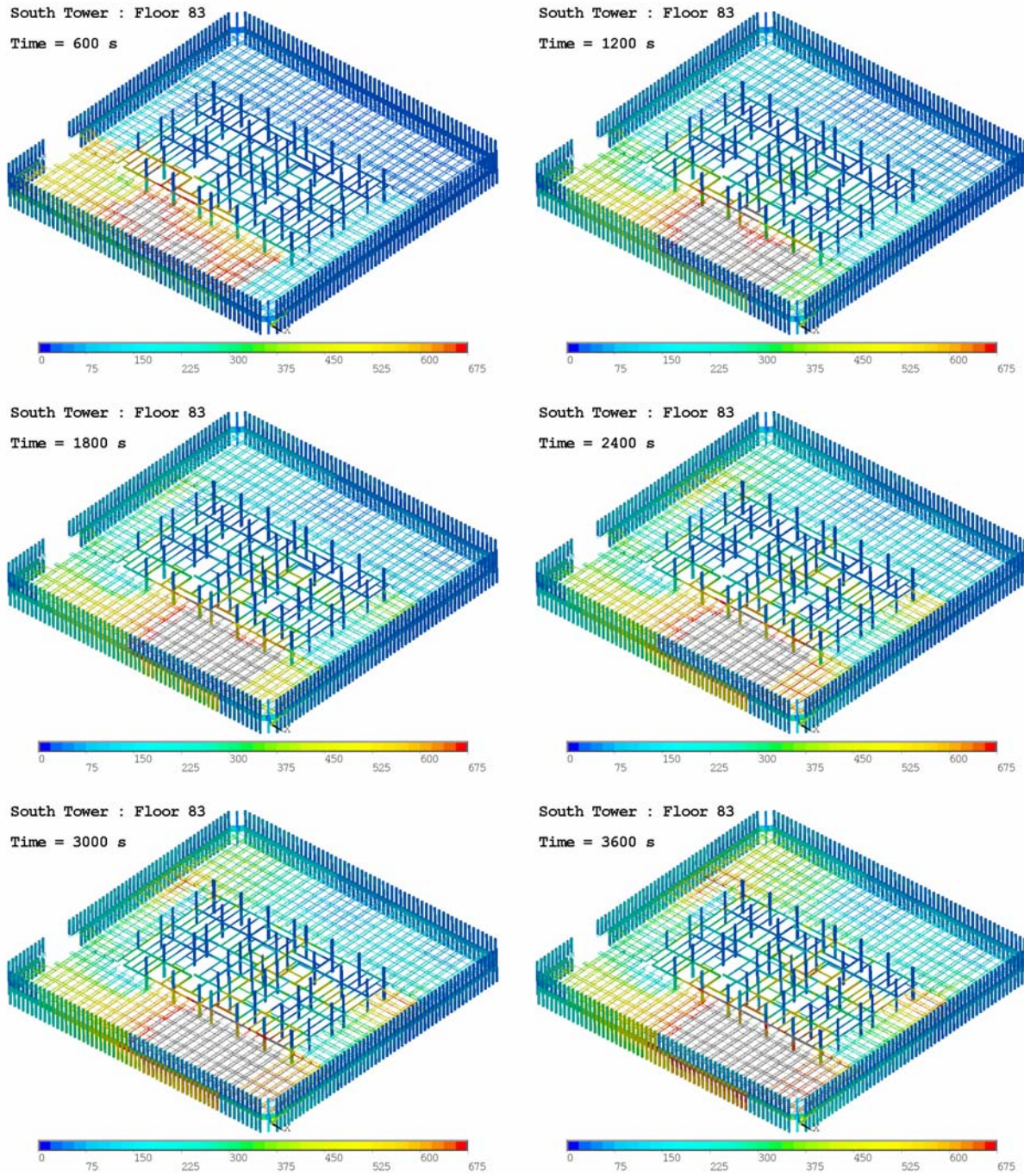


Figure 6–58. Thermal response of floor 83 of WTC 2, Case C.

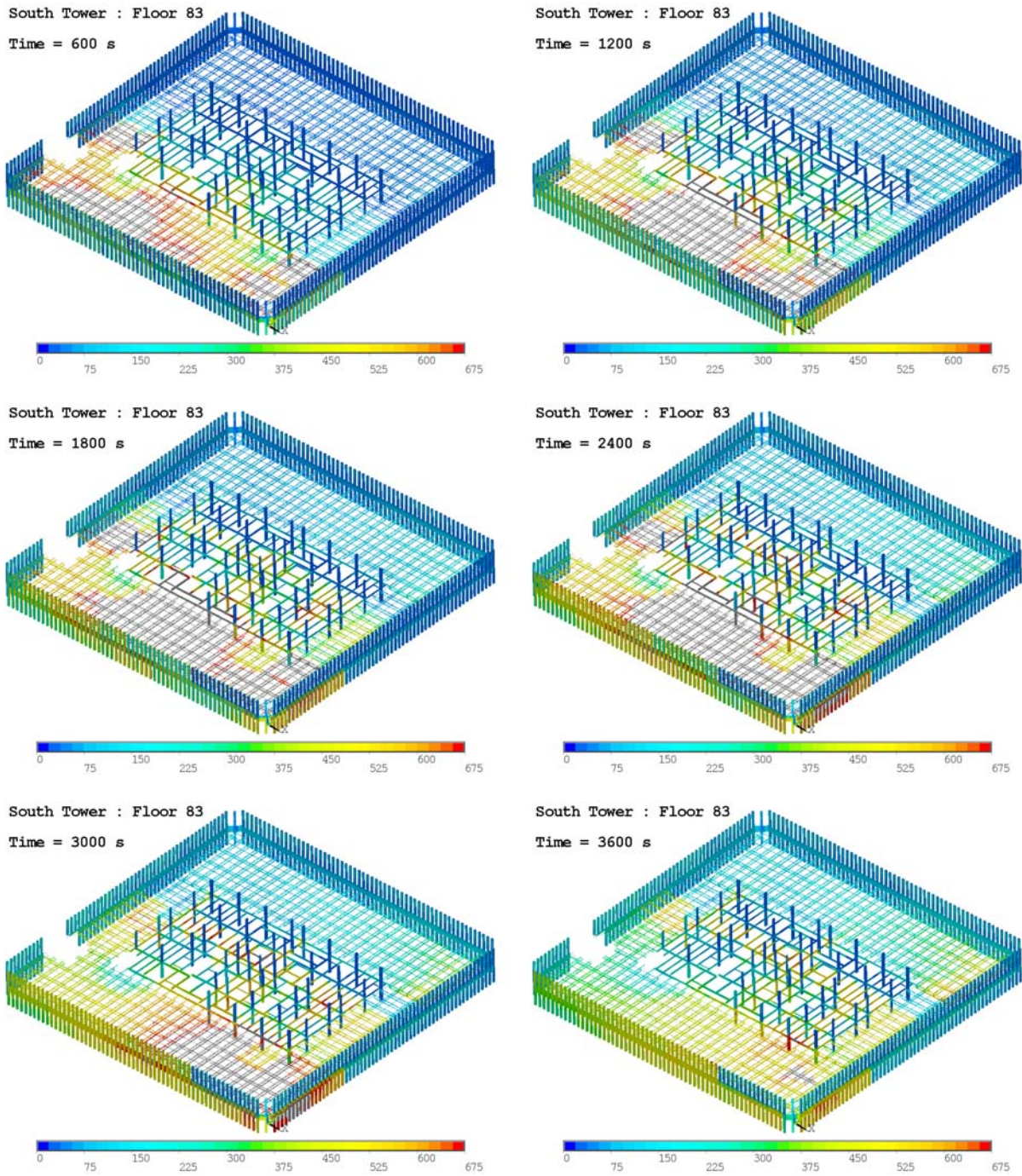


Figure 6-59. Thermal response of floor 83 of WTC 2, Case D.

6.12.1 Floor 79

Figure 6–60 shows the structural and insulation damage to floor 79.

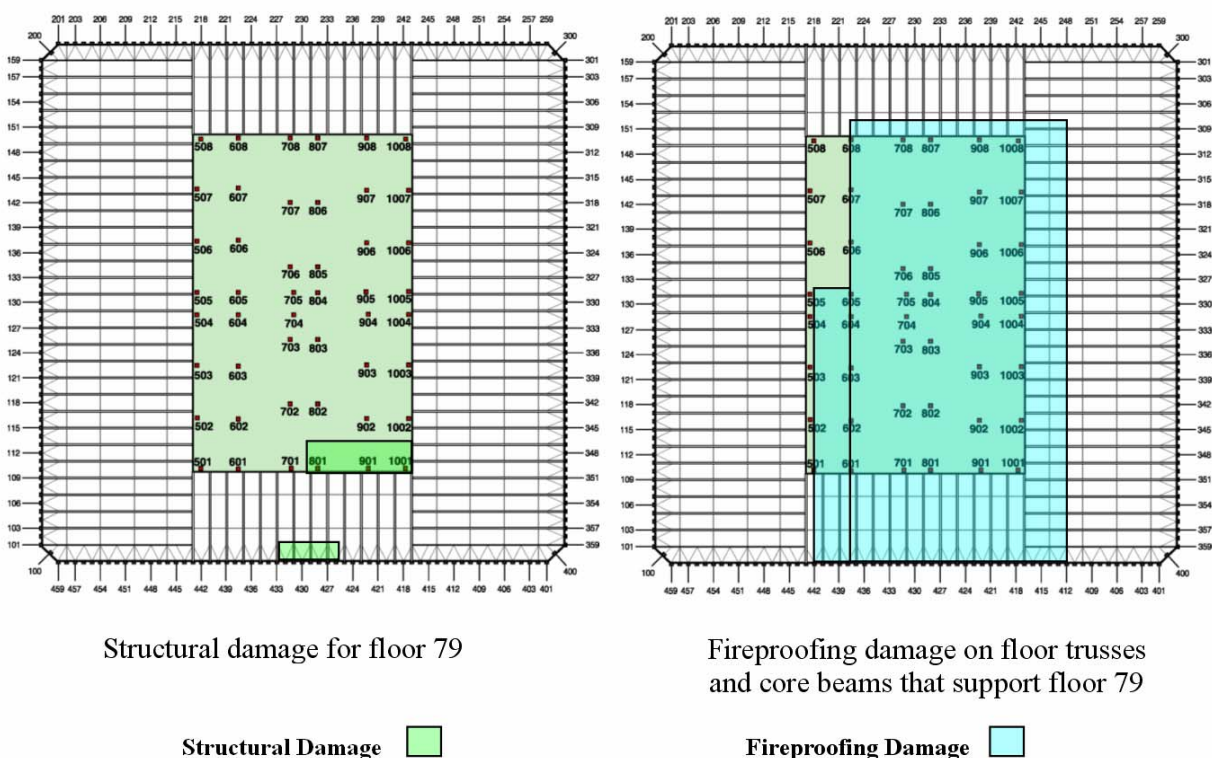


Figure 6–60. Structural and insulation damage on floor 79 of WTC 2, Case C.

In spite of extensive insulation damage on the trusses that supported the slab on the 79th floor, the trusses in the south face did not heat up significantly since there was only light fire activity on the 78th floor. The perimeter and core columns between floors 78 and 79 also remained relatively cold throughout the simulation, due to insufficient fire activity on the floor. Core columns on the east side (1000 series) above floor 79 indicated heating due to a combination of insulation damage and fire activity on the 79th floor. Core column 1008 had insulation damage but showed only gradual heating because of its high thermal inertia (thicker, heavier cross-section).

6.12.2 Floor 80

Figure 6–61 shows the structural and insulation damage to floor 80.

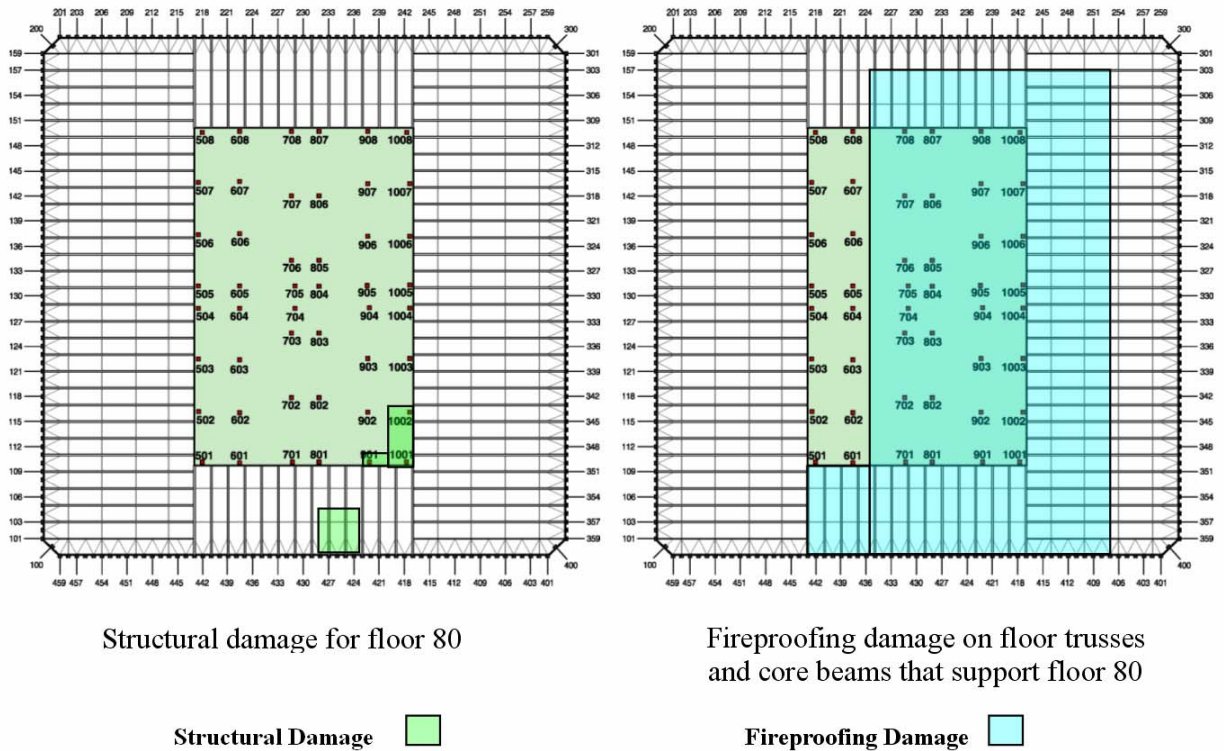


Figure 6–61. Structural and insulation damage on floor 80 of WTC 2, Case C.

The trusses and core beams that had insulation damage showed higher temperatures in the area where there was intense fire activity (10 min and 20 min after impact). There were portions of the floor trusses that did not heat up as quickly (even though they had lost their insulation) due to lack of fire activity in this area. Fire simulations indicated little fire activity near the south face and moderate activity at the north face. Some fire activity was predicted in the east and west faces. The trusses in the South Tower were covered with 0.6 in. equivalent thickness of sprayed fire-resistive materials (SFRM). These elements showed thermal heating in the northeast corner and at the east face. The simulations also predicted heating of the truss elements on the west face due to fire activity in this area. However, the collected photographs did not indicate the predicted level of fire activity. Thus, the heating of the truss elements in this area might have been significantly lower.

The northeast perimeter columns above floor 80 showed heating to over 500 °C due to the lack of insulation and intense fire activity. There was also some heating of the perimeter columns on the west face of floor 79. Heating of core columns was predicted on the east side on floor 79, but relatively cool core columns were predicted above floor 80. This was due to lack of high upper layer temperatures in the core on floor 80.

6.12.3 Floor 81

Figure 6–62 shows the structural and insulation damage on floor 81.

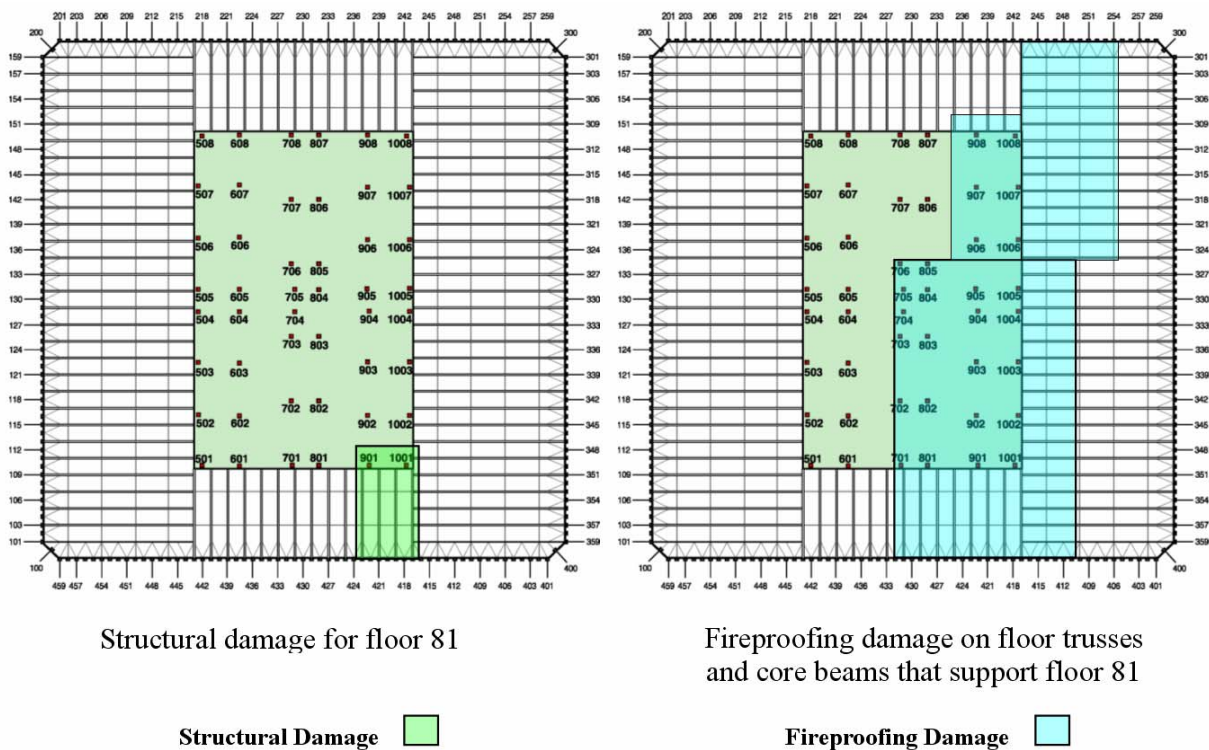


Figure 6–62. Structural and insulation damage on floor 81 of WTC 2, Case C.

Some heating of the trusses in the northwest corner was observed at 50 min to 60 min after impact. Although there was no insulation damage to the trusses in this region, the truss elements were covered with 0.6 in. of insulation, which allowed gradual heating in the region where there was fire activity. Fire simulations indicated less activity in the northeast corner on floor 80 compared to floors 81 and 82.

The perimeter columns above floor 81 showed significant heating due to lack of the insulation and intense fire activity in this area. This heating was observed over the entire east face and northeast corner. These perimeter columns reached temperatures above 600 °C at 30 min after impact. The rest of the perimeter columns stayed relatively cool. Core column heating was observed for the 1000 series columns above floor 81 due to a combination of insulation damage and fire activity in this area.

6.12.4 Floor 82

Figure 6–63 shows the structural and insulation damage on floor 82.

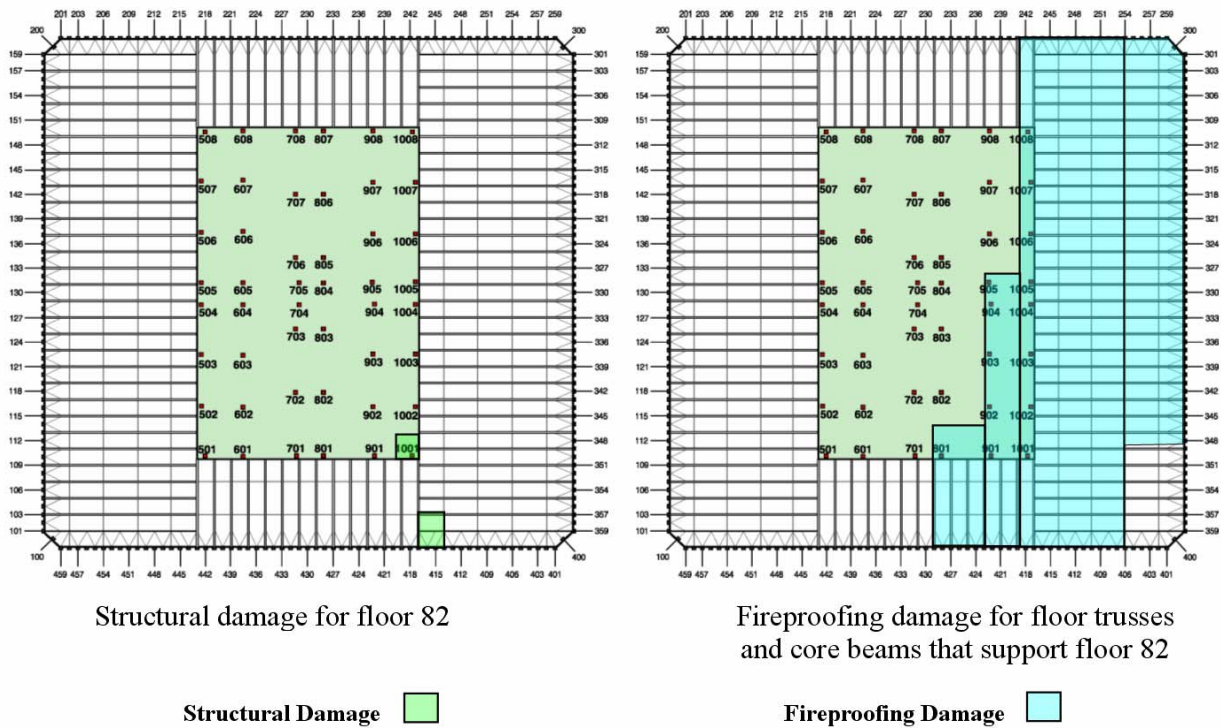


Figure 6–63. Structural and insulation damage on floor 82 of WTC 2, Case C.

The extensive insulation damage to the floor trusses and core beams on the east face of the tower resulted in significant heating of the trusses to over 675 °C for the entire duration of the simulation. Some heating was also observed in the southwest corner at 60 min after impact, due to the thinness of the insulation. The perimeter columns above floor 82 showed high temperatures at 40 min to 60 min after impact on the east face, and the core columns on the east side of the core also indicated thermal heating. The west side of the core stayed relatively cool, and there was very little activity in the northwest corner.

6.12.5 Floor 83

Figure 6–64 shows the structural and insulation damage on floor 83.

The thermal response of floor 83 was consistent with the insulation damage and the predicted fire activity on floors 82 and 83.

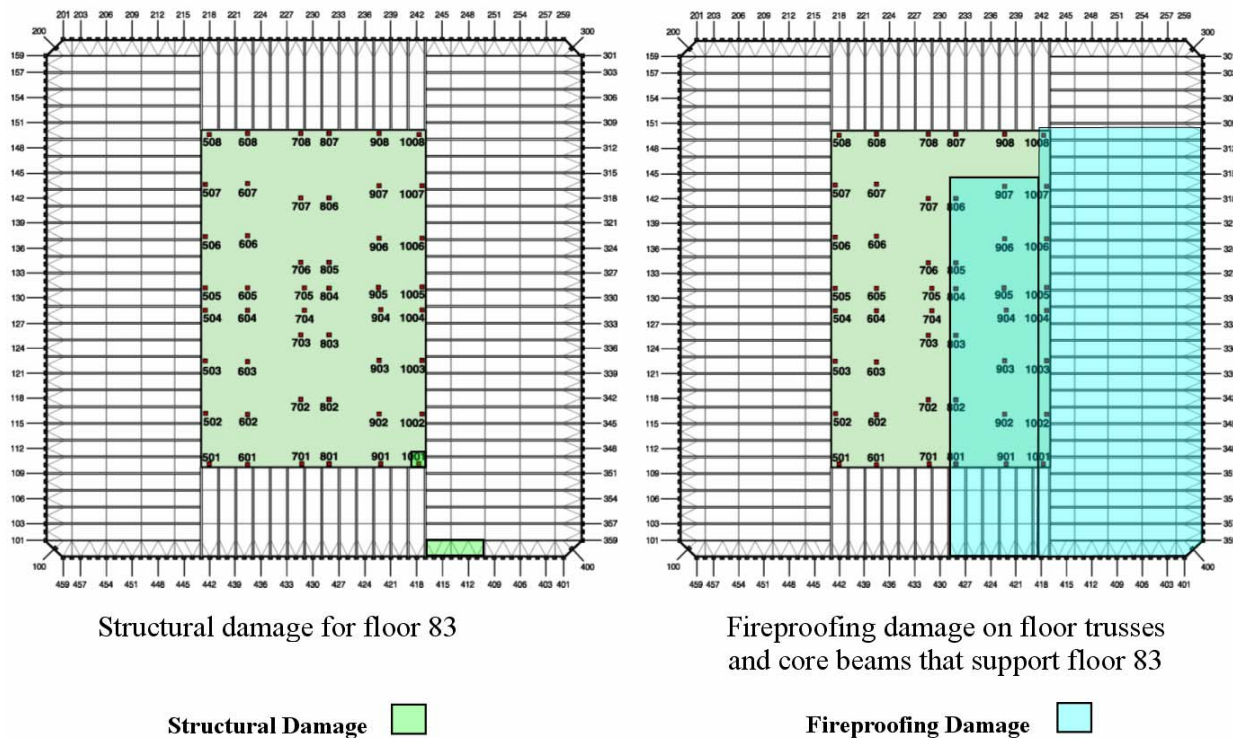


Figure 6–64. Structural and insulation damage on floor 83 of WTC 2, Case C.

6.13 GLOBAL THERMAL RESPONSE OF WTC 2, CASE D

6.13.1 Floor 79

The truss system that supported floor 79 showed slightly higher temperatures for Case D compared to Case C, especially in the southeast corner at 20 min after impact. This was due to continuous fire activity on floor 78 in this area.

6.13.2 Floor 80

The east side of the truss system that supported floor 80 showed higher temperatures than in Case C, due to continuous fire activity on floor 79. The insulation damage was more extensive in Case D, especially in the east side of the core. The insulation damage resulted in higher temperatures on the core columns.

6.13.3 Floor 81

The truss system that supported floor 81 showed intense heating at the east face and in the northeast corner. The perimeter columns in the northeast corner as well as core columns showed significant heating, due to a combination of insulation damage and fire activity in this area. The insulation damage in Case D was more extensive in the truss and floor systems and core columns.

6.13.4 Floor 82

Most of the perimeter and core columns along the east, and especially northeast, tenant space showed very high temperatures. This floor was one of the most severely insulation-damaged floors in these simulations. The fires in the northeast corner burned out at 50 min to 60 min, which resulted in cooling of the temperatures of the trusses and columns in this area.

6.13.5 Floor 83

Like floor 82, floor 83 showed very intense fire activity throughout the simulation, resulting in temperatures highly likely to result in structural weakening on the east side of the building.

6.14 SUMMARY OF THERMAL RESPONSE OF STRUCTURAL COMPONENTS

Tables 6–3 and 6–4 summarize the regions of the floors in which the structural steel reached temperatures at which their yield strengths would have been significantly diminished. Instances of brief heating of one or two columns early in the fires were not included.

Table 6–3. Regions in WTC 1 in which temperatures of structural steel exceeded 600 °C.

Floor Number	Trusses		Perimeter Columns		Core Columns	
	Case A	Case B	Case A	Case B	Case A	Case B
93	--	--	--	--	--	--
94	--	--	--	--	N, S	NE, S
95	N	N, S	--	--	S	NW, S
96	N	N, S	--	S	S	W, S
97	N, S	N, S	--	S	N	W, S
98	N	N, S	--	--	--	--
99	--	--	--	--	--	--

Key: E, east; N, north; S, south; W, west; NE: northeast; NW, northwest.

Table 6–4. Regions in WTC 2 in which temperatures of structural steel exceeded 600 °C.

Floor Number	Trusses		Perimeter Columns		Core Columns	
	Case C	Case D	Case C	Case D	Case C	Case D
79	--	--	--	--	--	--
80	--	--	--	--	--	--
81	NE	NE	NE	NE	--	NE
82	E	E	E	E	E	E
83	E	E	--	E	--	E

Key: E, east; N, north; S, south; W, west; NE, northeast; NW, northwest.

A principal conclusion from these results is that the columns and trusses for which the insulation was intact did not heat to temperatures where significant loss of strength occurred.

6.15 FIRE IN AN UNDAMAGED TOWER

After incurring the direct damage from two different aircraft strike conditions, WTC 1 and WTC 2 stood for 102 min and 56 min, respectively. Structural models of the two aircraft-damaged buildings indicated that, in the absence of weakening by fires or other substantial insult, the buildings would have continued to stand indefinitely (NIST NCSTAR 1-6D). The application of the fire scenarios in Cases B and D to the aircraft-damaged towers resulted in collapse.

To complete the assessment of the relative roles of aircraft impact and ensuing fires, NIST examined whether an intense, conventional fire, occurring without the aircraft impact, could have led to the collapse of a WTC tower, were it in the same condition as it was prior to the aircraft impact on the morning of September 11, 2001. The characteristics of such an intense fire could have been:

- Ignition on a single floor by a small bomb or other explosion. If arson were involved, there might have been multiple small fires ignited on a few floors.
- Air supply initially determined by the building ventilation system.
- Moderate fire growth rate. In the case of arson, several gallons of an accelerant might have been applied to the building combustibles, igniting the equivalent of several workstations.
- Water supply to the sprinklers and standpipes maliciously compromised.
- Intact structural insulation and interior walls.

The four cases described in this report represented fires that were far more severe than this:

- The incident jet fuel created large and widespread early fires on several floors.
- The aircraft and subsequent fireballs created large open areas in the building exterior, through which air could flow to support the fires. In Case A, the fire was still limited by the total vent area (broken windows plus aircraft gash). In Case C, the fire had sufficient air. The fires in both cases were immense.
- About 10,000 gal of jet fuel were sprayed into multiple stories, simultaneously igniting hundreds of workstations.
- The impact and debris removed the insulation from a large number of structural elements that were then subjected to the heat from the fires.

In the four cases reported earlier in this chapter, none of the columns with intact insulation reached temperatures over 300 °C. Only a few isolated truss members with intact insulation were heated to temperatures over 400 °C in the WTC 1 simulations and to temperatures over 500 °C in the WTC 2 simulations.

In WTC 1, if the fires had been allowed to continue past the time of building collapse, complete burnout would likely have occurred within a short time since the fires had already traversed around the entire floor and most of the combustibles would already have been consumed. (See Figure 6–30.)

In a simulation of WTC 2 that allowed the fires to continue to burn for 3 hours, the temperatures in the truss steel on the west side of the building (where the insulation was undamaged) did continue to increase. In WTC 2, if the fire simulation was extended for 2 hours past the time of building collapse with all windows broken, the temperatures in the truss steel on the west side of the building (where the insulation was undamaged) would likely have increased for about 40 min before falling off rapidly as the combustibles were consumed. Temperatures of 700 °C to 760 °C were reached over approximately 15 percent of the west floor area for less than 10 min. Approximately 60 percent of the floor steel had temperatures between 600 °C and 700 °C for about 15 min. Approximately 70 percent of the floor steel had temperatures that exceeded 500 °C for about 45 min. Based on Cases C and D, the temperatures of the insulated exterior and core columns would not have increased to the point where they would have experienced significant loss of strength or stiffness.

6.16 REFERENCES

- McGrattan, K., ed. 2004. *Fire Dynamics Simulator (Version 4) Technical Reference Guide*. NIST Special Publication 1018. National Institute of Standards and Technology, Gaithersburg, MD. September.
- Rehm, R.G., W.M. Pitts, H.R. Baum, D.D. Evans, K. Prasad, K.B. McGrattan, and G.P. Forney. 2002. *Initial Model for Fires in the World Trade Center*, NISTIR 6879. National Institute of Standards and Technology, Gaithersburg, MD. May.

This page intentionally left blank.

Chapter 7

FINDINGS

7.1 CHARACTERISTICS OF THE BUILDINGS

- The floors which the aircraft impacted and on which the major fires occurred were mostly occupied by a single tenant. The floor plans were generally open, with few interior walls.
- The principal combustibles on the fire floors were workstations, each capable of generating a peak heat release rate of 7 MW and a total (integrated) heat release of 4 GJ. The total fuel load on the World Trade Center (WTC) floors was about 4 psf, 20 kg/m².
- The aircraft added significant combustible material to their paths (and the paths of their breakup fragments) through the buildings.
- The ceiling tile systems in the fire zones were heavily damaged by the shocks from the aircraft impacts and would have provided little, if any, barrier to fire exposure of the ceiling structure. This was consistent with multiple observations during the evacuation.

7.2 CHARACTERISTICS OF THE FIRES

- Upon aircraft impact, a significant fraction of 10,000 gal of jet fuel ignited within the building. The expansion of the hot combustion gases broke windows and blew some of the remaining fuel through them in large fireballs.
- The jet fuel fires consumed most of the oxygen within the fire floors, and the fires quickly died down. The fires grew as fresh air became available through broken windows and the primed solid combustibles reached their full burning rates.
- The jet fuel was the primer for near-simultaneous ignition of large fires on multiple floors.
- The dominant fuel for the fires in the towers was the office combustibles. On the floors where the aircraft fuselage impacted, there was a significant, but secondary contribution from the combustibles in the aircraft. Most of the jet fuel in the fire zones was consumed in the first few minutes after impact, although there may have been unburned pockets of jet fuel that led to flare-ups late in the morning.
- The major fires in World Trade Center (WTC) 1 were on the 93rd through 99th floors. The fires generally moved both clockwise and counterclockwise from the north to the south of the tenant spaces. The fires were generally ventilation limited, i.e., they burned and spread only as fast as fresh air became available, generally from additional window breakage.
- The major fires in WTC 2 were on the 79th through 83rd floors, with the most important fires being in the northeast corner of the 81st and 82nd floors. The fires moved far less than those in

WTC 1, remaining in the east half of the floors. The fires had sufficient air to burn at a rate determined by the properties of the combustibles. This was in large part due to the extensive breakage of windows in the fire zone by the aircraft impact.

- At the time of the building collapses, there were still vigorous fires, indicating the unchecked fires could have continued to burn.

7.3 CAPABILITY FOR LARGE FIRE RECONSTRUCTION

- It was possible to reconstruct a complex fire in a large building, even if the building is no longer standing. However, this required extraordinary information to replace what might have been gleaned from an inspection of the post-fire premises. In the case of the WTC tower, this information included floor plans of the fire zones, burning behavior of the combustibles, simulations of damage to the building interior, and frequent photographic observations of the fire progress from the building exterior.
- Proper design and interpretation of laboratory fires over two orders of magnitude smaller (heat release rates of 10 MW and 12 GJ in total heat output) than the WTC fires provided valuable information for simulating the WTC fires.
- Conventional office workstations reached a peak burning rate in about 10 min and continued burning for a total of about a half hour. Partial covering of surfaces with inert material, such as ceiling tiles, reduced the peak burning rate proportional to the fraction covered, but did not affect the total amount of heat release during the entire burning.
- Jet fuel sprayed onto the surfaces of typical office workstations burned away within a few minutes. The jet fuel accelerated the burning of the workstation, but did not affect the overall heat released.
- The Fire Dynamics Simulator (FDS) was capable of prediction of the room temperatures and heat release rates for complex fires to within 20 percent, when the building geometry, fire ventilation, and combustibles were properly described. Parallel processing was essential to keep computation times tractable.
- The Fire Structure Interface, developed for this Investigation, was able to map the fire-generated temperature and radiation fields onto and through layered structural materials to within the accuracy of the fire-generated fields and the thermophysical data for the structural components.

7.4 SIMULATIONS OF THE WTC FIRES

- Insulation damage due to the aircraft impact was the single most important parameter affecting whether a structural member reached a temperature range likely to cause loss of structural strength.
- The fire spread rates in WTC 1 were consistent with a combusted fuel load of 4 psf (20 kg/m²). Higher combusted fuel loadings resulted in slower fire spread rates that did not

match the patterns observed in the photographic evidence. Since these fires were ventilation-limited, the flame temperatures would not have varied significantly within a range of reasonable combusted fuel loadings.

- The plateau heat release rates from the fires were about 2 GW for WTC 1 and 1 GW for WTC 2. The total heat outputs were about 8,000 GJ from WTC 1 and 3,000 GJ from WTC 2.
- For fires of this magnitude, the important factors in determining burning rates were the ventilation area and location, the mass loading of the combustibles, their spatial distribution, and their heats of gasification. The presence of high volatility materials, such as jet fuel, were instrumental during the initiation phase, but mostly burned away rapidly and (except for a few flare-ups observed in WTC 2) played little or no role later.
- In the simulations, none of the columns with intact insulation reached temperatures over 300 °C. Only a few isolated truss members with intact insulation were heated to temperatures over 400 °C in the WTC 1 simulations and to temperatures over 500 °C in the WTC 2 simulations. In WTC 1, if the fires had been allowed to continue past the time of building collapse, complete burnout would likely have occurred within a short time since the fires had already traversed around the entire floor, and most of the combustibles would already have been consumed. In WTC 2, the temperatures in the truss steel on the west side of the building (where the insulation was undamaged) would likely have continued to increase. These temperatures could have exceeded 600 °C for about 15 min for large sections of the floor steel. The temperatures of the insulated exterior and core columns would not have increased to the point where they would have experienced significant loss of strength or stiffness.

This page intentionally left blank.